

SYNTHESIS PROCEDURE FOR LINEAR TIME-VARYING  
FEEDBACK SYSTEMS WITH LARGE PARAMETER IGNORANCE

by

Thomas Edwin McDonald Jr.

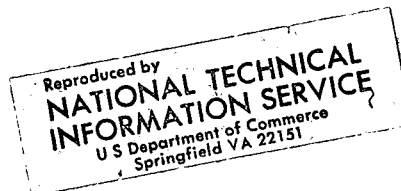
(NASA-CR-116777) SYNTHESIS PROCEDURE FOR  
LINEAR TIME-VARYING FEEDBACK SYSTEMS WITH  
LARGE PARAMETER IGNORANCE T.E. McDonald,  
Jr. (Colorado Univ.) 1 Apr. 1972 312 p

N72-27252

Unclas

CSSL 09C G3/10 34094

This research was jointly sponsored by the National Science  
Foundation and the National Aeronautics and Space  
Administration under research grant NGR 06-003-083



Department of Electrical Engineering  
University of Colorado  
Boulder, Colorado

APR 1 1972



No distribution limitation

312

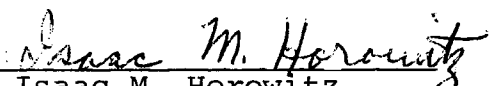
SYNTHESIS PROCEDURE FOR LINEAR TIME-VARYING  
FEEDBACK SYSTEMS WITH LARGE PARAMETER IGNORANCE

by

Thomas Edwin McDonald Jr.

This research was jointly sponsored by the National Science  
Foundation and the National Aeronautics and Space  
Administration under research grant NGR 06-003-083

  
Thomas Edwin McDonald Jr.

  
Isaac M. Horowitz  
Research Supervisor

Department of Electrical Engineering  
University of Colorado  
Boulder, Colorado

## SYNTHESIS PROCEDURE FOR LINEAR TIME-VARYING FEEDBACK SYSTEMS WITH LARGE PARAMETER IGNORANCE

Abstract--This work is addressed to the development of synthesis procedures for linear time-varying feedback systems. It is assumed that the plant can be described by linear differential equations with time-varying coefficients; however, ignorance is associated with the plant in that only the range of the time-variations are known instead of exact functional relationships. As a result of this plant ignorance the use of time-varying compensation is ineffective so that only time-invariant compensation is employed. In addition, there is a noise source at the plant output which feeds noise through the feedback elements to the plant input. Because of this noise source the gain of the feedback elements must be as small as possible. No attempt is made to develop a stability criterion for time-varying systems in this work.

Two synthesis procedures are developed and investigated. Both procedures assume system specifications to be given in the frequency domain (i.e., specifications on the Fourier transform of the system signals) and both procedures arrive at the transfer function for the linear compensation. The method used in the procedures takes an iterative approach in that a design is made, then the system is simulated on a computer to test its adequacy. If the design is unsatisfactory, a subsequent design is made until either the system is satisfactory or instability is reached. Application of the procedures to general systems is limited because of the lack of a stability criterion; however, the procedures can be successfully applied to systems with time-varying gains since a stability criterion exists for such systems.

TABLE OF CONTENTS

CHAPTER	PAGE
I	INTRODUCTION..... 1
	1.1 Description of the System..... 1
	1.2 Historical Background..... 2
	1.3 General Considerations..... 6
II	DEVELOPMENT OF INPUT-OUTPUT RELATIONS AND SYSTEMS EQUATIONS..... 16
	2.1 General..... 16
	2.2 Properties of the Frequency Impulse Response.. 18
	2.3 Discussion of the Frequency Impulse Response.. 27
	2.4 Development of System Equations..... 32
III	DEVELOPMENT OF SYNTHESIS PROCEDURES..... 37
	3.1 Introduction..... 37
	3.2 Synthesis Procedure One..... 38
	3.3 Synthesis Procedure Two..... 76
	3.4 Summary..... 91
IV	DESIGN EXAMPLE..... 94
	4.1 Introduction..... 94
	4.2 Methods of Calculations..... 96
	4.3 Specification..... 100
	4.4 First Design..... 131
	4.5 Second Design: Procedure One..... 184
	4.6 Second Design: Procedure Two..... 196
	4.7 Third Design..... 205
	4.8 Addition of High Frequency Poles..... 234
	4.9 Summary..... 272
V	CONCLUSIONS..... 278
	BIBLIOGRAPHY..... 283
	APPENDIX A..... 287
	APPENDIX B, DERIVATION OF $I_o(j\gamma)$ ..... 294
	APPENDIX C, DERIVATION OF $P_o(j\omega)/P_{eq}(j\omega)$ ..... 297
	APPENDIX D..... 299

# LIST OF ILLUSTRATIONS

FIGURE		PAGE
1.1	Block Diagram of the Feedback System Under Study....	1
1.2	Illustration of the Ignorance Assumed to Be Associated with Each Coefficient.....	7
1.3	Step Response Due to a Step Input Applied at $t = \gamma$ ..	11
1.4	System with Time-varying Gain.....	14
2.1	Block Diagram of a Linear System.....	19
2.2	Combining Systems in Parallel.....	23
2.3	Combining Systems in Cascade.....	24
2.4	Illustration of System and Inverse.....	26
2.5	Graph of $f(t)$ Used in Example.....	29
2.6	Type of Plant for Which an Expression of the Inverse Frequency Impulse Response Can Be Obtained.....	31
2.7	System under Study.....	33
3.1	System under Study.....	39
3.2	Block Diagram of System in Example.....	49
3.3	Boundaries of Acceptable Regions of $L(j\omega)$ with Polar Plot of $L_o(j\omega)$ .....	57
3.4	Envelope of $ E_o(j\omega) $ of First Design.....	60
3.5	Boundaries of Acceptable Regions of $L_1(j\omega)$ .....	61
3.6	Polar Plot of $L_1(j\omega)$ .....	63
3.7a	Envelope of $E_1(j\omega)$ of Second Design.....	64
3.7b	Low Frequency Specification of Design Example Two...	68
3.8	Boundaries of Acceptable Regions of $H(j\omega)$ with Polar Plot of $H(j\omega)$ .....	73
3.9a	Envelope of $ E(j\omega) $ for $0 \leq \omega \leq 10$ .....	75
3.9b	Envelope of $E(j\omega)$ for $10 \leq \omega \leq 20$ .....	75
3.10a	Low Frequency Range of $P_o(j\omega)/P_{eq}(j\omega)$ .....	84
3.10b	High Frequency Range of $P_o(j\omega)/P_{eq}(j\omega)$ .....	85
3.11a	Low Frequency Boundaries of Acceptable Regions of $L(j\omega)$ with Comparison of $L_1(j\omega)$ .....	87
3.11b	High Frequency Boundaries of Acceptable Regions of $L(j\omega)$ with Comparison of $L_1(j\omega)$ .....	88
3.12	Range of $P_o(j\omega)/P_{eq}(j\omega)$ .....	89
3.13	Acceptable Regions of $L(j\omega)$ with Comparison of $L_1(j\omega)$ .....	90
4.1	Design Example.....	94
4.2	General Structure of Plant Where Only Time-varying Element Is a Gain.....	95
4.3	General System with Time-varying Gain.....	95
4.4	Time Domain Specifications as Envelope About Desired Step Response.....	102
4.5	Time Domain Specifications as Upper Bound on Error..	102
4.6	Time Domain Specifications for Example; Envelope about Desired Step Response.....	104
4.7	Time Domain Specification for Example; Bound on Error.....	105

FIGURE		PAGE
4.8	Form of Frequency Domain Specification.....	106
4.9a	Error Function Series One.....	108
4.9b	Fourier Transform Magnitudes of Error Function Series One.....	109
4.10a	Error Function Series Two.....	111
4.10b	Fourier Transform Magnitudes of Error Function Series Two.....	112
4.11a	Error Function Series Three.....	114
4.11b	Fourier Transform Magnitudes of Error Function Series Three.....	115
4.12a	Error Function Series Four.....	116
4.12b	Fourier Transform Magnitudes of Error Function Series Four.....	117
4.13a	Error Function with Single Fast Variation.....	118
4.13b	Fourier Transform Magnitude of Function with Single Fast Variation.....	119
4.14	Possible Frequency Domain Specification Envelopes..	120
4.15a	Functions Which Violate Time Domain Specifications But May Not Violate Frequency Domain Specifi- cations; Series I.....	123
4.15b	Fourier Transform Magnitudes of Functions Which Violate Time Domain Specifications; Series I.....	124
4.16a	Functions Which Violate Time Domain Specifications But May Not Violate Frequency Domain Specifi- cations; Series II.....	126
4.16b	Fourier Transform Magnitudes of Functions Which Violate Time Domain Specifications; Series II.....	127
4.17	Frequency Domain Specification.....	129
4.18	Region Defined by Second Form of Frequency Domain Specifications.....	130
4.19	Region Defined by First Form of Frequency Domain Specifications.....	131
4.20	Illustration Showing the Determination of Acceptable Region of $-\tilde{L}_0(j\omega)$ .....	137
4.21	Acceptable Region of $-L_0$ for $\omega = 2$ .....	138
4.22	Acceptable Regions of $-L_0$ .....	140
4.23	Acceptable Regions of $C(j\omega)/C_0(j\omega)$ .....	143
4.24	Determining a Point on the Boundary of the Acceptable Region for $-L_0(j\omega)$ .....	144
4.25	Illustration of the Use of the Modified Region of $C/C_0$ .....	145
4.26	Determining the Modified Region of $C(j\omega)/C_0(j\omega)$ ....	146
4.27a	Modified Region of $C(j\omega)/C_0(j\omega)$ : $\omega = 0.628$ .....	148
4.27b	Modified Region of $C(j\omega)/C_0(j\omega)$ : $\omega = 1.25$ .....	149
4.27c	Modified Region of $C(j\omega)/C_0(j\omega)$ : $\omega = 1.88$ .....	150
4.27d	Modified Region of $C(j\omega)/C_0(j\omega)$ : $\omega = 4.39$ .....	151
4.27e	Modified Region of $C(j\omega)/C_0(j\omega)$ : $\omega = 6.28$ .....	152
4.27f	Modified Region of $C(j\omega)/C_0(j\omega)$ : $\omega = 9.42$ .....	153

## FIGURE

## PAGE

4.28	Determination of a Point on the Boundary of the Region of Acceptable $-L_O(j\omega)$ : $= 1.25$ .....	154
4.29	Polar Plot of Time Invariant Design.....	156
4.30	Type of Function for Time-varying Gain.....	158
4.31	Functions Resulting in Maximum Error During First Series.....	160
4.32	Step Response and Error Function Corresponding to Maximum Error at $\omega = 0$ during First Series.....	161
4.33	Step Response and Error Function Corresponding to Maximum Error at $\omega = 0.628$ during First Series....	162
4.34	Functions Resulting in Maximum Error during Second Series.....	163
4.35	Step Response and Error Function Corresponding to Maximum Error at $\omega = 0$ during Second Series.....	164
4.36	Step Response and Error Function Corresponding to Maximum Error at $\omega = 0$ during Second Series.....	165
4.37	Maximum Error Due to Time Variations.....	167
4.38	Region of $P_O/P_{eq}$ for $\omega = 0.628$ .....	169
4.39	Region of $P_O/P_{eq}$ for $\omega = 1.25$ .....	170
4.40	Region of $P_O/P_{eq}$ for $\omega = 1.88$ .....	171
4.41	Region of $P_O/P_{eq}$ for $\omega = 4.39$ .....	172
4.42	Region of $P_O/P_{eq}$ for $\omega = 6.28$ .....	173
4.43	Region of $P_O/P_{eq}$ for $\omega = 9.42$ .....	174
4.44	Step Response of Time-varying System Time-Invariant Design.....	177
4.45	Step Response of Time-varying System Time-Invariant Design.....	178
4.46	Step Response of Time-varying System Time-Invariant Design.....	179
4.47	Step Response of Time-varying System Time-Invariant Design.....	180
4.48	Step Response of Time-varying System Time-Invariant Design.....	181
4.49	Step Response of Time-varying System Time-Invariant Design.....	182
4.50	Step Response of Time-varying System Time-Invariant Design.....	183
4.51	Polar Plot of $-L_O(j\omega)$ with Boundaries of Acceptable Regions of $-L_O$ and $-L_O'$ .....	187
4.52	Plot of Maximum $ E $ for Second Design Using Procedure One.....	190
4.53	Time Variations Resulting in Maximum $ E $ at $\omega = 0$ with Corresponding Step Response and Error Function.....	192
4.54	Time Variations Resulting in Maximum $ E $ at $\omega = 0.628$ with Corresponding Step Response and Error Function.....	193
4.55	Sample Time Variation with Corresponding Step Response and Error Function.....	194

## FIGURE

## PAGE

4.56	Sample Time Variation with Corresponding Step Response and Error Function.....	195
4.57	Boundaries of Acceptable Regions of $-L'_0$ with Polar Plot of $-L'_0(j\omega)$ .....	197
4.58	Region of $P_o/P_{eq}$ for $\omega = 0.628$ .....	199
4.59	Region of $P_o/P_{eq}$ for $\omega = 1.25$ .....	200
4.60	Region of $P_o/P_{eq}$ for $\omega = 1.88$ .....	201
4.61	Region of $P_o/P_{eq}$ for $\omega = 4.39$ .....	202
4.62	Region of $P_o/P_{eq}$ for $\omega = 6.28$ .....	203
4.63	Region of $P_o/P_{eq}$ for $\omega = 9.42$ .....	204
4.64	Step Response of System with Gain Constant at 10, Second Design, Procedure Two.....	206
4.65	Step Response of System with Gain Constant at 1, Second Design, Procedure Two.....	207
4.66	Sample Step Response of Time-varying System, Second Design, Procedure Two.....	208
4.67	Sample Step Response of Time-varying System, Second Design, Procedure Two.....	209
4.68	Sample Step Response of Time-varying System, Second Design, Procedure Two.....	210
4.69	Sample Step Response of Time-varying System, Second Design, Procedure Two.....	211
4.70	Sample Step Response of Time-varying System, Second Design, Procedure Two.....	212
4.71	Sample Step Response of Time-varying System, Second Design, Procedure Two.....	213
4.72	Comparison of Maximum $ E $ for First and Second Designs.....	215
4.73	Boundaries of Acceptable $-L_0$ with Polar Plot of $-L_0$ for the Third Design.....	216
4.74	Maximum $ E $ for Third Design.....	219
4.75	Region of $P_o/P_{eq}$ for $\omega = 0.628$ , Third Design.....	220
4.76	Region of $P_o/P_{eq}$ for $\omega = 1.25$ , Third Design.....	221
4.77	Region of $P_o/P_{eq}$ for $\omega = 1.88$ , Third Design.....	222
4.78	Region of $P_o/P_{eq}$ for $\omega = 4.39$ , Third Design.....	223
4.79	Region of $P_o/P_{eq}$ for $\omega = 6.28$ , Third Design.....	224
4.80	Region of $P_o/P_{eq}$ for $\omega = 9.42$ , Third Design.....	225
4.81	Time-variation Causing Maximum $ E $ at $\omega = 0$ .....	226
4.82	Time-variation Causing Maximum $ E $ at $\omega = 0.628$ ...	227
4.83	Sample Step Response of Time-varying System, Third Design.....	228
4.84	Sample Step Response of Time-varying System, Third Design.....	229
4.85	Sample Step Response of Time-varying System, Third Design.....	230
4.86	Sample Step Response of Time-varying System, Third Design.....	231
4.87	Sample Step Response of Time-varying System, Third Design.....	232



## FIGURE

## PAGE

4.88	Sample Step Response of Time-varying System, Third Design.....	233
4.89	Polar Plot of $-L_O$ for Fourth Design with Boundaries of Acceptable Regions of $-L_O$ .....	238
4.90	Bode Plot of $ L_O $ for Fourth Design, $ L_O $ for Third Design and $ P_O $ .....	240
4.91	Maximum $ E $ for Fourth Design.....	241
4.92	Step Response Sample of Fourth Design.....	243
4.93	Bode Plot of $ L_O $ for Mod 1, $ L_O $ for Fourth Design and $ P_O $ .....	245
4.94	Maximum $ E $ for Fourth Design, Mod 1.....	246
4.95	Step Response Sample of Fourth Design, Mod 1.....	248
4.96	Boundaries of Acceptable Regions of $-L_O$ with Polar Plot of $-L_O$ for Fourth Design, Mod 2.....	249
4.97	Bode Plot of $L_O$ for Fourth Design and Mod 2, Fourth Design.....	250
4.98	Maximum $ E $ for Fourth Design, Mod 2.....	252
4.99	Step Response of Fourth Design, Mod 2.....	253
4.100	Polar Plot of $-L_O$ for Fifth Design with Boundaries of Acceptable Regions of $-L_O$ for Fourth Design....	255
4.101	Bode Plot of $ L_O $ for Fifth Design and Fourth Design Mod 1, Fourth Design Mod 2 and $ P_O $ .....	256
4.102	Maximum $ E $ for Fifth Design.....	258
4.103	Sample Step Response of Fifth Design.....	260
4.104	Sample Step Response of Fifth Design.....	261
4.105	Sample Step Response of Fifth Design.....	262
4.106	Sample Step Response of Fifth Design.....	263
4.107	Sample Step Response of Fifth Design.....	264
4.108	Sample Step Response of Fifth Design.....	265
4.109	Region of $P_O/P_{eq}$ , Fifth Design, $\omega = 0.628$ .....	266
4.110	Region of $P_O/P_{eq}$ , Fifth Design, $\omega = 1.25$ .....	267
4.111	Region of $P_O/P_{eq}$ , Fifth Design, $\omega = 1.88$ .....	268
4.112	Region of $P_O/P_{eq}$ , Fifth Design, $\omega = 4.39$ .....	269
4.113	Region of $P_O/P_{eq}$ , Fifth Design, $\omega = 6.28$ .....	270
4.114	Region of $P_O/P_{eq}$ , Fifth Design, $\omega = 9.42$ .....	271
4.115	Bode Plot of $ L_O $ for Time-varying and Time- invariant Designs.....	274
A.1	Block Diagram of System Under Study.....	287

## LIST OF TABLES

TABLE		PAGE
3-1	System Specifications.....	83
4-1	Values of the Right Side of Inequality (4-7).....	136
4-2	Summary of Specifications.....	185

## CHAPTER I

### INTRODUCTION

#### 1.1 Description of the System

A block diagram of the system with which this work is concerned is shown in Figure 1.1.

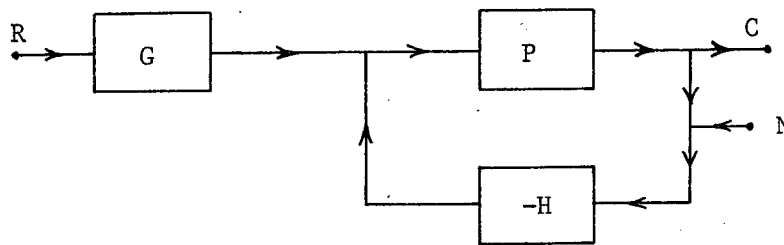


Figure 1.1  
Block Diagram of the Feedback  
System Under Study

The block P represents the plant which can be described by a linear differential equation with time-varying coefficients and blocks G and H represent compensations. There is also associated with the plant a form of ignorance in that it is assumed the time-varying coefficients have known bounds on their variations but the exact functional relationships of the variations are unknown. All components are considered to be single input-single output. The compensations are to be designed so that the desired system response is obtained while the effects of the plant time variations on the system output are reduced to an acceptable level. This is to be done with a minimum amount of noise transmitted to the plant input due to N.

## 1.2 Historical Background

Prior to 1950 there appeared to be little interest in time-varying control systems, and consequently little research had been done on such systems.<sup>1</sup> However, since 1950 more interest has been shown in time-varying control systems primarily due to the advent of such modern technology as rocket flight, space exploration, and control of high performance aircraft. The behavior of the plants of these systems can often be approximately described by linear differential equations with time-varying coefficients; thus, techniques have been sought which will aid the control engineer in designing a suitable system around a linear time-varying plant.<sup>2</sup>

The major portion of the work to date on linear time-varying control systems has been done either directly in the time domain, or some type of transform has been defined with the subsequent investigation of this transform.

### Time Domain Approach:

The time domain approach is the study of the system behavior as functions of time. It is well-known that the output of a linear system  $y(t)$  is related to the input of the system  $x(t)$  by the superposition integral

$$y(t) = \int_{-\infty}^t \phi(t, \tau) x(\tau) d\tau \quad (1-1)$$

where  $\phi(t, \tau)$  is the output of the system due to a unit impulse applied at  $t = \tau$  and is defined as the system impulse response.<sup>3</sup> For the time invariant case  $\phi(t, \tau)$  is a function of  $t - \tau$ .

Friedland<sup>4</sup> has formulated a representation of the impulse response  $\phi(t, \tau)$  as a lower diagonal matrix where the  $i, j$ th element in the matrix is the value of  $\phi(t, \tau)$  at time  $t = t_i$  due to an impulse applied at time  $\tau = t_j$ . This type of representation lends itself readily to the analysis of sampled data systems since at the sampling instances the integration is replaced by matrix multiplication. Cruz<sup>5</sup> has worked on the synthesis of time-varying control systems using the Friedland representation. The compensations which he obtains are in the form of impulse responses. These compensations are inevitably time-varying themselves, which leads to the study of the synthesis of prescribed impulse responses of time-varying systems.<sup>6,7</sup>

An algebra has been presented independently by Darlington,<sup>8</sup> A. V. Solodav,<sup>9</sup> and Stubberud<sup>10</sup> which allows block diagram manipulations of a system represented by differential equations. This would allow the blocks of the system shown in Figure 1.1 to be combined into a single block represented by a linear time-varying differential equation and could then be more easily analyzed. Stubberud also recognized that if the system specifications were given in the form of a desired differential equation of the overall system, then the method could be used as a synthesis procedure. He has thus presented two synthesis techniques for synthesizing a desired system differential equation from the time-varying differential equation describing the plant. As in the techniques employed by Cruz, the compensations which are obtained by Stubberud are inevitably time-varying.

### Transform Approach:

Largely due to the success with which the Laplace and Fourier transforms can be applied to differential equations with time invariant coefficients, a number of investigators have sought transform techniques which can be applied with equal success to linear differential equations with time-varying coefficients. The desired goal in these investigations is to arrive at a technique which will yield general solutions to linear time-varying differential equations merely by solving an algebraic equation in the transform domain in much the same manner as a differential equation with constant coefficients can be solved by using the Laplace transform. Unfortunately, up to the present time no transform technique has been found that can be applied to a linear time-varying system in a practical manner.

Transforms have been found for special types of time-varying differential equations. These special integral transforms include the Laplace transform, the Mellin transform, and the Hankel transform.<sup>11,12</sup> The Laplace transform is used in the solution of linear differential equations with constant coefficients, while the Mellin transform is used to solve the equidimensional (Euler-Cauchy) differential equation which is of the form

$$t^n \frac{d^n}{dt^n} y(t) + a_{n-1} t^{n-1} \frac{d^{n-1}}{dt^{n-1}} y(t) + \dots + a_0 y(t) = f(t),$$

and the Hankel transform can profitably be applied to Bessel's equation which is of the form

$$t^2 \frac{d^2 y(t)}{dt^2} + t \frac{dy(t)}{dt} + (\sigma t^2 - n^2) = f(t).$$

Unfortunately, neither the equidimensional equation nor Bessel's equation possesses sufficient generality to be applied to the time-varying system synthesis problem.

Aseltine<sup>13</sup> has proposed a method of deriving a compatible transform for a linear time-varying differential equation; however, practically, the transform can only be obtained for a second order time-varying system. Further, a block diagram algebra cannot be developed since a transform which is compatible with one part of a system will not generally be compatible with another part of the system.

Naylor<sup>14,15</sup> has taken an interesting approach in attempting to obtain a system transformation. Working with the Friedland characterization, he has defined the system transformation as a matrix which, when properly applied to the Friedland characterization of a system, results in a system matrix which is diagonal and is thus easily manipulated. However, the transform domain of the Naylor Transformation does not have a simple interpretation, so that synthesis in this transform domain appears to be as difficult as working directly in the time domain.

L. A Zadeh<sup>16,17,18,19</sup> has defined a system transformation that is similar to the transfer function of a time-invariant system. The transformation proposed by Zadeh which is referred to as the system function is defined as

$$\Phi(t, j\omega) = \int_{-\infty}^t \phi(t, \tau) e^{-j\omega(t-\tau)} d\tau$$

where  $\phi(t, \tau)$  is the impulse response of the system. Cruz<sup>20</sup> has made a study of the system function and has proposed a technique for synthesizing a desired system function provided, of course, that such a desired system function is known. This work does not consider the feedback problem. Kaplin<sup>21</sup> has considered the system function from a more analytical viewpoint and has presented theorems which give some of its mathematical properties. Other researchers<sup>22,23,24,25</sup>, have also considered the Zadeh transformation, but no significant progress has been made past the purely mathematic description and the study of its general characteristics.

### 1.3 General Considerations

In this section three of the more important aspects which will affect the design of the system described in Section 1.1 will be considered.

#### Plant Ignorance:

Although the plant can be described by a linear differential equation with time-varying coefficients, it is assumed that these variations are not known explicitly as functions of time. That is, the plant has associated with it some type of ignorance. Such an assumption is necessary in the formulation of the feedback problem; otherwise, it would be possible in theory, at least, to design a prefilter which would effectively cancel the parameter



variations of the plant and feedback would not be mandatory<sup>26</sup>.

It will, therefore, be assumed that ranges for the values and the rates of variations of the time-varying coefficients are known but that the time of occurrence of the variation is unknown and the exact rate and values of the variations are unknown. Figure 1.2 gives an illustration of what is assumed to be known and unknown about the coefficients. Referring to Figure 1.2, the range of  $a_n(t)$  is assumed to be  $A \leq a_n(t) \leq B$ , and the range of  $K$  is assumed to be  $K_1 \leq K \leq K_2$ ; however, the actual values of  $A'$ ,  $B'$ , and  $K$  as well as  $\tau$  are assumed to be unknown.

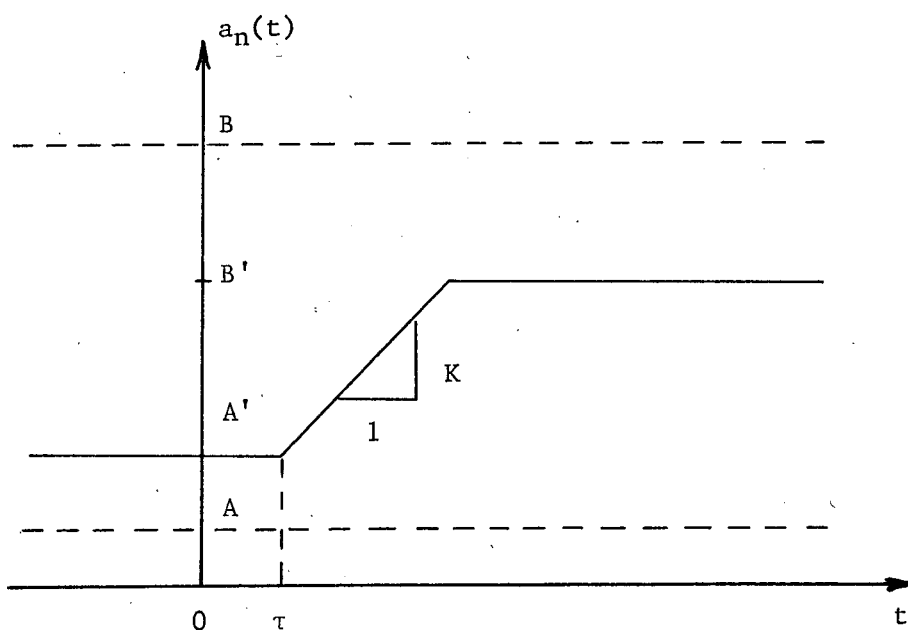


Figure 1.2  
Illustration of the Ignorance Assumed to  
Be Associated with Each Coefficient

Due to the assumption that the plant is not completely known, it is evident that the synthesis procedures of Stubberud<sup>10</sup> and Cruz,<sup>7</sup> which arrive at time-varying compensations as mentioned in

Section 1.1, cannot be used since these procedures rely on knowing the equation coefficients explicitly as functions of time. Nevertheless, one may still consider whether or not time-varying compensation might be superior to time-invariant compensation. Under the ignorance assumptions just outlined, time-varying compensation has no particular advantage over time-invariant compensation. The argument leading to this conclusion is as follows. The compensation cannot be used to cancel out the plant parameter variations since they are not known exactly; therefore, if time-varying compensation has an advantage over time-invariant compensation, it must be due to the time-varying compensator's superior signal processing properties or filtering properties. However, to take advantage of the time-varying compensator's signal processing properties, the time-varying characteristics of the signal to be processed must be known. But, these are not known in general due to the assumption of plant ignorance which thus leads to the conclusion that there is no particular advantage in using time-varying compensation. A second consideration from a more practical point of view is the fact that a time-varying compensator is much more difficult and expensive to fabricate and would in all probability be physically larger than a time-invariant compensator. Thus, even when the plant is known exactly, it may be more advantageous to use time-invariant compensation. For these reasons only time-invariant

compensations will be considered in the synthesis of the system of Figure 1.1

Specifications:

Several performance criteria have been established for linear time-invariant systems which include step response criteria, steady state error criteria, stability criteria and frequency response criteria.<sup>27</sup> Because of the linearity of the system, a modified form of the majority of these criteria can still be used in the linear time-varying system. Unfortunately, the stability criteria of a linear time-invariant system cannot be applied to a linear time-varying system.

The design criteria which will be used in this work is the step response of the system. To justify the use of the step response to judge system performance of linear time-varying systems, one can argue that any input signal can be approximated by a sum of step functions; and, due to the linearity of the system, the system output will be the sum of the step responses due to each individual step function in the input. Thus, a reasonably well-behaved step response will imply a reasonably well-behaved response to any input. A second justification can be made by examining the reason for using the step response as a performance criteria in a linear time-invariant system. In a linear time-invariant system the impulse response  $\phi(t - \tau)$  and the step response  $c(t)$  are related by

$$\phi(t - \tau) = \frac{d}{d\xi} c(\xi) \Big|_{\xi = t - \tau}$$

and knowing  $\phi(t - \tau)$  the system response to any input can be determined. Thus, the performance of a linear time-invariant system can be determined from its step response. If one could obtain the impulse response of a time-varying system from its step responses, then it would be possible to associate system behavior with these step responses in the same way as is done in the time-invariant system. Note that in time-varying systems one would actually consider a number of different step responses, each step response corresponding to a particular time of interest.

It will now be shown that the impulse response for a linear time-varying system can be constructed from a set of step responses of the system. Suppose the values of all system step responses starting in the interval from  $t = 0$  to  $t = t_1$  are known at  $t = t_1$ . Figure 1.3 shows one such step response  $c_\gamma(t)$  which is due to a step input applied at  $t = \gamma$ . The value of a step response evaluated at  $t = t_1$  due to a step input applied at  $t = \gamma$  is given by

$$c_\gamma(t_1) = \int_{\gamma}^{t_1} \phi(t_1, \tau) d\tau. \quad (1-2)$$

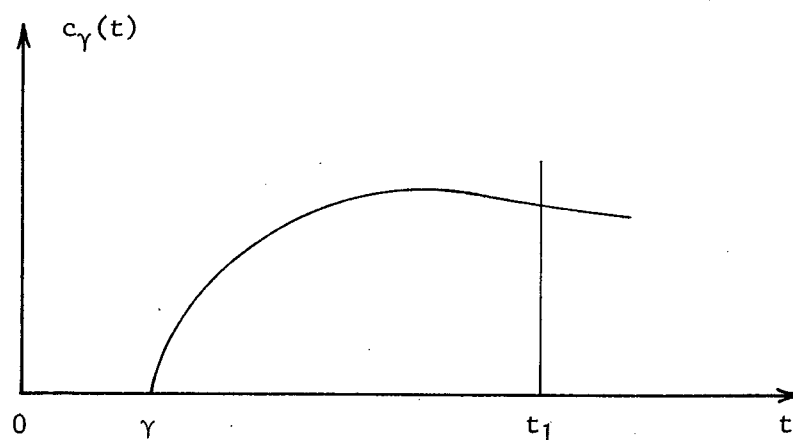


Figure 1.3.

Step Response Due to a  
Step Input Applied at  $t = \gamma$

By considering  $t_1$  fixed and varying  $\gamma$ ,  $c_\gamma(t_1)$  becomes a function of  $\gamma$ . Let

$$\lambda(\gamma) = -c_\gamma(t_1)$$

so that Equation (1-2) can be written

$$\lambda(\gamma) = \int_{t_1}^{\gamma} \phi(t_1, \tau) d\tau.$$

Differentiating  $\lambda(\gamma)$  with respect to  $\gamma$  one obtains the desired result

$$\frac{d\lambda(\gamma)}{d\gamma} = \phi(t_1, \gamma).$$

Thus, with a time-varying system it is possible to associate system behavior with its step responses.

The design specifications will be assumed to be given in the form of an acceptable step response. In principle step response specifications can be given either in the time domain or the frequency domain. Generally, step response specifications are given in the time domain since one is normally aware of the desired time domain response. The difficulty with frequency domain specifications lies in the fact that it is not known precisely what constitutes acceptable specifications. The basic problem of translating time domain specifications into frequency domain specifications and vice versa has yet to be solved<sup>28</sup>, although investigations of single responses have been made by researchers in the field.<sup>29,30</sup> Nevertheless, frequency domain specifications are desirable since by using such specifications general design procedures can be developed which are not dependent upon the order of the differential equation describing the system, and thus such procedures are not limited to simple systems. Further, the "cost of feedback" is clearly evident in the frequency domain.<sup>28</sup>

This study will not attempt to solve the problem of translating time domain specifications into frequency domain specifications; rather, the necessary frequency domain specifications will be assumed known. These specifications will be of the form of a limit on the magnitude of the Fourier transform of the difference in the actual system step response  $c(t)$  and a desired system step response  $c_0(t)$ . Some justification for such

specifications can be seen from the Fourier transform of this difference

$$E(j\omega) = \int_{-\infty}^{\infty} e(t)e^{-j\omega t} dt$$

where

$$e(t) = c(t) - c_o(t).$$

If  $E(j\omega)$  is "small" over the entire frequency range then  $e(t)$  will also be "small". The exact relation between the magnitude of the argument of  $E(j\omega)$  and the magnitude of  $e(t)$  has yet to be determined.

#### Stability Considerations:

Although a number of researchers have investigated the stability of linear time-varying systems, necessary and sufficient conditions have yet to be found which will insure the stability of the system of Figure 1.1.<sup>31</sup> A number of definitions and concepts of stability exists; however, in this work a system will be considered stable when it is bounded-input bounded-output stable. That is, if the system input is bounded, then the system output will also be bounded for a stable system.

Research in the stability of a time-varying system has taken basically two approaches. The first is to examine the system's differential equation or impulse response in the time domain;<sup>32,33</sup> however, no practical results have been obtained which lend themselves directly to the application to the system of Figure 1.1.

The second approach has been to obtain a frequency domain stability criterion similar to the Nyquist stability criterion of time-invariant systems.<sup>34,35</sup> Results have been limited to systems in which the only time-varying element is the plant gain. Such a system is illustrated in Figure 1.4.

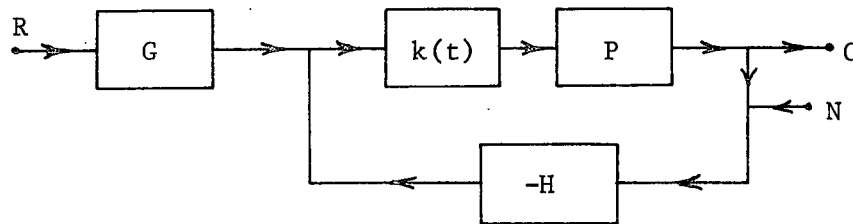


Figure 1.4  
System with Time-varying Gain

However, even for this case only sufficient conditions for stability have been determined rather than the necessary and sufficient conditions which would be required for a completely satisfactory stability criterion.

This thesis will not attempt to develop a stability criterion for linear time-varying systems; rather, synthesis procedures will be developed under the assumption of a stable system. It will be seen that the procedures can easily be modified to include any applicable stability criterion that specifies constraints on the transfer function of the feedback compensation  $H$ . The sufficient conditions for stability which have been developed for the system



of Figure 1.4 represent such a criterion and the synthesis procedures will be modified appropriately to include this criterion in the design of systems of the type shown in Figure 1.4.

## CHAPTER II

### DEVELOPMENT OF INPUT-OUTPUT RELATION AND SYSTEMS EQUATIONS

#### 2.1 General

A number of representations exist which relate the output of a linear system to its input. The differential equation itself can be considered as one such representation. Unfortunately, the differential equation is not directly useful as a design tool because it does not allow for the system characteristics to be readily observed in order that a suitable design can be developed. It is thus desired that an input-output relation be found which is suitable for the development of a design procedure.

An investigation of input-output relations was made in an effort to find one which is well suited for design purposes. The investigation centered on four functions in particular. The four functions which were considered are:

- (1) The impulse response  $\phi(t, \tau)$  which is defined as the output of the system at time  $t$  due to a unit impulse applied at time  $\tau$ .<sup>21</sup>
- (2) The system function which was introduced by Zadeh<sup>16</sup> and is defined as

$$\Phi(t, j\omega) = \int_{-\infty}^t \phi(t, \tau) e^{-j\omega(t-\tau)} d\tau$$

- (3) The complementary function which is defined by

$$\Phi(j\omega, \tau) = \int_{\tau}^{\infty} \phi(t, \tau) e^{-j\omega(t-\tau)} dt$$

- (4) The frequency impulse response which is defined by

$$\Phi(j\omega, j\gamma) = \int_{-\infty}^{\infty} \int_{-\infty}^t \phi(t, \tau) \frac{e^{j\delta\tau}}{2\pi} e^{-j\omega t} d\tau dt$$

is the Fourier transform of the output at frequency  $j\omega$

due to the input of an unit impulse of frequency at  $j\gamma$ .

A good deal of time was devoted to the study of these four functions and a number of interesting properties were found and investigated. However, none of the functions were found to lend themselves to the development of a practical design procedure. The difficulties encountered ranged from not being able to evaluate the functions to not being able to determine the output in terms of the input for systems having a feedback loop. An in-depth discussion of this study will not be presented because the results which were obtained generally have little bearing on the design problem.

The frequency impulse response was found to be useful because of its notational convenience when studying the Fourier transform of the various signals of the system. Because it is used later in the work, the general characteristics of the frequency impulse response will be presented and a discussion of the difficulties in employing the frequency impulse response will be given. The difficulties encountered with the frequency impulse response are representative of the type of difficulties encountered with the other three.

A clarification of notation should be made before going further. The term "frequency domain" refers to expressions as

functions of frequency such as the Fourier transform representation of signals, the transfer function of a system or the frequency impulse response of a system. The term "time domain" refers to expressions as functions of time such as the impulse response or a signal expressed as a function of time.

## 2.2 Properties of the Frequency Impulse Response

It would be possible to relate the frequency domain representation of the system output to that of the system input by first employing a time domain relation such as the impulse response and then taking the necessary Fourier transforms. However, it is more convenient to employ the frequency impulse response since it is a direct relation between the frequency domain representation of the system output to that of the input. The frequency impulse response is defined as

$$\Phi(j\omega, j\gamma) = \int_{-\infty}^{\infty} \int_{-\infty}^t \phi(t, \tau) \frac{e^{j\delta\tau}}{2\pi} e^{-j\omega t} d\tau dt \quad (2-1)$$

where  $\phi(t, \tau)$  is the system impulse response. This function was first mentioned by Zadeh who referred to it as the bi-frequency transform;<sup>19</sup> however, Zadeh gave no results of any study he may have made of this function. Kailath<sup>37</sup> uses similar forms in his study of time-varying filters. The author feels justified in referring to this function as the frequency impulse response since it possesses many characteristics in the frequency domain that the impulse response exhibits in the time domain.

Figure 2.1 is an illustration of a linear time-varying system having an impulse response denoted by  $\phi(t, \tau)$  and a frequency impulse response denoted by  $\Phi(j\omega, j\gamma)$ . The differential equation describing the system is assumed to be of the form

$$a_n(t) \frac{d^n}{dt^n} x(t) + \dots + a_0(t) x(t) = b_m(t) \frac{d^m}{dt^m} y(t) + \dots + b_0(t) y(t) \quad (2-2)$$

where  $a_n(t) \neq 0$  and  $n \geq m$ .

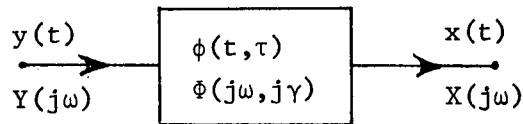


Figure 2.1  
Block Diagram of a Linear System

The primary reason for referring to  $\Phi(j\omega, j\gamma)$  as the frequency impulse response is because it is the Fourier transform of the system output evaluated at frequency  $j\omega$  due to an impulse of frequency at  $j\gamma$ . This, of course, is the frequency domain equivalent of the impulse response. The property can be easily demonstrated as follows. Let the system input be given by  $y(t) = \frac{e^{j\gamma t}}{2\pi}$  which is a unit impulse at frequency  $j\gamma$  in the frequency domain.<sup>49</sup> The system output is given by<sup>38</sup>

$$x(t) = \int_{-\infty}^t \phi(t, \tau) \frac{e^{j\gamma\tau}}{2\pi} d\tau.$$

Taking the Fourier transform of  $x(t)$ , one obtains

$$X(j\omega) = \int_{-\infty}^{\infty} \int_{-\infty}^t \phi(t, \tau) \frac{e^{j\gamma\tau}}{2\pi} d\tau e^{-j\omega t} dt$$

which is the definition of the frequency impulse response given in Equation (2-1).

If the system is time-invariant, the frequency impulse response is given by

$$\Phi(j\omega, j\gamma) = \Phi(j\omega) \delta(j\gamma - j\omega) \quad (2-3)$$

where  $\Phi(j\omega)$  is the transfer function of the system. This result is obtained as follows. Since the system is time-invariant, the system impulse response is given by  $\phi(t, \tau) = \phi(t - \tau)$ . Letting  $\tau = t - u$  the frequency impulse response can be written as

$$\Phi(j\omega, j\gamma) = \frac{1}{2\pi} \int_{-\infty}^{\infty} \left[ \int_{-\infty}^{\infty} \phi(u) e^{-j\gamma u} du \right] e^{-(j\omega - j\gamma)t} dt.$$

The integral inside the brackets is the system transfer function so that one can write

$$\Phi(j\omega, j\gamma) = \frac{1}{2\pi} \int_{-\infty}^{\infty} \Phi(j\gamma) e^{-(j\omega - j\gamma)t} dt$$

or upon performing the integration<sup>49</sup> one obtains

$$\Phi(j\omega, j\gamma) = \Phi(j\gamma) \delta(j\omega - j\gamma).$$

Another important property of the frequency impulse response is that the Fourier transform of the system output  $X(j\omega)$  is given by the relation

$$X(j\omega) = \int_{-\infty}^{\infty} \Phi(j\omega, j\gamma) Y(j\gamma) d\gamma. \quad (2-4)$$

This expression is obtained by taking the Fourier transform of the output as

$$X(j\omega) = \int_{-\infty}^{\infty} x(t) e^{-j\omega t} dt. \quad (2-5)$$

Expressing  $x(t)$  by

$$x(t) = \int_{-\infty}^t \phi(t, \tau) y(\tau) d\tau$$

and expressing  $y(\tau)$  as the inverse Fourier transform of  $Y(j\omega)$ , Equation (2-5) can be written

$$X(j\omega) = \int_{-\infty}^{\infty} \int_{-\infty}^t \phi(t, \tau) \left[ \frac{1}{2\pi} \int_{-\infty}^{\infty} Y(j\gamma) e^{-j\gamma\tau} d\gamma \right] d\tau e^{-j\omega t} dt.$$

Interchanging the order of integration, the relation becomes

$$X(j\omega) = \int_{-\infty}^{\infty} \left[ \frac{1}{2\pi} \int_{-\infty}^{\infty} \int_{-\infty}^t \phi(t, \tau) e^{j\gamma\tau} e^{-j\omega t} d\tau dt \right] Y(j\gamma) d\gamma.$$

Recognizing the term inside the brackets as the definition of the frequency impulse response establishes Equation (2-4). The frequency impulse response can be thought of as an operator which operates through the relation expressed in Equation (2-4). Thus,

Equation (2-4) can be referred to as  $\Phi(j\omega, j\gamma)$  operating on  $Y(j\gamma)$  with the result of the operation being  $X(j\omega)$ .

Special consideration should be given to Equation (2-4) because this relation demonstrates a basic difference in time-varying systems and time-invariant systems. Suppose the system were time-invariant with transfer function  $\Phi(j\omega)$ . Equation (2-4) becomes the well-known relation

$$X(j\omega) = \Phi(j\omega) Y(j\omega).$$

Observe that in the time-invariant system the value of the output at frequency  $\omega$  is due only to the value of the input at  $\omega$  which is weighted by the value of the transfer function at frequency  $\omega$ . Thus, to determine the value of the output at a given frequency, one only needs to determine the value of the input and the transfer function at that frequency. For the time-varying system on the other hand, Equation (2-4) shows that the system output at  $\omega$  is not only influenced by the system input at  $\omega$  but also by all other frequencies in the system input. The amount of influence each frequency has on the system output is determined by the weighting of the frequency impulse response at each frequency. Therefore, to evaluate the output of a time-varying system, one must determine the values of the system input at all frequencies and the corresponding values of the frequency impulse response instead of just the two values required in the time-invariant system. The basic difficulty in time-varying systems is



that a much larger number of frequencies must be considered than in the time-invariant case.

If two systems are considered in parallel as shown in Figure 2.2, the frequency impulse response for the parallel combination is the sum of the frequency impulse responses of the two systems. This is easily obtained from the fact that the impulse response of two parallel systems is the sum of the impulse responses of the two parallel systems.

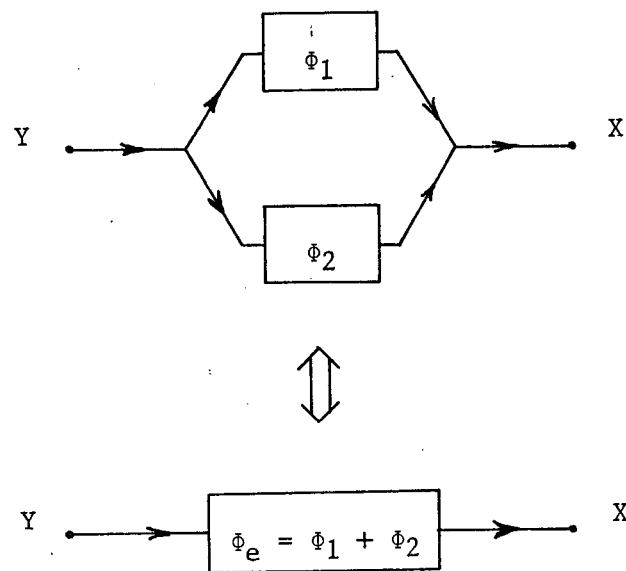


Figure 2.2  
Combining Systems in Parallel

Thus, the equivalent impulse response of the parallel system shown in Figure 2.2 is given by

$$\phi_e(t, \tau) = \phi_1(t, \tau) + \phi_2(t, \tau)$$

Applying the definition of the frequency impulse response, Equation (2-1), to this relation yields the same property for the frequency impulse response.

Cascade systems, unfortunately, do not combine as easily as do parallel systems. The equivalent impulse response of two systems in cascade as shown in Figure 2.3 is given by

$$\Phi_e(j\omega, j\gamma) = \int_{-\infty}^{\infty} \Phi_2(j\omega, j\xi) \Phi_1(j\xi, j\gamma) d\xi \quad (2-6)$$

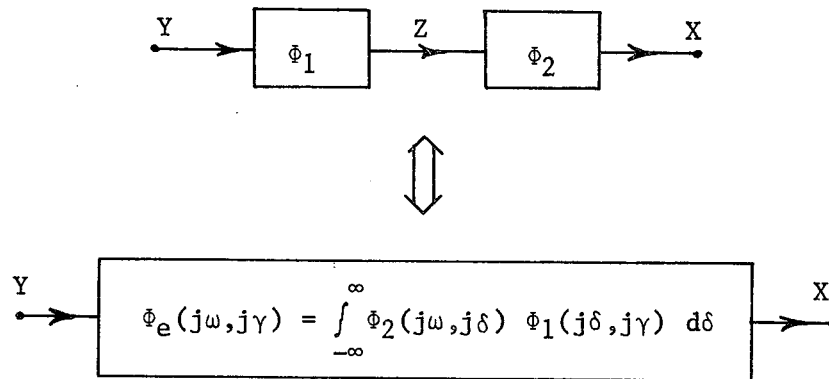


Figure 2.3  
Combining Systems in Cascade

This relation can be obtained by letting  $Y(j\lambda) = \delta(j\lambda - j\gamma)$ . Since the input is a unit impulse in the frequency domain, the Fourier transform of the system output is the frequency impulse response of the system. From Equation (2-4) the Fourier transform of the

system output is obtained from the intermediate signal  $Z(j\omega)$  by the relation

$$X(j\omega) = \Phi_e(j\omega, j\gamma) = \int_{-\infty}^{\infty} \Phi_2(j\omega, j\xi) Z(j\xi) d\xi \quad (2-7)$$

and  $Z(j\xi)$  is given by

$$Z(j\xi) = \int_{-\infty}^{\infty} \Phi_1(j\xi, j\lambda) Y(j\lambda) d\lambda.$$

Substituting  $Y(j\lambda) = \delta(j\lambda - j\gamma)$  and performing the integration, one obtains

$$Z(j\xi) = \Phi_1(j\xi, j\gamma).$$

Substituting the above relation into Equation (2-7) gives the desired expression, Equation (2-6). Again, thinking of the frequency impulse response as an operator, the cascading of two operators results in a new operator  $\Phi_e$  which is obtained by letting the second operator  $\Phi_2$  operate on the first operator  $\Phi_1$ . Note that  $\Phi_2$  operating on  $\Phi_1$  is not the same in general as  $\Phi_1$  operating on  $\Phi_2$ .

Cascading a time-invariant system with a time-varying system is quite simple. First assume that  $\Phi_2$  in Figure 2.3 is time-invariant. From Equation (2-3) the frequency impulse response of  $\Phi_2$  is

$$\Phi_2(j\omega, j\gamma) = \Phi_2(j\omega) \delta(j\gamma - j\omega).$$

Substituting this expression for  $\phi_2$  into Equation (2-6), the equivalent frequency impulse response is found to be

$$\phi_e(j\omega, j\gamma) = \phi_2(j\omega) \phi_1(j\omega, j\gamma).$$

Likewise, if  $\phi_1$  is time-invariant,  $\phi_e$  is given by

$$\phi_e(j\omega, j\gamma) = \phi_2(j\omega, j\gamma) \phi_1(j\gamma).$$

Thus the time-invariant portions of a time-varying system are easily handled by ordinary multiplication rather than the more difficult integration process.

The concept of the inverse system<sup>9</sup> is also important in using the frequency impulse response. Figure 2.4 shows an illustration of a system represented by  $\phi$  and its inverse represented by  $\phi^{-1}$ .

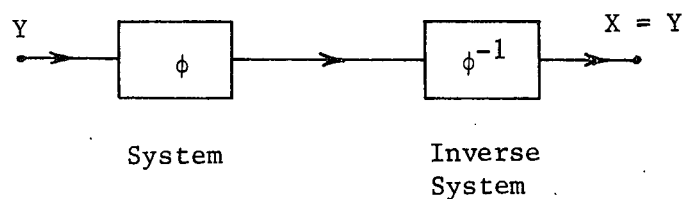


Figure 2.4  
Illustration of System and Inverse

The cascading of a system with its inverse results in a system in which the output is equal to the input. Such a system will be referred to as the unit system. The frequency impulse response

of the unit system is found from the definition to be

$$\Phi(j\omega, j\gamma) = \delta(j\omega - j\gamma).$$

Thus, if either the inverse operates on the system or if the system operates on the inverse, the resulting frequency impulse response is  $\delta(j\omega - j\gamma)$ .

### 2.3 Discussion of the Frequency Impulse Response

In the early stages of the investigation it was hoped that the frequency impulse response could be represented explicitly as a function of frequency and could thus then be utilized in much the same manner as is the transfer function for time-invariant systems. This hope was not realized for all efforts to obtain an explicit functional representation were, in general, unsuccessful. However, in some instances it is possible to represent the frequency impulse response by an explicit function of frequency.

Any attempt to obtain the frequency impulse response from a direct application on the definition is impossible except for systems which can be described by first order differential equations or by simple time-varying gains. This is due to the fact that the impulse response of higher order time-varying systems cannot be found in general. Also, for systems which can be described by first order differential equations a closed functional form cannot be obtained even with the time-varying function specially chosen to aid the calculation.

The simplest time-varying system consists of a time-varying gain  $f(t)$ . The frequency impulse response for this system is obtained from a direct application of the definition, Equation (2-1), and is found to be

$$\Phi(j\omega, j\gamma) = \frac{F(j\omega - j\gamma)}{2\pi}$$

where  $F(j\lambda)$  is the Fourier transform of  $f(t)$ .

The next type of system to consider is one which can be described by a first order differential equation of the form

$$\dot{x}(t) + f(t)x(t) = y(t) \quad (2-8)$$

where  $y(t)$  is the system input and  $x(t)$  is the output. The impulse response for this system is given by

$$\phi(t, \tau) = \exp \left[ - \int_{\tau}^t f(t) dt \right].$$

The frequency impulse response is found by applying Equation (2-1); however, it is evident that unless  $f(t)$  is selected very carefully the integrals cannot be evaluated and an explicit functional representation of the frequency impulse response is not possible.

As an example, consider a system which is described by the first order differential equation given in Equation (2-8) where

$$f(t) = \frac{2e^{2t} + e^t}{e^{2t} + e^t}.$$

The graph of  $f(t)$  is shown in Figure 2.5.

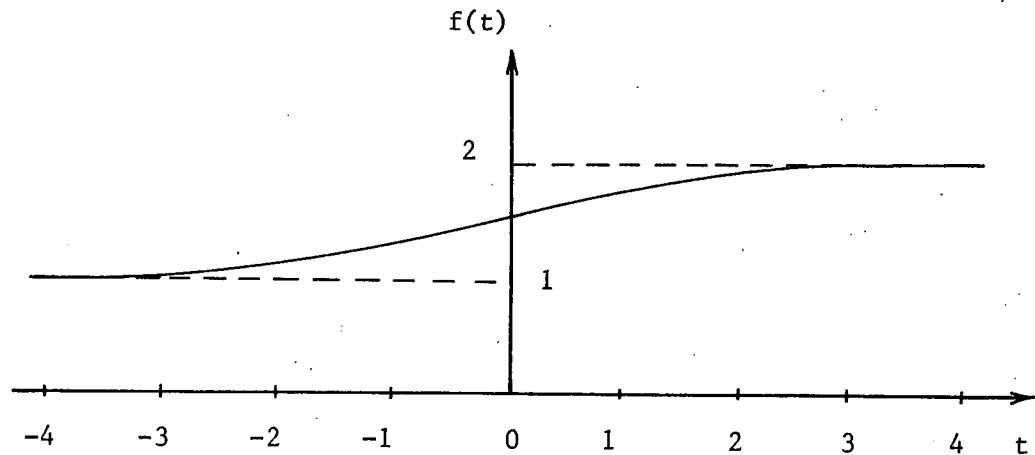


Figure 2.5  
Graph of  $f(t)$  Used in Example

It is easily verified that the system impulse response is given by

$$\phi(t, \tau) = \frac{e^{2\tau} + e^{\tau}}{e^{2t} + e^t} u(t - \tau).$$

A straightforward application of Equation (2-1) yields for the frequency impulse response

$$\Phi(j\omega, j\gamma) = \frac{\delta(j\omega - j\gamma)}{j\gamma + 2} + \frac{1}{(j\gamma + 1)(j\omega + 2)} \int_{-\infty}^{\infty} \frac{e^t}{e^{2t} + e^t} e^{-(j\omega - j\gamma)t} dt.$$

Note that even though the function  $f(t)$  was especially chosen, a closed functional form of the frequency impulse response is still not possible.

If the function is described by a differential equation of order higher than one as given in Equation (2-2), the impulse response cannot be determined in general and thus an expression for the frequency impulse response cannot be found.

It is possible, however, to determine the inverse frequency impulse response of a differential equation of the form

$$a_n(t) \frac{d^n}{dt^n} x(t) + \dots + a_0(t)x(t) = y(t) \quad (2-9)$$

where  $y(t)$  is the system input and  $x(t)$  is the system output.

The inverse system is also described by Equation (2-9); however, in the inverse system  $x(t)$  is the input and  $y(t)$  is the output.

The frequency impulse response of the inverse system can be found by employing the property that it is the Fourier transform of the system output evaluated at  $j\omega$  due to an impulse of frequency at  $j\gamma$  applied to the input. An impulse of frequency is applied to the input by setting

$$x(t) = \frac{e^{j\gamma t}}{2\pi}.$$

The output is easily found to be

$$y(t) = \left[ a_n(t)(j\gamma)^n + \dots + a_0(t) \right] \frac{e^{j\gamma t}}{2\pi}. \quad (2-10)$$

Taking the Fourier transform of  $y(t)$  results in

$$\begin{aligned} \Phi^{-1}(j\omega, j\gamma) &= \mathcal{F} [y(t)] = \int_{-\infty}^{\infty} y(t) e^{-j\omega t} dt \\ &= \frac{1}{2\pi} \left[ A_n(j\omega - j\gamma) (j\gamma)^n + \dots + A_0(j\omega - j\gamma) \right] \end{aligned} \quad (2-11)$$

where  $A_i(j\lambda)$  is the Fourier transform of  $a_i(t)$ . Presumably the



frequency impulse response can now be obtained by finding the function  $\Phi(j\omega, j\gamma)$  which satisfies the equation

$$\delta(j\omega - j\gamma) = \int_{-\infty}^{\infty} \Phi(j\omega, j\lambda) \Phi^{-1}(j\lambda, j\gamma) d\lambda.$$

Unfortunately, it was not possible to find the proper function  $\Phi(j\omega, j\lambda)$  which satisfies the above relation for a general  $\Phi^{-1}(j\lambda, j\gamma)$ .

Note that the right hand side of Equation (2-9) can contain a first order derivative of  $y(t)$  and the frequency impulse response of the inverse system can still be found since the first order differential equation can be solved. Thus, an expression for the inverse frequency impulse response of a system of the general form shown in Figure 2.6 can be obtained although the expression will generally contain integrals which cannot be evaluated in a closed functional form.

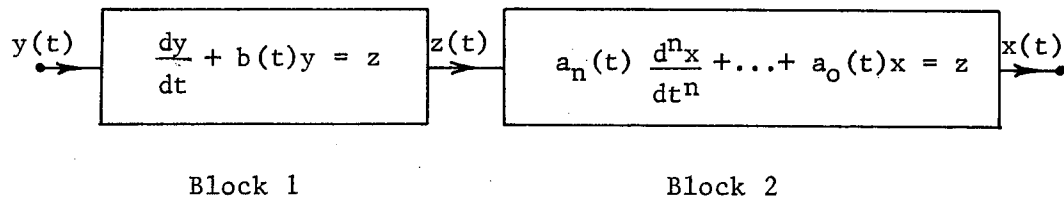


Figure 2.6  
Type of Plant for Which an Expression of the Inverse  
Frequency Impulse Response Can Be Obtained

It should be emphasized that if the differential equation in block 1 of Figure 2.6 is of order higher than one, an expression for the inverse frequency impulse response cannot be obtained.

To summarize, it is seen that an expression for the frequency impulse response cannot be obtained for all types of systems. However, an expression can be obtained for time-varying gains and for systems that can be described by first order differential equations. Also, an expression for the inverse frequency impulse response can be obtained for a system of the type shown in Figure 2.6.

#### 2.4 Development of System Equations

The system equations will now be developed utilizing the frequency impulse response. The desired objective is to develop an expression which will allow one to determine the Fourier transform of the system output from the Fourier transform of the system input. Equations will be found which give the desired relation, but, unfortunately, cannot be solved to yield the values of the system output.

For convenience the system is shown in Figure 2.7. A detailed discussion of the noise transmission from the noise source  $N$  is given in Section 4.7 and will not be considered at this point. It is assumed that the time-invariant prefilter has a transfer function  $G(j\omega)$ , and the time-invariant feedback element has a transfer function  $H(j\omega)$ , while the time-varying plant has a frequency impulse response  $P(j\omega, j\gamma)$ .

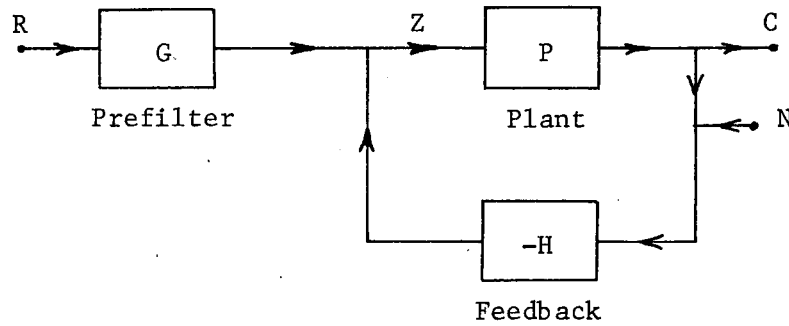


Figure 2.7  
System under Study

One form of the basic equation is developed as follows. The system output is given in terms of the plant input by the expression

$$C(j\omega) = \int_{-\infty}^{\infty} P(j\omega, j\gamma) Z(j\gamma) d\gamma \quad (2-12)$$

and the plant input is given by the expression

$$Z(j\gamma) = G(j\gamma) R(j\gamma) - H(j\gamma) C(j\gamma).$$

Substituting  $Z(j\gamma)$  into Equation (2-12) one obtains

$$C(j\omega) = \int_{-\infty}^{\infty} P(j\omega, j\gamma) G(j\gamma) R(j\gamma) d\gamma - \int_{-\infty}^{\infty} P(j\omega, j\gamma) H(j\gamma) C(j\gamma) d\gamma. \quad (2-13)$$

This is a potentially useful relation since it relates the system output to the system input. However, the equation is known as a singular integral equation and, unfortunately, no general methods of solution are known for such equations.<sup>42</sup> Obtaining a solution

is doubly difficult in this case because of the complex expression for the frequency impulse response.

Equation (2-13) can be put in an alternate form by operating on both sides with the frequency impulse response of the inverse plant  $P^{-1}(j\omega, j\gamma)$ . The resulting equation is

$$\int_{-\infty}^{\infty} P^{-1}(j\omega, j\gamma) C(j\gamma) d\gamma = G(j\omega) R(j\omega) - H(j\omega) C(j\omega) \quad (2-14)$$

Again, this equation is a singular integral equation and cannot in general be solved. However, because of the less complex expression for the inverse frequency impulse response of the class of plants which can be described by Equation (2-9), one can come closer to obtaining a solution from Equation (2-14) than from Equation (2-13). As an example, assume the plant is a time-varying gain  $f(t)$ , the inverse of which can be described by a function of the form

$$f^{-1}(t) = K + Ae^{-bt} u(t).$$

Applying the results obtained in the last section, the inverse frequency impulse response is found to be

$$P^{-1}(j\omega, j\gamma) = K \delta(j\omega - j\gamma) + \frac{1}{2\pi} \frac{A}{(b + j\omega - j\gamma)}$$

Substituting this expression into the integral term of Equation (2-14), one obtains

$$\int_{-\infty}^{\infty} P^{-1}(j\omega, j\gamma) C(j\gamma) d\gamma = \int_{-\infty}^{\infty} A \delta(j\omega - j\gamma) C(j\gamma) d\gamma$$

$$+ \frac{1}{2\pi} \int_{-\infty}^{\infty} \frac{A}{(b - j\omega - j\gamma)} C(j\gamma) d\gamma$$

The first integral on the right hand side is equal to  $C(j\omega)$ . With a proper interpretation the second integral can be evaluated by contour integration. Instead of integrating the real variable from minus infinity to plus infinity, the integral is first multiplied and divided by  $j$ , then the complex variable  $s$  is substituted for the variable  $j\gamma$  with the path of integration along the imaginary axis. Since  $C(s)$  is the Laplace transform of the system output,  $|C(s)|$  goes to zero as  $|s|$  goes to infinity, and the integral can thus be thought of as being integrated around a closed path where the path encloses the right half plane. Therefore, the integral can be written in the form

$$\frac{1}{2\pi j} \int \frac{-A}{(s - b - j\omega)} C(s) ds$$

where the path of integration encloses the right half plane. This is in the form of Cauchy's integral formula<sup>50</sup> and is evaluated as  $-AC(j\omega + b)$ .

Equation (2-14) thus can be written as

$$[A + H(j\omega)] C(j\omega) - A C(j\omega + b) = G(j\omega) R(j\omega) \quad (2-15)$$

The problem now is to determine a function  $C(j\omega)$  which satisfies Equation (2-15). Unfortunately, a method of determining the

solution of Equation (2-15) has not been found. The most promising approach has been to represent  $C(j\omega)$  as an infinite series; however, no real success has been achieved by this method. Although the above approach has not yielded an analytical solution for the time-varying system, it does come the closest of any method attempted.

An attempt to obtain an analytical expression for the system output from either Equation (2-13) or (2-14) has been unsuccessful. Thus, a different approach must be taken to develop a representation which may be used for design purposes.

## CHAPTER III

### DEVELOPMENT OF SYNTHESIS PROCEDURES

#### 3.1 Introduction

In the last chapter an attempt to obtain a solution to the time-varying system equations in the form of an explicit function of frequency proved to be unsuccessful. Design procedures based on the knowledge of such functions, therefore, cannot be developed. The approach in this chapter is to develop equations and design methods which lend themselves to numerical solutions of the system equations. This approach should be more successful since numerical solutions can be obtained from analog and digital computer simulations. The difficulty is the development of design procedures which can utilize such solutions.

A degree of success has been achieved in that two design procedures based on numerical solutions have been developed. Unfortunately, as was pointed out in Chapter I, a general stability criterion is not available for linear time-varying systems. Thus, it is not known whether the designs obtained by these procedures are stable. When the plant has only a time-varying gain, however, sufficient conditions for stability do exist so that in such cases it is usually possible to arrive at a stable design.

The two synthesis procedures will be presented in the following sections together with illustrating examples.

### 3.2 Synthesis Procedure One

This design procedure is based on a comparison of the actual system step response to a desired system step response. The approach is to design the system such that the magnitude of the difference in the Fourier transforms of the actual system step response and the desired step response falls within some specified level. For this method the specifications are assumed to be in the form

$$|E| = |C - C_0| \leq M \quad (3-1)$$

where  $C_0$  is the Fourier transform of the desired step response and  $C$  is the Fourier transform of the actual step response. (See Section 1.3.)

The primary reason for selecting such an approach is that the system equation describing  $|E|$  lends itself to the development of a practical design method. The procedure requires that a series of designs be made in which each new design comes closer to satisfying the specifications than the previous design. This iterative procedure is continued until either a satisfactory design is obtained or until the system becomes unstable.

The system design equations will now be developed. The system is shown in Figure 3.1.



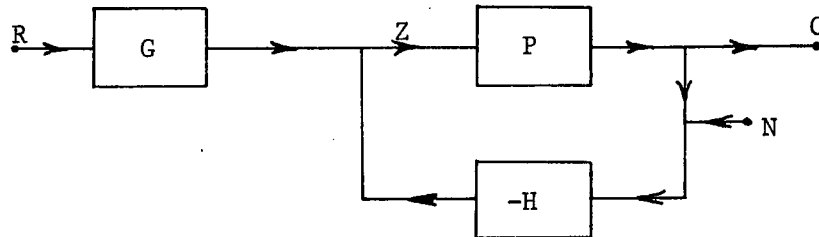


Figure 3.1  
System under Study

In order to simplify the notation, let

$$X = PY \quad (3-2)$$

be the symbolical representation between the input  $Y$  of a block and its corresponding output  $X$ . The inverse representation is denoted by

$$Y = P^{-1}X. \quad (3-3)$$

Using this notation the system equation, Equation (2-14), can be written

$$P^{-1}C = GR - HC. \quad (3-4)$$

Let the inverse time-varying plant be written in the form of the sum of a time-varying component  $\Delta P^{-1}$  and a time-invariant component  $P_0^{-1}$ . That is,

$$P^{-1} = P_0^{-1} + \Delta P^{-1}. \quad (3-5)$$

Also, the system output  $C$  can be written as

$$C = C_o + E \quad (3-6)$$

where  $C_o$  is the desired output and  $E$  is the error. Substituting these expressions for  $P^{-1}$  and  $C$  into Equation (3-4) one can obtain

$$P^{-1}E + P_o^{-1}C_o + \Delta P^{-1}C_o + HC_o + HE = GR. \quad (3-7)$$

The prefilter  $G$  is now defined such that if the plant becomes  $P_o$ , the system step response is the desired response  $C_o$ . Thus, the following equation is also satisfied

$$P_o^{-1}C_o + HC_o = GR. \quad (3-8)$$

Employing the relationship expressed in Equation (3-8), Equation (3-7) becomes

$$P_o^{-1}E + HE = -\Delta P^{-1}(C_o + E). \quad (3-9)$$

Equation (3-9) is the design equation which is employed in this design procedure. The equation is expressed in full notational form as

$$P_o^{-1}(j\omega) E(j\omega) + H(j\omega) E(j\omega) = -\int_{-\infty}^{\infty} \Delta P^{-1}(j\omega, j\gamma) [C_o(j\gamma) + E(j\gamma)] d\gamma \quad (3-10)$$

where  $P_o^{-1}(j\omega)$  is the transfer function of the time-invariant portion of the inverse plant. As was discussed in Section (2.4)

this equation is a singular integral equation and no general method of solution is known. Thus, it is not possible to solve for  $E$  as an explicit function of frequency. Nonetheless, the equation can be used to arrive at a design procedure.

Equation (3-10) is written in the form

$$E(j\omega) = \frac{-1}{P_O^{-1}(j\omega) + H(j\omega)} \int_{-\infty}^{\infty} \Delta P^{-1}(j\omega, j\gamma) \left[ C_O(j\gamma) + E(j\gamma) \right] d\gamma. \quad (3-11)$$

Applying the specifications given in Inequality (3-1), one obtains

$$|E(j\omega)| = \left| \frac{-1}{P_O^{-1}(j\omega) + H(j\omega)} \right| \left| \int_{-\infty}^{\infty} \Delta P^{-1}(j\omega, j\gamma) \left[ C_O(j\gamma) + E(j\gamma) \right] d\gamma \right| \leq M. \quad (3-12)$$

From the above relation it appears that if system stability can be maintained, it may be possible to reduce the magnitude of the error to any desired level by increasing the magnitude of  $H$ .

Note that  $H$  is the only term over which the designer has direct control. It is shown in Appendix A that except in one case the magnitude of the error can indeed be reduced to as small a value as desired by increasing the magnitude of  $H$  provided system stability can be maintained. The one exception is at  $\omega = 0$  and with the plant not having an integrator. That is, if the plant were time-invariant, the system would be classified as type 0.<sup>41</sup>

It is possible to design a system which will meet the specifications simply by increasing the magnitude of  $H$  to some

arbitrarily large value. This is not a satisfactory approach, however, because as the magnitude of  $H$  is increased, the transmission of the noise from the noise source  $N$  to the plant input is increased proportionately. Thus, it is desired to increase the magnitude of  $H$  no more than absolutely necessary in order to satisfy the specifications. The design method presented in this section will not directly yield the optimal design, but the method does provide a systematic approach to increasing the magnitude of  $H$ . In order to approach the optimal design, the designer must utilize the insight gained from the application of the design procedure. As has been mentioned, the procedure involves an iteration technique where a design is made and then tested. If the specifications are not satisfied, a subsequent design is made based on the previous design. The subsequent design will come closer to satisfying the specification than the previous design.

In order to begin the iteration procedure an initial design must first be made. Any stable design could be used as the starting design; however, such an approach could yield excessive iterations and would not lend itself to the systematic study of the system. One possible approach would be to assume that the plant were time-invariant but that the parameters could take on any constant value within their ranges of variation. The design could be made under this assumption using the methods presented by Horowitz.<sup>28</sup>

Another approach is to begin with Equation (3-13) and assume that the integral term involving the error is zero. If the time-variations were known as functions of time, the remainder of the equation could usually be solved analytically and a design made based on this analytical solution.

The second approach of obtaining a starting design will be presented with the design procedure; however, this is not to imply that the second approach is superior to the first. The second approach is given because it is not included in the literature elsewhere as is the first approach. The second approach is also used in the examples given in this section because the time-variations are assumed to be functions of time.

The design method will now be presented. For convenience, the design equation is rewritten in Equation (3-13) as

$$E(j\omega) = \lambda(j\omega) \left[ I_0(j\omega) + \int_{-\infty}^{\infty} \Delta P^{-1}(j\omega, j\gamma) E(j\gamma) d\gamma \right] \quad (3-13)$$

where

$$\lambda(j\omega) = \frac{-1}{P_0^{-1}(j\omega) + H(j\omega)} \quad (3-14)$$

and

$$I_0(j\omega) = \int_{-\infty}^{\infty} \Delta P^{-1}(j\omega, j\gamma) C_0(j\gamma) d\gamma . \quad (3-15)$$

### First Iteration:

The function to be determined is  $\lambda(j\omega)$ . For the first iteration let  $\lambda(j\omega)$  be denoted by  $\lambda_0(j\omega)$ .

#### Step 1

Assume that

$$\int_{-\infty}^{\infty} \Delta P^{-1}(j\omega, j\gamma) E(j\gamma) d\gamma = 0 \quad (3-16)$$

so that Equation (3-13) becomes

$$E(j\omega) = \lambda_0(j\omega) I_0(j\omega). \quad (3-17)$$

Applying the specifications one obtains

$$|E(j\omega)| = |\lambda_0(j\omega)| |I_0(j\omega)| \leq M(\omega) \quad (3-18)$$

which by using Equation (3-14) can be rewritten as

$$\frac{|I_0(j\omega)|}{M(\omega)} \leq |P_0^{-1}(j\omega) + H(j\omega)|. \quad (3-19)$$

#### Step 2

Since the term  $|I_0(j\omega)|$  depends upon the plant parameter variations, it will take on a range of values in the complex plane. This range is determined for several frequencies of interest. Regions are then determined in the complex plane which correspond to the values of  $I_0(j\omega)/M(\omega)$ . From these regions a region of acceptable values of  $H(j\omega)$  is determined in the complex plane for each frequency of interest.

### Step 3

Determine an  $H(j\omega)$  as a function of  $j\omega$  such that it lies within the acceptable regions found in Step 2 and such that  $|H(j\omega)|$  is as small as possible. This step is actually an exercise in curve fitting and the  $H(j\omega)$  which is selected will depend upon the desired simplicity of the compensation network as well as the experience of the designer. Let the  $H(j\omega)$  selected in this step be denoted  $H_o(j\omega)$ .

### Step 4

The prefilter  $G(j\omega)$  is determined from Equation (3-4).

Solving Equation (3-4) for  $G(j\omega)$  one obtains

$$G(j\omega) = \left[ P_o^{-1}(j\omega) + H_o(j\omega) \right] \frac{C_o(j\omega)}{R(j\omega)} \quad (3-20)$$

which completes the first design.

Since  $H_o(j\omega)$  was designed under the assumption expressed in Equation (3-16), it will in all probability not be a satisfactory design. In order to determine whether or not this first design satisfies the specifications the design is simulated on an analog or digital computer and the frequency domain representation of the error is obtained. Let the error of the first design be denoted  $E_o(j\omega)$ . Note that the simulation is merely the means of obtaining the solution to the equation

$$E_o(j\omega) = \lambda_o(j\omega) \left[ I_o(j\omega) + \int_{-\infty}^{\infty} \Delta P^{-1}(j\omega, j\gamma) E_o(j\gamma) d\gamma \right]. \quad (3-21)$$

The magnitude of  $E_o(j\omega)$  can now be compared to the specifications  $M(\omega)$ . If  $E_o(j\omega)$  does not meet the specifications over part of the frequency range, another compensation which will be denoted  $\lambda_1(j\omega)$  must be designed. In order to see the philosophy behind the design of  $\lambda_1(j\omega)$  let the error which corresponds to the  $\lambda_1(j\omega)$  design be written as

$$E_1(j\gamma) = E_o(j\gamma) + \varepsilon_1(j\gamma). \quad (3-22)$$

The equation which gives  $E_1(j\omega)$  can then be written

$$E_1(j\omega) = \lambda_1(j\omega) \quad (3-23)$$

$$\left[ I_o(j\omega) + \int_{-\infty}^{\infty} \Delta P^{-1}(j\omega, j\gamma) E_o(j\gamma) d\gamma + \int_{-\infty}^{\infty} \Delta P^{-1}(j\omega, j\gamma) \varepsilon_1(j\gamma) d\gamma \right].$$

The first integral in Equation (3-23) is obtained from Equation (3-21) as

$$\int_{-\infty}^{\infty} \Delta P^{-1}(j\omega, j\gamma) E_o(j\gamma) d\gamma = \frac{E_o(j\omega)}{\lambda_o(j\omega)} - I_o(j\gamma). \quad (3-24)$$

The value of the second integral in Equation (3-23) is unknown; thus, as with the assumption expressed in Equation (3-16) it is assumed that

$$\int_{-\infty}^{\infty} \Delta P^{-1}(j\omega, j\gamma) \varepsilon_1(j\gamma) d\gamma = 0. \quad (3-25)$$

Substituting Equations (3-24) and (3-25) into Equation (3-23) and applying the specifications one obtains



$$\frac{|\lambda_1(j\omega)|}{|\lambda_0(j\omega)|} \leq \frac{|E_0(j\omega)|}{M(\omega)}. \quad (3-26)$$

This inequality is then used to determine  $\lambda_1(j\omega)$ .

### Second Iteration:

#### Step 1

Simulate the design which was obtained in the first iteration on an analog or digital computer and obtain the maximum value of the magnitude of the frequency domain representation of the error which is denoted  $E_{om}(j\omega)$  for the frequencies of interest.

#### Step 2

Determine the maximum value of  $\lambda_1(j\omega)$  from the relation

$$|\lambda_1(j\omega)| \leq \frac{M(\omega)}{E_{om}(j\omega)} |\lambda_0(j\omega)| \quad \text{for} \quad E_{om}(j\omega) \geq M(\omega) \quad (3-27a)$$

$$|\lambda_1(j\omega)| \leq |\lambda_0(j\omega)| \quad \text{for} \quad E_{om}(j\omega) \leq M(\omega). \quad (3-27b)$$

Employing equation (3-14) this relation can be rewritten as

$$\frac{E_{om}(j\omega)}{|\lambda_0(j\omega)| M(\omega)} \leq |P_0^{-1}(j\omega) + H_1(j\omega)| \quad \text{for} \quad E_{om}(j\omega) \geq M(\omega) \quad (3-28a)$$

$$\frac{1}{|\lambda_0(j\omega)|} \leq |P_0^{-1}(j\omega) + H_1(j\omega)| \quad \text{for} \quad E_{om}(j\omega) \leq M(\omega). \quad (3-28b)$$

Step 3

Determine the region of acceptable  $H(j\omega)$  in the complex plane from Inequality (3-28) for the frequencies of interest.

Step 4

Determine an  $H_1(j\omega)$  as a function of  $j\omega$  such that it lies within the regions of acceptable  $H(j\omega)$  found in Step 3 and such that  $|H_1(j\omega)|$  is as small as possible.

Step 5

Determine the prefilter  $G(j\omega)$  from Equation (3-20).

The subsequent iterations are identical to the second iteration. If the compensation can be designed to yield a stable system at each iteration, the method will eventually yield an acceptable design since  $|\lambda(j\omega)|$  of each new design is smaller than  $|\lambda(j\omega)|$  of the previous design. The method itself implies nothing concerning the stability of the system so that a stability criterion must be applied as a separate part of the design. Any stability criterion which is expressed in the frequency domain can be integrated into the design procedure by using the criterion to modify the regions of acceptable  $H(j\omega)$  while the basic procedure remains unchanged.

An example will now be presented. The purpose of the example is to illustrate the mechanism of the procedure so the design itself will not be carried to completion. Discussion of the important considerations in setting specifications and

in choosing the desired transfer function and the nominal plant is also given in this example.

#### Design Example One

Let the plant be described by the first order differential equation

$$f(t)\dot{c}(t) = y(t) \quad (3-29)$$

where

$$f(t) = k_1 + k_2 \left[ 1 - e^{-\alpha(t-\tau)} \right] u(t-\tau) \quad (3-30)$$

and

$$0.1 \leq k_1 \leq 1$$

$$0.1 \leq k_1 + k_2 \leq 1$$

$$0.1 \leq \alpha \leq 10.$$

It is assumed that the value of  $\tau$  is unknown. From the above statement it is seen that the function  $f(t)$  can vary exponentially between any value in the range from .1 to 1 with no restrictions on when the variation can take place. A block diagram of the system is shown in Figure 3.2.

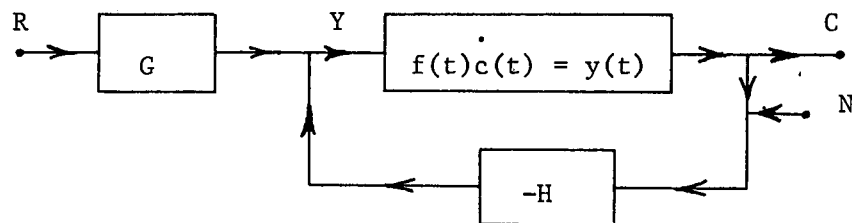


Figure 3.2  
Block Diagram of System in Example

Let the desired step response be given by

$$c_o(t) = (1 - e^{-t})u(t).$$

In specifying  $c_o(t)$  one should insure that it is possible for the plant to deliver such a response. That is, the designer should insure that there exists a reasonable plant input such that the actual output of the plant will be close to the desired output. This qualitative check is an obvious one since no amount of feedback can make the plant deliver what it is not capable of delivering. For this example if the plant output  $c(t)$  were to equal  $c_o(t)$  then the plant input would be given by

$$y(t) = f(t) e^{-t}u(t)$$

which is a function that imposes no unreasonable demands, in theory at least, on the compensations  $G$  and  $H$ . That is,  $y(t)$  contains no impulses or derivatives of impulses.

A second consideration is the specification  $M$ . At high frequencies the time-varying plant can be approximated by a time-invariant plant<sup>43</sup> so that at high frequencies  $|E(j\omega)|$  can be rewritten

$$|E| = \left| \frac{PGR}{1 + PH} - \frac{P_o GR}{1 + P_o H} \right| \leq M(\omega). \quad (3-31)$$

The magnitude of the functions  $G$ ,  $R$ ,  $H$ ,  $P$ , and  $P_o$  must all go to zero as  $\omega$  becomes large and since  $1 \gg |PH|$  then

$$|E| \approx |P - P_o| \quad |GR| \leq M(\omega). \quad (3-32)$$

But by Equation (3-20) GR is chosen as

$$GR = (P_o^{-1} + H)C_o \quad (3-33)$$

so that

$$|E| \approx |(P - P_o) \left[ \frac{1}{P_o} + H \right] C_o| \leq M(\omega)$$

or

$$\left| \frac{P}{P_o} - 1 + PH - P_o H \right| \leq M(\omega). \quad (3-34)$$

Note that since  $P_o$  is time-invariant then

$$P_o^{-1} = \frac{1}{P_o}.$$

Since  $|PH| \ll 1$  and  $|P_o H| \ll 1$  then one can write

$$|E(j\omega)| \approx \left| \frac{P(j\omega)}{P_o(j\omega)} - 1 \right| |C_o(j\omega)| \leq M(\omega). \quad (3-35)$$

From this formulation it is evident that  $M(\omega)$ ,  $C_o(j\omega)$  and  $P_o(j\omega)$  cannot be chosen in a completely arbitrary manner if the specifications at high frequency are to be met. Note that if a poor selection of  $M$  is made such that  $M$  goes to zero faster than  $C_o$  at high frequency, the specifications can never be satisfied at the higher frequencies. This difficulty can be avoided if  $M$  is

chosen as a constant at high frequencies. With  $M$  as a constant at high frequencies, the specifications can always be met by choosing the magnitude of the feedback compensation  $H$  large enough to satisfy the specifications over the lower frequencies (provided stability can be maintained) up to the point where Inequality (3-35) will be satisfied by  $C_o$  going to zero. Intuitively it appears that there should be no difficulty in letting  $M$  be some arbitrarily small number at high frequencies although this may not be true in all cases. At any rate, Inequality (3-35) must be satisfied in the high frequency range.

The specification for the example must now be chosen. Since frequency domain specifications have received little study there is no definite basis on which to choose the specifications for the example. Rather than attempt to relate time domain and frequency domain specifications at this point, specifications will be chosen arbitrarily. Let  $M$  for the example be chosen as a constant of value 0.06. Thus

$$M(\omega) = 0.06$$

so that

$$|E(j\omega)| = |C(j\omega) - C_o(j\omega)| \leq 0.06$$

The nominal plant  $P_o(j\omega)$  must now be chosen. No definite rule can be deduced concerning the selection of  $P_o(j\omega)$ ; however, a guide line can be determined upon examination of Equation (3-13). Equation (3-13) can be written in the form

$$E(j\omega) =$$

$$\lambda(j\omega) \int_{-\infty}^{\infty} \left[ P^{-1}(j\omega, j\gamma) - P_0^{-1}(j\omega, j\gamma) \right] \left[ C_0(j\gamma) + E(j\gamma) \right] d\gamma.$$

The object is to choose  $|\lambda(j\omega)|$  as large as possible and still have  $|E(j\omega)|$  fall within specifications. Obviously, the smaller the value of the magnitude of the integral, the larger  $|\lambda(j\omega)|$  can be for a given  $|E(j\omega)|$ . The nominal plant  $P_0^{-1}(j\omega, j\gamma)$  should be chosen such that the magnitude of the integral will be as small as possible.

The design equation for this example will now be determined. Note that the differential equation describing the plant is in the general form of Equation (2-9) so that the frequency impulse response of the inverse plant is evaluated as shown in Equations (2-10) and (2-11). The frequency impulse response of the inverse plant is found to be

$$P^{-1}(j\gamma, j\omega) = j\omega \left[ k_1 + \frac{k_2}{2} \right] \delta(j\gamma - j\omega) + \frac{j\omega e^{-(j\gamma - j\omega)\tau}}{2\pi} \left[ \frac{1}{j\gamma - j\omega} - \frac{1}{j\gamma - j\omega + \alpha} \right].$$

The nominal plant must now be determined. Let the transfer function of the nominal plant be given by  $P_0(j\omega)$ . Referring to Section 2.2, since the nominal plant is time-invariant, the frequency impulse response of the nominal plant is given by

$$P_0^{-1}(j\gamma, j\omega) = P_0^{-1}(j\omega) \delta(j\gamma - j\omega)$$

so that  $\Delta P^{-1}(j\gamma, j\omega)$  is found to be

$$\begin{aligned} \Delta P^{-1}(j\gamma, j\omega) = & \left[ \left[ k_1 + \frac{k_2}{2} \right] j\omega - P_o^{-1}(j\omega) \right] \delta(j\gamma - j\omega) \\ & + \frac{j\omega k_2 e^{-(j\gamma - j\omega)\tau}}{2\pi} \left[ \frac{1}{j\gamma - j\omega} - \frac{1}{j\gamma - j\omega + \alpha} \right]. \end{aligned} \quad (3-36)$$

Substituting the above expression for  $\Delta P^{-1}(j\gamma, j\omega)$  into Equation (3-13) and rearranging terms, one obtains

$$\begin{aligned} E(j\gamma) \left[ \left[ k_1 + \frac{k_2}{2} \right] j\gamma + H(j\gamma) \right] = & - \left[ \left[ k_1 + \frac{k_2}{2} \right] j\gamma - P_o^{-1}(j\gamma) \right] C_o(j\gamma) \\ & + \int_{-\infty}^{\infty} \frac{k_2 e^{-(j\gamma - j\omega)\tau}}{2\pi} \left[ \frac{1}{j\gamma - j\omega} - \frac{1}{j\gamma - j\omega + \alpha} \right] C(j\omega) d\omega. \end{aligned}$$

It is desired to select  $P_o^{-1}(j\gamma)$  such that the magnitude of the right hand side of this equation is as small as possible. The only term in the equation that involves  $P_o^{-1}(j\omega)$  is the first term on the right hand side. The possible values of the second term which is the integral term are not known so that the "best"  $P_o^{-1}(j\omega)$  cannot be determined. As an alternative  $P_o^{-1}(j\omega)$  will be chosen such that the magnitude of the first term will be a minimum. Since  $k_1 + k_2/2$  can range from .1 to 1, the nominal plant is chosen to fall half way between .1 and 1 or  $P_o^{-1}(j\omega) = 0.55j\omega$ . Thus  $\Delta P^{-1}(j\gamma, j\omega)$  is given by Equation (3-36) with  $P_o^{-1}(j\omega) = 0.55j\omega$ .

The first step in the first iteration of the design procedure is to determine  $I_o(j\gamma)$  which is given by



$$I_o(j\gamma) = \int_{-\infty}^{\infty} \Delta P^{-1}(j\gamma, j\omega) C_o(j\omega) d\omega$$

or

$$I_o(j\gamma) = \int_{-\infty}^{\infty} P^{-1}(j\gamma, j\omega) C_o(j\omega) d\omega - \int_{-\infty}^{\infty} P^{-1}(j\gamma, j\omega) C_o(j\omega) d\omega. \quad (3-37)$$

The first integral in Equation (3-37) is the Fourier transform of the input to the plant when the plant output is  $c_o(t)$  and the second integral is the Fourier transform of the input to the nominal plant when the output is  $c_o(t)$  so that the expression for  $I_o(j\gamma)$  can be written as

$$I_o(j\gamma) = \int_{-\infty}^{\infty} \left[ (k_1 - 0.55) + k_2 \left[ 1 - e^{-\alpha(t - \tau)} \right] u(t - \tau) \right] e^{-t} u(t) e^{-j\gamma t} dt.$$

Evaluating this integral one obtains

$$I_o(j\gamma) = \begin{cases} \frac{k_1 - 0.55}{j\omega + 1} + k_2 \left[ \frac{1}{j\omega + 1} - \frac{e^{\alpha t}}{j\omega + \alpha + 1} \right] & \tau \leq 0 \\ \frac{k_1 - 0.55}{j\omega + 1} + k_2 \left[ \frac{1}{j\omega + 1} - \frac{1}{j\omega + \alpha + 1} \right] e^{-(1 + j\omega)\tau} & \tau \geq 0 \end{cases} \quad (3-38)$$

The second step in the first iteration is to determine the regions in the complex plane for several frequencies of interest such that  $H(j\omega)$  falling within these regions insures that

Inequality (3-27) is satisfied. Inequality (3-27) can be written as

$$\frac{|I_o(j\omega)|}{|P_o^{-1}(j\omega) + H(j\omega)|} \leq M(\omega) = 0.06$$

which is equivalent to

$$\frac{|I_o(j\omega)| |P_o(j\omega)|}{|1 + P_o(j\omega)H(j\omega)|} \leq 0.06$$

Letting

$$P_o(j\omega)H(j\omega) = L_o(j\omega)$$

the inequality can be expressed as

$$\frac{|I_o(j\omega)| |P_o(j\omega)|}{0.06} \leq |1 + L_o(j\omega)|.$$

The problem now becomes that of determining acceptable regions for  $L_o(j\omega)$ . Notice that the acceptable regions of  $L_o(j\omega)$  take on the form of circles in the complex plane centered at the point  $-1$  and having radius equal to  $|P_o(j\omega)| |I_{om}(j\omega)|/0.06$  where  $|I_{om}(j\omega)|$  is the maximum value of  $|I_o(j\omega)|$  for the particular frequency of interest. Using a digital computer, the maximum value of  $I_o(j\omega)$  was obtained from Equation (3-38) for values of  $\omega$  equal to 0.5, 1, 2, and 5. The boundaries of the acceptable regions of  $L_o(j\omega)$  for these values of  $L_o(j\omega)$  are shown plotted in Figure 3.3. Note

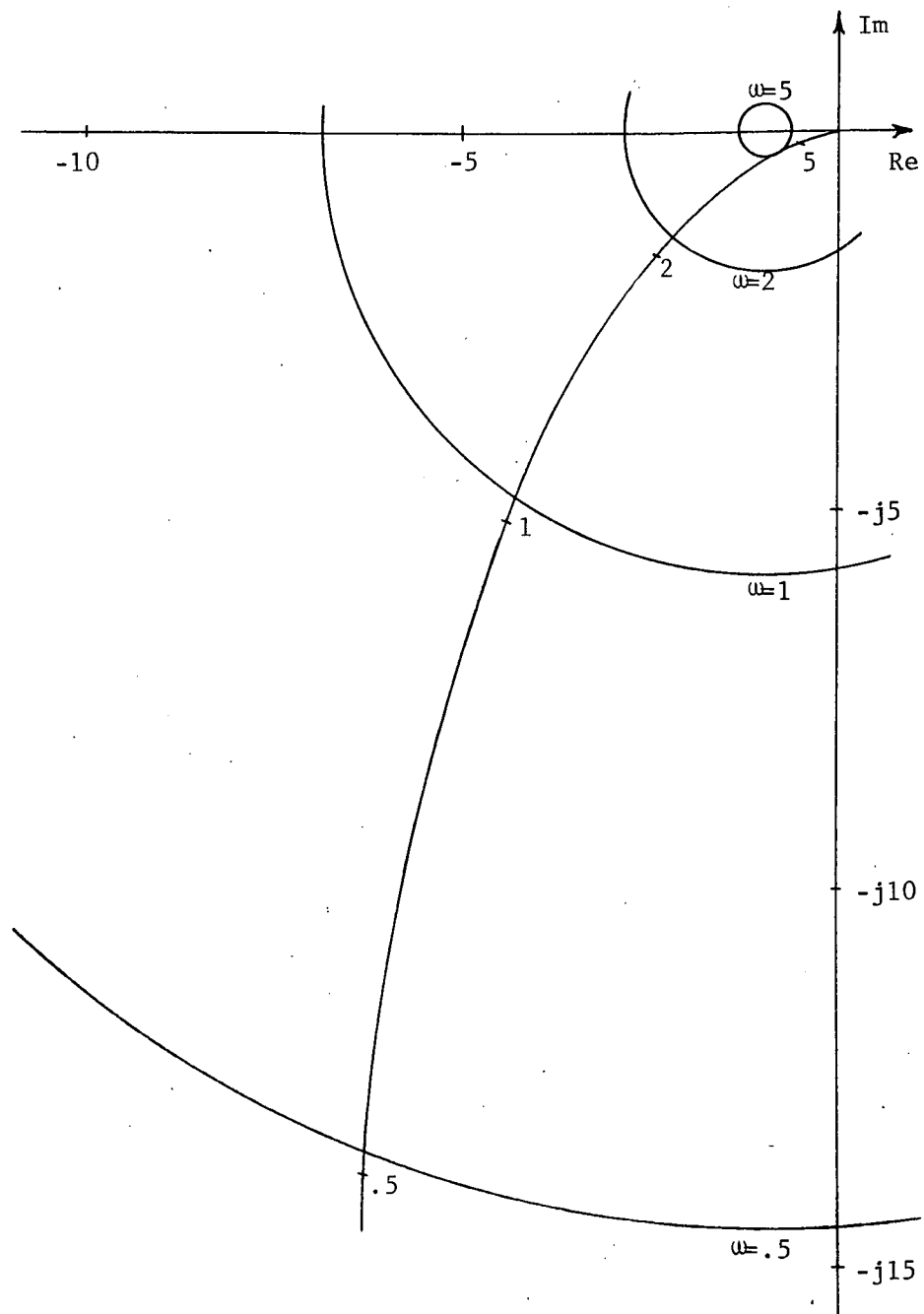


Figure 3.3  
Boundaries of Acceptable Regions of  $L(j\omega)$   
with Polar Plot of  $L_o(j\omega)$

that the acceptable regions of  $L_O(j\omega)$  lie on the outside of these circles. The third step in the design procedure is to determine a  $L_O(j\omega)$  which will just lie within the acceptable region found above. The function selected for  $L_O(j\omega)$  is

$$L_O(j\omega) = \frac{24.8(j\omega + 2)}{j\omega(j\omega + 1)(j\omega + 4)}$$

and is also shown plotted in Figure 3.3.

The fourth and final step in the first iteration of the design procedure is to determine the prefilter  $G(j\omega)$  from the equation

$$G(j\omega) = \left[ 1 + L_O(j\omega) \right] \frac{C_O(j\omega)}{P_O(j\omega)R(j\omega)} . \quad (3-39)$$

This is a straightforward matter of substituting  $L_O(j\omega)$ ,  $P_O(j\omega)$ , and  $C_O(j\omega)/R(j\omega)$  into the expression for  $G(j\omega)$  and simplifying. The expression for  $G(j\omega)$  was found to be

$$G(j\omega) = \frac{0.55(j\omega)^3 + 2.75(j\omega)^2 + 18.56(j\omega) + 32.73}{(j\omega)^3 + 6(j\omega)^2 + 9(j\omega) + 4} .$$

In order to determine whether or not this design actually meets the specification, the system was simulated on an analog computer and  $|E_O(j\omega)|$  was obtained at selected frequencies for a number of step responses using different values of  $k_1$ ,  $k_2$ ,  $\alpha$  and  $\tau$ . The values of  $|E_O(j\omega)|$  were determined directly from the analog computer using the method presented by Dick and Wertz<sup>44</sup> for obtaining the Fourier transform of a signal on an

analog computer. An envelope of the maximum values of  $|E_o(j\omega)|$  is shown plotted in Figure 3.4. Observe that the specifications are not met and that a second iteration must be made.

The first step in the second iteration which is the simulation of the design and the obtaining of  $|E_o(j\omega)|$  has been accomplished. The second iteration will start directly with the second step. The second step in the procedure is determining the values of  $|P_o^{-1}(j\omega) + H_1(j\omega)|$  such that Inequality (3-28) is satisfied for a number of frequencies of interest. Inequality (3-28) can be written in the following form

$$\frac{|1 + L_o(j\omega)|}{M(\omega)} \frac{|E_o(j\omega)|}{M(\omega)} \leq |1 + L_1(j\omega)| \quad \text{for } |E_o(j\omega)| \geq M(\omega)$$

$$|1 + L_o(j\omega)| \leq |1 + L_1(j\omega)| \quad \text{for } |E_o(j\omega)| \leq M(\omega)$$

which, for this example, becomes

$$\frac{|1 + L_o(j\omega)|}{0.06} \frac{|E_o(j\omega)|}{0.06} \leq |1 + L_1(j\omega)| \quad \text{for } |E_o(j\omega)| \geq 0.06 \quad (3-40a)$$

$$|1 + L_o(j\omega)| \leq |1 + L_1(j\omega)| \quad \text{for } |E_o(j\omega)| \leq 0.06. \quad (3-40b)$$

Note that the left hand side of the above inequalities can easily be determined from the plot of  $|E_{om}(j\omega)|$  shown in Figure 3.4 and the plot of  $L_o(j\omega)$  shown in Figure 3.3.

The third step is the determination of the regions of acceptable values of  $L_1(j\omega)$  in the complex plane. These regions are found from Inequalities (3-40) and are shown plotted in

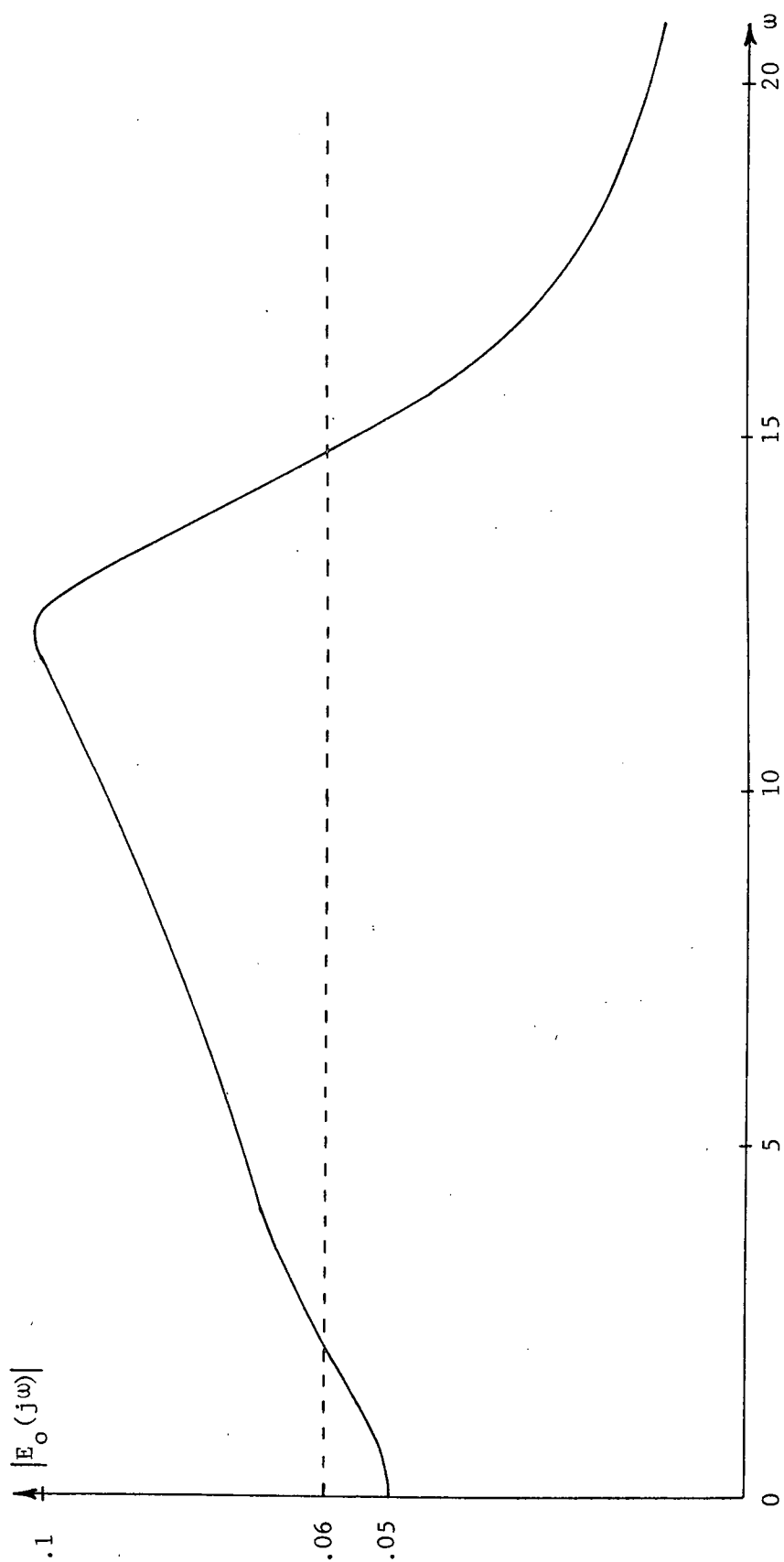


Figure 3.4  
Envelope of  $|E_o(j\omega)|$  of First Design

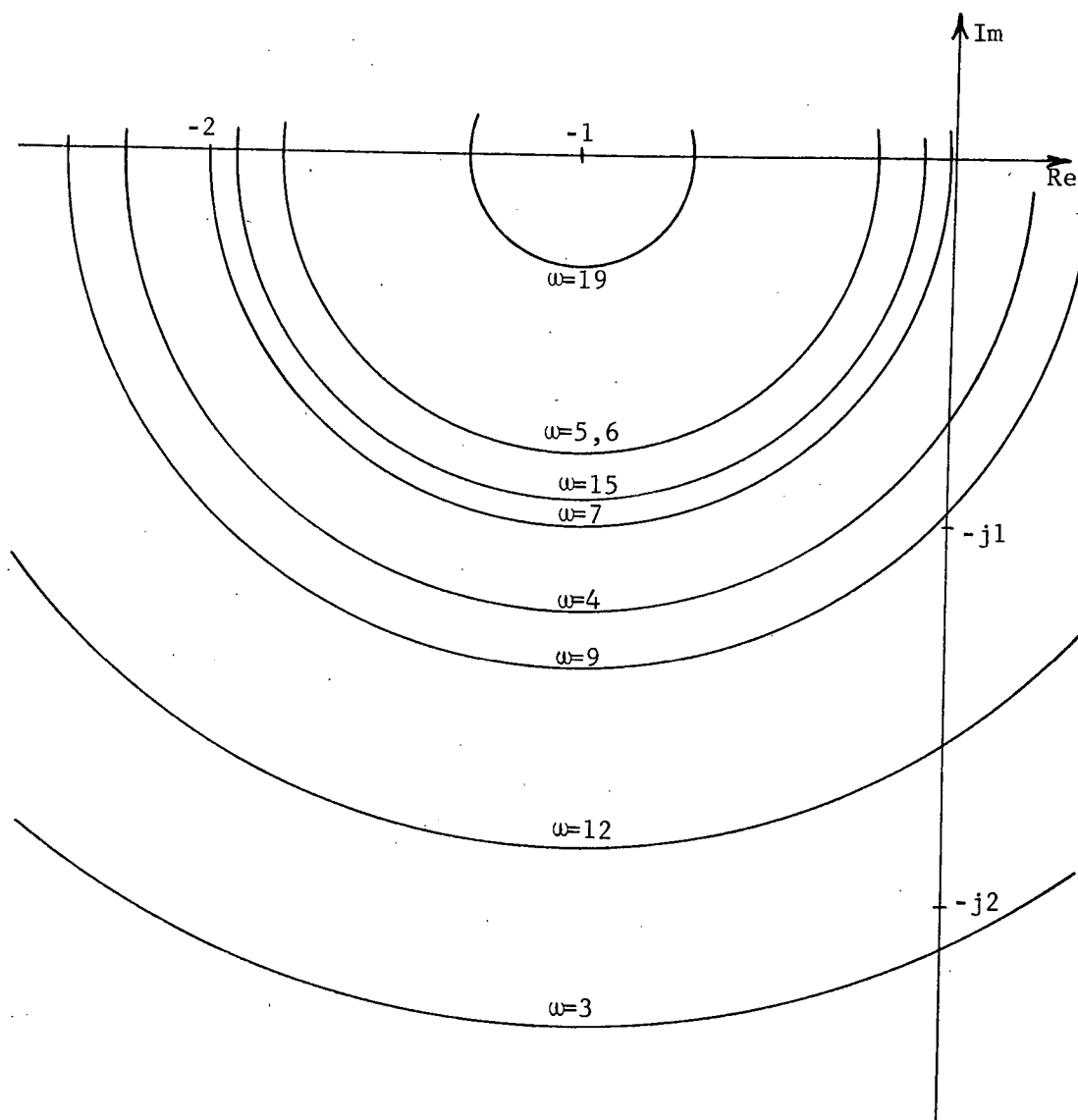


Figure 3.5  
Boundaries of Acceptable Regions of  $L_1(j\omega)$

Figure 3.5 for several values of  $\omega$ . The boundaries take on the form of circles centered about the point  $-1$  with radius equal to the larger of the two values  $|1 + L_O(j\omega)|$   $|E_{om}(j\omega)|/0.06$  or  $|1 + L_O(j\omega)|$ . The acceptable regions lie on the outside of these circles.

The fourth step is determining  $L_1(j\omega)$  such that it lies within the acceptable regions found in step three and is as small in magnitude as possible. The  $L_1(j\omega)$  which was selected is

$$L_1(j\omega) = \frac{476 (j\omega + 1.5) [(j\omega)^2 + 6(j\omega) + 36]}{j\omega(j\omega + 1) [(j\omega)^2 + 12(j\omega) + (12)^2](j\omega + 12)}$$

The polar plot of this function is shown in Figure 3.6.

The fifth and final step in the second iteration of the design procedure is determining  $G(j\omega)$  from Equation (3-39) which was found to be

$$G(j\omega) =$$

$$\frac{.55(j\omega)^5 + 13.75(j\omega)^4 + 433.4(j\omega)^3 + 3,072(j\omega)^2 + 12,732j\omega + 14,138}{(j\omega)^5 + 26(j\omega)^4 + 337(j\omega)^3 + 2,328(j\omega)^2 + 3,744j\omega + 1,728}$$

This completes the second iteration of the design procedure.

In order to determine whether or not this design meets specifications, the system was simulated on an analog computer and  $|E_1(j\omega)|$  was found for a number of step responses corresponding to different values of  $k_1$ ,  $k_2$ ,  $\alpha$ , and  $\tau$  at selected frequencies. The envelope of these is shown in Figure 3.7a. It is seen that the specifications are satisfied; thus, the design may be considered acceptable.



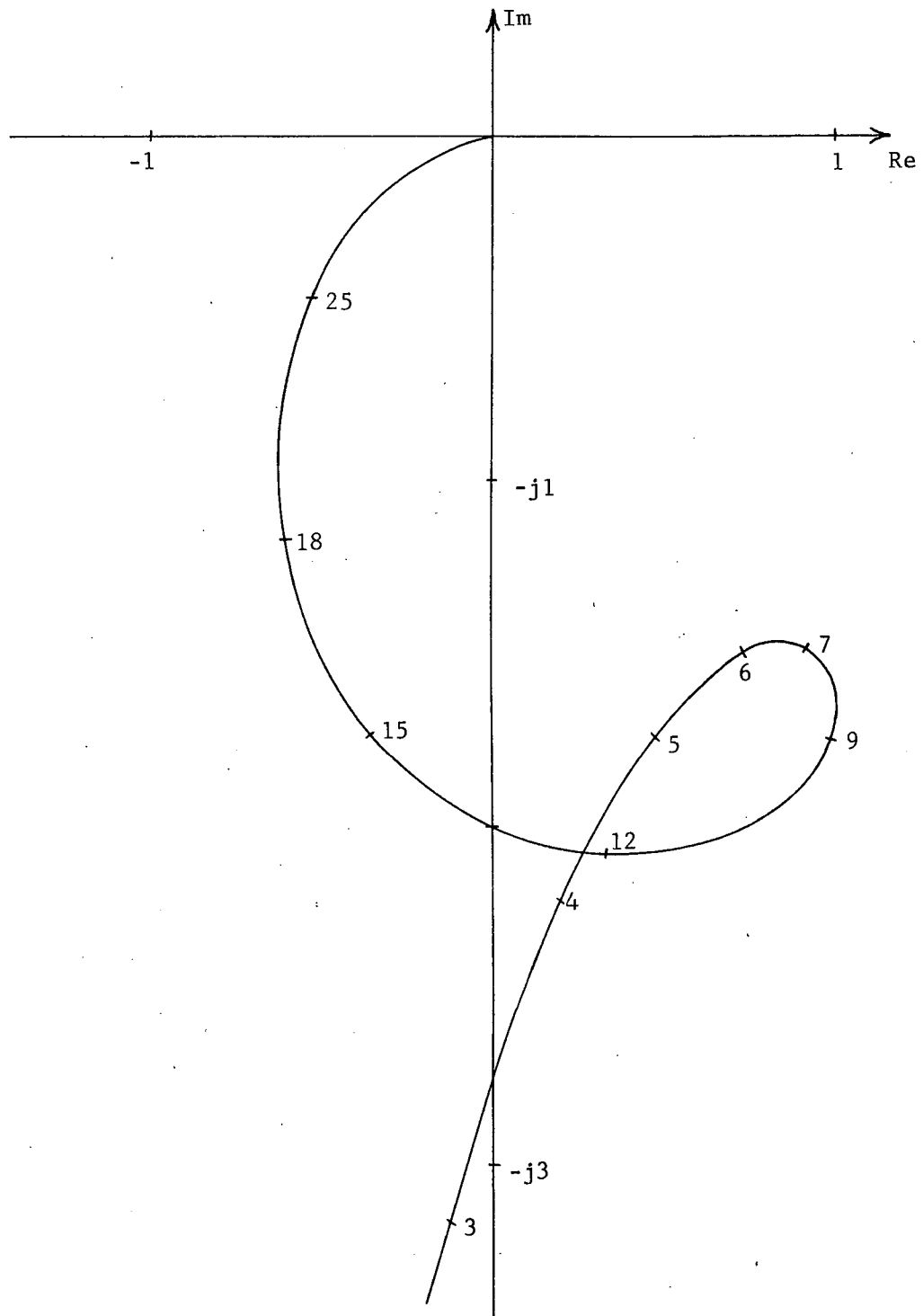


Figure 3.6  
Polar Plot of  $L_1(j\omega)$

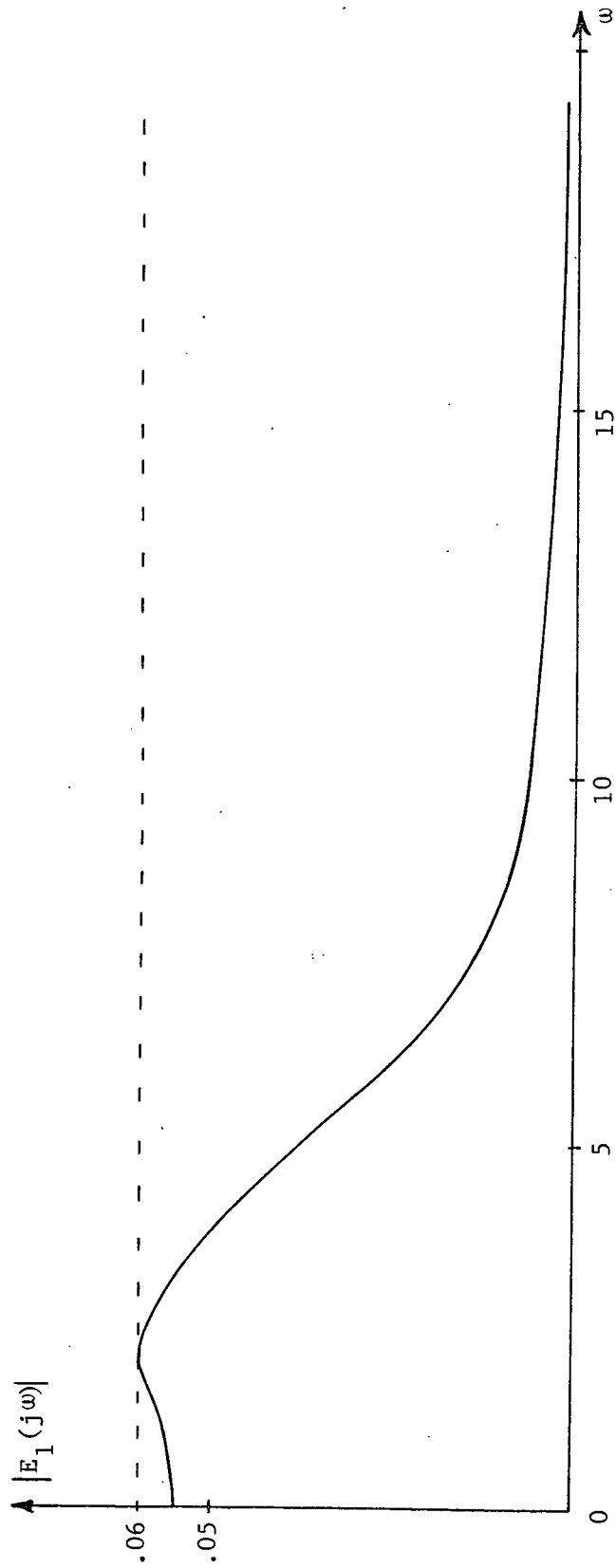


Figure 3.7a  
Envelope of  $|E_1(j\omega)|$  of Second Design

Although this completes the first example, some comments are in order. Even though the system meets specifications it must be noted that the design is not necessarily the best design possible. As has been pointed out, the best design is that design which will meet specification with as small a value of  $H(j\omega)$  as possible in order to minimize the noise transmission from the plant output to the plant input. When the best design has been obtained the design inequalities will become equalities except at high frequencies. In a system where it is particularly important to have  $|H(j\omega)|$  as small as possible, more iterations may be made using the inequality

$$\frac{|1 + L_0(j\omega)| |E_0(j\omega)|}{M(\omega)} \leq |1 + L_1(j\omega)|$$

for all values of  $\omega$ . The subscript zero represents the present design and the subscript one represents the subsequent design. Using this procedure the designer should be able to gain considerable insight into a particular system and thus arrive at a design which is closer to the best design. It should also be noted that system stability was not considered in the example. If an applicable stability criterion is determined, the criterion will place restrictions on  $H(j\omega)$  which can then be incorporated into the procedure by modifying the acceptable region of  $H(j\omega)$  or equivalently  $L(j\omega)$  in the complex plane.

A second design example will now be presented which illustrates a modification that can be made in the design equation although the procedure basically remains unchanged.

### Design Example Two

The plant of this design example is described by the second order differential equation

$$g(t)\ddot{x}(t) + f(t)\dot{x}(t) = y(t)$$

where

$$f(t) = F_1 + F_2(1 - e^{-a(t - \tau_1)})u(t - \tau_1)$$

$$g(t) = G_1 + G_2(1 - e^{-b(t - \tau_2)})u(t - \tau_2)$$

and

$$0.01 \leq G_1 \leq 1 \quad ; \quad 0.01 \leq G_1 + G_2 \leq 1$$

$$0.1 \leq F_1 \leq 0.25 \quad ; \quad 0.1 \leq F_1 + F_2 \leq 0.25$$

$$0.1 \leq a \leq 10 \quad ; \quad 0.1 \leq b \leq 10$$

It is also assumed that  $\tau_1$  and  $\tau_2$  are unknown. The desired step response is given by

$$c_o(t) = \left[ 1 - e^{-1.4t} \cos(1.414t) + 0.98 \sin(1.414t) \right] u(t).$$

The frequency domain representation of  $c_o(t)$  is

$$C_o(j\omega) = \frac{4}{j\omega \left[ (j\omega)^2 + 2.8j\omega + 4 \right]}$$

The specifications are arbitrarily chosen as

$$M(\omega) = \text{Max} \left\{ \left| \frac{5}{(j\omega + 1)(j\omega + 5)} \right|; 0.01 \right\}$$

A plot of these specifications for low frequency is shown in Figure 3.7b. Note that the specifications are consistent with the considerations discussed in Example One. That is, the desired plant output does not impose unreasonable demands on the plant input and it is possible for  $|H(j\omega)|$  to go to zero at high frequency and still meet the specifications since  $M(\omega)$  goes to a constant value at high frequency. Following the procedure illustrated in Example One, the nominal plant was chosen as

$$P_o^{-1}(j\omega) = 0.505(j\omega)^2 + 0.175j\omega$$

and the frequency impulse response of the inverse plant was found to be

$$\begin{aligned} P^{-1}(j\gamma, j\omega) = & \left[ (G_1 + \frac{G_2}{2})(j\omega)^2 + (F_1 + \frac{F_2}{2})j\omega \right] \delta(j\gamma - j\omega) \\ & + \frac{(j\omega)^2 e^{-(j\gamma - j\omega)\tau_2} + j\omega e^{-(j\gamma - j\omega)\tau_1}}{2\pi(j\gamma - j\omega)} \\ & - \frac{(j\omega)^2 e^{-(j\gamma - j\omega)\tau_1}}{2\pi(j\gamma - j\omega + b)} - \frac{j\omega e^{-(j\gamma - j\omega)}}{2\pi(j\gamma - j\omega + a)}. \end{aligned} \quad (3-41)$$

Let the portion of  $P^{-1}(j\gamma, j\omega)$  which is multiplied by  $\delta(j\gamma - j\omega)$  be denoted by  $P_a^{-1}(j\omega)$ . Note that  $P_a^{-1}(j\omega)\delta(j\gamma - j\omega)$  has the form of a time-invariant plant (see Section 2.2), while  $P_b^{-1}(j\gamma, j\omega)$

represents a time-varying plant. Thus, separating the frequency impulse response of the inverse plant into components

$P_a^{-1}(j\omega)\delta(j\gamma - j\omega)$  and  $P_b^{-1}(j\gamma, j\omega)$  effectively separates the plant into its time-varying and time-invariant components.

The function  $\Delta P^{-1}(j\gamma, j\omega)$  can now be written as

$$\Delta P^{-1}(j\gamma, j\omega) = P^{-1}(j\gamma, j\omega) - P_o^{-1}(j\gamma, j\omega)$$

or

$$\Delta P^{-1}(j\gamma, j\omega) = \left[ P_a^{-1}(j\omega) - P_o^{-1}(j\omega) \right] \delta(j\gamma - j\omega) + P_b^{-1}(j\gamma, j\omega). \quad (3-42)$$

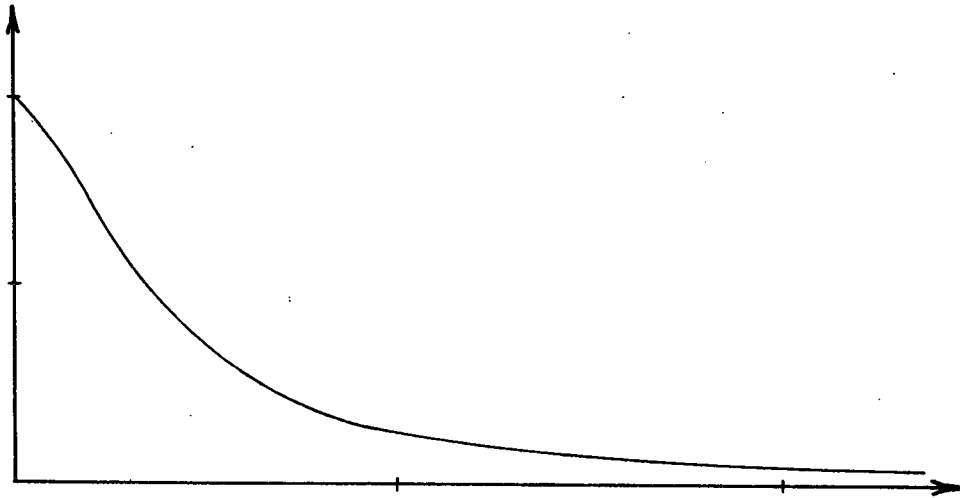


Figure 3.7b  
Low Frequency Specification  
Of Design Example Two

The design equation, Equation (3-13), can be written as

$$E(j\gamma) = \frac{1}{P_o^{-1}(j\gamma) + H(j\gamma)} \int_{-\infty}^{\infty} \Delta P^{-1}(j\gamma, j\omega) [C_o(j\omega) + E(j\omega)] d\omega . \quad (3-43)$$

Substituting Equation (3-42) into Equation (3-43) one obtains

$$E(j\gamma) = \frac{-1}{P_o^{-1}(j\gamma) + H(j\gamma)} \left[ \int_{-\infty}^{\infty} [P_a^{-1}(j\omega) - P_o^{-1}(j\omega)] \delta(j\gamma - j\omega) E(j\omega) d\omega \right. \\ \left. + \int_{-\infty}^{\infty} \Delta P^{-1}(j\omega, j\gamma) C_o(j\omega) d\omega + \int_{-\infty}^{\infty} P_b^{-1}(j\gamma, j\omega) E(j\omega) d\omega \right] \quad (3-44)$$

Evaluating the first integral and solving for  $E(j\gamma)$ , Equation (3-44) can be written

$$E(j\gamma) = \lambda(j\gamma) \left[ I_o(j\gamma) + \int_{-\infty}^{\infty} P_b^{-1}(j\gamma, j\omega) E(j\omega) d\omega \right] \quad (3-45)$$

where

$$I_o(j\gamma) = \int_{-\infty}^{\infty} \Delta P^{-1}(j\gamma, j\omega) C_o(j\omega) d\omega \quad (3-46)$$

and

$$\lambda(j\gamma) = \frac{-1}{P_a^{-1}(j\gamma) + H(j\gamma)} . \quad (3-47)$$

This equation can now be substituted in place of Equation (3-13) in the synthesis procedure. The advantage in using Equation (3-45) can be seen by comparing the terms which are ignored in the first step of the first iteration. By using Equation (3-13) the entire integral

$$\int_{-\infty}^{\infty} \Delta P^{-1}(j\omega, j\gamma) E(j\gamma) d\gamma$$

is assumed equal to zero (see Equation (3-16)), while by using Equation (3-45) only the term

$$\int_{-\infty}^{\infty} P_b^{-1}(j\gamma, j\omega) E(j\omega) d\omega$$

is assumed equal to zero.

The first step in the design procedure is to assume

$$\int_{-\infty}^{\infty} P_b^{-1}(j\gamma, j\omega) E(j\omega) d\omega = 0 \quad (3-48)$$

then apply the specifications to  $E(j\gamma)$  as follows

$$|E(j\gamma)| = |\lambda(j\gamma) I_o(j\gamma)| \leq M(\gamma).$$

Using Equation (3-47) this can be written

$$\frac{|I_o(j\gamma)|}{M(\gamma)} \leq |P_a^{-1}(j\gamma) + H(j\gamma)|. \quad (3-49)$$

Note that both  $I_o(j\gamma)$  and  $P_a^{-1}(j\gamma)$  depend upon the plant parameters so that the ranges in the complex plane of both of these functions must be considered in determining the acceptable range of  $H(j\gamma)$ .

It must be observed at this point that  $I_o(j\gamma)$  and  $P_a^{-1}(j\gamma)$  are not independent. However, to simplify the task of determining the acceptable regions of  $H(j\gamma)$  from Inequality (3-49) it will be assumed that  $I_o(j\gamma)$  and  $P_a^{-1}(j\gamma)$  are independent. This assumption



should not introduce any more error than is inherently present in the first iteration due to the assumption expressed in Equation (3-48).

Since  $P_a^{-1}(j\omega)$  is obtained by inspection from Equation (3-41), it only remains to determine  $I_o(j\gamma)$  which is given by

$$I_o(j\gamma) = \int_{-\infty}^{\infty} \Delta P^{-1}(j\gamma, j\omega) C_o(j\omega) d\omega$$

or

$$I_o(j\gamma) = \int_{-\infty}^{\infty} P^{-1}(j\gamma, j\omega) C_o(j\omega) d\omega - \int_{-\infty}^{\infty} P_o^{-1}(j\gamma, j\omega) C_o(j\omega) d\omega.$$

This is equivalent to the Fourier transform of the plant input with the plant output equal to  $c_o(t)$  minus the Fourier transform of the nominal plant input with the nominal plant output equal to  $c_o(t)$ . Thus,  $I_o(j\gamma)$  is given by

$$\begin{aligned} I_o(j\gamma) = \int_{-\infty}^{\infty} \left\{ \left[ G_3 + G_2 \left[ 1 - e^{-b(t - \tau_2)} \right] u(t - \tau_2) \right] \right. \\ \left[ 4e^{-1.4t} \cos(1.414t) - 3.96e^{-1.4t} \sin(1.414t) \right] u(t) \\ + \left[ F_3 + F_2 \left[ 1 - e^{-a(t - \tau_1)} \right] u(t - \tau_1) \right] \\ \left. \left[ 2.83 e^{-1.4t} \sin(1.414t) u(t) \right] \right\} e^{-j\gamma t} dt \end{aligned}$$

9

where

$$G_3 = G_1 - 0.505$$

and

$$F_3 = F_1 - 0.175.$$

Performing this straightforward but lengthy integration, a complicated expression for  $I_o(j\gamma)$  is obtained consisting of four functions for different ranges of  $\tau_1$  and  $\tau_2$ . This expression is given in Appendix B.

The second step in the synthesis procedure is to determine the regions in the complex plane at selected frequencies which correspond to  $I_o(j\gamma)$  and  $P_a^{-1}(j\omega)$  for different values of the plant parameters. From these two regions corresponding to  $I_o(j\gamma)$  and  $P_a^{-1}(j\gamma)$  one can determine acceptable regions of  $H(j\gamma)$ . This was done for  $\gamma$  equal to 1, 5, 10, 20, 30, and 50. The resulting acceptable regions for  $H(j\gamma)$  are shown in Figure 3.8.

The third step is to select an  $H(j\gamma)$  which falls within the acceptable regions determined in Step 2. Because of the limited size of the analog computer available, it was necessary to limit the feedback compensation to third order. The compensation which was chosen is

$$H(j\gamma) = 31.54 \frac{(j\gamma + 0.5)(j\gamma + 5)(j\gamma + 50)}{(j\gamma + 2)(j\gamma + 30)(j\gamma + 80)}.$$

The polar plot of  $H(j\gamma)$  is also shown in Figure 3.8.

The fourth and final step in the first iteration is the determination of the prefilter  $G(j\gamma)$  from Equation (3-28) which was found to be

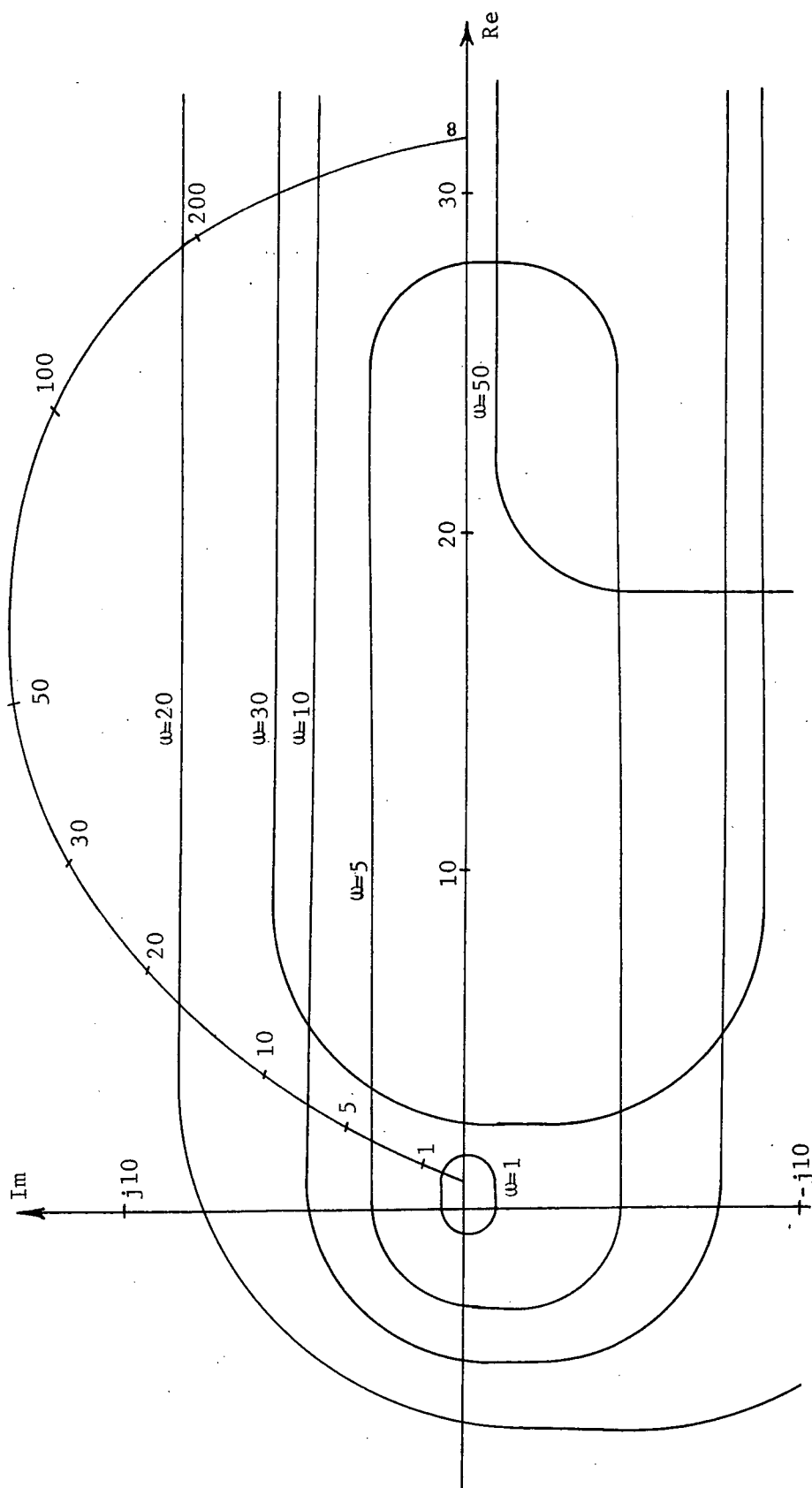


Figure 3.8  
Boundaries of Acceptable Regions of  $H(j\omega)$   
with Polar Plot of  $H(j\omega)$

$$G(j\gamma) =$$

$$\frac{2(j\gamma)^5 + 227(j\gamma)^4 + 5497(j\gamma)^3 + 1853(j\gamma)^2 + 38367j\gamma + 15769}{(j\gamma)^5 + 115(j\gamma)^4 + 2938(j\gamma)^3 + 12584(j\gamma)^2 + 23920j\gamma + 19200}$$

The system was simulated on an analog computer and  $E(j\gamma)$  was found for a number of step responses corresponding to different values of the plant parameters. The envelope of the maximum value of these  $E(j\gamma)$  is shown plotted in Figures 3.9a and 3.9b. Observe that the specifications are met except at very low frequencies. This illustrates the basic procedure so a second iteration will not be made. Note that  $|E|$  is reasonably close to the specifications except at low frequency. Thus, the second  $H$  would be similar to the first except for a higher gain at low frequencies.

Although the designs in the two examples were not carried to completion, it appears that there is no difficulty in carrying out the steps in design procedure one. It remains to be seen how easily a design that is close to optimal can be achieved through the procedure. A basic assumption in the procedure is that the regions of acceptable  $L(j\omega)$  are circular as shown in Figures 3.3 and 3.5. In the second example it was possible to arrive at acceptable regions which were not circular; however, this was only true for the initial design. It would be necessary in subsequent designs to assume circular regions. If the regions of acceptable  $L(j\omega)$  are, in fact, circular, especially in the region of  $L(j\omega)$ , then the design procedure should lead to a design that is close

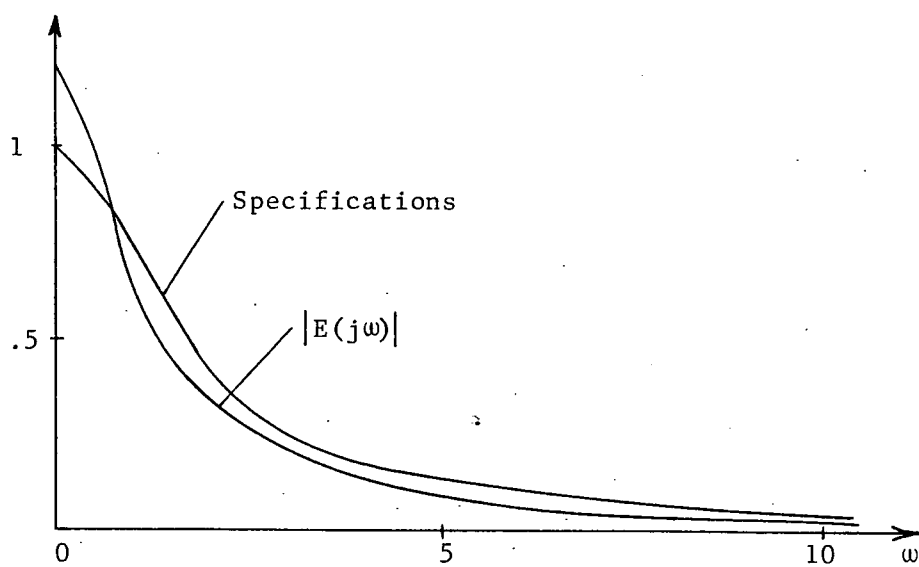


Figure 3.9a  
Envelope of  $|E(j\omega)|$  for  $0 \leq \omega \leq 10$

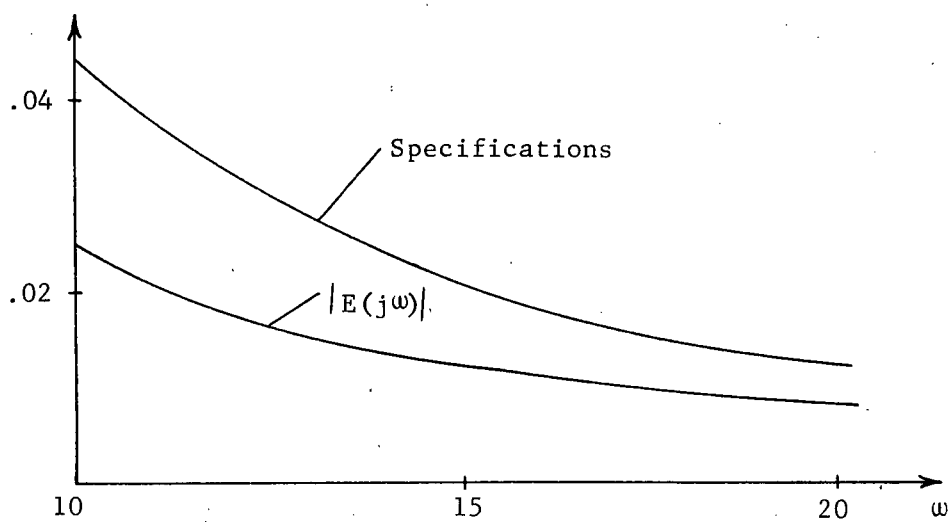


Figure 3.9b  
Envelope of  $|E(j\omega)|$  for  $10 \leq \omega \leq 20$

to optimal. If the assumption of circular regions is grossly in error, it would be more difficult to arrive at a design which is close to optimal.

The second design procedure will now be presented. Like the first procedure, the second procedure is an iterative process. However, the assumption that the regions of acceptable  $L$  are circular is not made in the second procedure so that a design which is close to optimal may be able to be obtained in a more straightforward manner than is possible in the first procedure.

### 3.3 Synthesis Procedure Two

The procedure is similar to the synthesis procedure presented by I. M. Horowitz<sup>45</sup> for time-invariant systems having ignorance, with the exception that iterations must be performed for a time-varying system. In this procedure the specifications are given in the form

$$k_1 \leq \left| \frac{C(j\omega)}{C_o(j\omega)} \right| \leq k_2 \quad (3-50a)$$

$$\theta_1 \leq \arg [C(j\omega) - C_o(j\omega)] \leq \theta_2. \quad (3-50b)$$

The design equation for this procedure will now be developed. Referring to Section 2.4, the system is described by the equation

$$H(j\omega)C(j\omega) + Y(j\omega) = G(j\omega)R(j\omega)$$

where  $Y(j\omega)$  is the Fourier transform of the input to the plant. Factoring  $C(j\omega)$  from the left hand side of the equation one obtains

$$\left[ H(j\omega) + \frac{Y(j\omega)}{C(j\omega)} \right] C(j\omega) = G(j\omega)R(j\omega) . \quad (3-51)$$

Under the conditions that the plant is at its nominal time-invariant value the system will be described by the equation

$$\left[ H(j\omega) + \frac{1}{P_o(j\omega)} \right] C_o(j\omega) = G(j\omega)R(j\omega) . \quad (3-52)$$

Dividing Equation (3-51) by Equation (3-52) one obtains

$$\frac{\left[ H(j\omega) + \frac{Y(j\omega)}{C(j\omega)} \right] C(j\omega)}{\left[ H(j\omega) + \frac{1}{P_o(j\omega)} \right] C_o(j\omega)} = 1 .$$

Multiplying the numerator and denominator of the right hand side by  $P_o(j\omega)$  and letting

$$P_o(j\omega)H(j\omega) = L_o(j\omega)$$

the equation can be written

$$\frac{C(j\omega)}{C_o(j\omega)} = \frac{1 + L_o(j\omega)}{\frac{Y(j\omega)}{C(j\omega)} P_o(j\omega) + L_o(j\omega)} . \quad (3-53)$$

Letting the ratio of the plant output to the plant input be denoted by

$$P_{eq}(j\omega) = \frac{C(j\omega)}{Y(j\omega)}$$

Equation (3-53) can be written

$$\frac{C(j\omega)}{C_o(j\omega)} = \frac{1 + L_o(j\omega)}{\frac{P_o(j\omega)}{P_{eq}(j\omega)} + L_o(j\omega)} . \quad (3-54)$$

For the time-invariant case with ignorance  $P_{eq}(j\omega)$  is the transfer function of the unknown time-invariant plant. Using the procedure presented by Horowitz, it is possible to determine acceptable regions for  $L_o(j\omega)$  from the region in the complex plane corresponding to the possible values of  $P_{eq}(j\omega)$ . For the time-invariant case the values of  $P_{eq}(j\omega)$  are dependent only upon the plant parameters so that knowing the ranges of these plant parameters it is possible to determine the range of  $P_{eq}(j\omega)$  in the complex plane. However, for the time-varying case  $P_{eq}(j\omega)$  is dependent not only upon the plant and its variations but also upon the plant input which in turn depends upon the feedback compensation  $H(j\omega)$ . Thus,  $P_{eq}(j\omega)$  depends upon  $L_o(j\omega)$  in the time-varying case. This presents difficulty since  $L_o(j\omega)$  is not known prior to the design.

To circumvent this difficulty an iteration procedure is employed where an initial design is made and tested. If the specifications are not satisfied, a second design is made based on the region of  $P_o/P_{eq}$  corresponding to the first design. If additional designs are required, each is based on the regions of  $P_o/P_{eq}$  corresponding to the previous design. In this scheme the designer must use his judgment because there is no guarantee that



the procedure will lead to a satisfactory design if mechanically followed. Intuitively, however, it appears that the procedure should lead to a satisfactory design. If large changes in  $H$  are required, the procedure will at least call for changes which are in the proper direction to improve the design. If relatively small changes in  $H$  are needed, the regions of  $P_O/P_{eq}$  should show little change from one design to the next so that regions of  $P_O/P_{eq}$  which are very close to being correct will be used in the design with the result that a proper design will be made. It is conceivable that difficulty could arise in starting with a design which requires large modifications in  $H$ . There is nothing in the procedure which prevents an oscillatory effect. That is, the first design may require a large increase in  $|H|$  and the second design may call for a large decrease in  $|H|$  back to the first design. Of course, in such a case the designer would apply his judgment and not decrease  $|H|$  as much as specified. It is important that the designer consider all previous designs and their corresponding regions of  $P_O/P_{eq}$  when making a new design to avoid one that is similar to a design which has previously been shown to be unacceptable.

The steps in the second design procedure will now be presented. As in design procedure one, the initial design is a starting point for the iteration procedure. As was discussed in design procedure one, the initial design may be any stable design; however, it would be better to start from a more definite design such as one based on a time-invariant plant with ignorance. The

approach to obtaining an initial design which is given is based on the assumption that the plant output is the desired plant output for all variations. It is also assumed that the time-variations are known as functions of time so that analytical calculations can be made.

### First Iteration

#### Step One

Assuming that

$$C(j\omega) = C_o(j\omega)$$

determine  $P_o(j\omega)/P_{eq}(j\omega)$  from the expression

$$\frac{P_o(j\omega)}{P_{eq}(j\omega)} = \frac{P_o(j\omega)Y(j\omega)}{C_o(j\omega)} = \frac{P_o(j\omega)}{C_o(j\omega)} \int_{-\infty}^{\infty} P^{-1}(j\omega, j\gamma) C_o(j\gamma) d\gamma \quad (3-55)$$

for a number of frequencies of interest. Plot the range of  $P_o(j\omega)/P_{eq}(j\omega)$  in the complex plane for the possible plant parameter variations.

#### Step Two

Using the procedure outlined by Horowitz<sup>45</sup> determine the acceptable regions of  $L_o(j\omega)$  at a number of frequencies of interest and design a  $L_o(j\omega)$  which falls within these acceptable regions.

#### Step Three

Determine the prefilter  $G(j\omega)$  from the relation

$$G(j\omega) = \left[ 1 + L_o(j\omega) \right] \frac{C_o(j\omega)}{P_o(j\omega)R(j\omega)} \quad (3-56)$$

The preliminary design is now complete.

This first design is simulated on a computer in order to determine whether or not the system satisfies its specifications. If the preliminary design is unsatisfactory, which presumably it will be, a second iteration must be made.

### Second Iteration

#### Step One

From the computer simulation of the previous design, determine the range of  $P_o/P_{eq}$  in the complex plane for the possible plant parameter variations.

#### Step Two

Repeat steps two and three of the First Iteration.

Subsequent iterations are made until a satisfactory design is obtained. It should again be emphasized that the designer must consider not only the ranges of  $P_o/P_{eq}$  corresponding to the last design, but also the ranges corresponding to all previous designs. What the designer must guard against is an iteration leading to a design which has previously been found to be unsatisfactory. There is nothing inherent in the design procedure itself which prevents such an occurrence so the designer must consider all previous ranges of  $P_o/P_{eq}$  in each new design. An example illustrating this synthesis procedure will now be presented. Again, the purpose of the design is to illustrate the procedure rather than arrive at an optimal design for the particular system considered.

### Design Example Three

The plant which was considered in Design Example Two will be used in this example. Since a design was made in Design Example Two, it will be of interest to compare the regions of  $P_o(j\omega)/P_{eq}(j\omega)$  with the  $L_o(j\omega)$  which was obtained in Design Example Two. In order to utilize the design of Design Example Two, the specifications of that example must be put in a form compatible with this design procedure. That is, the specifications must be put in the form

$$k_1 \leq \left| \frac{C(j\omega)}{C_o(j\omega)} \right| \leq k_2 \quad (3-57a)$$

$$\theta_1 \leq \text{Arg} [C(j\omega) - C_o(j\omega)] \leq \theta_2 \quad (3-57b)$$

instead of the form

$$|C(j\omega) - C_o(j\omega)| \leq M(\omega). \quad (3-58)$$

Note that Inequality (3-58) defines a region in the complex plane in which  $C(j\omega)$  must fall. Likewise, Inequalities (3-57) also define a region in the complex plane in which  $C(j\omega)$  must fall. The specifications are given in Figure 3.7 so that one must determine the values of  $k_1$ ,  $k_2$ ,  $\theta_1$ , and  $\theta_2$  such that the region defined by Inequalities (3-57) corresponds to the region defined by Inequality (3-58). The shapes of the two regions are not the same so that values of  $k_1$ ,  $k_2$ ,  $\theta_1$ ,  $\theta_2$  can only be chosen such that the region defined by Inequalities (3-57) is approximately the

same as the region defined by Inequality (3-58). The values which transfer the specifications of Figure 3.7 to specifications which can be used with Inequalities (3-57) are listed in Table 3.1.

$\omega$	$k_1$	$k_2$	$\theta_1$	$\theta_2$
1	.36	1.55	-35°	-35°
5	0	3.6	-180°	180°
10	0	11	-180°	180°
20	0	24	-180°	180°
100	0	$2.5 (10)^3$	-180°	180°
400	0	$1.6 (10)^7$	-180°	180°
500	0	$3.1 (10)^7$	-180°	180°

Table 3.1  
System Specifications

The first step of the first iteration is to determine the range in the complex plane of the values of  $P_O(j\omega)/P_{eq}(j\omega)$  under the assumption that  $C(j\omega) = C_O(j\omega)$ . The expression for  $P_O(j\omega)/P_{eq}(j\omega)$  is given in Appendix C. The regions in the complex plane corresponding to the values of  $P_O(j\omega)/P_{eq}(j\omega)$  for  $\omega$  equal to 1, 10, 20, 100, 400, and 500 are shown in Figures 3.10a and 3.10b.

Step two of the procedure is to determine the acceptable region for  $L_O(j\omega)$ . Using the specifications given in Table 3.1 the acceptable regions for  $L_O(j\omega)$  were determined from the regions shown in Figures 3.10a and 3.10b. These acceptable regions for

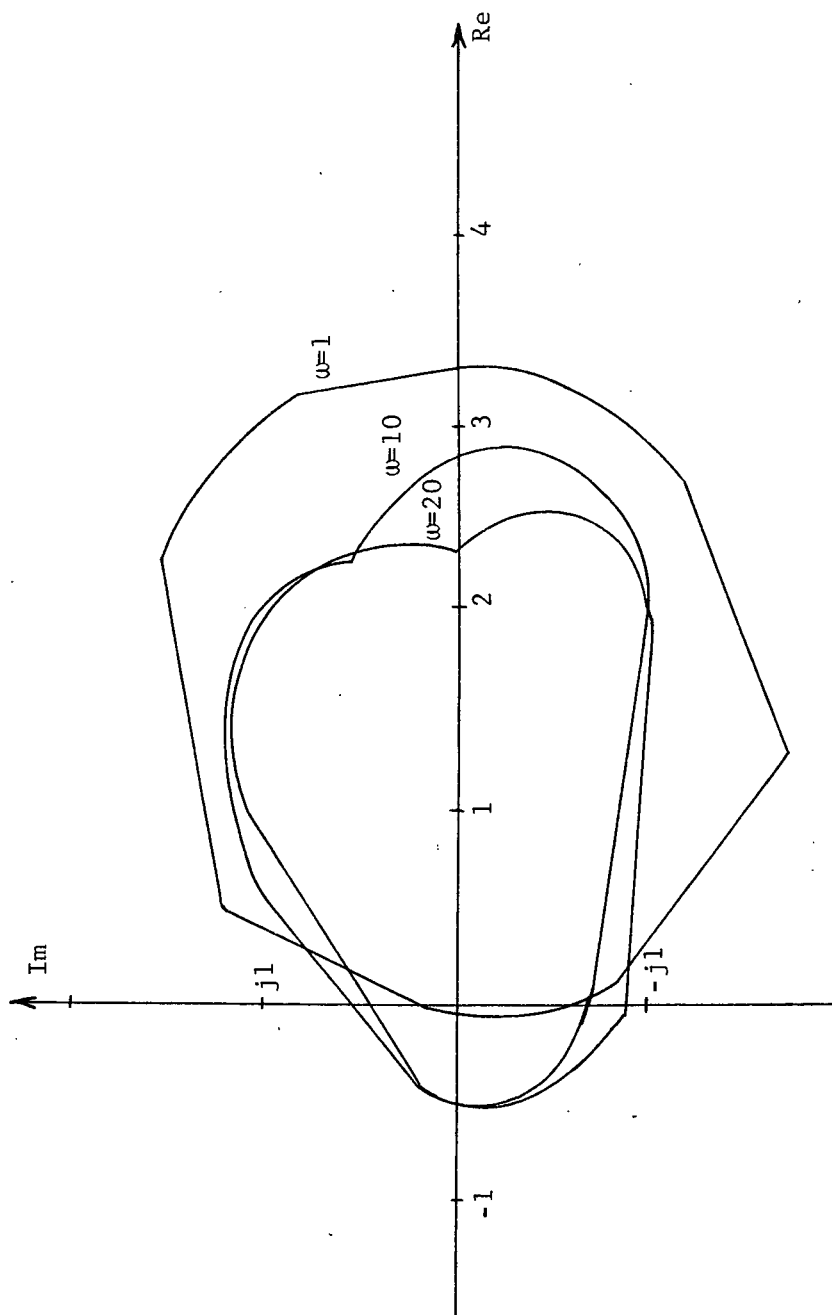


Figure 3.10a  
Low Frequency Range of  $P_o(j\omega)/P_{eq}(j\omega)$

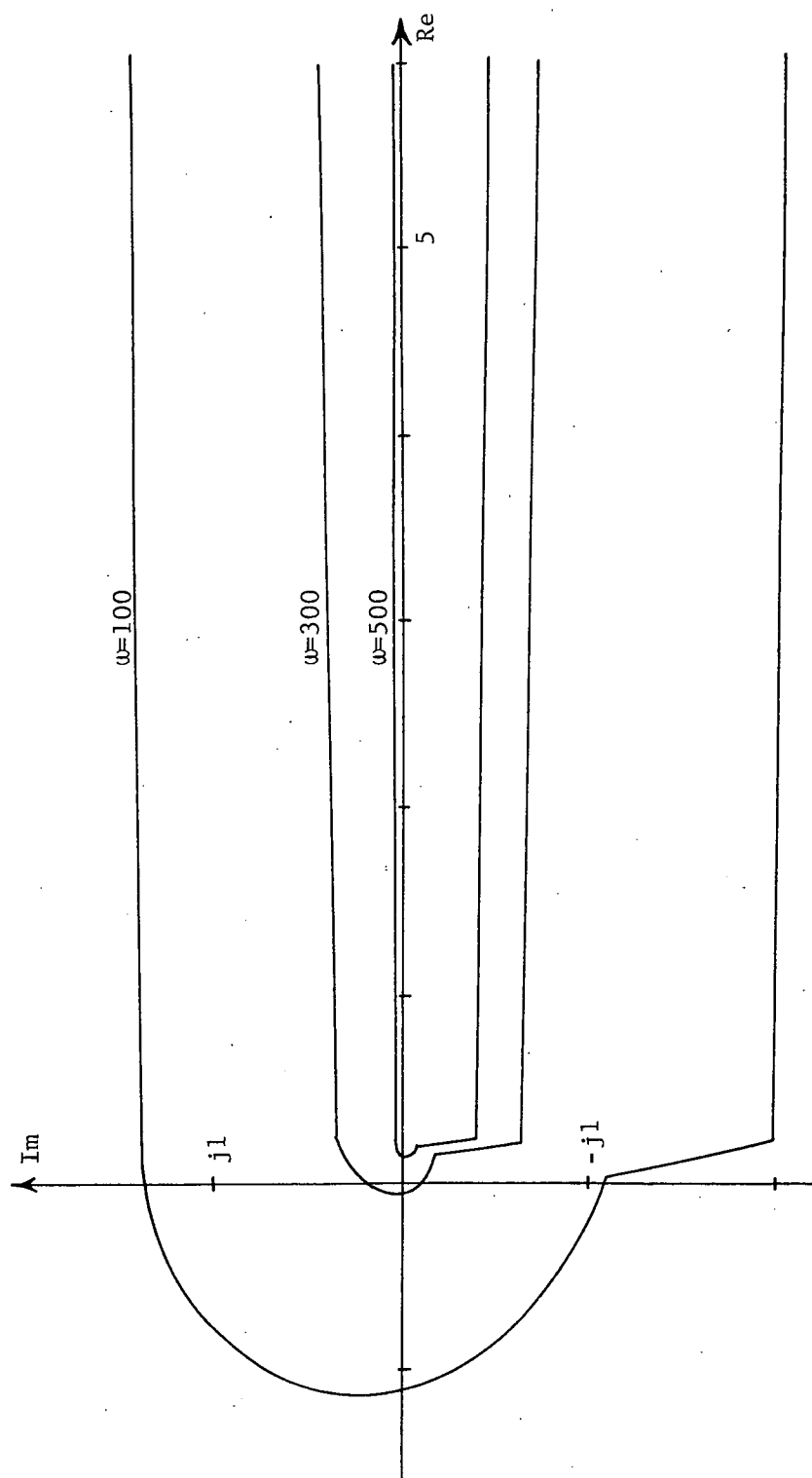


Figure 3.10b  
High Frequency Range of  $P_o(j\omega)/P_{eq}(j\omega)$

$L_0(j\omega)$  are shown in Figures 3.11a and 3.11b. Also shown on the figure is the polar plot of  $L_1(j\omega)$  which was designed in Design Example Two. It is known that this compensation satisfies the specifications except at very low frequency; however, it is seen from the figure that  $L_1(j\omega)$  does not fall within the acceptable regions. Two conclusions can be drawn from these figures. The first is that at least for this problem the approximation  $C(j\omega) = C_0(j\omega)$  is a poor one. The second is that a compensation which is designed on the basis of these acceptable regions will in all probability more than meet the specifications since its magnitude would be considerably larger than the magnitude of  $L_1(j\omega)$ .

A second iteration will now be made. However, instead of designing a compensation based on the regions of Figures 3.11a and 3.11b the  $L_1(j\omega)$  which was designed in Design Example Two will be used. The system was simulated on an analog computer and  $C(j\omega)$  and  $Z(j\omega)$  were evaluated from this computer simulation for a number of variations of  $g(t)$  and  $f(t)$ . The values of  $P_0(j\omega)Z(j\omega)/C(j\omega)$  for these variations were then plotted in the complex plane. This plot of points was used to determine the range of  $P_0(j\omega)/P_{eq}(j\omega)$ . These ranges of  $P_0(j\omega)/P_{eq}(j\omega)$  were determined for values of  $\omega$  equal to 1, 5, and 10 and are shown in Figure 3.12. The range of  $P_0(j\omega)/P_{eq}(j\omega)$  for higher frequencies could not be determined due to practical limitations of the analog computer available. These ranges were next used to determine the acceptable regions of  $L_0(j\omega)$  which are shown in Figure 3.13.



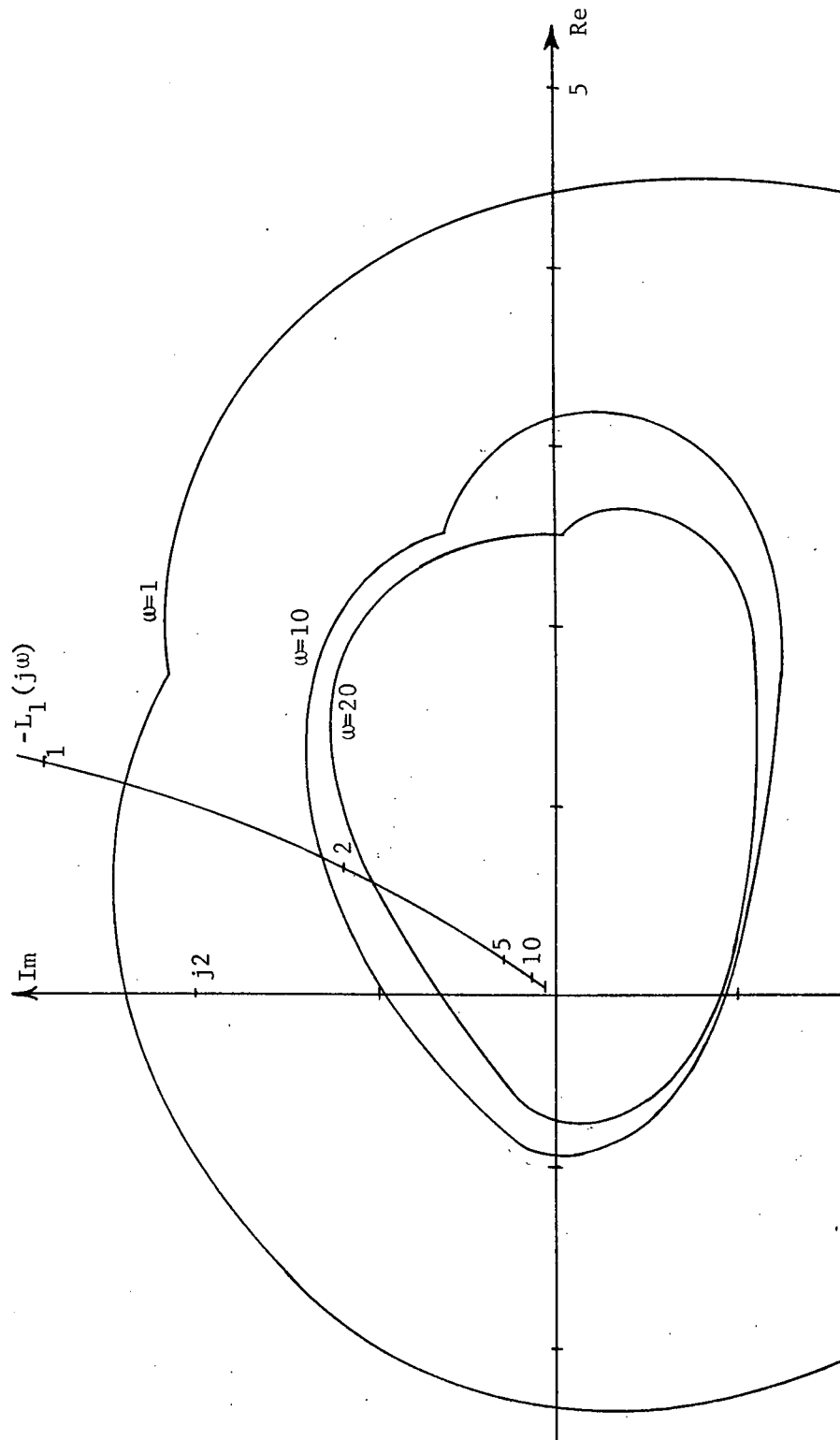


Figure 3.11a  
Low Frequency Boundaries of Acceptable Regions  
of  $L(j\omega)$  with Comparison of  $L_1(j\omega)$

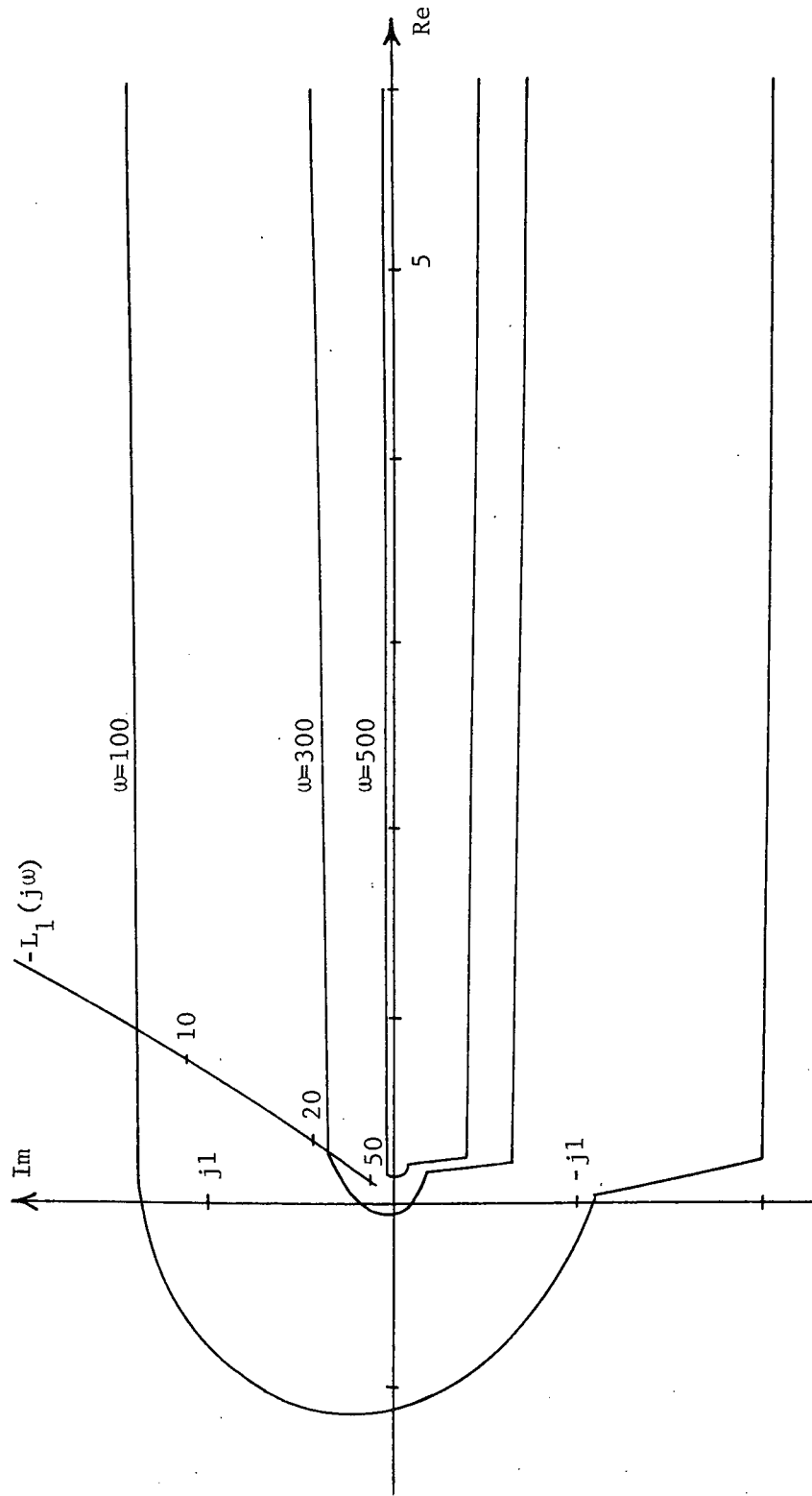


Figure 3.11b  
High Frequency Boundaries of Acceptable Regions  
of  $L(j\omega)$  with Comparison of  $L_1(j\omega)$

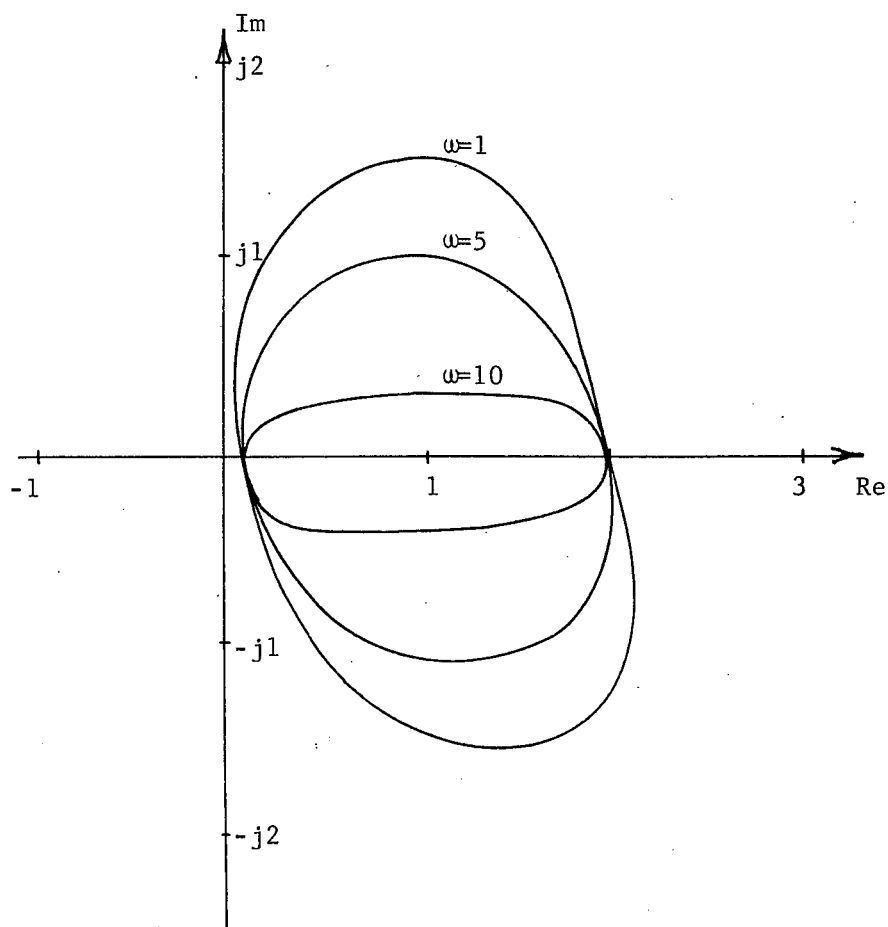


Figure 3.12

Range of  $P_o(j\omega)/P_{eq}(j\omega)$

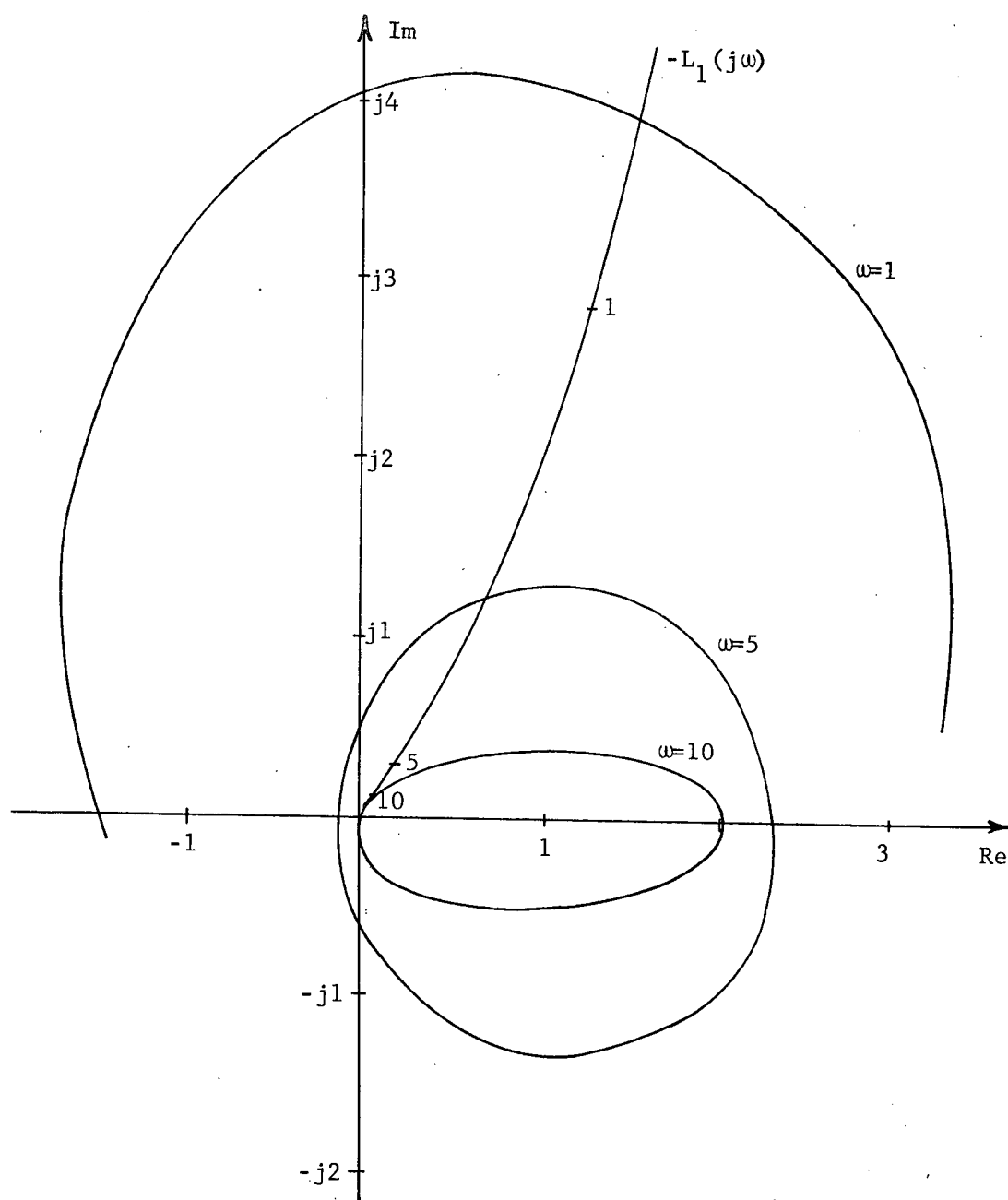


Figure 3.13  
Acceptable Regions of  $L(j\omega)$   
with Comparison of  $L_1(j\omega)$

A polar plot of  $L_1(j\omega)$  is also shown in Figure 3.13. It is first noted that  $L_1(j\omega)$  evaluated at  $\omega$  equal to one does not fall within the corresponding acceptable region for  $L_0(j\omega)$ . This is not surprising since the specifications in the last example were not met at low frequency using  $L_1(j\omega)$ . However, at  $\omega$  equal to 5 and 10,  $L_1(j\omega)$  does not fall within the corresponding acceptable region even though it is known that  $L_1(j\omega)$  does meet the specifications in Design Example Two at these frequencies. This is partially due to the fact that the specifications listed in Table 3.1 are not exactly equivalent to the specifications given in Figure 3.7; however, the primary error comes from the analog computer calculations and in determining the region of  $P_o(j\omega)/P_{eq}(j\omega)$  from these calculations.

The next step in the procedure would be to design a second  $L_0(j\omega)$  based on the regions shown in Figure 3.13. Such a design will not be carried out since the basic method has been illustrated; however, note that the magnitude of  $L_0(j\omega)$  of such a second design would be greater than the magnitude of  $L_1(j\omega)$ . Thus, a second design would be a step in the right direction toward meeting the specifications as given in Table 3.1.

### 3.4 Summary

Two design procedures which rely on the numerical solution of the system equation via computer simulation have been presented. Simple design examples have also been carried out which demonstrate that it is possible to perform the required steps in the

procedures; however, an optimal design has yet to be obtained.

It is of interest to consider the similarities and differences in the two procedures. Even though the procedures appear to be quite different they are actually very much alike. Note that in both procedures the design of the nominal loop gain  $L_0$  is carried out in the same manner in that acceptable regions are determined and an  $L_0$  is designed to fall within these acceptable regions. Also, it is shown in the next chapter that the specifications for the two procedures can be made identical. Thus, the only basic difference in the two procedures is that in procedure one it is assumed that the shape of the regions of acceptable  $L_0$  are circular, while in procedure two the shape of the regions of acceptable  $L_0$  are determined in the procedure itself. Observe that because of this assumption procedure one is more easily applied than procedure two. In procedure one it is only necessary to determine the maximum value of  $|E|$  while in procedure two it is necessary to determine the complete region of  $P_0/P_{eq}$ . It is seen in the next chapter that the price paid for the simpler calculation in procedure one is the greater difficulty in arriving at an optimal design.

A major difficulty in the procedures is the determination of the maximum value of  $|E|$  and the region of  $P_0/P_{eq}$ . The method which is presently employed is to run representations of all possible time-variations. Unfortunately, even where there are only one or two time-varying parameters a large number of runs are required. If a system has several time-varying parameters,

the number of combinations of time-variations are prohibitively large to test representative samples of all possible time-variations. Thus, for systems having several time-varying parameters a procedure is needed for determining the worst case variations without having to perform a search over all possible variations.

In this chapter the examples demonstrated that it is possible to carry out the steps in the procedures using numerical solutions from computer simulation. However, the examples do not have the depth necessary to observe the advantages and disadvantages of the procedures nor do they illustrate how a design close to the optimal design may be obtained. In the next chapter the design of a system having a time-varying gain is carried out in depth so that greater insight into the procedures can be obtained.

## CHAPTER IV

### DESIGN EXAMPLE

#### 4.1 Introduction

Previous examples have demonstrated the steps in the two design procedures with little consideration given to the practical problems encountered in carrying out these steps or of the performance of the system involved. In this chapter a design example will be considered with greater depth of study in an effort not only to gain further insight into the design procedures but also to consider the practical problems associated with the procedures, as well as to investigate the performance of the system. The example which will be considered is shown in Figure 4.1.

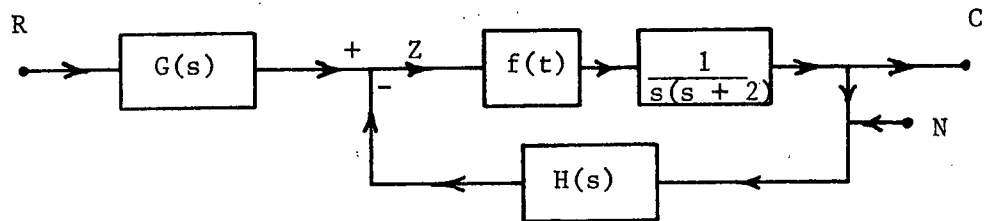


Figure 4.1  
Design Example

The function  $f(t)$  is a time-varying gain which can vary between 1 and 10. The general structure of  $f(t)$  will be discussed in more detail later in the chapter. Although this example may appear rather restricted, note that it is a special case of a more general class of systems where the only time-varying element is a time-varying gain as shown in Figure 4.2.



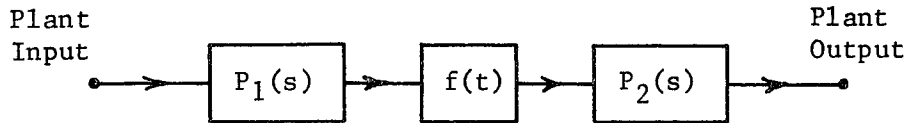


Figure 4.2  
General Structure of Plant Where Only  
Time-Varying Element Is a Gain

The portions of the plant  $P_1$  and  $P_2$  are linear and time-invariant with the time-varying gain represented by  $f(t)$ . Although  $P_1$  and  $P_2$  are integral portions of the plant and cannot be modified by the designer, any system having such a plant can be put in the form shown in Figure 4.3 so that  $P_1$  and  $P_2$  can be considered as integral portions of the compensations  $\tilde{G}$  and  $\tilde{L}$ .

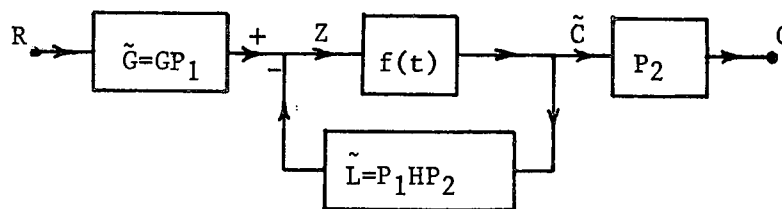


Figure 4.3  
General System with Time-Varying Gain

In addition since  $P_2(s)$  is a known transfer function at the system output, system specifications on  $\tilde{C}$  can be obtained from the system specifications on  $C$ . The portions of the plant  $P_1$  and  $P_2$ , therefore, need not be considered in the study of the time-varying characteristics of the system. Also, since  $G(s)$  is primarily a prefilter, the salient properties of the class of systems which have only a time-varying gain can be investigated by considering only the time-varying gain with a feedback loop for compensation.

Results of the design example shown in Figure 4.1 can thus be applied to the more general class of systems as shown in Figure 4.3 where  $f(t)$  varies by a factor of ten. The transfer function has been included in the plant of the example so that the wave forms of the time-invariant system will be familiar and the effects of the time-variation will be more clearly evident.

#### 4.2 Methods of Calculations

Since the design procedures require numerical calculations of the Fourier transform for various signals in the system, it was necessary to derive a method for performing these calculations. Due to the fact that both design procedures require a search over the possible time variations for several frequencies, any method used must not only be accurate but also must be able to be performed quickly in order that a fairly large number of calculations may be made within a reasonable period of time.

The first approach was to simulate the system on an analog computer and calculate the required Fourier transform directly on the computer. This technique, which is described in Reference (44), is relatively fast and the results are satisfactory as long as the value of the Fourier transform is above the noise level of the computer and the run time of the computer can be accurately timed. A disadvantage of this approach is that a separate run is required for each value of frequency unless a large computer is available with at least six amplifiers for each frequency of interest in addition to the system simulation requirements. A major difficulty in analog computation, however, is the synthesis of time variations. The method of producing variations must be of such precision that

the variations can be duplicated for repeated calculations of the Fourier transform at different frequencies, yet it must be flexible enough so that the characteristics of the variations may be quickly altered. The ability to precisely control and quickly change exponential variations on the analog computer is the primary reason for these type variations in the examples of the previous chapter. The computer system used for this first approach consisted of a Beckman 2200 analog computer and an SDS model 920 digital computer which had been combined into a hybrid system. The Beckman analog computer is a fully shielded, solid state,  $\pm 100$  volt machine. The particular configuration consisted of a total of 36 amplifiers and four multipliers along with a complement of logic and an accurate real time clock. In addition, there were sufficient servo potentiometers to provide satisfactory hybrid operation. The SDS digital computer had an 8K storage with a high speed paper tape reader and teletypewriter input-output.

Use of the analog computer alone proved to be, on the whole, unsatisfactory. It is required that the operator make each run, and read and record the values of the calculated Fourier transform. This in itself is a lengthy procedure; but, in addition, calculations must be made on each data point and the result plotted. The entire process proved to be extremely lengthy.

By utilizing the full hybrid capabilities of the computer, calculation times were significantly reduced. The digital computer was programmed to change the time variations, control the analog computer, read the computed values, perform the required calculation, and print the results. Thus, many more calculations could be

performed with the hybrid configuration in a given time than with the analog alone.

The analog computer's method of calculating the numerical Fourier transform proved satisfactory for the first design procedure; however, in the second design procedure difficulties were encountered with this method of computation. In the second design procedure it is necessary to compute the Fourier transform of the system output. Since the system input is a step function, the system output generally goes to a constant value which will be denoted  $C_{\infty}$ . In such a case the numerical computation methods yield the sum of the Fourier transform and the constant  $C_{\infty}$ . Thus, in order to determine the Fourier transform it is necessary to subtract the constant  $C_{\infty}$  from the computed result. For the majority of frequencies it was found that the difference in  $C_{\infty}$  and the computed results was small. This means that the inaccuracies, which are small in comparison to the large value of the computed result, are large when compared to the small value of the difference in  $C_{\infty}$  and the computed result. Thus, in many cases it was impossible to obtain an accurate value of the Fourier transform of the system output with the analog method of computation.

In an effort to eliminate this problem with the second design procedure, it was decided to use the digital computer to calculate the numerical Fourier transform instead of the analog computer. This approach would allow for a more accurate computation of the transform. The procedure was to simulate the system on the analog computer, sample and store the sample values of the signals of interest, which in the case of the second design procedure are the

plant input and plant output, then compute the values of the Fourier transform at the frequencies of interest. The algorithm described in Reference (48) was used to compute the numerical Fourier transform of the sampled signals. At this time the system was simulated on an EAI-TR20 analog computer with a PDP9-L digital computer being used to sample the signals and perform the numerical calculations. The combination could not be considered a hybrid computer since the digital computer could not be used to control the analog computer. Although a number of calculations were performed on this set of computers, the attempt on the whole was considered a failure. The lack of success was not due to the methods of computation which were basically sound but to the inadequacy of the computers themselves. This attempt illustrates the fact that relatively sophisticated computers are required for the necessary computations in the two design procedures.

The necessary simulations and Fourier transform calculations of the example in this chapter were done wholly on a digital computer. The computer used was an IBM 1130 with a core storage capacity of 16K with three disk drives. The basic program used to simulate the system was the Continuous System Modeling Program for the IBM 1130 computer. The program was modified by the addition of several subroutines for the purposes of storing signals, calculating the Fourier transform, modifying the time-variations, and printing results. The primary disadvantage to this approach is that it requires a good deal more time to make a calculation than with the hybrid computer. To illustrate the difference in run time, assume it is necessary to calculate the Fourier transform at five fre-

quencies for a signal of ten seconds duration. On a hybrid computer with the Fourier transform calculated on the analog portion of the computer, one run would require ten seconds of computation time with five runs being required. Add approximately 30 seconds additional time to allow for data reading and parameter changing and the total time becomes 80 seconds. The digital computer requires from two to four minutes to generate the required signals of a third or fourth order system plus approximately 30 seconds to calculate the Fourier transform at each frequency for a total run time of approximately five minutes. This time increases substantially as the order of the system increases. The primary advantage in using the digital simulation is the increase in accuracy that is obtainable. However, one also gains other advantages. Time-variations are easily simulated and modified on the digital computer so that it is possible to develop search techniques for determining the worst case variations which is required in the first design procedure and for generating randomly varying variations which is required in the second design procedure. Thus, once the program is started the operator need do nothing more until a solution is obtained.

#### 4.3 Specification

As was discussed in Chapter One, system specifications are more commonly given in the time domain than in the frequency domain; thus, there is no reservoir of experience upon which to draw in assigning frequency domain specifications as there is for time domain specifications. In order to determine realistic frequency domain specifications for the example considered in this chapter, it will be necessary to first consider the acceptable system step

response in the time domain and then attempt to relate these to the frequency domain. The approach will not be rigorous but will consist of examining the magnitude of the Fourier transform of a sampling of error functions and assigning a frequency domain specification based upon this examination.

Consider the first form of frequency domain specification which is given by

$$|C(j\omega) - C_0(j\omega)| = |E(j\omega)| \leq M(\omega) \quad (4-1)$$

where  $C_0$  is the desired step response,  $C$  is the actual step response, and  $M$  is a real number which can depend upon  $\omega$ . The form of this specification naturally suggests a time domain specification of the form

$$|c(t) - c_0(t)| = |e(t)| \leq m(t).$$

There are two graphical interpretations of this relation. The specification given by

$$|c(t) - c_0(t)| \leq m(t) \quad (4-2)$$

corresponds to a symmetrical envelope about the desired step response within which the actual step response must fall. Such a specification is shown in Figure 4.4.

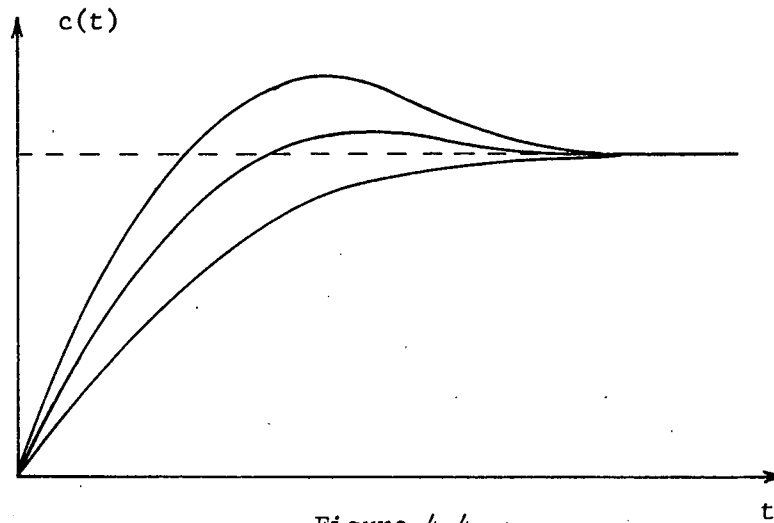


Figure 4.4  
Time Domain Specifications as Envelope  
About Desired Step Response

The specification can also be expressed in the form

$$|e(t)| \leq m(t) \quad (4-3)$$

which corresponds to a symmetrical envelope about the time-axis as shown in Figure 4.5.

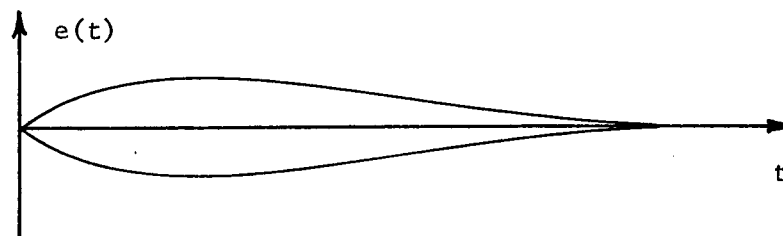


Figure 4.5  
Time Domain Specifications as Upper  
Bound on Error

In this form the specification represents an upper bound on the error. Although the specifications given in inequalities (4-2) and (4-3) are equivalent, the specification as given in inequality (4-3) is somewhat more convenient to study since it is independent of the



desired step response. In all probability, however, the specification for any particular system will first be established in the form of inequality (4-2) since one is generally more familiar with acceptable step responses than with acceptable error functions.

For the example considered in this chapter, it will be assumed that the desired system transfer function is given by

$$T(s) = \frac{4}{s^2 + 2.8s + 4}$$

This transfer function will occur in the system of the example if the gain is constant at 4 and the compensations are given by

$$H(s) = G(s) = \frac{s + 2}{s + 2.8}$$

The transfer function corresponds to a second order system having a damping ratio of 0.7 and an undamped natural frequency of 2. The step response of this transfer function, which is the desired step response, is shown in Figure 4.6.

In assigning the specification envelope, consideration must be given to the usual time domain specifications of rise time, overshoot and settling time. The rise time determines how quickly the lower bound of the envelope must increase while the peak overshoot determines the maximum values of the envelope's upper bound and the settling time determines how quickly the envelope must converge to the final value. In the final analysis, however, it will be necessary to assign an acceptable minimum step response and an acceptable maximum step response. These maximum and minimum step responses will constitute the specification envelope. Note that the time domain specification given in inequality (4-2) demands that the envelope be symmetrical about the desired step response. If the maximum and minimum step responses are not symmetrical about the desired step response, the desired step response must be redefined such that this

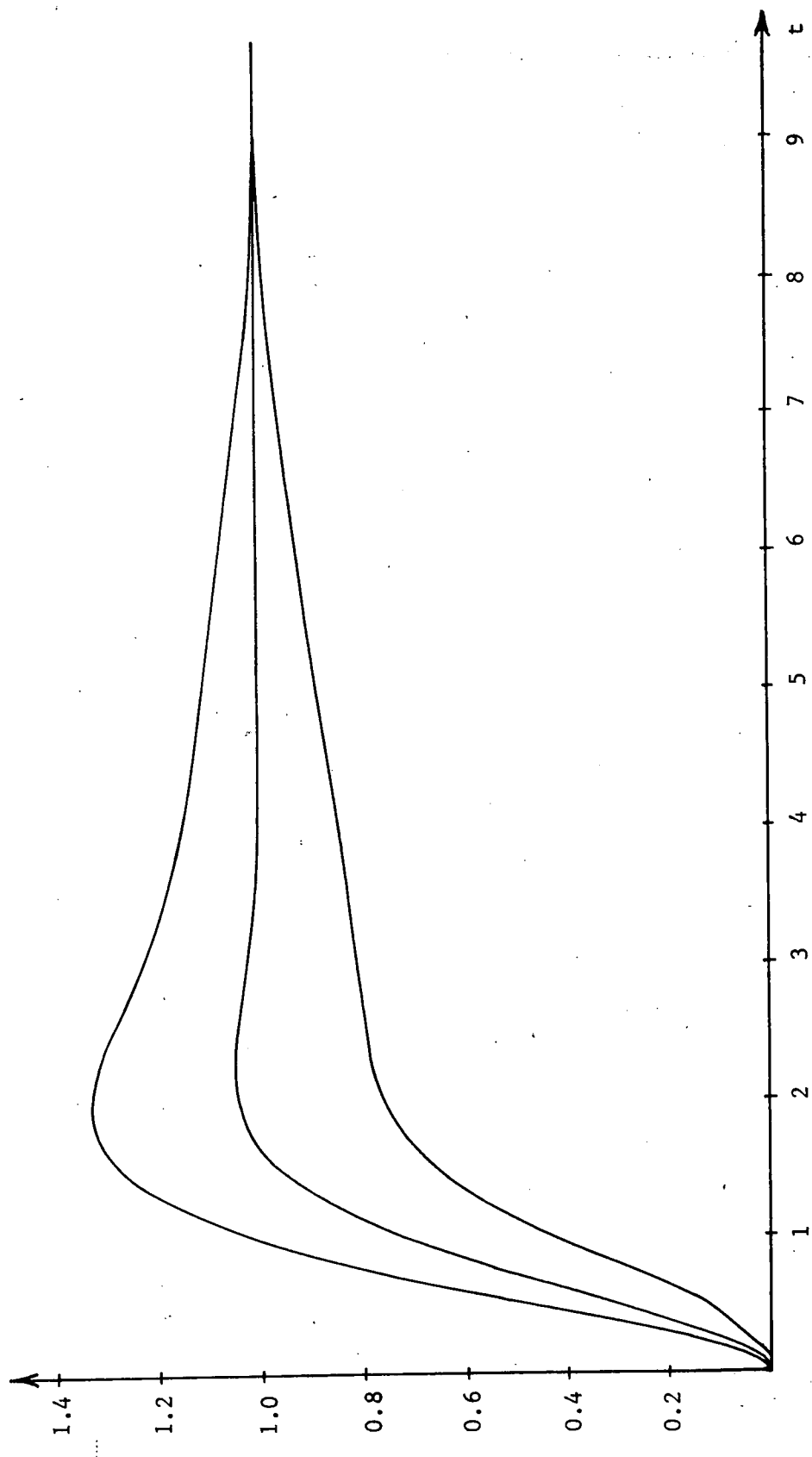


Figure 4.6  
Time Domain Specifications for Example; Envelope about Desired Step Response

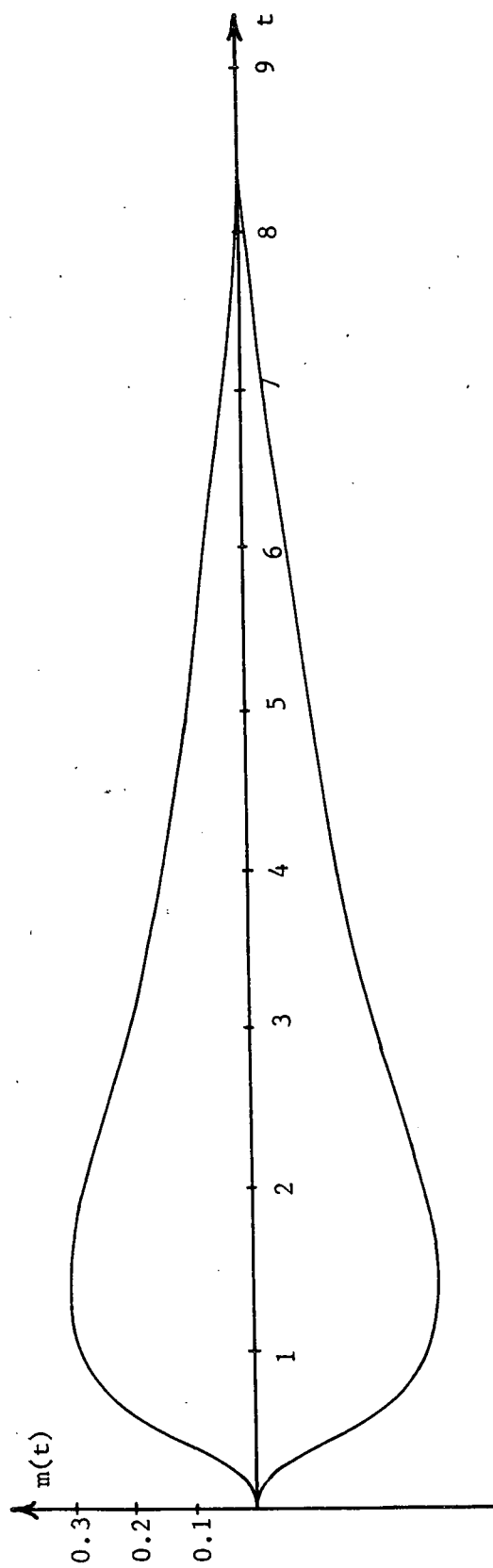


Figure 4.7  
Time Domain Specification for Example;  
Bound on Error

symmetry is achieved. The assumed specification envelope for the example is shown in Figure 4.6 with the desired step response. This envelope corresponds to a minimum rise time of approximately 1.5 seconds, a peak overshoot of 30% and a maximum settling time of 8.5 seconds.

The upper bound on the error which corresponds to the specification in Figure 4.6 is shown in Figure 4.7. The problem now is to determine the frequency domain equivalent of this specification in the form of an upper bound on the magnitude of the Fourier transform of the error. This frequency domain specification will be in a form as shown in Figure 4.8.

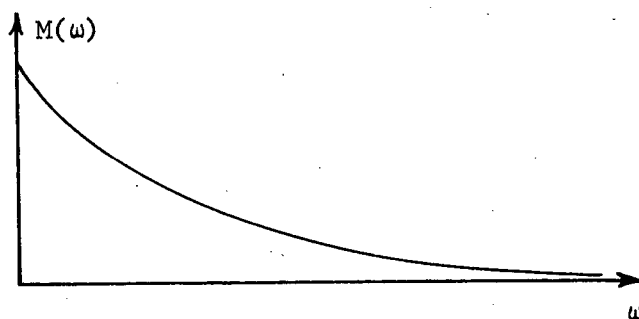


Figure 4.8  
Form of Frequency Domain Specification

The desired objective is to determine the frequency domain envelope  $M(\omega)$  such that if the magnitude of the Fourier transform of the error is less than or equal to the maximum value  $M(\omega)$ , the error will fall within the time domain envelope given in Figure 4.7.

A difficulty is now encountered which again emphasizes the complexity of the problem of obtaining frequency domain specifications from time domain specifications and vice-versa. Assume that an error  $e(t)$  satisfies the time domain specification of Figure 4.7 and the magnitude of the Fourier transform  $|E(j\omega)|$  satisfies the frequency domain specification of Figure 4.8. Let the error  $e(t)$  be shifted in time by the amount  $\tau$  such that  $e(t - \tau)$  now lies

outside the time domain specification. The Fourier transform of  $e(t-\tau)$  is  $E(j\omega)e^{-j\omega\tau}$  which has the same magnitude as the Fourier transform of  $e(t)$  and thus will still satisfy the frequency domain specification. The reason for this difficulty is due to the fact that  $e(t-\tau)$  is nonminimum phase so that the uniqueness between phase and magnitude does not hold. Thus there is no unique relationship between the error  $e(t)$  and the magnitude of its Fourier transform. It is easily seen then that if the frequency domain specification is given in the form shown in Figure 4.8 and the time domain specification is given in the form shown in Figure 4.7, there will always be functions which will satisfy the frequency domain specifications and yet violate the time domain specifications.

In stable systems it is generally the case that the maximum error will occur relatively close to the origin, then will settle to zero. Otherwise, the actual step response would closely follow the desired step response through its maximum change; then, after attaining the final value would show a deviation. It would be necessary for a system to possess some form of large time delay to exhibit such behavior. Since there is a large class of systems which do not possess such time delays and therefore will not exhibit a delayed error, it will still be assumed that the time domain specification is given in the form of Figure 4.7.

A number of possible error functions and their Fourier transform magnitudes will now be examined in order to determine the error function characteristics in the frequency domain.

Figure 4.9a shows four functions which, for different values of time, lie on but do not exceed the error bound  $m(t)$ . Figure 4.9b

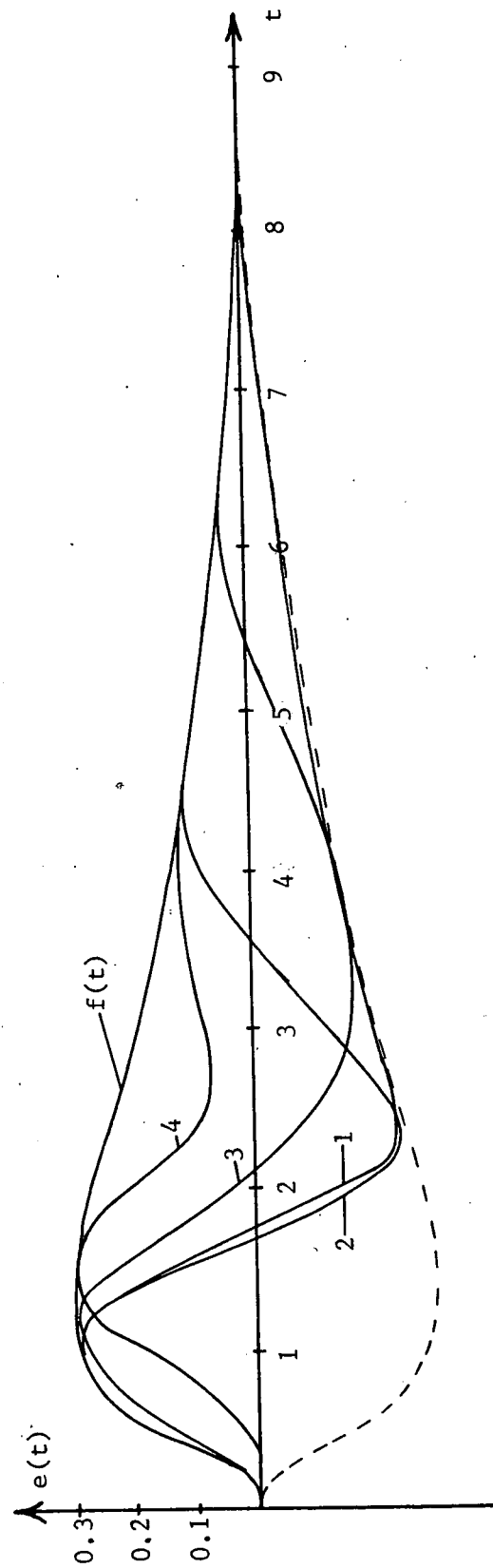


Figure 4.9a  
Error Function Series One

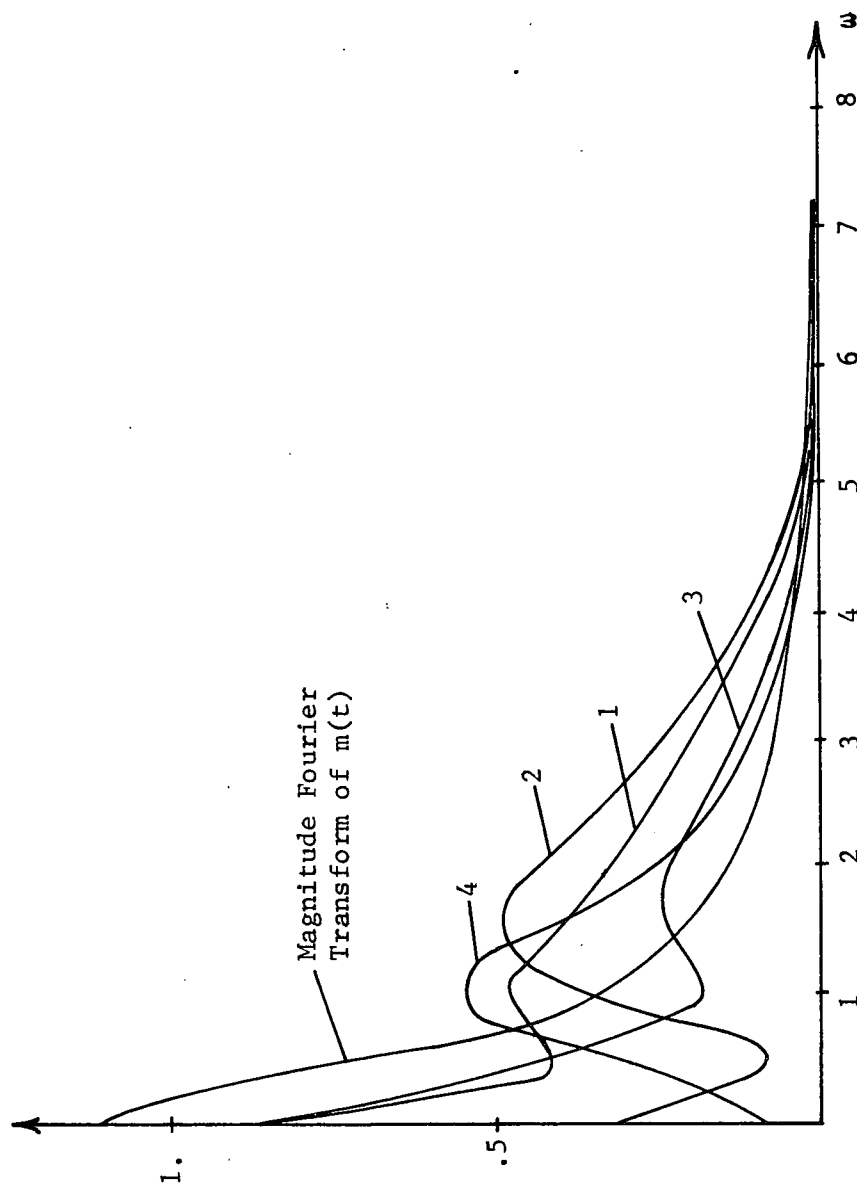


Figure 4.9b  
Fourier Transform Magnitudes of  
Error Function Series One

shows a plot of the magnitude of their Fourier transforms. Also shown for comparison is the magnitude of the Fourier transform of the time domain envelope  $m(t)$ . An error function that is exactly equal to  $m(t)$  has the largest zero frequency component allowable since this component is equal to the area under the curve. But since  $m(t)$  has few variations, its higher frequency component would be smaller than might be allowed. Functions 2 and 3 shown in Figure 4.9a cross the zero axis leaving about as much negative area as positive area and thus would be expected to have a relatively small low frequency component. Note that the type of variation for all four functions is similar so they would be expected to have similar higher frequency components. This is shown in Figure 4.9b where all four functions exhibit peaking around  $\omega = 1.5$ , then decrease rather quickly toward zero. Function 2 exhibits the greatest amount of variations in the time domain which shows up in the frequency domain as a little larger high frequency component than is observed in the other three functions.

Figure 4.10a shows a series of error functions which has a relatively large variation then settles fairly quickly to zero. The frequency domain representations are shown in Figure 4.10b. As expected, all exhibit a relatively small zero frequency component since the areas under the curves are relatively small. The higher frequency components depend upon the particular variations. If the variations show an oscillation effect as does Function 5, the higher frequency components will be larger; whereas, if the error deviates from zero only once then returns to zero as does Function 6, the higher frequency component will be smaller.



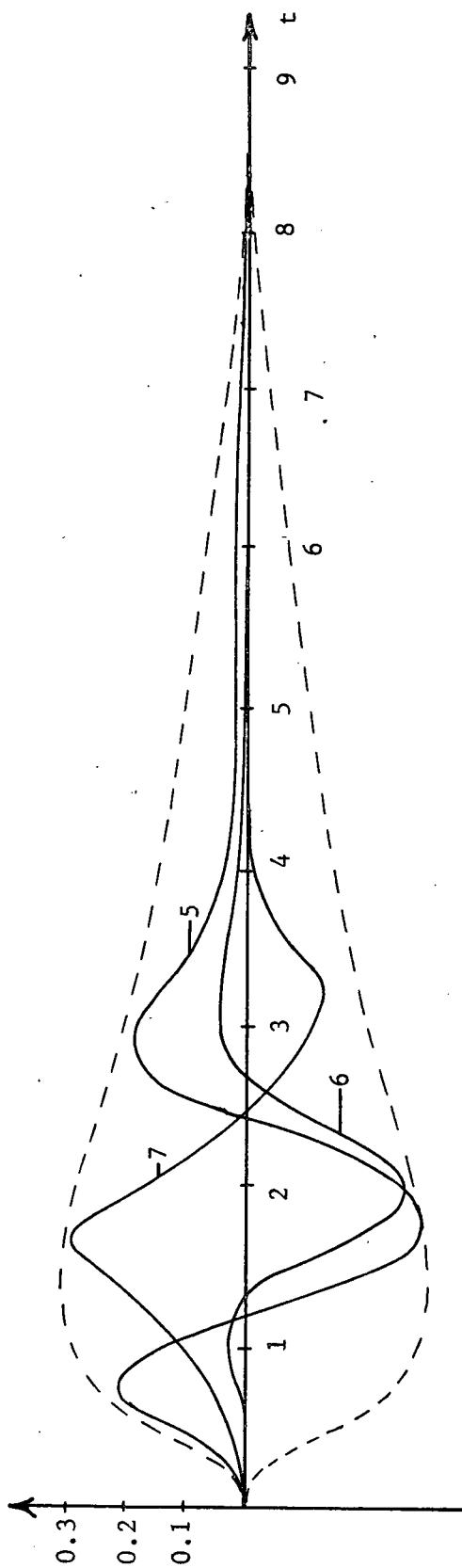


Figure 4.10a  
Error Function Series Two

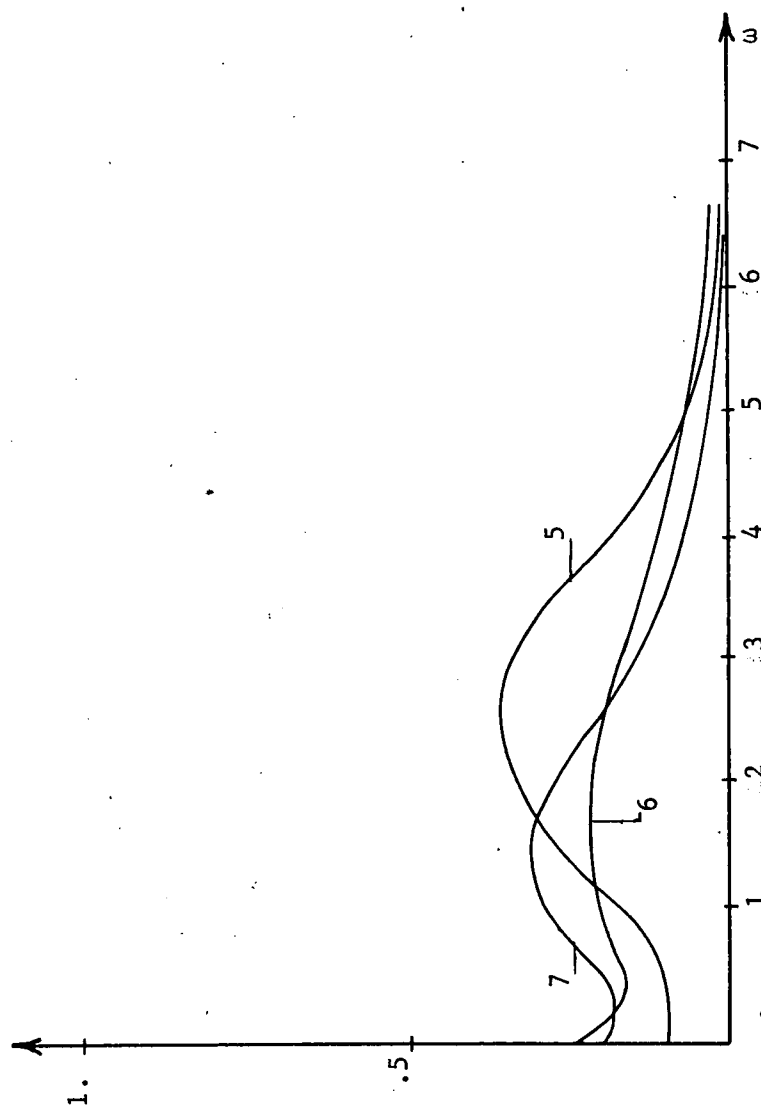


Figure 4.10b  
Fourier Transform Magnitudes  
of Error Function Series Two

Shown in Figure 4.11a is a series of functions having relatively low frequency oscillatory tendencies but remaining within the time domain error bounds. The magnitudes of their Fourier transforms are shown in Figure 4.11b. The oscillatory tendency is evident in large frequency components in the region of  $\omega$  equal from 2 to 3. Note that Function 10 is smaller than the other three, and thus its Fourier transform is also smaller in magnitude.

Figure 4.12a shows two functions which fall within the time domain error bound but are highly oscillatory. The magnitudes of their Fourier transforms are shown in Figure 4.12b. As expected, the oscillations show up as large high frequency components.

It would also be of interest to observe the effects in the frequency domain of a single fast variation. Figure 4.13a shows such a function with its frequency domain representation shown in Figure 4.13b.

Although the error functions shown in Figures 4.9 through 4.13 represent a small sample of the possible error functions, they were selected from the functions investigated because they give a good representation of the error functions possessing Fourier transforms with large magnitudes which are the types of functions that will establish the error bound in the frequency domain. The low frequency bound, that is, in the region from 0 to 1 radian per second, will be established by the Fourier transform of  $m(t)$  which is shown in Figure 4.9b. This is because as was previously mentioned  $m(t)$  has the largest low frequency component allowable. To establish the high frequency bound, it is observed that the magnitude of the

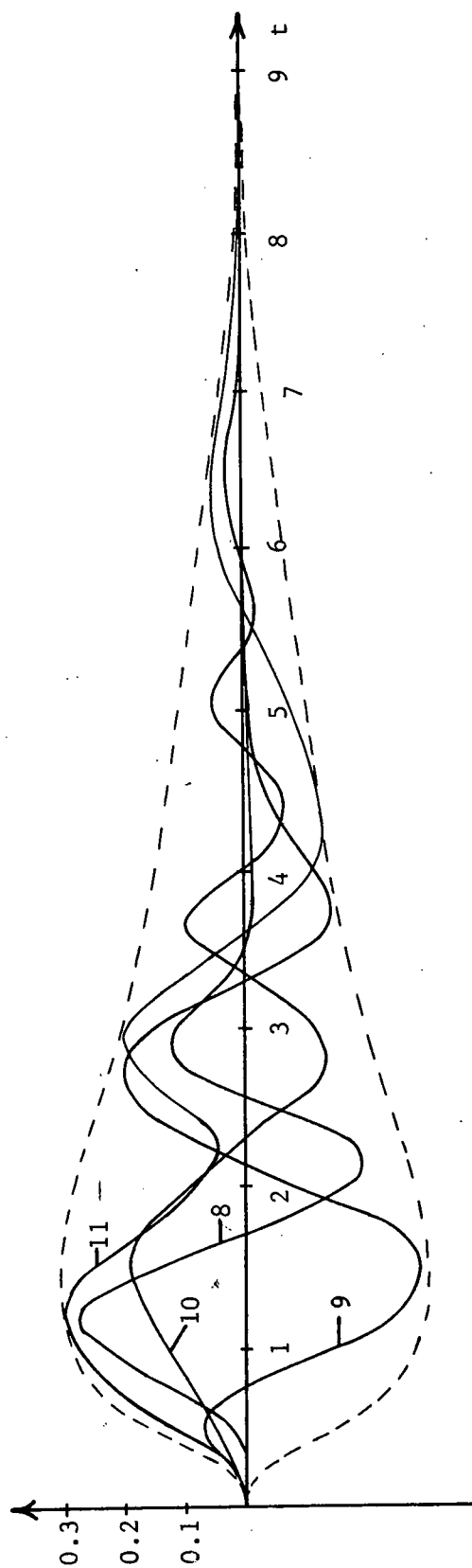


Figure 4.11a  
Error Function Series Three

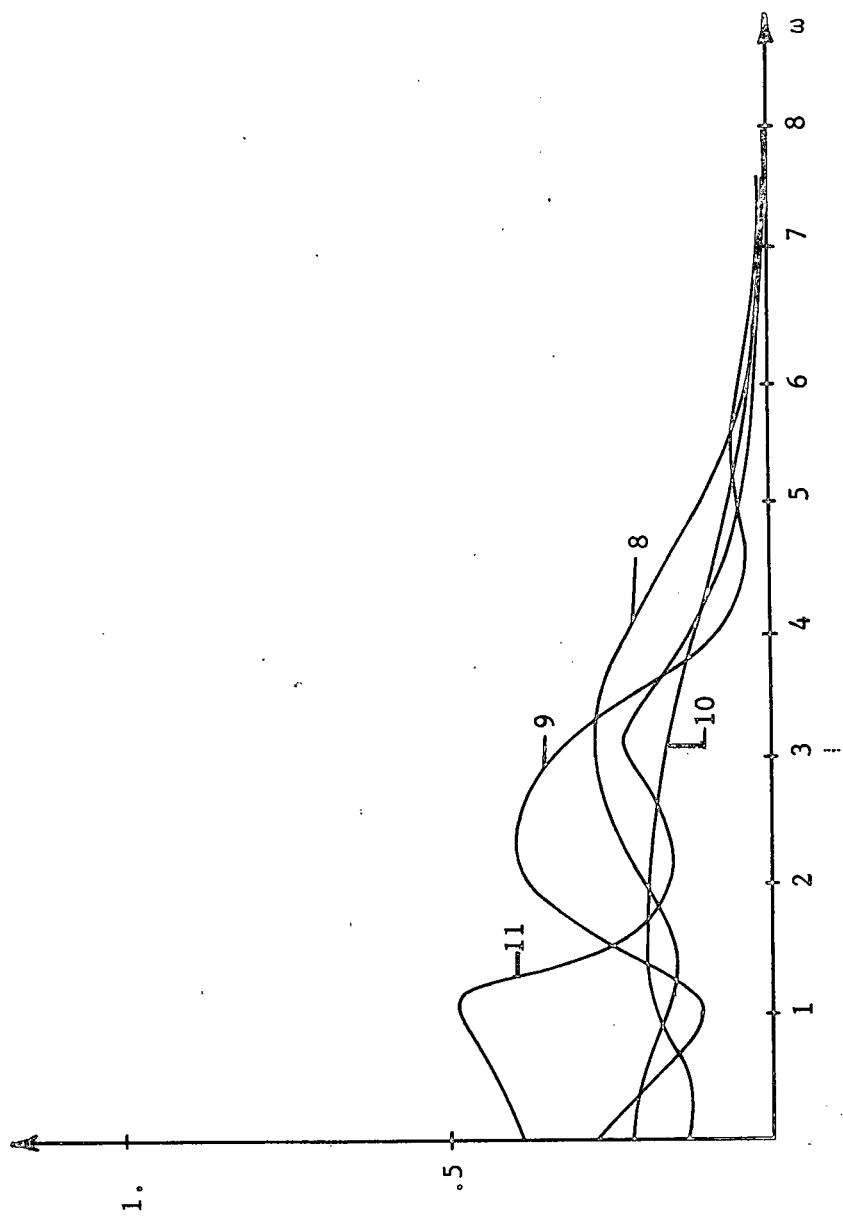


Figure 4.11b  
Fourier Transform Magnitudes  
of Error Function Series Three

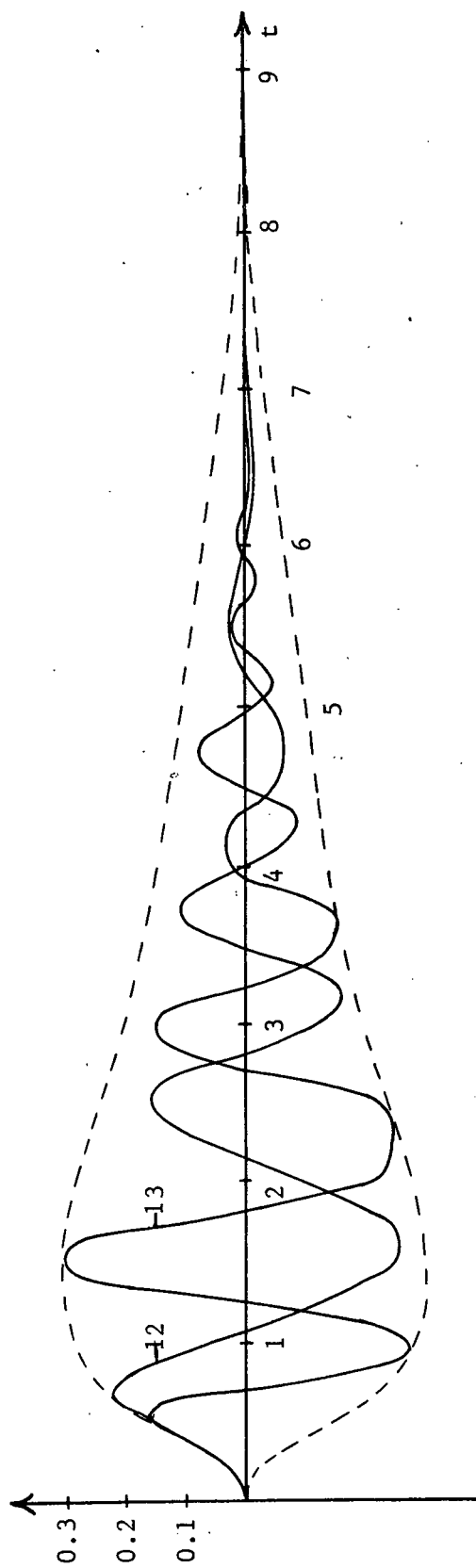


Figure 4.12a  
Error Function Series Four

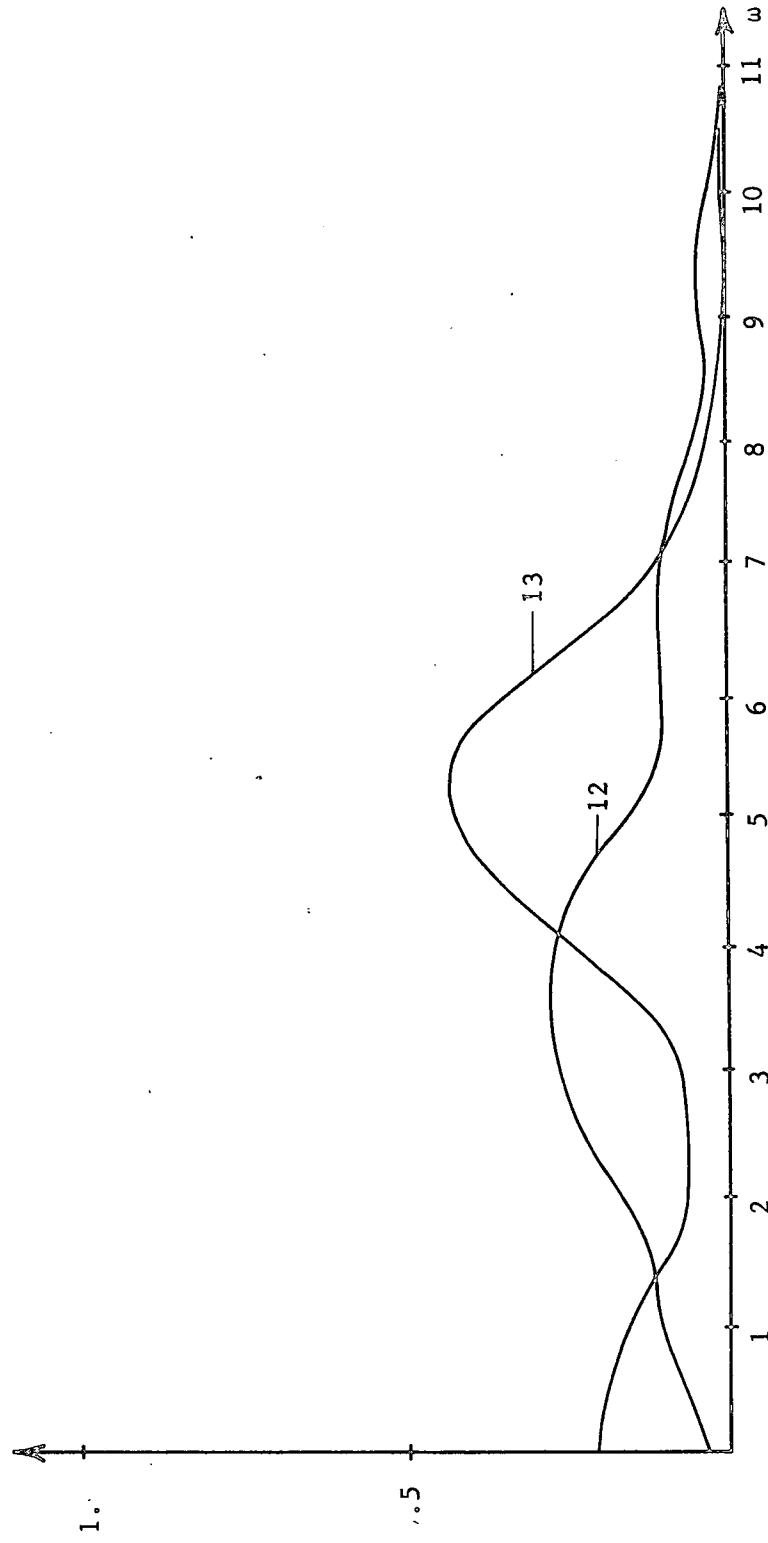


Figure 4.12b  
Fourier Transform Magnitudes  
of Error Function Series Four

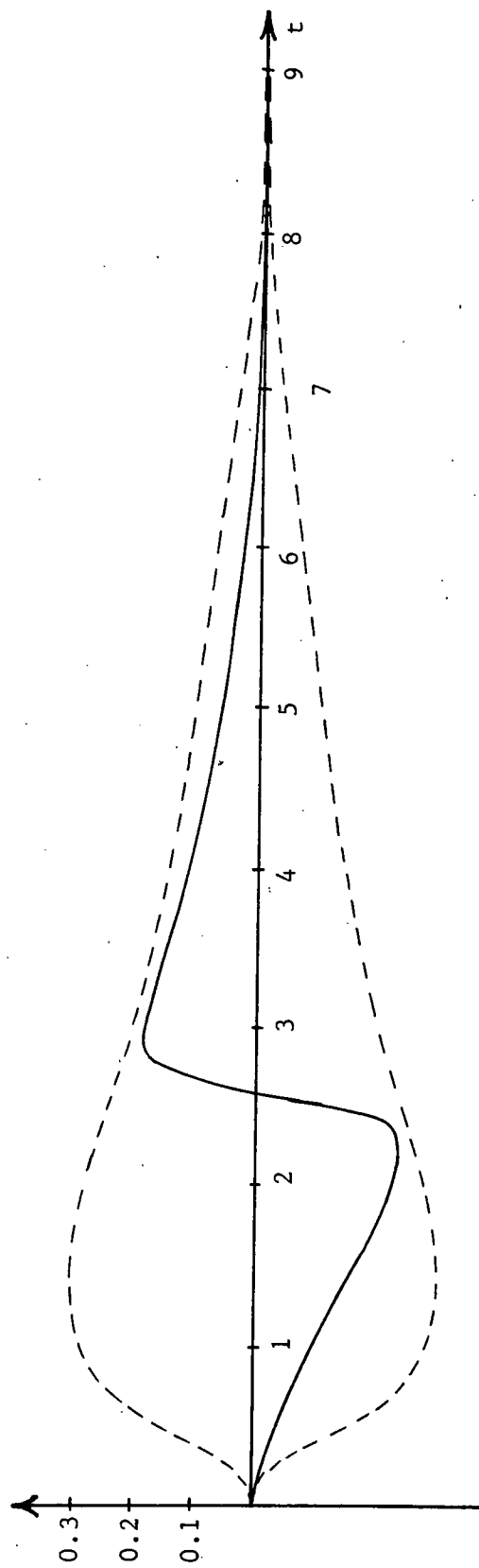


Figure 4.13a  
Error Function with Single Fast Variation



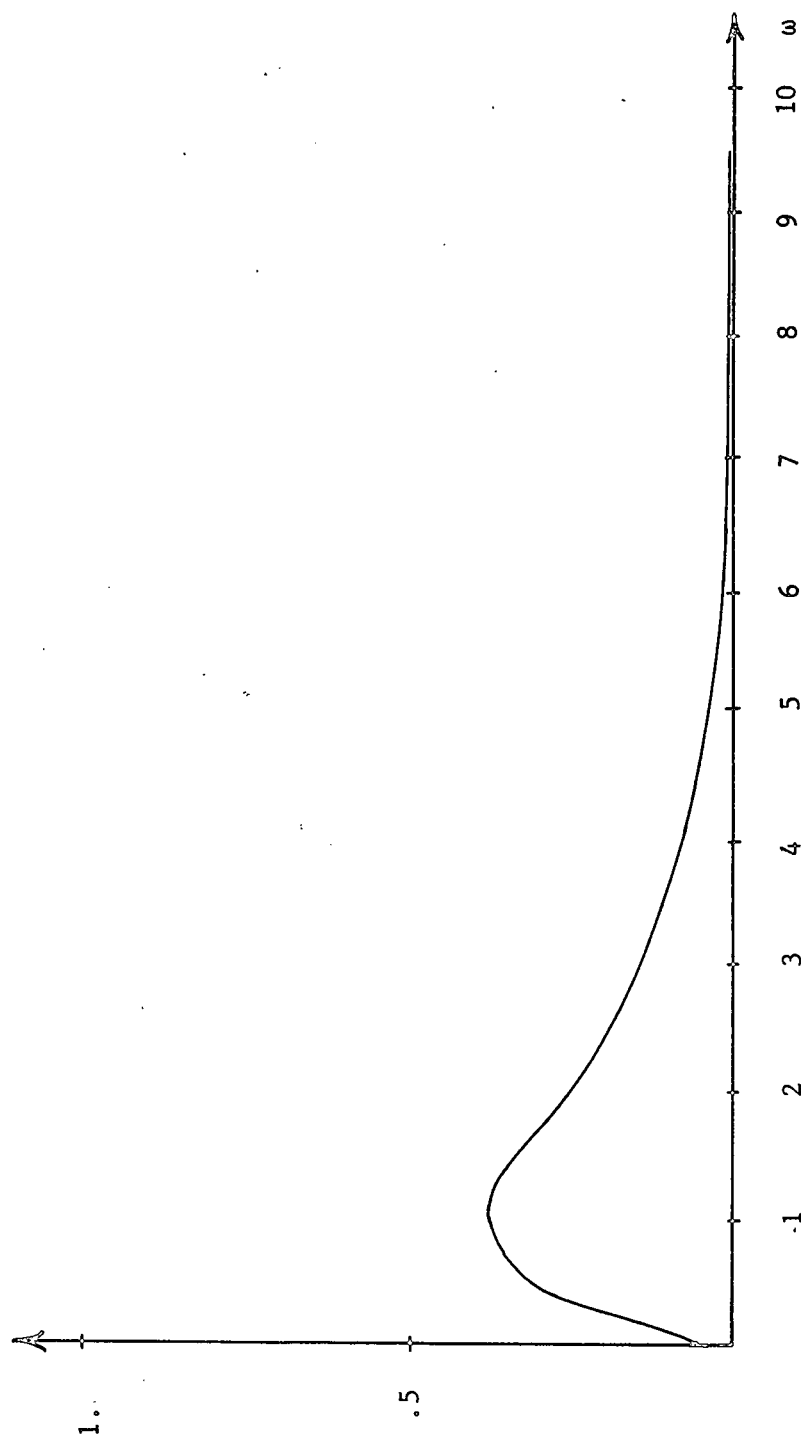


Figure 4.13b  
Fourier Transform Magnitude of  
Function with Single Fast Variation

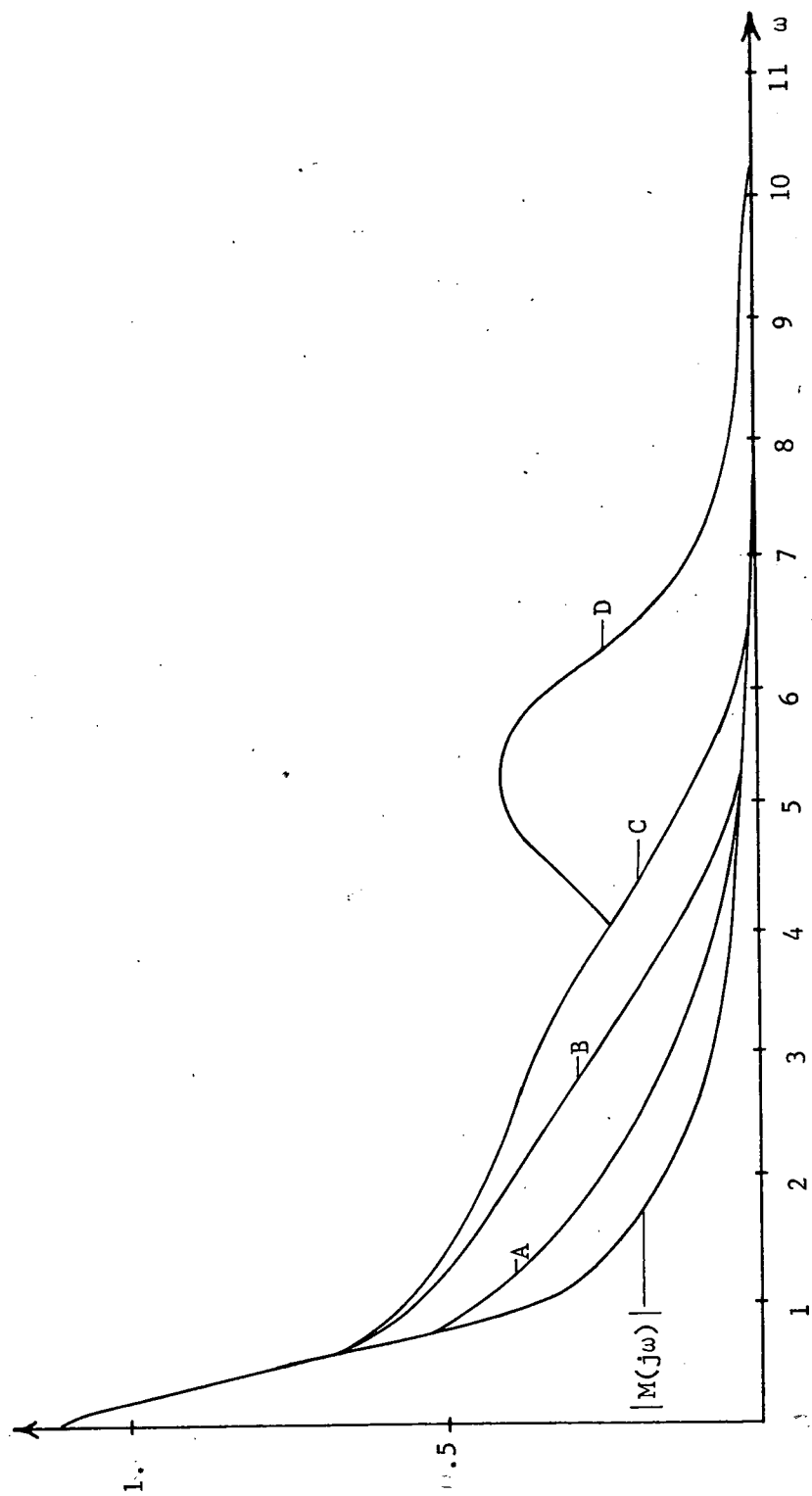


Figure 4.14  
Possible Frequency Domain Specification Envelopes

functions shown is less than .03 for  $\omega$  greater than seven radians per second unless the functions are highly oscillatory as shown in Figure 4.10a. Such oscillatory functions are generally undesirable even though they do not exceed the time domain error bound, and thus the high frequency bound should be set small enough to exclude these undesirable functions. Nevertheless, a high frequency oscillation of small magnitude is often considered acceptable; thus, instead of assigning a very small value for high frequencies, a relatively large value will be selected for the high frequency bound. The minimum value of the frequency domain bound at high frequencies will be selected as 0.05.

The frequency domain specification must now be established in the mid-frequency range. A minimum frequency domain envelope would be established by the magnitude of the Fourier transform of the time domain envelope  $m(t)$  which is shown in Figure 4.14. Also shown in Figure 4.14 are additional envelopes, the inclusion of which will allow additional types of functions. The envelope labeled A will allow Function 7 of Figures 4.10 and the Function shown in Figures 4.13. Note the similarity of these two functions. The envelope labeled B will allow the functions shown in Figures 4.9 and the functions shown in Figures 4.10 with the exception of Function 5. Observe that the large oscillatory nature of Function 5 excludes it from this set. The envelope labeled C allows all functions shown in Figures 4.10 and 4.11. The envelope labeled D is included in Figure 4.14 to demonstrate the large magnitude required in the region of  $\omega$  equal to five to six to include the highly oscillatory

functions shown in Figures 4.12. The error functions allowed by the envelope labeled B will be assumed to be acceptable in the example; thus, the magnitude labeled B will be selected as the frequency domain specifications. This selection will exclude the oscillatory type of functions shown in Figures 4.11 and 4.12 but will include functions having a high degree of variations.

As was discussed earlier, it is possible for the frequency domain specifications to be satisfied and the time domain specifications to be violated. With this in mind, it would be of interest to examine the magnitudes of the Fourier transform of a sampling of functions which violate the time domain specification but may be expected to satisfy the frequency domain specifications. Such functions could not have large oscillations for they would surely violate the frequency domain specification at high frequency, nor could such functions have large deviation without being oscillatory for they would then violate the low frequency specifications. One possible type of function that may violate the time domain specification but satisfy the frequency domain specification would increase slowly to a value outside the time domain specification then return to zero before the frequency domain specifications are violated at low frequency. Three possible functions are shown in Figure 4.15a with their Fourier transform magnitudes shown in Figure 4.15b. Even though functions 15 and 16 violate the time domain specification only a relatively small amount, the frequency domain specifications are nonetheless violated at low frequency. Function 17, on the other hand, does not violate the frequency domain specifications while the time domain specifications are violated. This, of course,

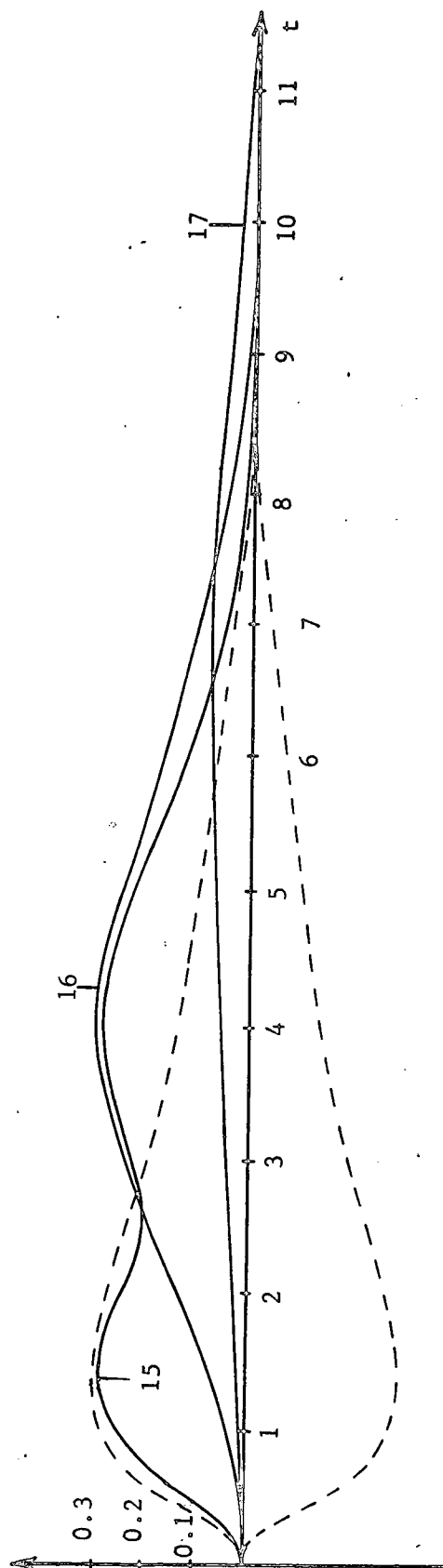


Figure 4.15a  
 Functions Which Violate Time Domain Specifications  
 But May Not Violate Frequency Domain Specifications; Series I

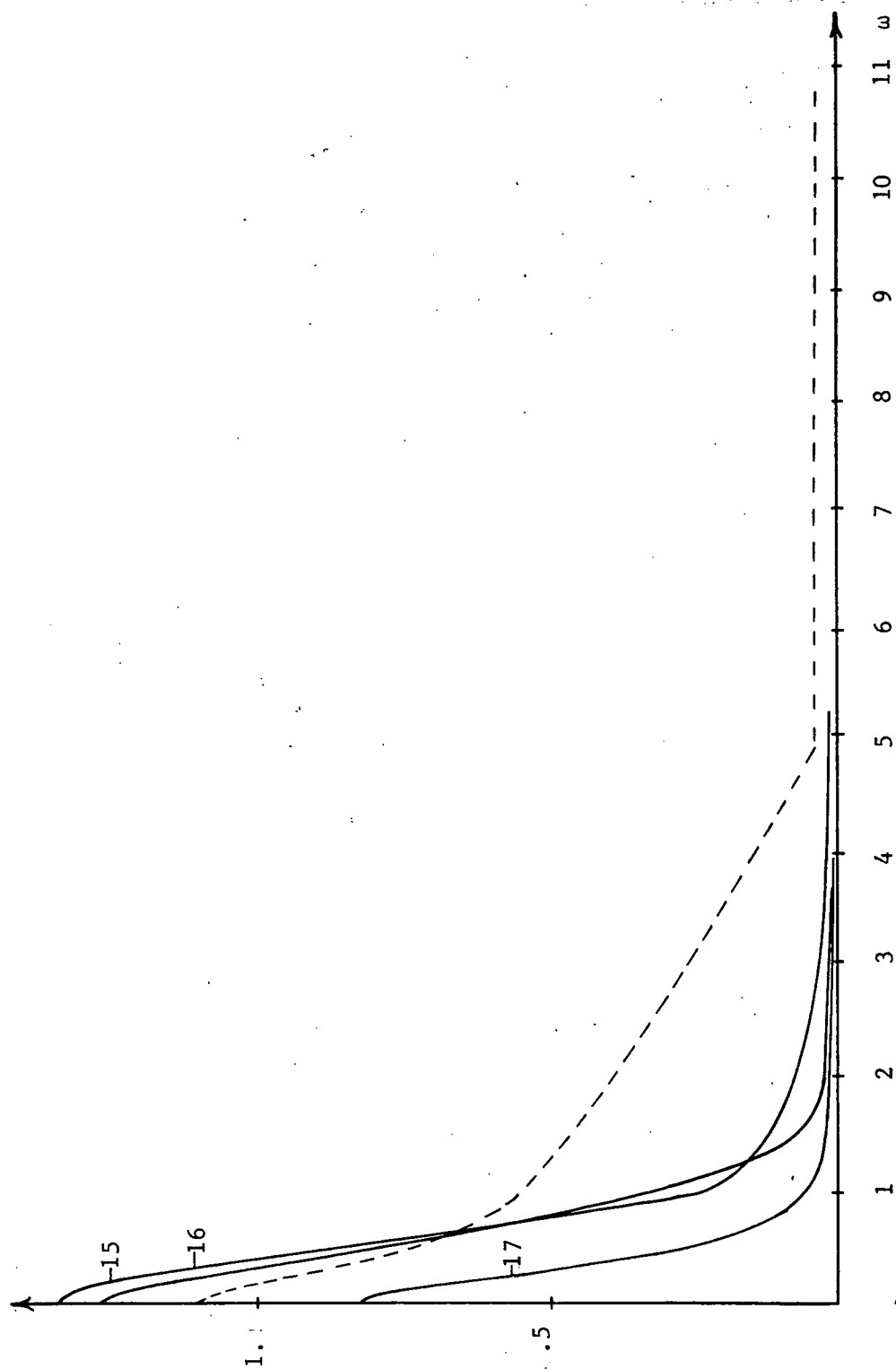


Figure 4.15b  
Fourier Transform Magnitudes of Functions Which Violate Time Domain Specifications; Series I

is because the magnitude of function 17 does not become large enough to have too large an area under the curve but does not return to zero quickly enough to avoid violating the time domain specifications. Functions such as function 17 cannot be eliminated by altering the frequency domain specifications without also excluding the desirable functions. However, the slowly settling component in such functions is probably due to poles near the origin as would occur if  $L(j\omega)$  (see Figure 4.3) were assigned a zero near the origin and the magnitude of  $L(j\omega)$  were not sufficiently large in the low frequency range. If functions of this type occur, the cause will probably be evident and can thus be eliminated from the design.

Another type of function which could possibly violate the time domain specification but not the frequency domain specification would quickly reach a point outside the time domain specification then return to zero to avoid violating the frequency domain specification at low frequency. Two such functions are shown in Figure 4 16a with their Fourier transform magnitudes shown in Figure 4 16b. Even though function 18 violates the time domain specifications, it would in fact satisfy these specifications if it were shifted properly in time. Function 18 violates the frequency domain specification only slightly at  $\omega$  equal to five radians per second while function 19 completely satisfies the frequency domain specification. Note that the magnitude of the Fourier transform of both functions remains relatively large at frequencies around six to nine radians per second. This is undoubtedly due to the fast

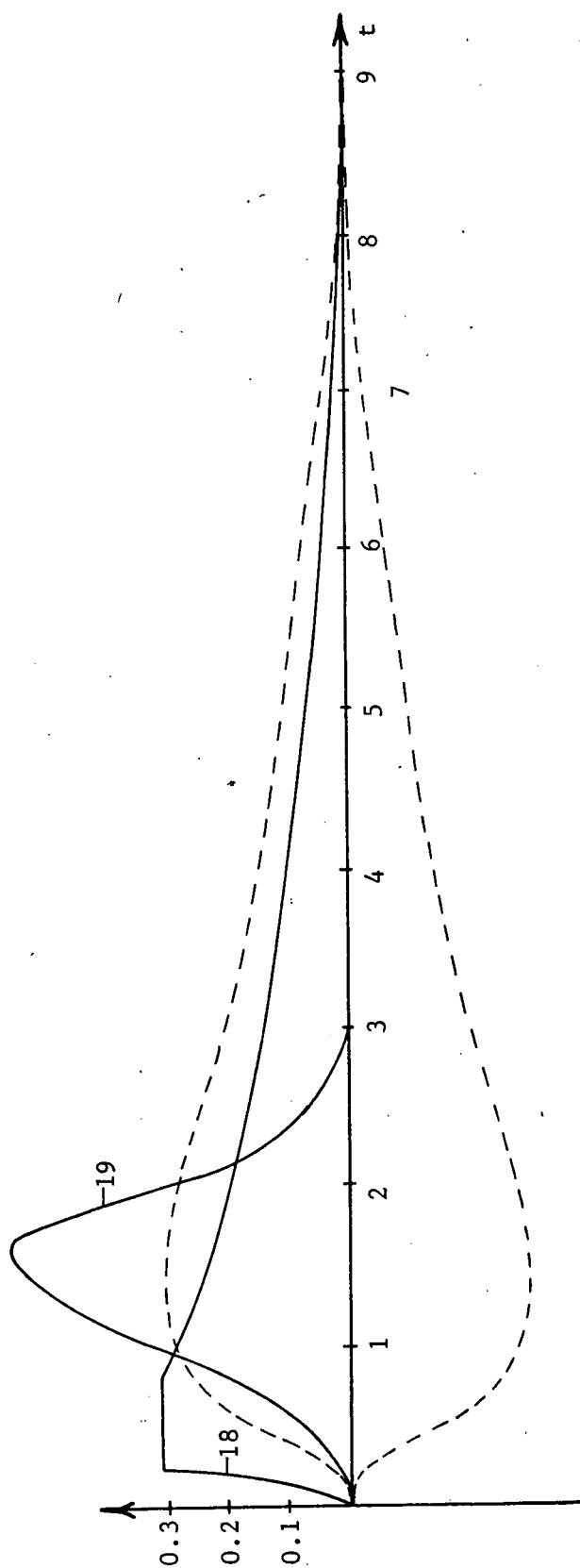


Figure 4.16a  
 Functions Which Violate Time Domain Specifications  
 But May Not Violate Frequency Domain Specifications; Series II



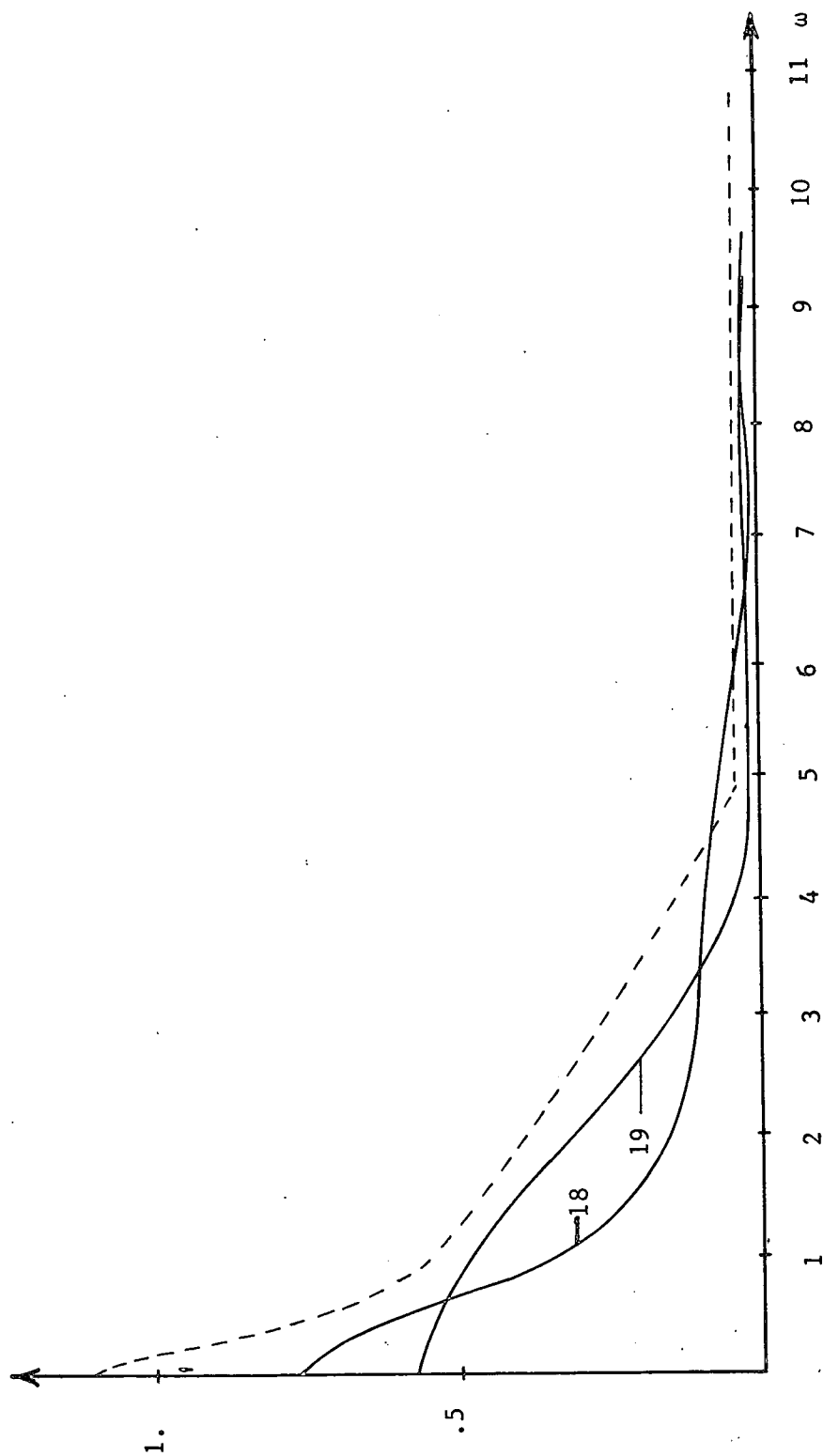


Figure 4.16b  
 Fourier Transform Magnitudes of Functions  
 Which Violate Time Domain Specifications; Series II

rate of variations of the functions. It is likely that such functions can be controlled by reducing the high frequency specification. A reduction at high frequency will not be made on the frequency domain specification which has been chosen, but careful attention will be paid as to whether or not such error functions become present in the design of the example.

To summarize, the frequency domain specification which is shown in Figure 4.17 has been chosen as a counterpart to the time domain specification shown in Figure 4.7. The selection was based on a small but what is felt to be a representative sampling of error functions. It was also pointed out that an error function satisfying the frequency domain specification will not necessarily satisfy time domain specifications as shown in Figure 4.15; however, such instances would have to be due to some form of time delay within the system or a slowly settling component within the system. In such instances the particular portion of the system which is causing the difficulty would have to be examined separately to see if it can be eliminated or its effect reduced to an acceptable level.

The frequency domain specifications used in the second design procedure must now be determined. These specifications have been assumed to be given in the form

$$k_1(\omega) \leq \left| \frac{C(j\omega)}{C_o(j\omega)} \right| \leq k_2(\omega) \quad (4-4)$$

$$\theta_1(\omega) \leq \text{Arg} \left[ \frac{C(j\omega)}{C_o(j\omega)} \right] \leq \theta_2(\omega)$$

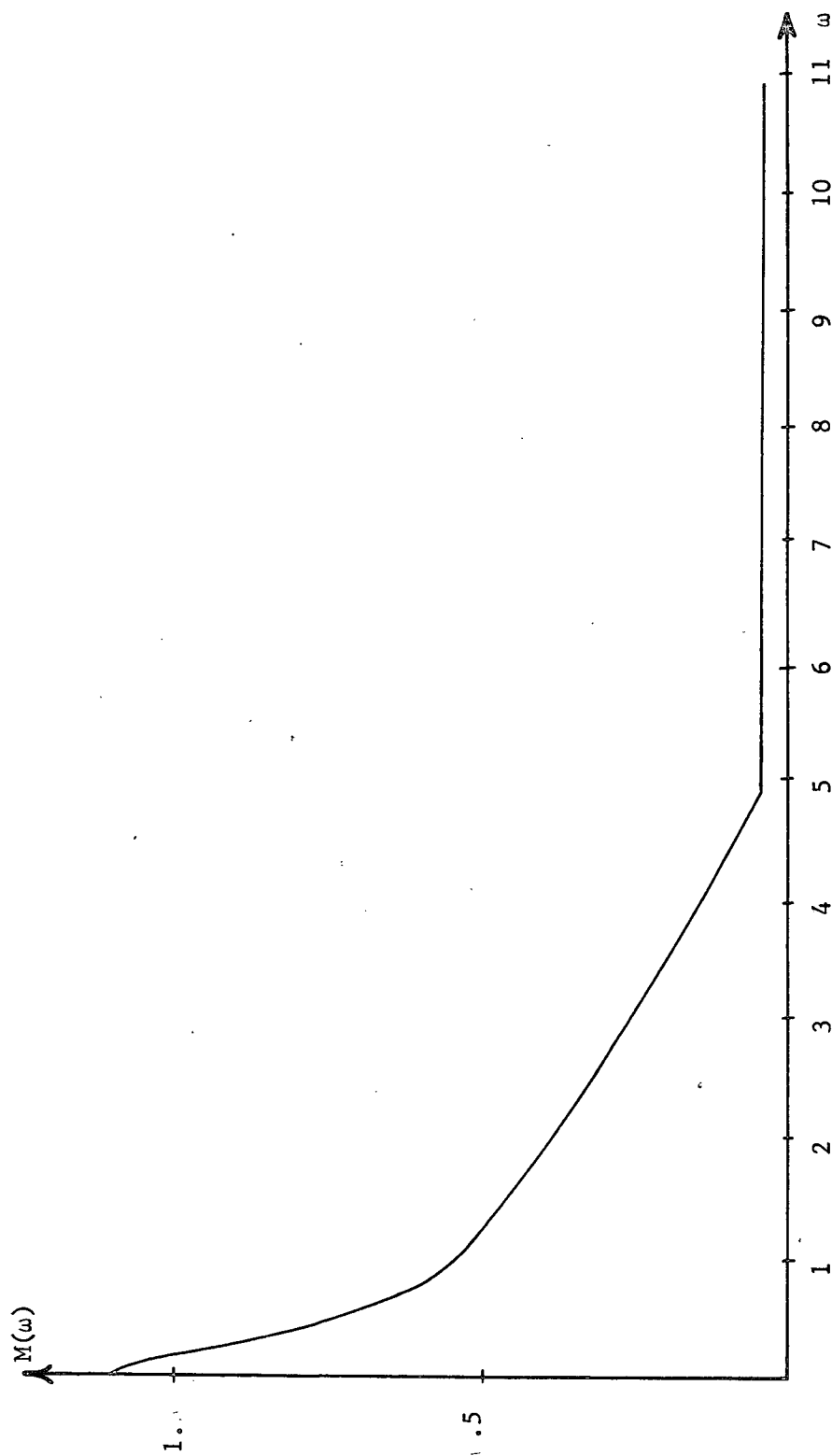


Figure 4.17  
Frequency Domain Specification

In order to compare the two design procedures, it will be desirable to have the specifications as given in Inequality (4-4) to be equivalent to the specifications shown in Figure 4.17. Such an equivalence is easily established if the two sets of specifications are properly interpreted. Note that the specifications given in Inequality (4-4) define a region in the complex plane which is illustrated in Figure 4.18.

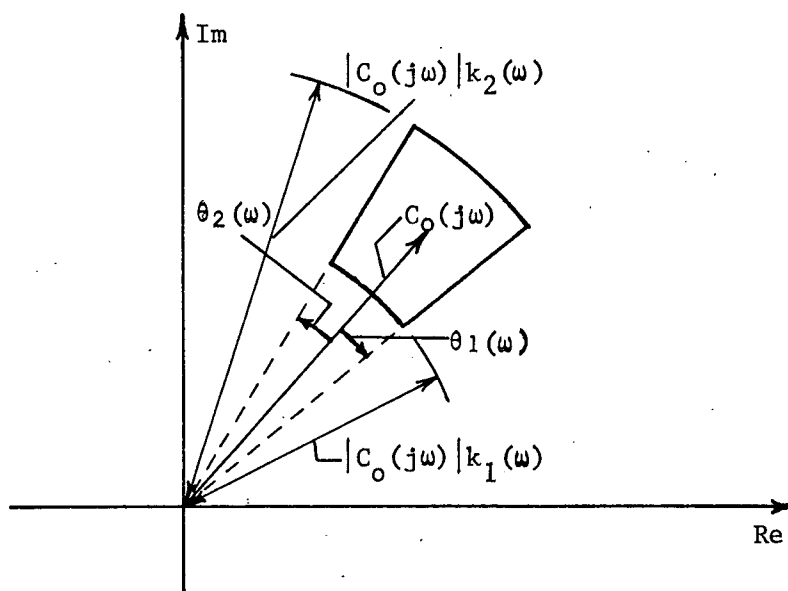


Figure 4.18

Region Defined by Second Form of  
Frequency Domain Specifications

Also observe that the specification given in Figure 4.17 defines a region in the complex plane. This region is shown in Figure 4.19.

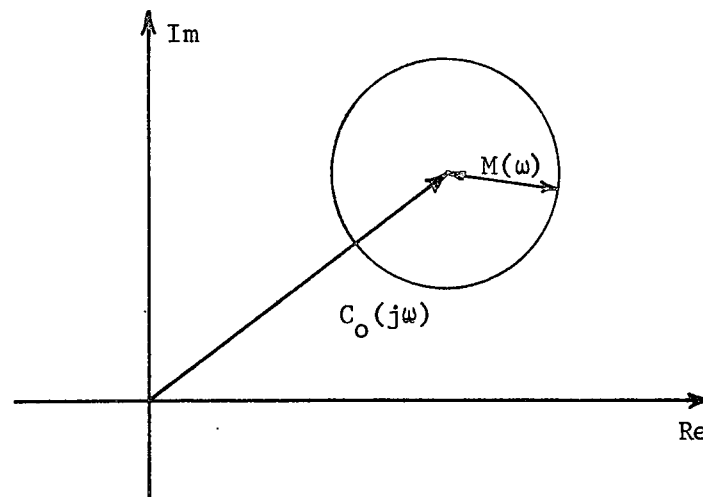


Figure 4.19  
Region Defined by First Form of  
Frequency Domain Specifications

It is evident that since the regions shown in Figure 4.18 and 4.19 are basically different, one region can only be an approximation to the other. However, the procedure for using the specification given in Inequality (4-4) is a graphical procedure and the region shown in Figure 4.19 can be used as satisfactorily as the region shown in Figure 4.18. Thus, the specifications used in the second design procedure will be the regions defined by the frequency domain specification given in Figure 4.17 and illustrated in Figure 4.19 in place of the region shown in Figure 4.18.

#### 4.4 First Design

In design procedures number one and two, the first design is a starting point from which a final design is reached. In the previous chapter the methods of obtaining a first design assumed that the time variations were known as an explicit function in order that the necessary integrals could be evaluated. In the example

given in this chapter the time variations are not assumed known as an explicit function, so that some other method of determining the first design must be used rather than that previously given. It would be possible to assume any stable compensation as the starting design; however, not only may this lead to an excessive number of designs in the procedure, but such an indiscriminate approach does not lend itself to an orderly study of time-varying systems. The most logical starting design would be one based on a time-invariant system with plant ignorance. Since the plant is time-invariant, such a design can be made analytically; and, in addition, the effects of the time variations on the system can be directly observed while the additional feedback required to compensate for these time variations is clearly evident.

The first step in the time invariant design is to find the acceptable regions in the complex plane for  $H(j\omega)$ . However, instead of determining the acceptable regions of  $H(j\omega)$  what will actually be found are the acceptable regions for  $-L_0(j\omega) = -H(j\omega)P_0(j\omega)$  where  $P_0(j\omega)$  is the nominal plant. In designing the time invariant system one should bear in mind that the design equations for both design procedure one and two stem from the same basic equation. The difference in the two procedures is that procedure one bases the design upon the difference in the actual system output and the desired system output, while procedure two bases the design upon the ratio of the actual system output to the desired system output. Since the specifications found in the previous section for the two procedures are exactly equivalent,

the acceptable regions for  $-L_O(j\omega)$  found by either procedure one or two will be identical. For illustration purposes the acceptable regions will be found using both procedure one and two.

The acceptable regions for  $-L_O(j\omega)$  will first be obtained for design procedure one. The design equation for design procedure one is given as

$$E(j\omega) = \frac{-1}{P_O(j\omega) + H(j\omega)} \int_{-\infty}^{\infty} \Delta P^{-1}(j\omega, j\gamma) C(j\gamma) d\gamma.$$

Since the system is assumed time invariant, the design equation can be written

$$E(j\omega) = \frac{-[P^{-1}(j\omega) - P_O^{-1}(j\omega)] [C_O(j\omega) + E(j\omega)]}{P_O^{-1}(j\omega) + H(j\omega)}.$$

Solving for  $E(j\omega)$  and rearranging one can obtain

$$E(j\omega) = \frac{\frac{1}{P_O(j\omega)} - \frac{1}{P(j\omega)}}{\frac{1}{P(j\omega)} + H(j\omega)} C_O(j\omega). \quad (4-5)$$

In selecting the nominal plant, observe that  $|E(j\omega)|$  may be reduced by either increasing the magnitude of the denominator of Equation (4-5) or by decreasing the magnitude of its numerator. It is the design objective, of course, to increase the magnitude of the denominator no more than necessary while maintaining as small a value of  $|H(j\omega)|$  as possible. Thus,  $P_O(j\omega)$  should be selected such that the magnitude of the numerator will be reduced to as small a value as possible. The inverse plant is given by

$$\frac{1}{P(j\omega)} = \frac{j\omega(j\omega + 2)}{k}$$

where  $1 \leq k \leq 10$

and the inverse nominal plant is given by

$$\frac{1}{P_o(j\omega)} = \frac{j\omega(j\omega + 2)}{k_o}.$$

The expression for the magnitude of the numerator of Equation (4-5) becomes

$$\begin{aligned} \left| \frac{1}{P_o(j\omega)} - \frac{1}{P(j\omega)} \right| &= \left| \frac{j\omega(j\omega + 2)}{k_o} - \frac{j\omega(j\omega + 2)}{k} \right| \\ &= \left| \frac{1}{k_o} - \frac{1}{k} \right| \left| j\omega(j\omega + 2) \right|. \end{aligned}$$

For any  $\omega$  the maximum value of this expression will be minimized for all  $k$  when  $1/k_o$  is given by

$$\frac{1}{k_o} = \left| \frac{\frac{1}{k_{\min}} + \frac{1}{k_{\max}}}{2} \right| = \frac{1.1}{2} = 0.55$$

or  $k_o = 1.818$ .

Thus, the nominal plant is selected as

$$P_o(j\omega) = \frac{1.818}{j\omega(j\omega + 2)}.$$

The regions of acceptable  $-L_o(j\omega)$  can now be found. Rearranging Equation (4-5) as shown on the following page



$$E(j\omega) = \frac{1 - \frac{P_O(j\omega)}{P(j\omega)}}{\frac{P_O(j\omega)}{P(j\omega)} - 1 + 1 + H(j\omega)P_O(j\omega)} C_O(j\omega)$$

one can write

$$E(j\omega) = \frac{-Q(j\omega)}{Q(j\omega) + \tilde{L}_O(j\omega)} C_O(j\omega) \quad (4-6)$$

where

$$Q(j\omega) = \frac{P_O(j\omega)}{P(j\omega)} - 1$$

and

$$\tilde{L}_O(j\omega) = H(j\omega)P_O(j\omega) + 1 = L_O(j\omega) + 1.$$

Applying the specifications to Equation (4-6), one obtains the inequality

$$|C_O(j\omega)| \left| \frac{Q(j\omega)}{Q(j\omega) + \tilde{L}_O(j\omega)} \right| \leq M(\omega)$$

or

$$|Q(j\omega) + \tilde{L}_O(j\omega)| \geq \frac{|Q(j\omega)| |C_O(j\omega)|}{M(\omega)} \quad (4-7)$$

At any specific frequency  $\omega$  the function  $Q(j\omega)$  takes on a range of possible values in the complex plane depending upon the plant  $P(j\omega)$ . For each value of  $Q(j\omega)$  the right hand term of Inequality (4-7) takes on a specific value which then specifies a forbidden region

for  $-L_O(j\omega)$ . Determining the forbidden regions for all values of  $Q(j\omega)$  then determines the forbidden region of  $-\tilde{L}_O(j\omega)$  at frequency  $\omega$ . The compliment of the forbidden region automatically gives the acceptable region of  $-\tilde{L}_O(j\omega)$ . To illustrate the procedure, the acceptable region for  $-\tilde{L}_O(j\omega)$  at  $\omega$  equal to two will be found. The range of  $Q(j\omega)$  must first be determined. The expression for  $Q(j\omega)$  is given by

$$\begin{aligned} Q(j\omega) &= \frac{P_O(j\omega)}{P(j\omega)} - 1 \\ &= \frac{1.818}{j\omega(j\omega + 2)} \frac{j\omega(j\omega + 2)}{k} - 1 \\ &= \frac{1.818}{k} - 1. \end{aligned}$$

Since the constant  $k$  takes on all values between one and ten,  $Q(j\omega)$  takes on all real values between  $-0.818$  and  $0.818$ . From Figure 4.17 the value of  $M(2)$  is found to be  $0.4$  and the value of  $|C_O(j2)|$  is calculated as  $0.352$ . Table 4-1 gives the values of the right side of Inequality (4-7) for different values of  $Q(j\omega)$  at  $\omega$  equal to 2.

$Q$	$\frac{ Q(j\omega)  \cdot  C_O(j\omega) }{M(\omega)}$
$-0.818$	$0.731$
$-0.5$	$0.446$
$-0.2$	$0.179$
$0$	$0$
$0.2$	$0.179$
$0.5$	$0.446$
$0.818$	$0.731$

Table 4-1  
Values of the Right Side of Inequality (4-7)

To determine the forbidden region of  $-\tilde{L}_O(j\omega)$  for a particular  $Q$ , consider the value of  $Q$  equal to  $-0.818$ . At this value of  $Q$  one finds from Table 4-1 that the magnitude of  $Q(j\omega) + \tilde{L}_O(j\omega)$  must be greater than or equal to  $0.731$ . The region where this is true is illustrated graphically in Figure 4.20. The distance from  $Q$  to  $-\tilde{L}_O$  is the magnitude of  $Q + \tilde{L}_O$ , so that the forbidden region of  $-\tilde{L}_O$  for  $Q$  equal to  $-0.818$  corresponds to the region inside a circle with center at  $-0.818$  and radius  $0.731$ .

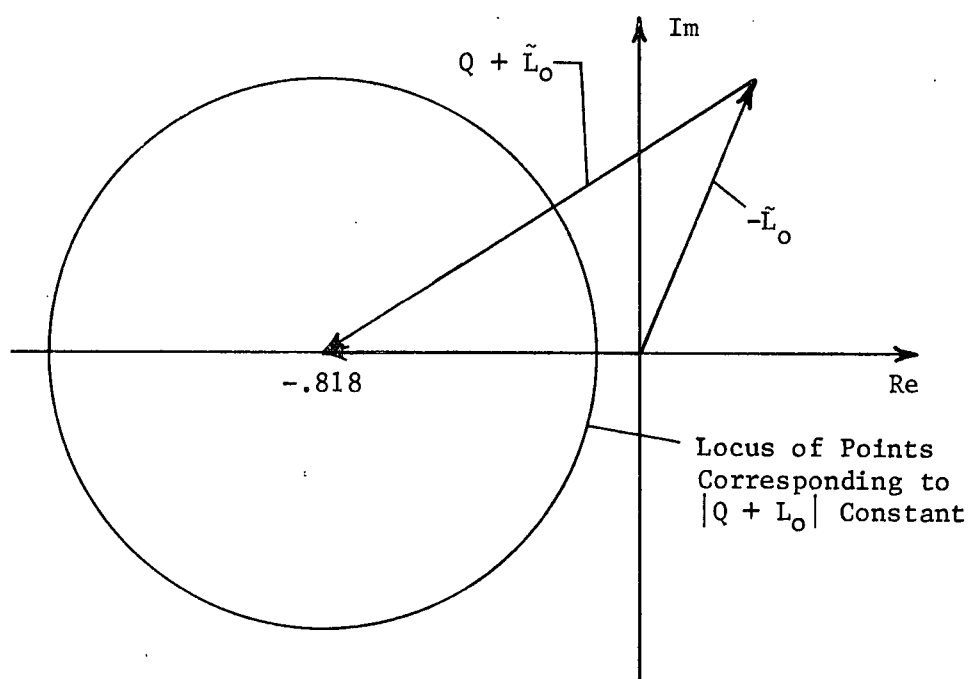


Figure 4.20  
Illustration Showing the Determination of  
Acceptable Region of  $-\tilde{L}_O(j\omega)$

Repeating this procedure for several values of  $Q$ , one is able to determine the forbidden regions corresponding to each value which, when superimposed upon one another, gives the total forbidden

region. The acceptable region is then the region outside the forbidden region. Figure 4.21 shows the total acceptable region of  $-\tilde{L}_O$  for  $\omega$  equal to 2.

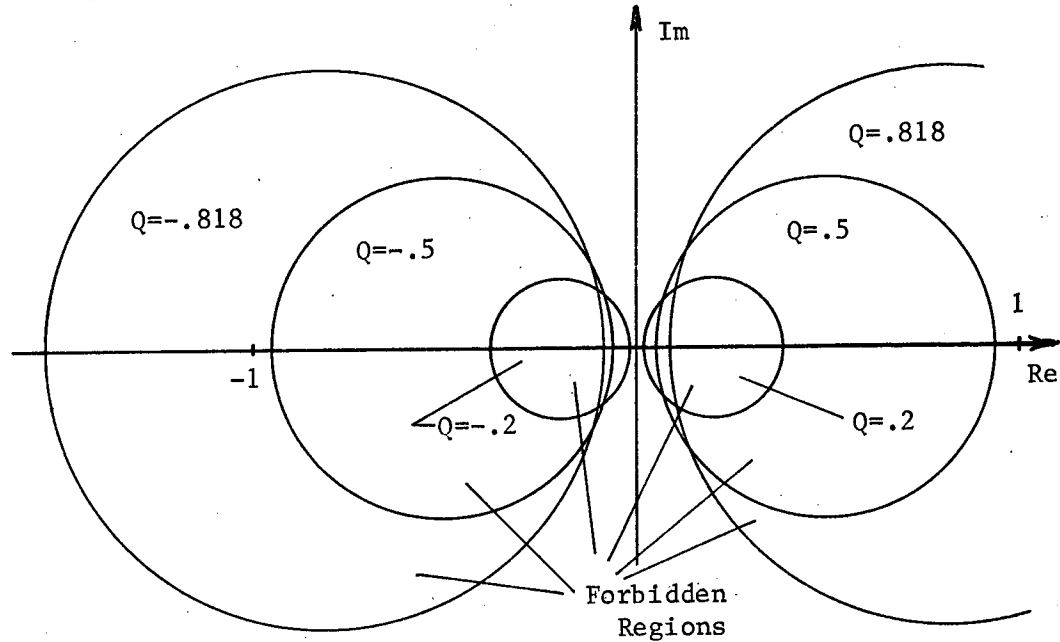


Figure 4.21  
Acceptable Region of  $-\tilde{L}_O$  for  $\omega = 2$

Having the acceptable regions of  $-\tilde{L}_O$ , it is a simple matter to determine the acceptable region of  $-L_O$ . Since  $\tilde{L}_O$  is given by

$$\tilde{L}_O = 1 + L_O,$$

then

$$-L_O = 1 - \tilde{L}_O.$$

Thus by adding one to each point in the acceptable region of  $-\tilde{L}_O$ , the acceptable region of  $-L_O$  is obtained. This corresponds to a shifting of the acceptable regions of  $-\tilde{L}_O$  to the right by one to obtain the acceptable regions of  $-L_O$ .

The frequencies of interest for which the acceptable regions are to be found for the example must now be selected. In calculating the Fourier transform on the computer, the frequencies which may be calculated are multiples of the fundamental frequency given by

$$\omega_0 = \frac{2\pi}{T}$$

where  $T$  is the total system time of the calculation. It will be assumed that the system will be close to steady state in ten seconds so that  $T$  is taken as ten seconds. If, in practice the system does not reach steady state in ten seconds,  $T$  can be doubled or quadrupled until steady state is reached and the appropriate harmonic selected. With  $T$  equal to ten seconds,  $\omega_0$  is equal to 0.628. The multiples of this frequency which were chosen are 0, 1, 2, 3, 7, 10 and 15. This selection gives frequencies fairly equally spaced on a Bode plot and should also give adequate representation of the functions of interest. The frequencies corresponding to these multiples are 0, 0.628, 1.25, 1.88, 4.39, 6.28, and 9.42. The acceptable regions of  $-L_0(j\omega)$  which correspond to these frequencies are shown in Figure 4.22. An acceptable region for  $\omega = 0$  cannot be found since  $L_0(j\omega)$  is indeterminate at  $\omega = 0$ . If it is found that the error is too large at  $\omega = 0$ , a correction will be made in the second design. The reduction of the magnitude of  $L_0(j\omega)$  is not as critical at low frequencies as it is at high frequencies since at low frequencies the loop gain is adequate to limit the noise transmission to the plant input.

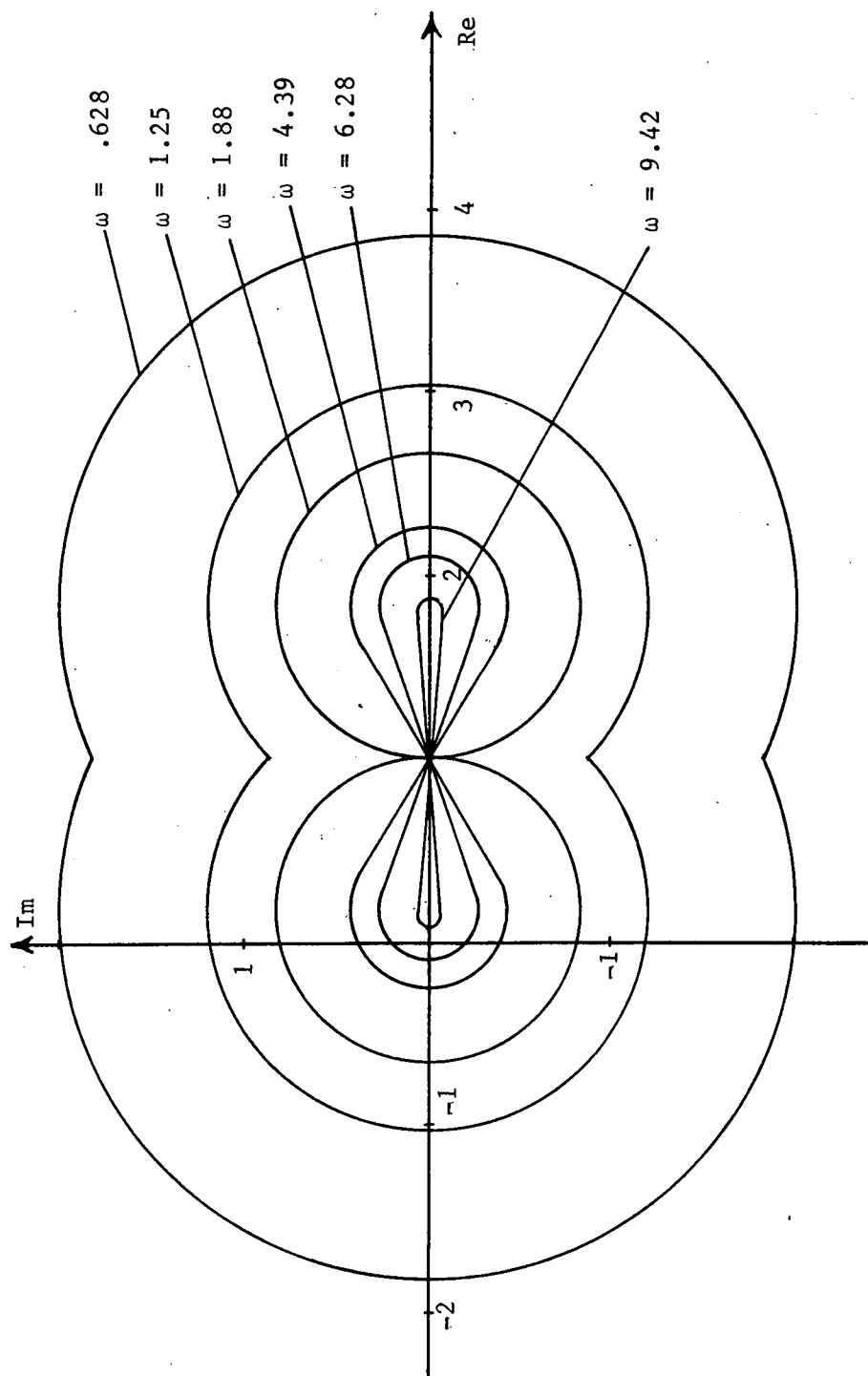


Figure 4.22  
Acceptable Regions of  $-L_o$

The acceptable regions for  $-L_O(j\omega)$  will now be found for design procedure two. The design equation for design procedure two is given by

$$\frac{C(j\omega)}{C_O(j\omega)} = \frac{1 + L_O(j\omega)}{\frac{P_O(j\omega)}{P(j\omega)} + L_O(j\omega)} .$$

The nominal plant is chosen the same as was selected for design procedure one.

$$P_O(j\omega) = \frac{1.818}{j\omega(j\omega + 2)}$$

Since the system is assumed to be time-invariant, the equivalent plant is given by

$$P_{eq}(j\omega) = \frac{k}{j\omega(j\omega + 2)}$$

where

$$1 \leq k \leq 10.$$

The ratio of the nominal plant to the equivalent plant is thus found to be

$$\frac{P_O(j\omega)}{P_{eq}(j\omega)} = \frac{\frac{1.818}{j\omega(j\omega + 2)}}{\frac{k}{j\omega(j\omega + 2)}} = \frac{1.818}{k}$$

so that the design equation becomes

$$\frac{C(j\omega)}{C_O(j\omega)} = \frac{1 + L_O(j\omega)}{\frac{1.818}{k} + L_O(j\omega)} . \quad (4-8)$$

The objective is to choose an  $L_0(j\omega)$  such that the value of  $C(j\omega)/C_0(j\omega)$  as given by Equation (4-8) falls within the appropriate specification regions for all values of  $k$ .<sup>(28)</sup>

As discussed in the previous section, one form of the specification region is a circle in the complex plane of radius  $M(\omega)$  and centered at the point  $C_0(j\omega)$ . The specifications will be satisfied if  $C(j\omega)$  falls within this region. Dividing every point in the region by  $C_0(j\omega)$ , one obtains a region into which  $C(j\omega)/C_0(j\omega)$  must fall for the specification to be satisfied. This region consists of a circle centered at the point one with radius  $M(\omega)/|C_0(j\omega)|$ . As with design procedure one, the frequencies of interest are selected as 0, 0.628, 1.25, 1.88, 4.39, 6.28, and 9.42. The regions of acceptable  $C(j\omega)/C_0(j\omega)$  for these frequencies are shown in Figure 4.23.

The regions shown in Figure 4.23 are still not in the most convenient form for determining the acceptable region of  $-L_0(j\omega)$ , however. To determine the appropriate form, consider Figure 4.24 as shown on page 144.

Shown in Figure 4.24 is a hypothetical region of  $P_0/P_{eq}$  and a line  $\alpha$  passing through the point one. To determine whether or not any point A on the line  $\alpha$  lies within the acceptable region of  $-L_0$ , one draws the vector from point A to one which is equal to  $1 + L_0$ . A vector from A to any point within the region of  $P_0/P_{eq}$  gives  $P_0/P_{eq} + L_0$ . These two vectors give the numerator and denominator of Equation (4-8) so that  $C/C_0$  can be determined. If  $C/C_0$  as determined by Equation (4-8) falls within the acceptable



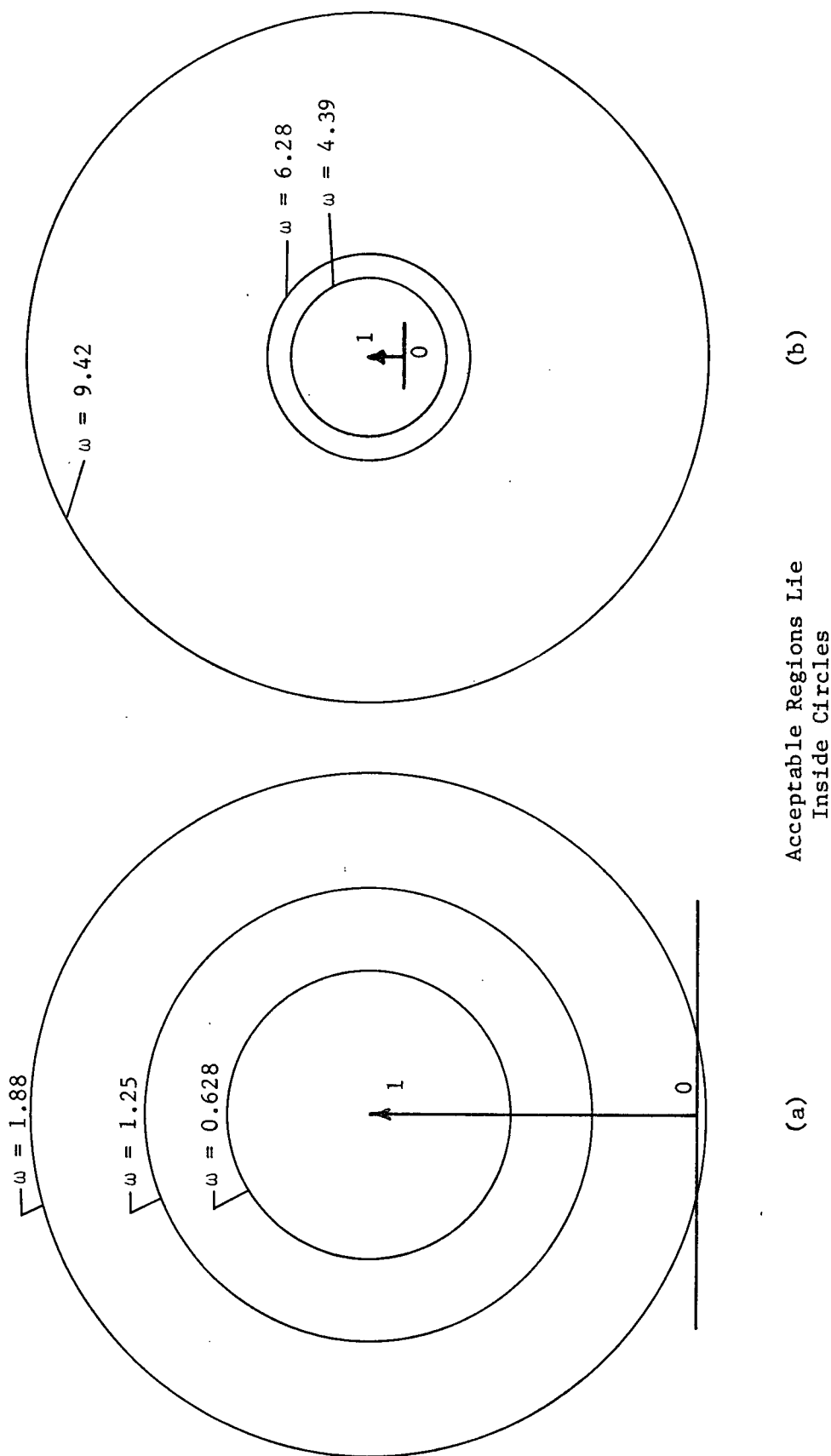


Figure 4.23  
Acceptable Regions of  $C(j\omega)/C_0(j\omega)$

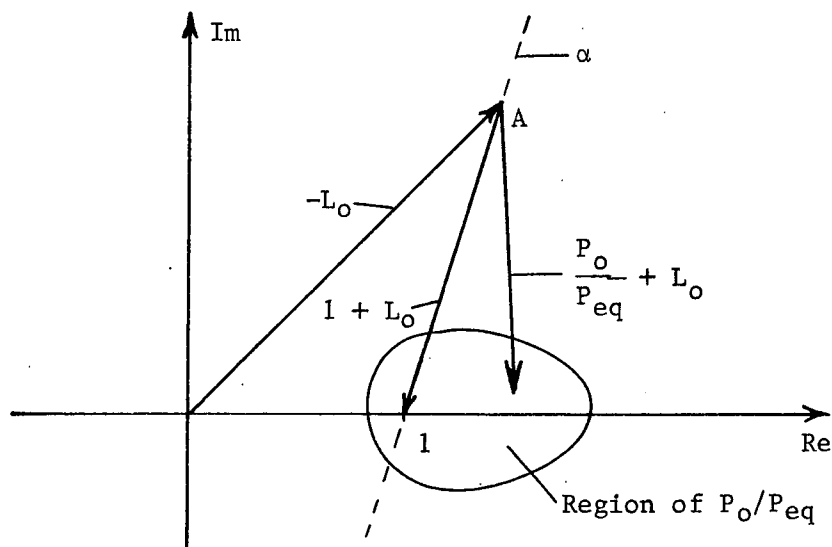


Figure 4.24  
Determining a Point on the Boundary of the  
Acceptable Region for  $-L_O(j\omega)$

region of  $C/C_O$  for all the points within the region of  $P_O/P_{eq}$ , point A then falls within the acceptable region of  $-L_O$ . Point A lies on the boundary of the acceptable region of  $-L_O$  if  $C/C_O$  just falls within the acceptable region of  $C/C_O$  for all  $P_O/P_{eq}$ . The object is to determine the boundary points for a number of lines passing through the point one. These boundary points then determine the region of acceptable  $-L_O$ .

The determination of the boundary points by the procedure just described is a trial and error method and can become fairly lengthy. However, if the specification region for  $C/C_O$  were modified so that the numerator appears to be a constant and the denominator a variable, which corresponds to the form of Equation (4-8), the determination of the boundary of acceptable  $-L_O$  becomes

a simpler matter. To illustrate, Figure 4.25 shows the region of  $P_0/P_{eq}$ , and superimposed is an assumed modified region of  $C/C_0$ .

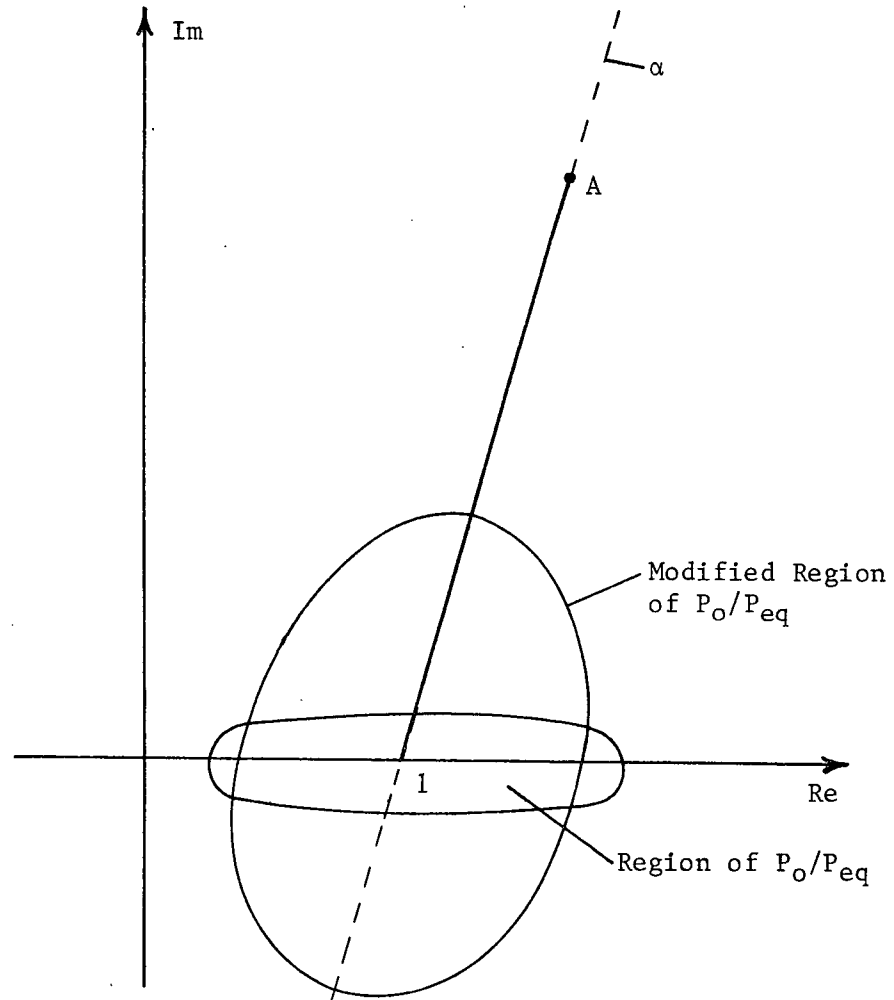


Figure 4.25  
Illustration of the Use of the Modified  
Region of  $C/C_0$

The point one is common to both regions and the vector from point A to one which is  $1 + L_0$  also corresponds to C. Observe that if point A is moved away from one along line  $\alpha$ , the region of  $C/C_0$  becomes proportionally larger while retaining the same

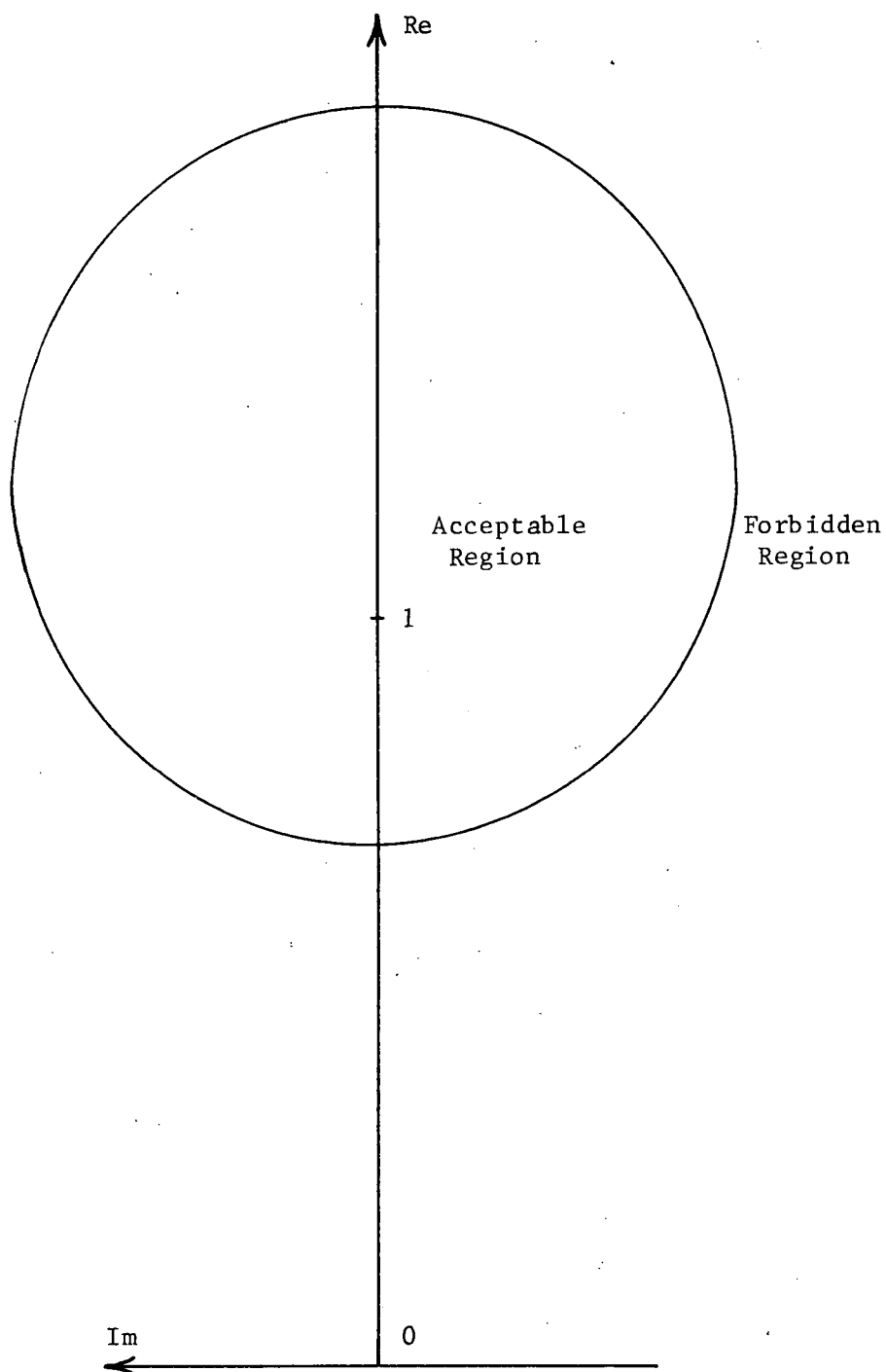


Figure 4.27a  
Modified Region of  $C(j\omega)/C_o(j\omega)$ :  $\omega = 0.628$

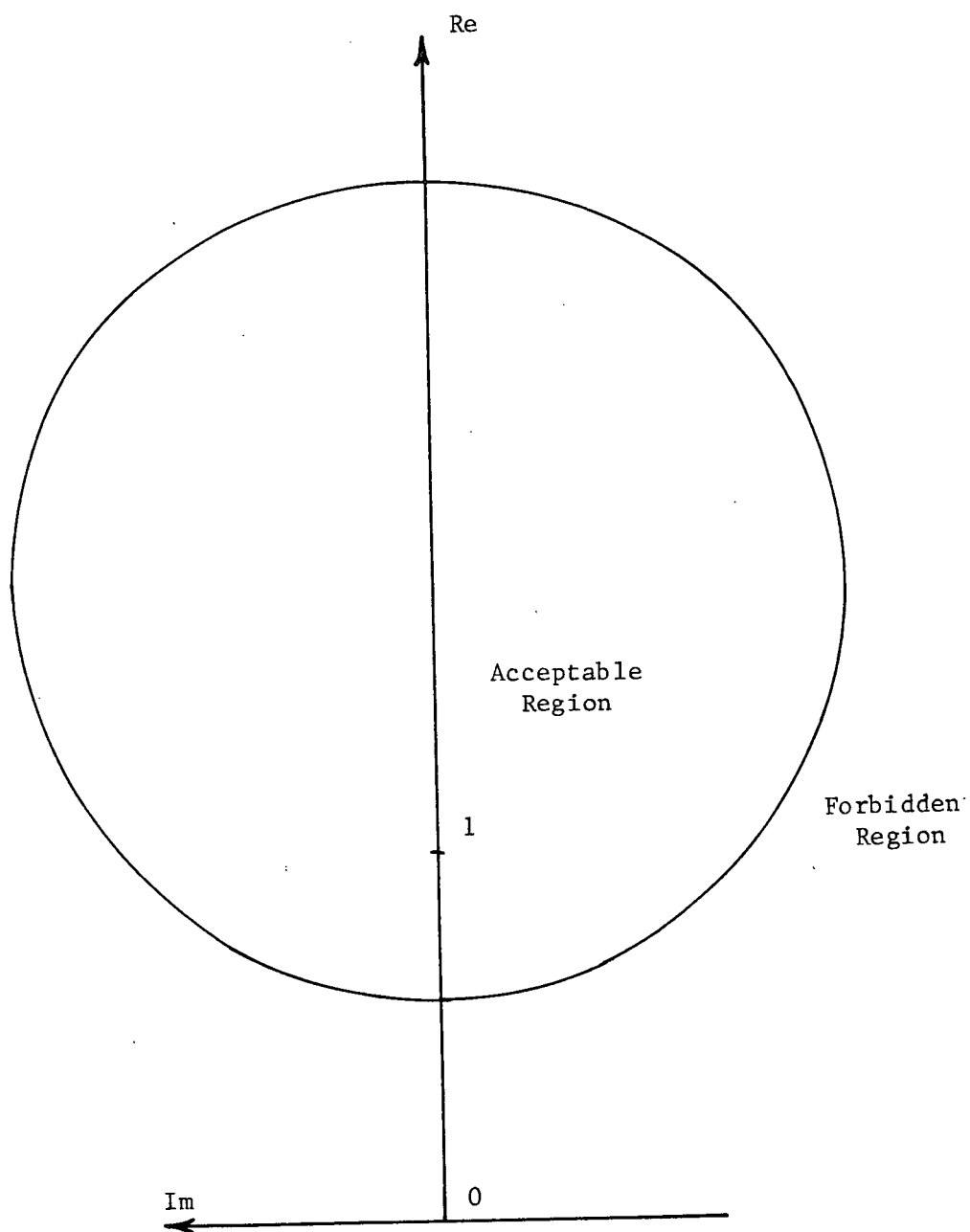


Figure 4.27b  
Modified Region of  $C(j\omega)/C_o(j\omega)$ :  $\omega = 1.25$

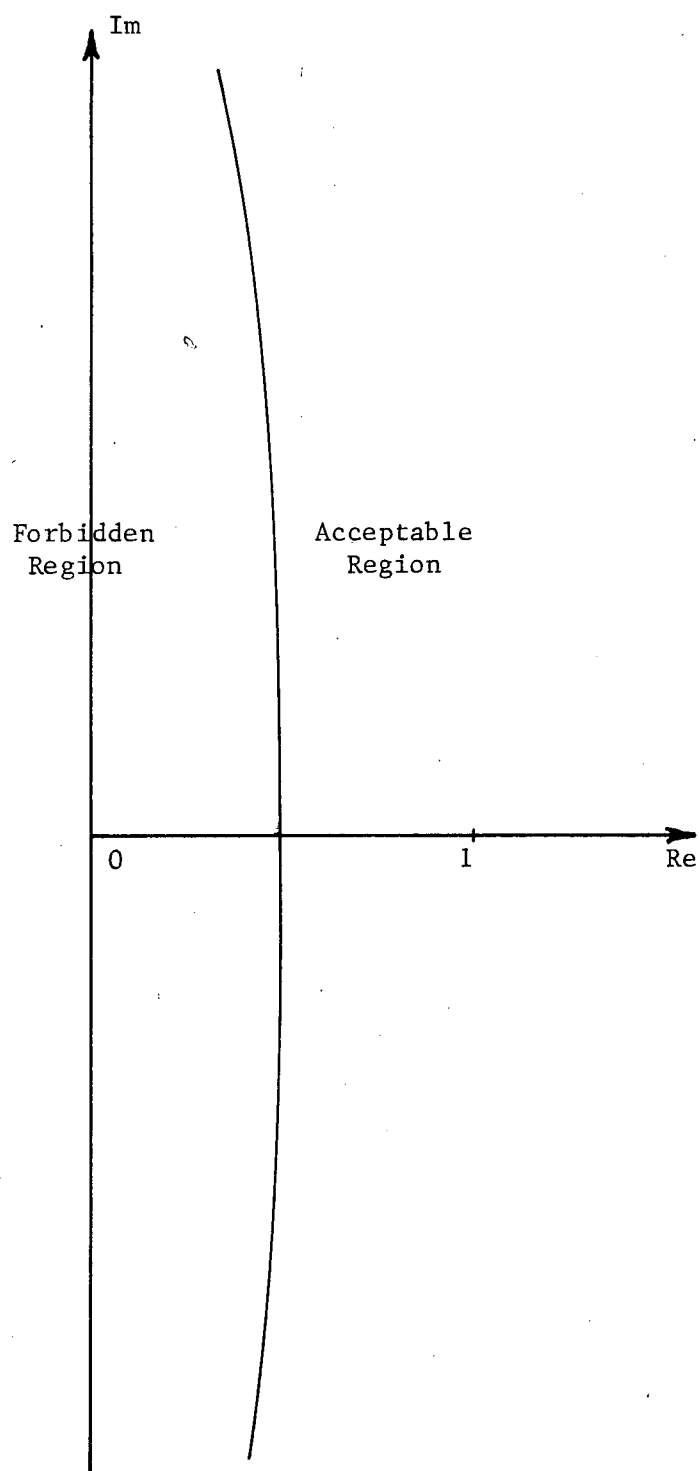


Figure 4.27c  
Modified Region of  $C(j\omega)/C_0(j\omega)$ :  $\omega = 1.88$

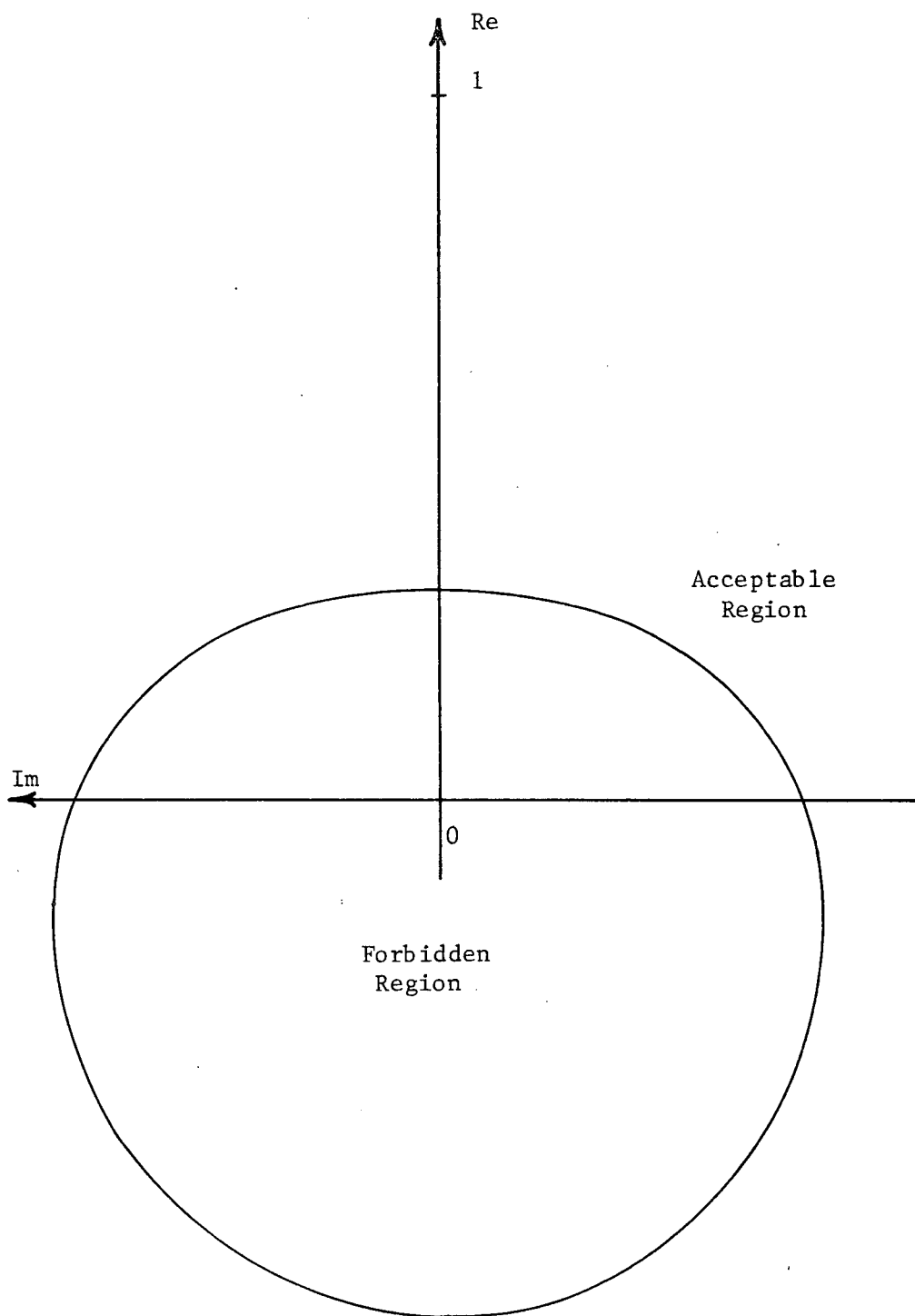


Figure 4.27d  
Modified Region of  $C(j\omega)/C_o(j\omega)$ :  $\omega = 4.39$

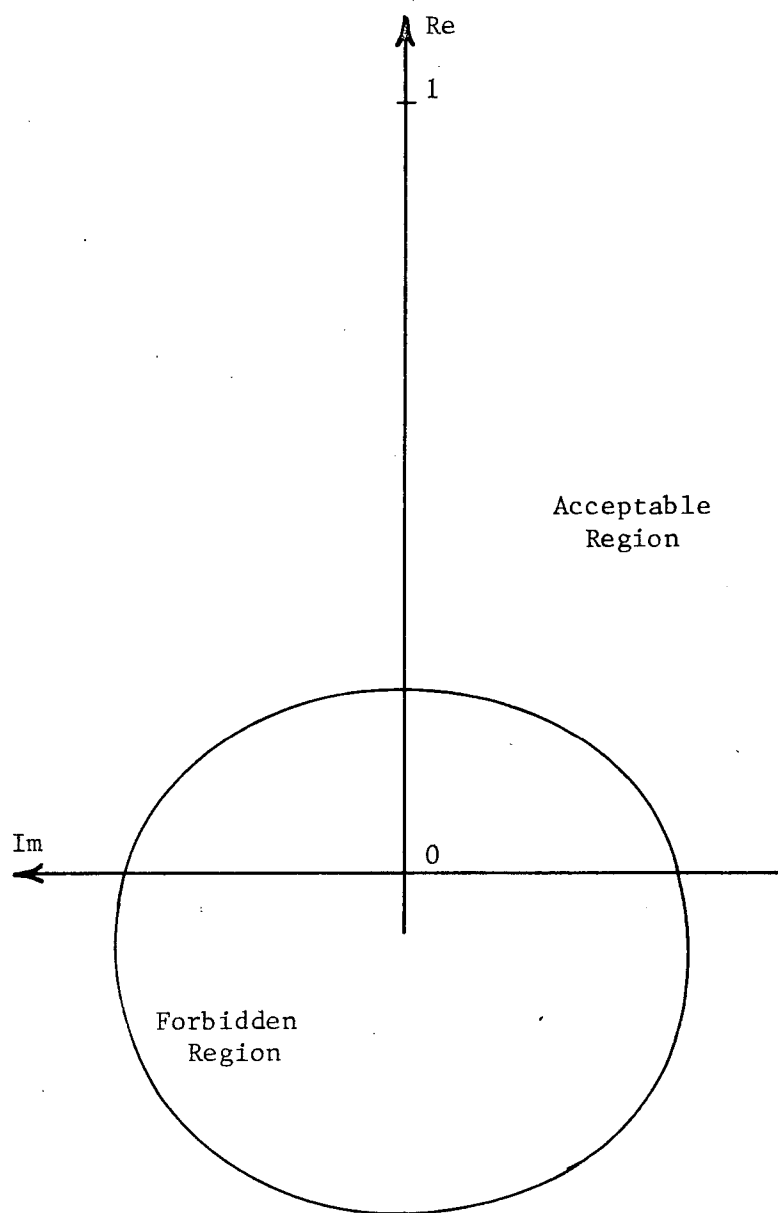


Figure 4.27e  
Modified Region of  $C(j\omega)/C_o(j\omega)$ :  $\omega = 6.28$



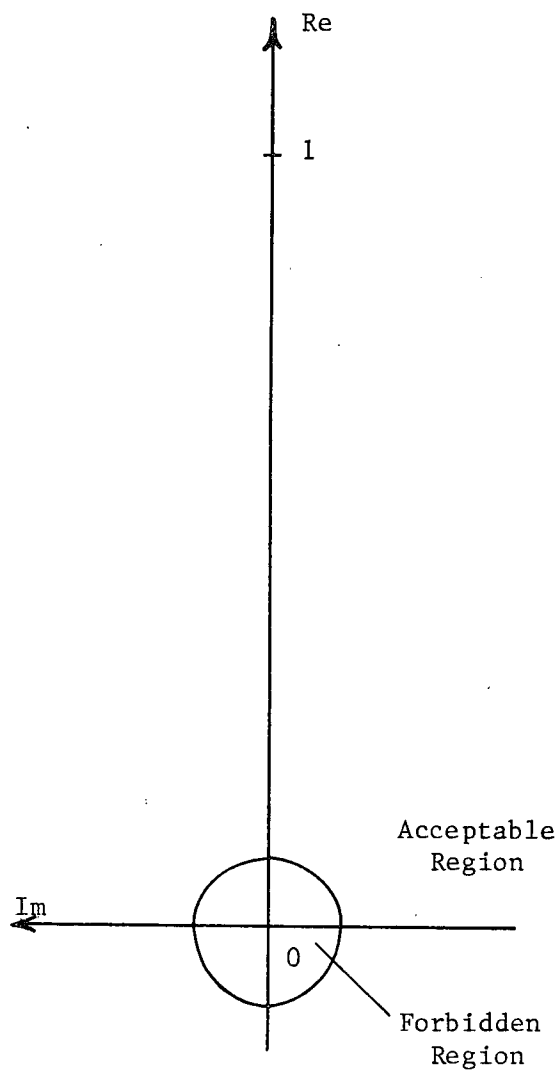


Figure 4.27f  
Modified Region of  $C(j\omega)/C_o(j\omega)$ :  $\omega = 9.42$

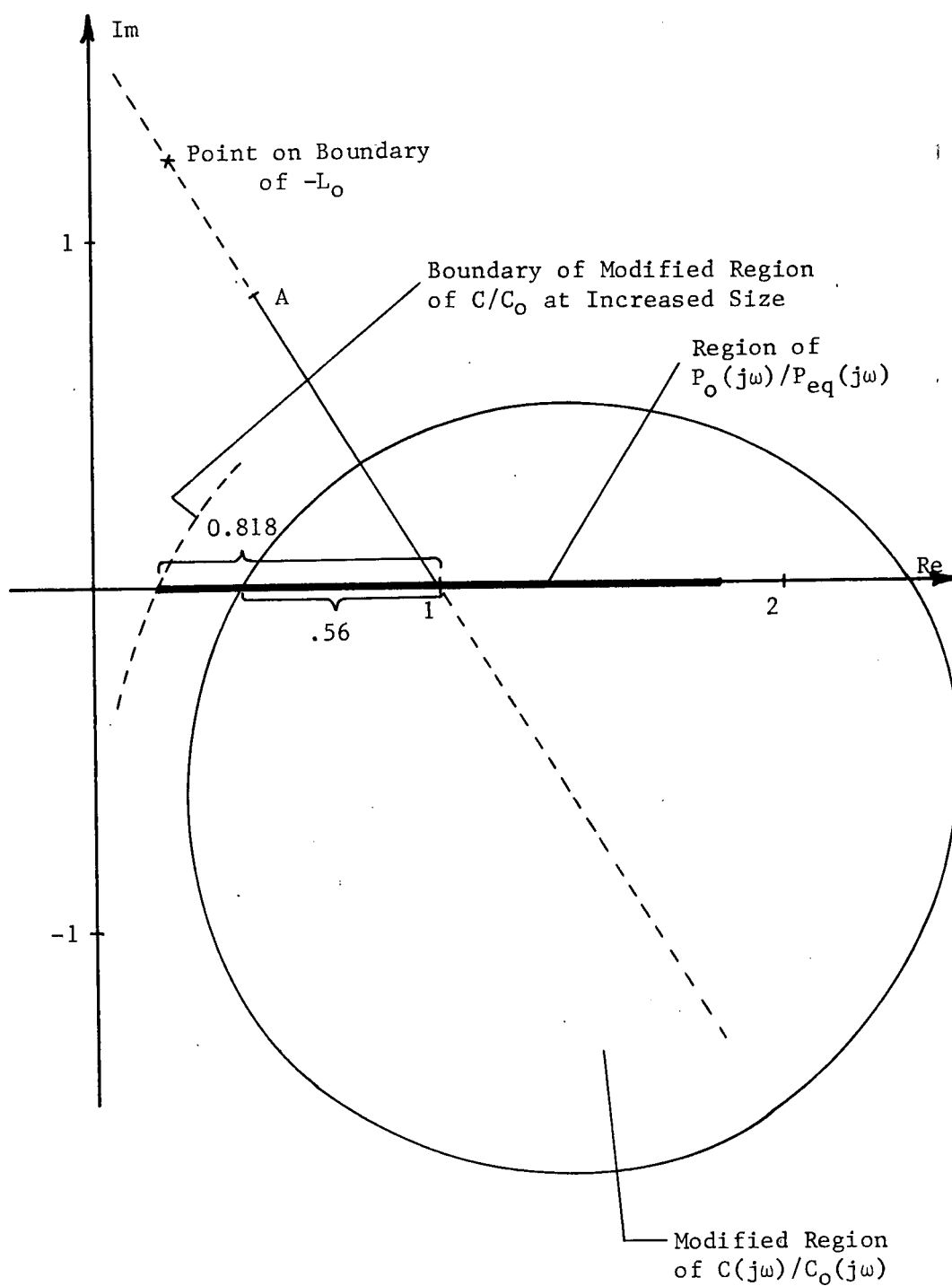


Figure 4.28  
 Determination of a Point on the Boundary  
 of the Region of Acceptable  $-L_O(j\omega)$ :  $\omega = 1.25$

of acceptable  $-L_O(j\omega)$ . The acceptable regions of  $-L_O(j\omega)$  obtained by this method are identical to the regions obtained for design procedure one which are shown in Figure 4.22. Figures 4.27a through 4.27f show the modified regions which correspond to the specification regions given in Figure 4.23.

Since the acceptable regions of  $-L_O(j\omega)$  are known, a suitable  $L_O(j\omega)$  can now be designed for the time-invariant system. It is desired to have  $-L_O(j\omega)$  just lie on the boundaries of acceptable  $-L_O$  at the point where the distance to the origin is a minimum. For the acceptable regions shown in Figure 4.22, the points closest to the origin lie on the negative real axis. However, for the magnitude of  $L_O(j\omega)$  to decrease there must be some degree of lag associated with  $L_O(j\omega)$ . Thus, the design of  $L_O$  will be a compromise between maintaining as small a magnitude as possible while obtaining the necessary rate of decrease. The design of  $L_O(j\omega)$  was made by trial and error. A preliminary design was first made using the Bode plot, then the final design was reached by adjusting the preliminary design so that the polar plot of  $-L_O(j\omega)$  came as close as possible to lying on the boundaries of the acceptable regions of  $-L_O(j\omega)$ . The expression for the  $L_O(s)$  which was selected is

$$L_O(s) = \frac{24.17 (s + 0.9) (s + 6)}{s(s + 1.4) (s + 7) (s + 12)}$$

and has a polar plot as shown in Figure 4.29. The expression of  $H(s)$  is easily found from the relation

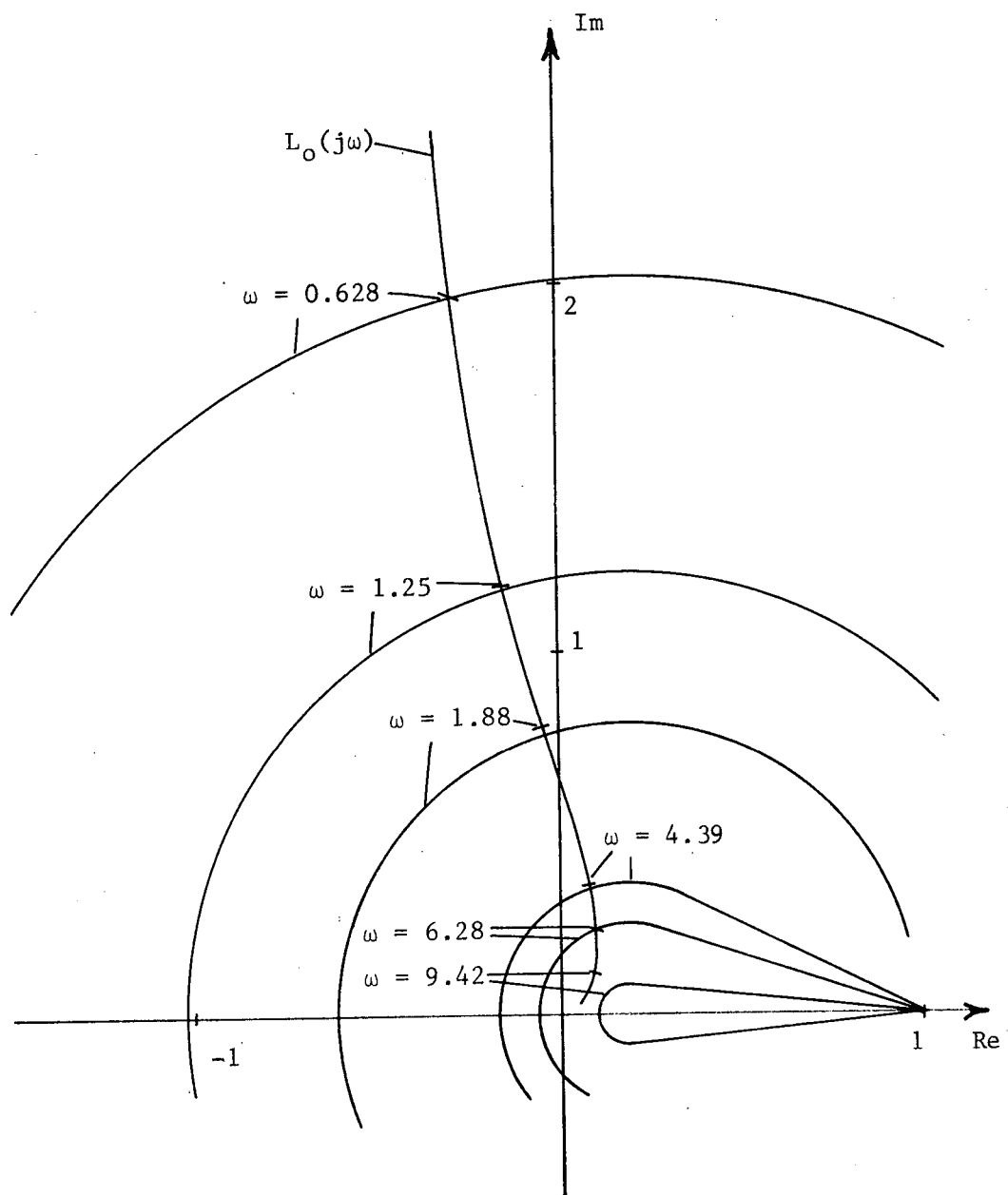


Figure 4.29  
Polar Plot of Time Invariant Design

$$H(s) = \frac{L_o(s)}{P_o(s)}$$

and is found to be

$$H(s) = 13.3 \frac{s^3 + 8.9s^2 + 19.2s + 10.8}{s^3 + 20.4s^2 + 110.6s + 117.6}$$

Generally, the number of poles over zeroes will be greater than in the above  $L_o(s)$  and  $H(s)$ . The high frequency poles were not included in order to keep the solution time for the computer simulations as short as possible. The high frequency poles will be added after a suitable time-varying design has been made.

The prefilter  $G(s)$  is determined from the expression

$$G(s) = \frac{1 + L_o(s)}{P_o(s)} T_o(s)$$

Making the appropriate substitutions one obtains

$$G(s) = 2.2 \frac{s^5 + 22.4s^4 + 175.6s^3 + 553.9s^2 + 699.3s + 261.1}{s^5 + 23.2s^4 + 171.7s^3 + 508.9s^2 + 771.7s + 470.4}$$

Note that the far off poles of  $L_o(s)$  will also be in  $G(s)$ ; however, the far off poles in  $G(s)$  are not necessary as they are in  $L(s)$ . In fact, the far off poles of  $G(s)$  can be assumed to be in  $T_o(s)$ . This will give a simpler expression for  $G(s)$  and will result in little change in the system response.

To determine whether or not the design is adequate for the system under time-varying conditions, a simulation was made on an

IBM 1130 digital computer using the Continuous System Modeling Program for the 1130 in conjunction with the algorithm for calculating the numerical Fourier transform as given in Reference (48). A more detailed discussion of the simulation procedure is given in Appendix D.

The results of the search for the maximum value of the error will first be presented. A series of runs was made with the function representing the time-varying gain having the general form as shown in Figure 4.30. The function has 11 equally spaced points starting from time equal zero to nine seconds. The points can take on any value between one and ten with the function varying linearly between points. Thus, the maximum slope for the function is ten except at the selected points.

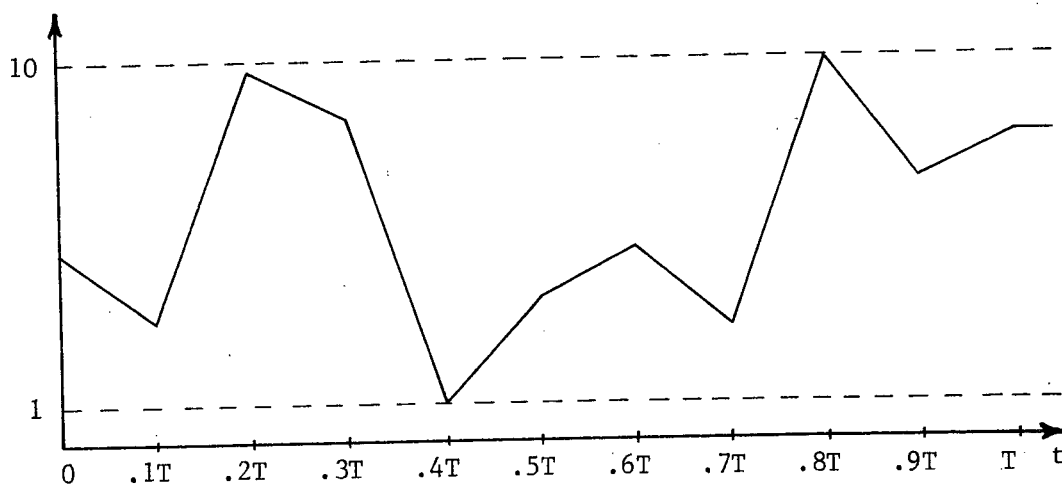


Figure 4.30  
Type of Function for Time-Varying Gain

In searching for the function which would give the maximum error, it was quickly found that the larger errors occur when the

specified points take on either maximum or minimum values. The variations having the greatest effect on the error occur near time equal zero, and any variation after five or six seconds has little effect on the error. By far the largest error occurs when the time variations start at ten and decrease quickly to one. In fact, variations starting at values other than near ten produce errors no larger than those observed when the gain is held constant at ten, no matter what the subsequent variation.

It was found that a significant increase in error occurred only at frequencies zero and 0.628, while the design appeared to be adequate for all higher frequencies. Figures 4.32 and 4.33 show the step responses and error functions corresponding to these maximum errors. Figure 4.37 shows the magnitude of the Fourier transform of these error functions. Note that the error functions in both cases increase quickly, then slowly decrease to the final value with the result of an excess area under the curve. What apparently happens in the system during these particular time-variations is that when the gain starts at ten, the system has the ability to accelerate quickly to a relatively high velocity; however, after the system has attained the velocity the gain is suddenly reduced to one, so that the rapid acceleration effect is lost, thus allowing the system to coast to a higher value than would be the case if the gain remained at ten. With the gain at the lower value, the system returns to the final value more slowly than if the gain were at ten. The effect is also observed in Figure 4.33 when the system decreases to zero

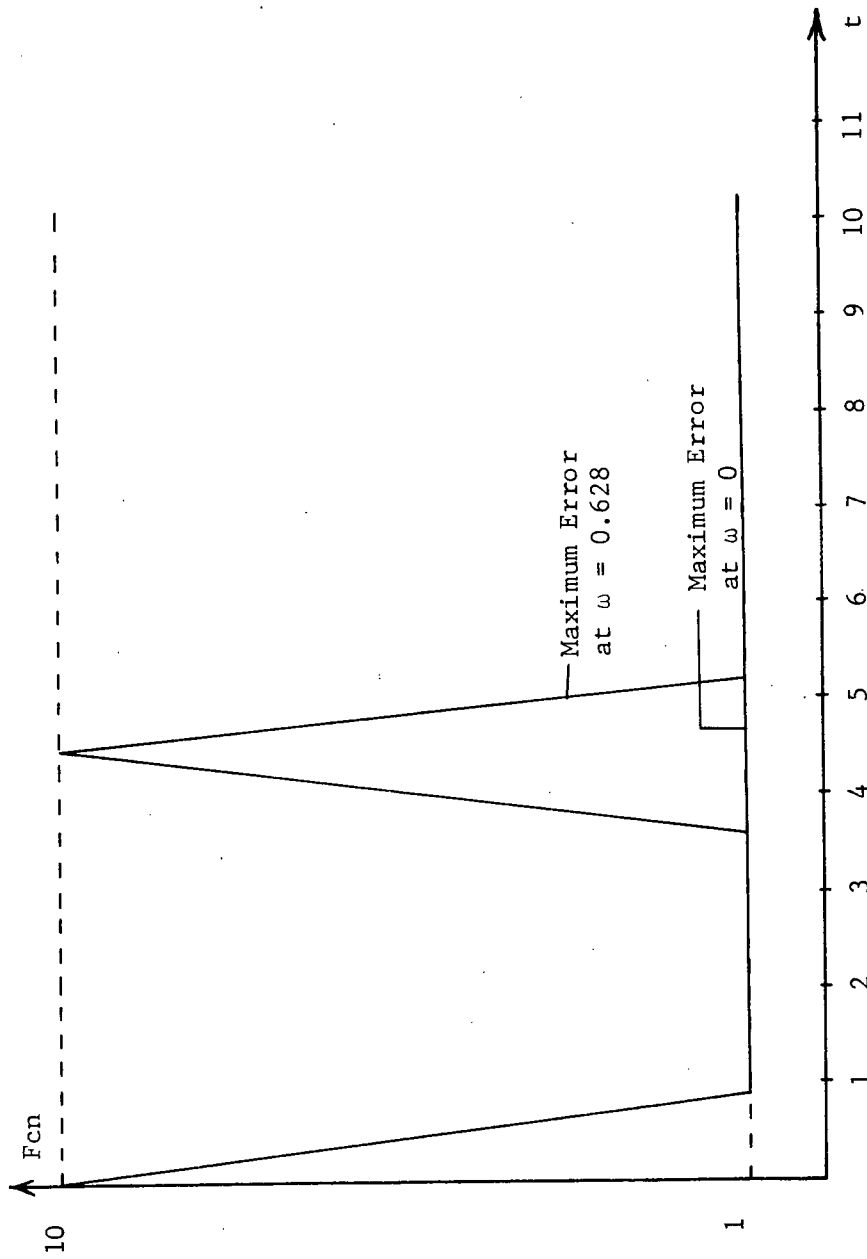


Figure 4.31  
Functions Resulting in Maximum Error  
During First Series



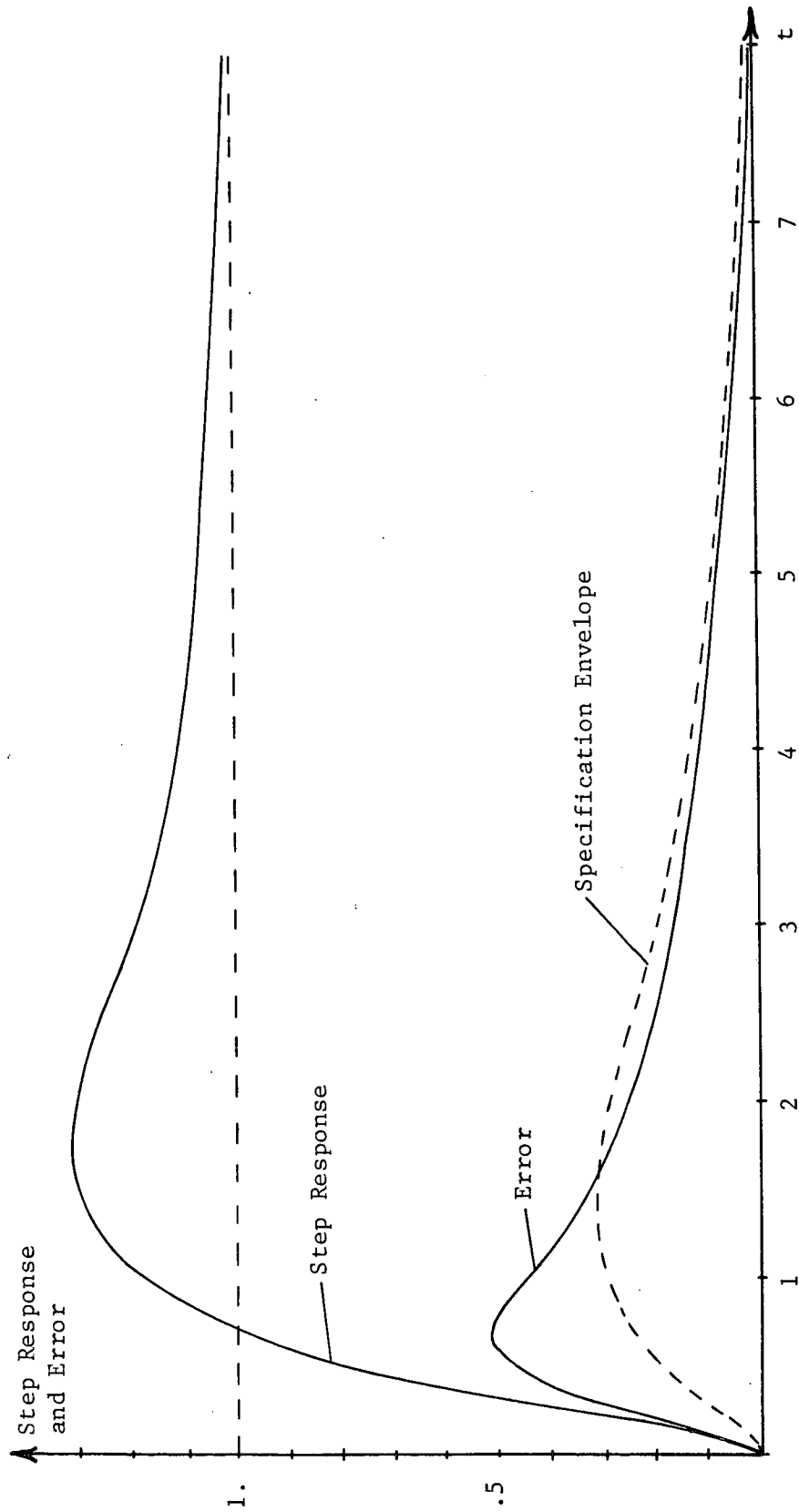


Figure 4.32  
Step Response and Error Function Corresponding  
To Maximum Error at  $\omega = 0$  During First Series

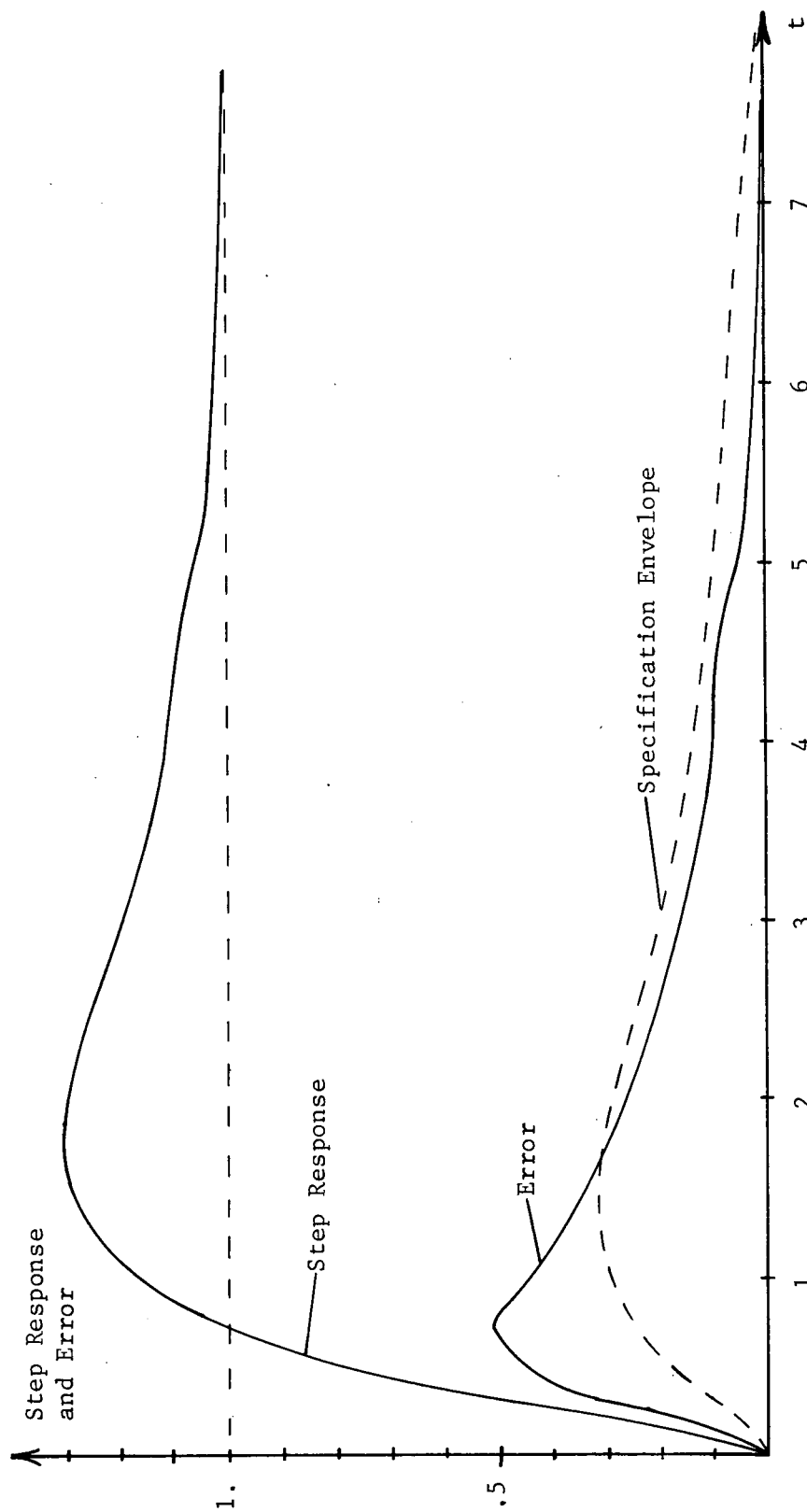


Figure 4.33  
 Step Response and Error Function Corresponding  
 To Maximum Error at  $\omega = 0.628$  During First Series

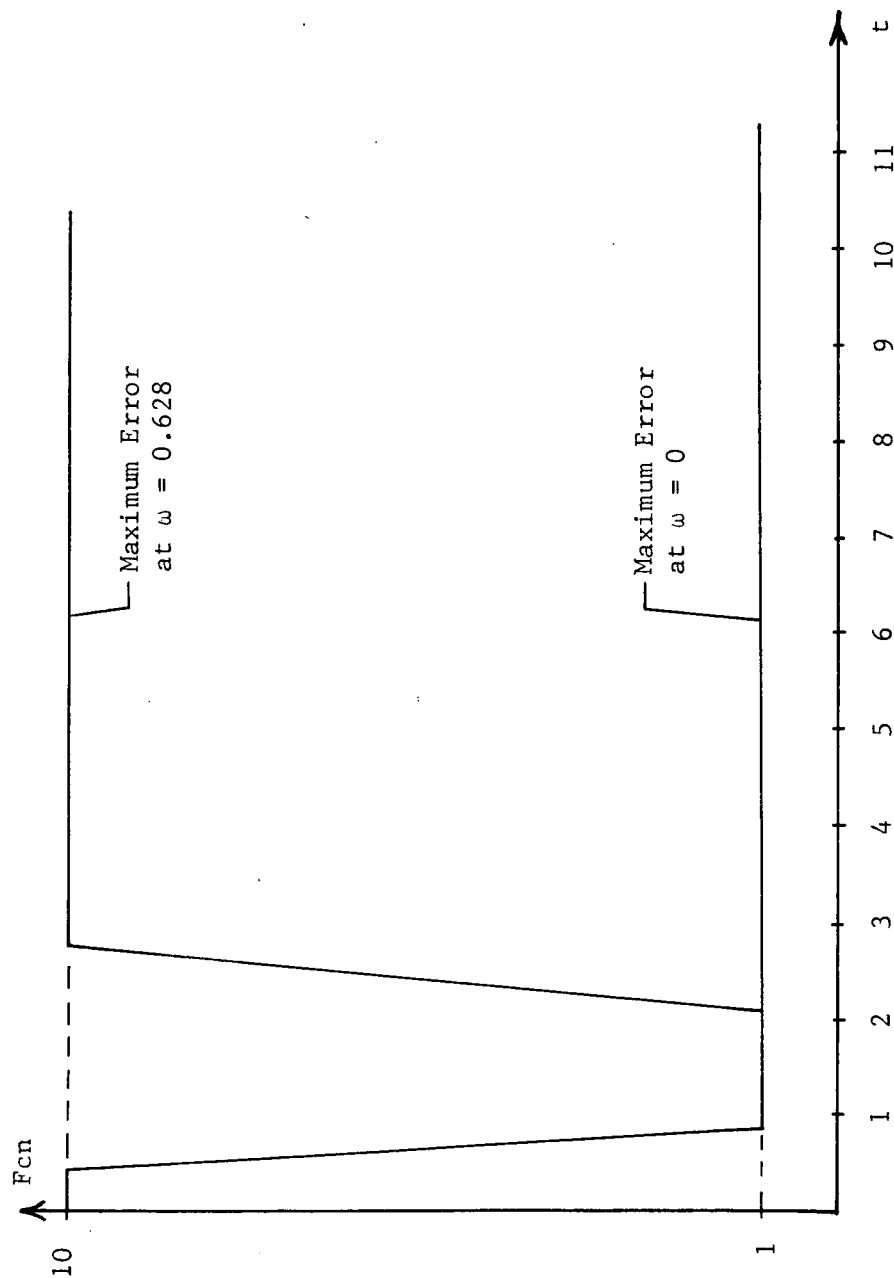


Figure 4.34  
Functions Resulting in Maximum Error  
During Second Series

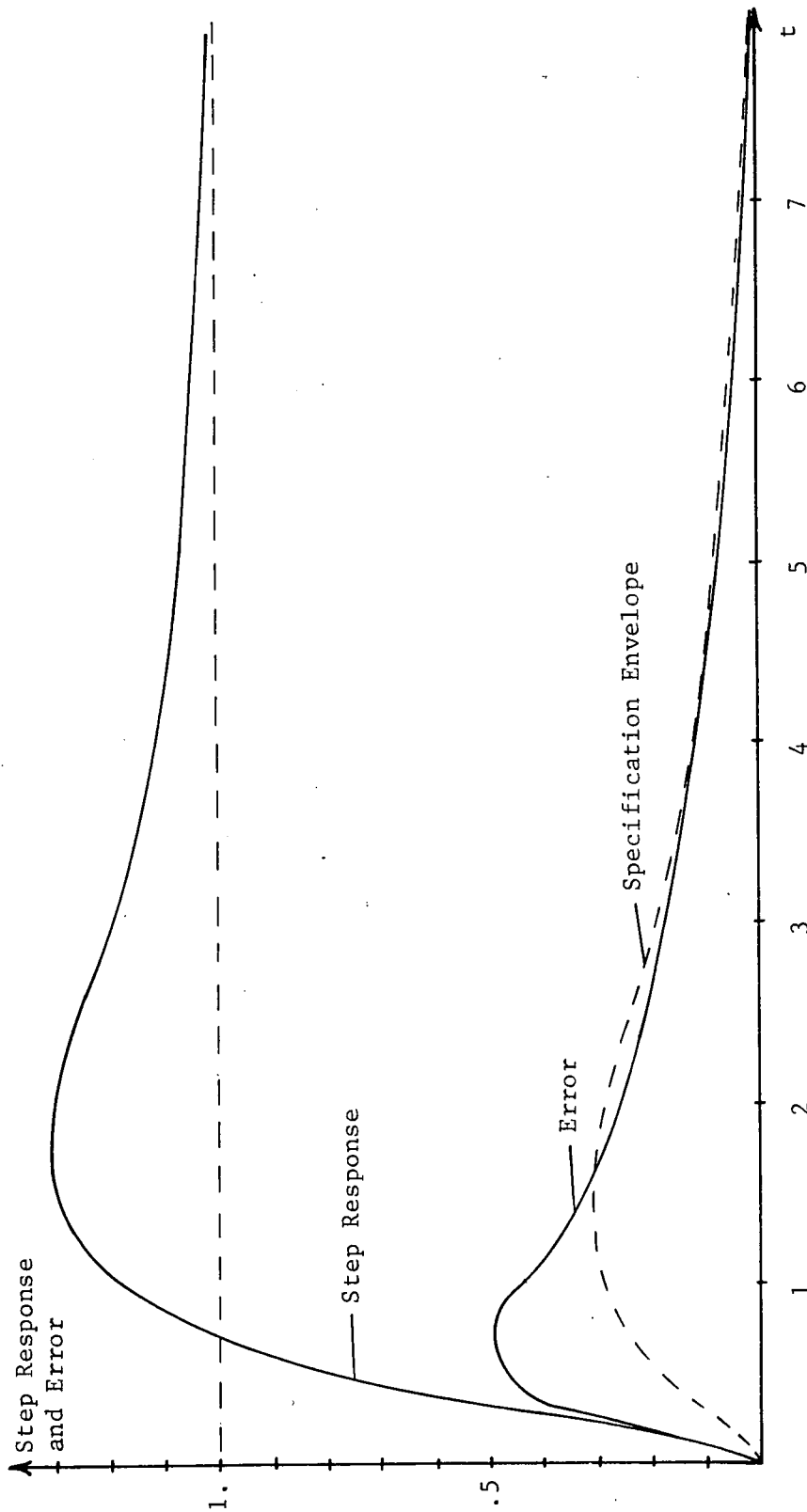


Figure 4.35  
 Step Response and Error Function Corresponding  
 To Maximum Error at  $\omega = 0$  During Second Series

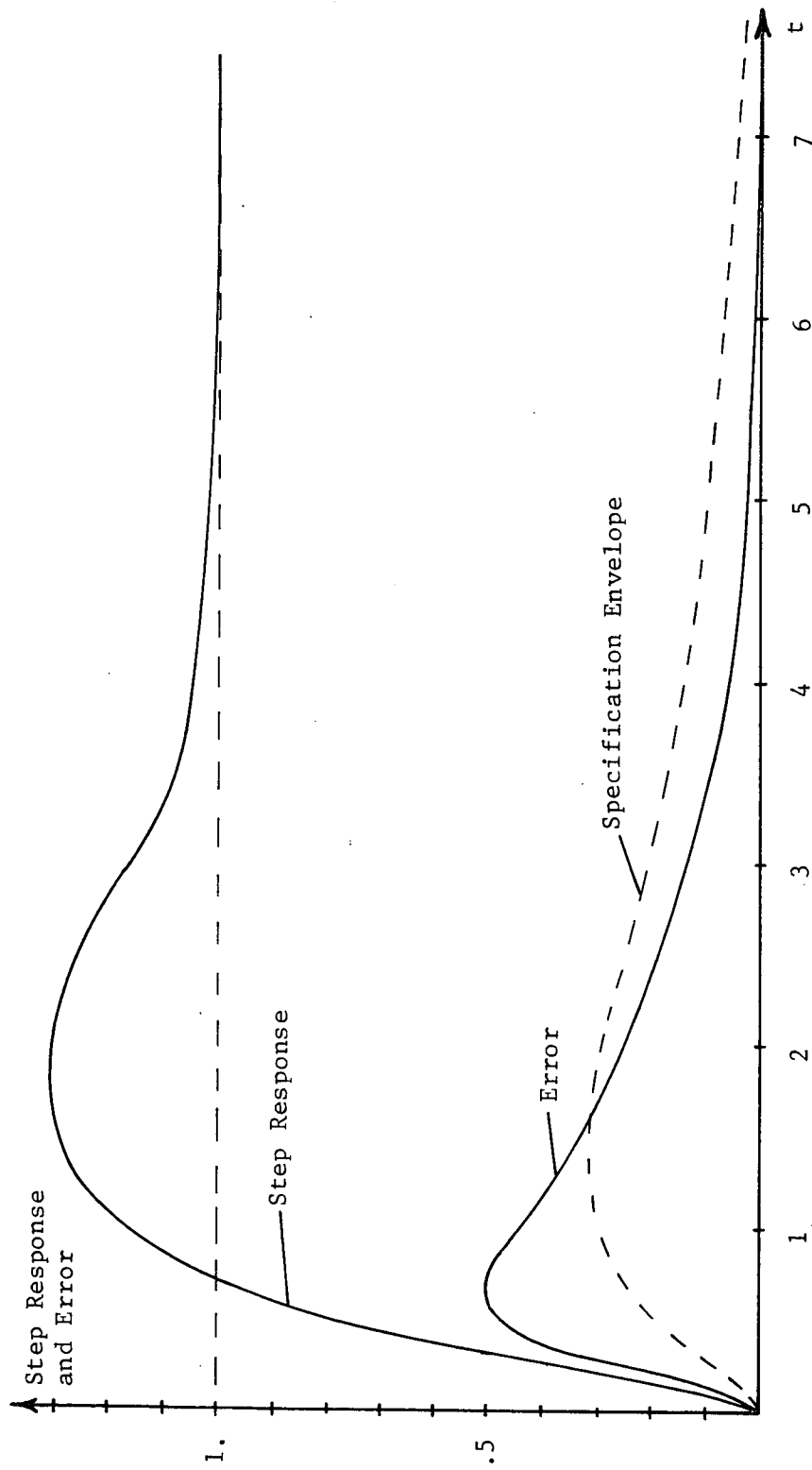


Figure 4, 36  
Step Response and Error Function Corresponding  
To Maximum Error at  $\omega = 0$  During Second Series

more quickly after four seconds as a result of an increase in gain between four and five seconds.

In an effort to observe the effect of an increase in slope on the error, a second series of time-varying runs was made with the same time-varying gain as shown in Figure 4.30, except the variations are completed in 4.5 seconds instead of nine seconds, thus increasing the maximum gain from ten to 20. A slight increase in the error at the two frequencies zero and 0.628 was observed; but, again, the design proved to be adequate for the higher frequencies. Figure 4.34 shows the variations causing the maximum error at the two frequencies and Figures 4.35 and 4.36 show the corresponding step responses and error functions. The magnitude of the Fourier transforms of the error functions is shown in Figure 4.37. Note the close similarity of these functions to those shown in Figure 4.31 through 4.33.

A final effort was made to cause errors at the higher frequencies by having the time-varying gain make discrete jumps between the values at each of the 11 points instead of varying linearly between points. Only negligibly higher values of error were observed, however, over those obtained in the second series of runs.

It is felt that an excellent representation of possible time-variations were obtained in these runs. A number of preliminary runs were first made and analyzed to determine the types of variations causing the larger errors. It was these preliminary runs that showed the larger errors to occur when the specified

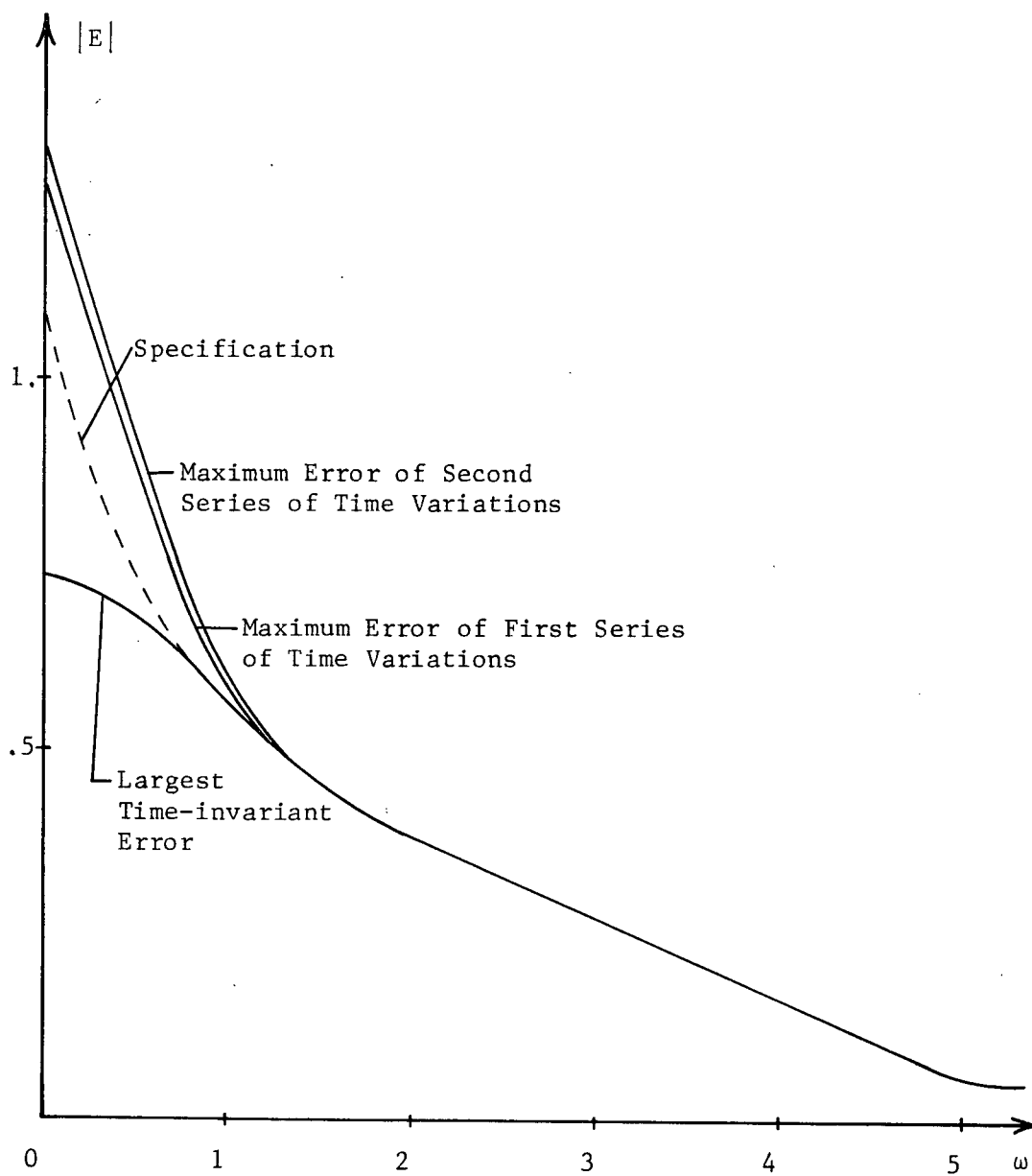


Figure 4.37  
Maximum Error Due to Time Variations

points of the function take on either the maximum or minimum values and that the largest errors occur when the function started at ten and quickly decreased to one. Special functions such as oscillations of various frequencies and step functions were then selected and run. Finally, a large number of functions were selected at random to help insure that some possible variation resulting in larger errors had not been overlooked. None of the errors due to these special or random selections, however, caused errors larger than those observed in the preliminary runs. In all, more than five hundred functions were run requiring approximately 70 hours of computer time on the IBM 1130.

The determination of the regions of  $P_o/P_{eq}$  for  $\omega = 6.28$  will now be discussed. In reality, the determination of the regions of  $P_o/P_{eq}$  were carried out simultaneously with the search for the maximum  $|E|$  since both  $P_o/P_{eq}$  and  $|E|$  were calculated for each function. The procedure for determining the region of  $P_o/P_{eq}$  was to plot the values of  $P_o/P_{eq}$  for each time-varying function from which the general outline of the region could be observed. It must be recognized that the procedure is not exact but, nonetheless, yields useable results. Because of the relatively large number and wide diversity of functions which were run, it is felt that a reasonably good representation of the regions of  $P_o/P_{eq}$  was obtained. The regions are shown in Figures 4.38 through 4.43, along with the specification regions of acceptable  $P_o/P_{eq}$  for the  $L_o$  of the design. The only frequency at which the specifications are not met is 0.628, which is in agreement with the results obtained in the maximum  $|E|$



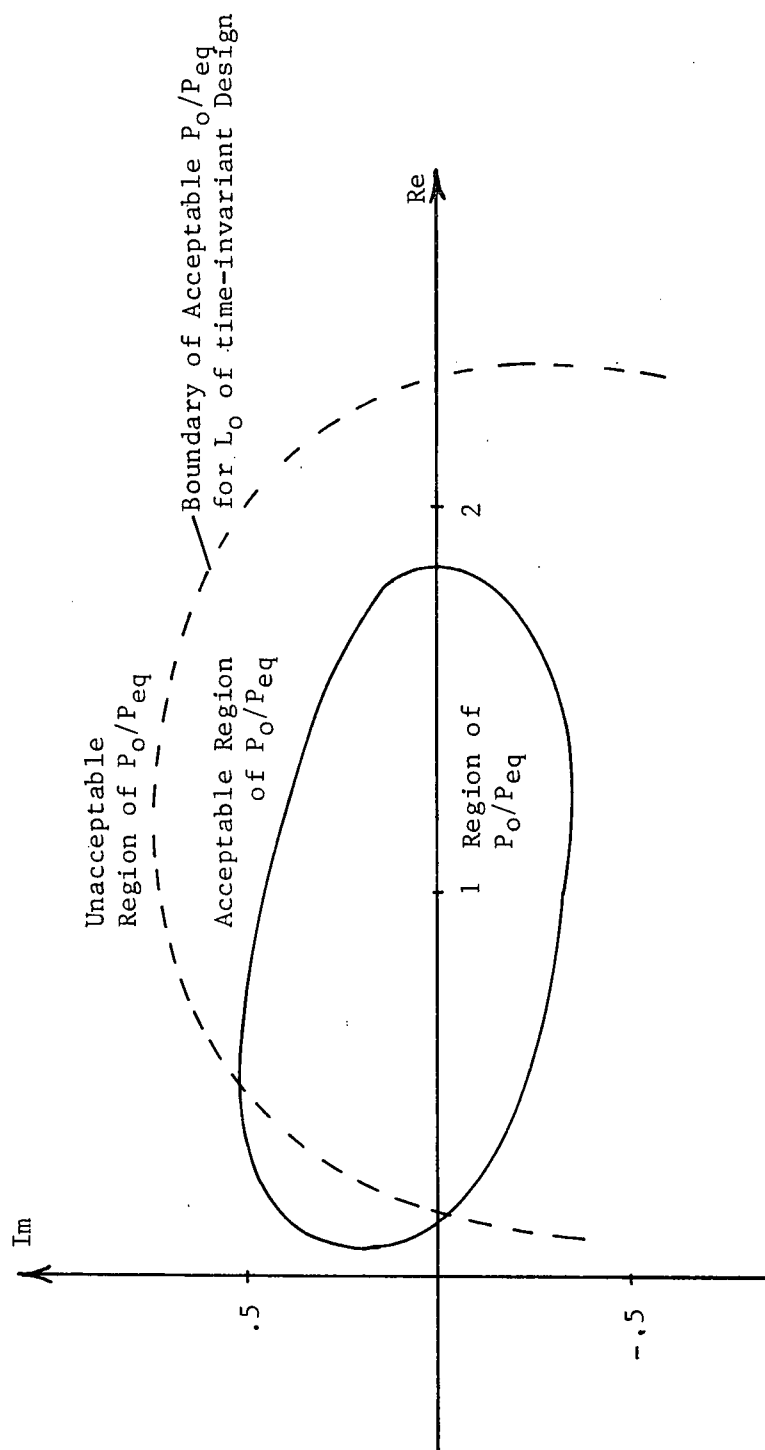


Figure 4.38  
Region of  $P_O/P_{eq}$  for  $\omega = 0.628$

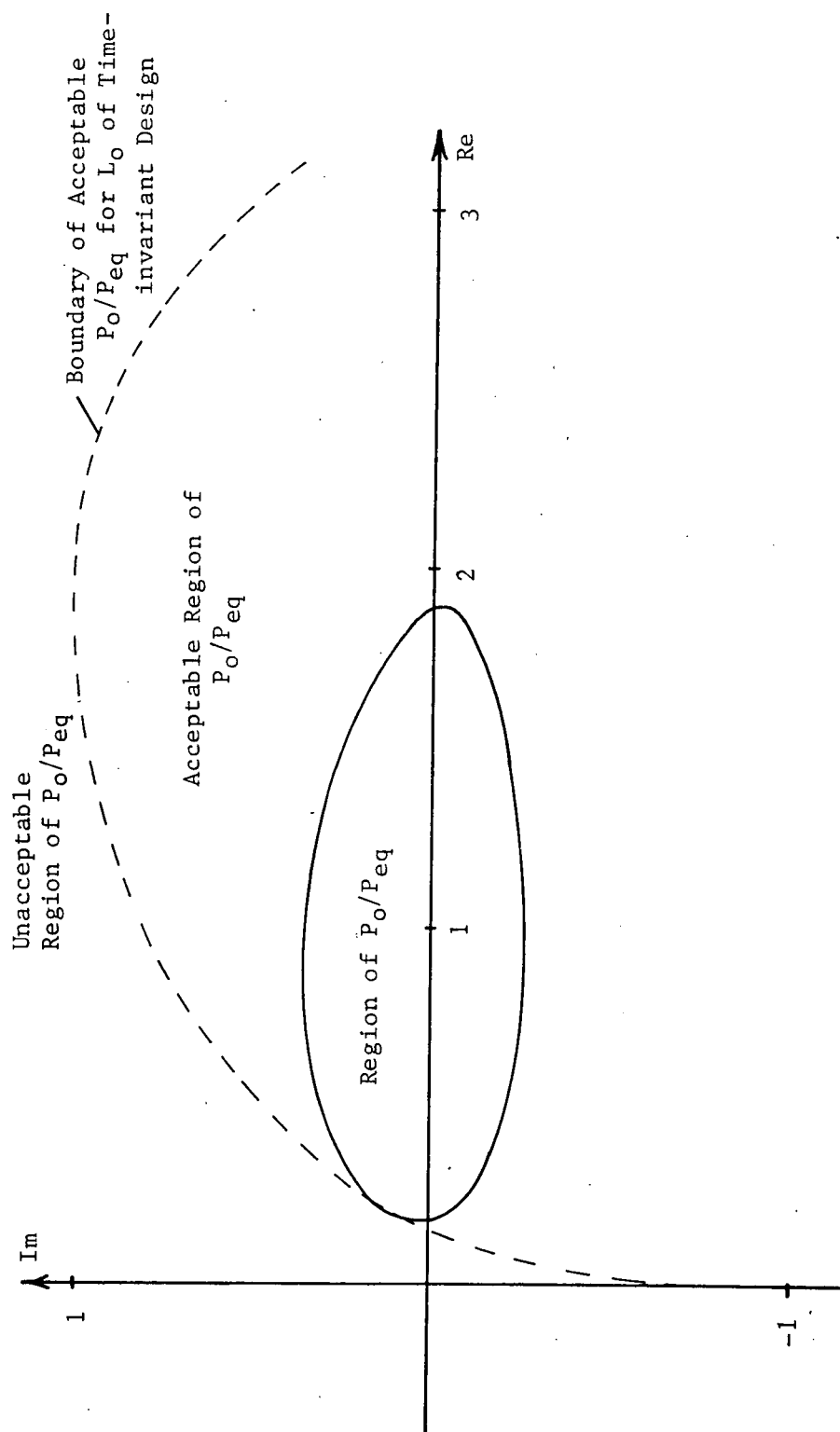


Figure 4.39  
Region of  $P_O/P_{eq}$  for  $\omega = 1.25$

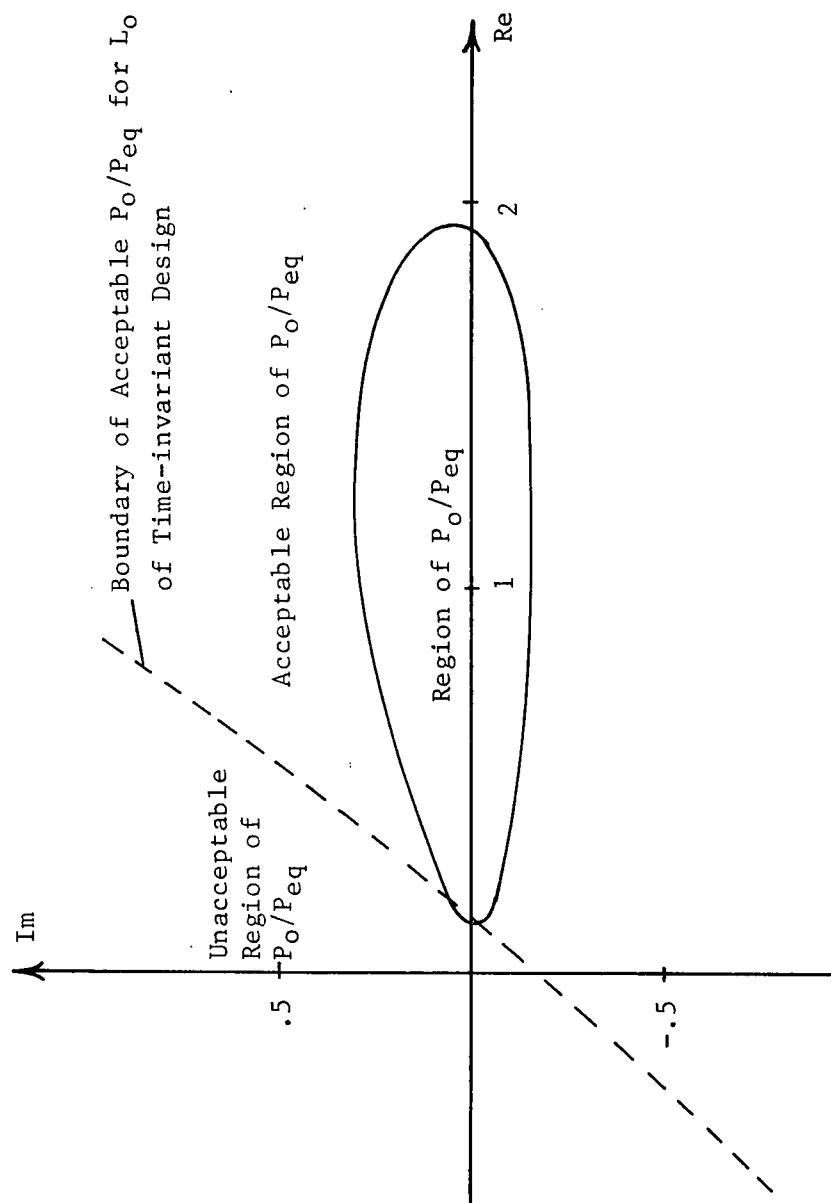


Figure 4.40  
Region of  $P_O/P_{eq}$  for  $\omega = 1.88$

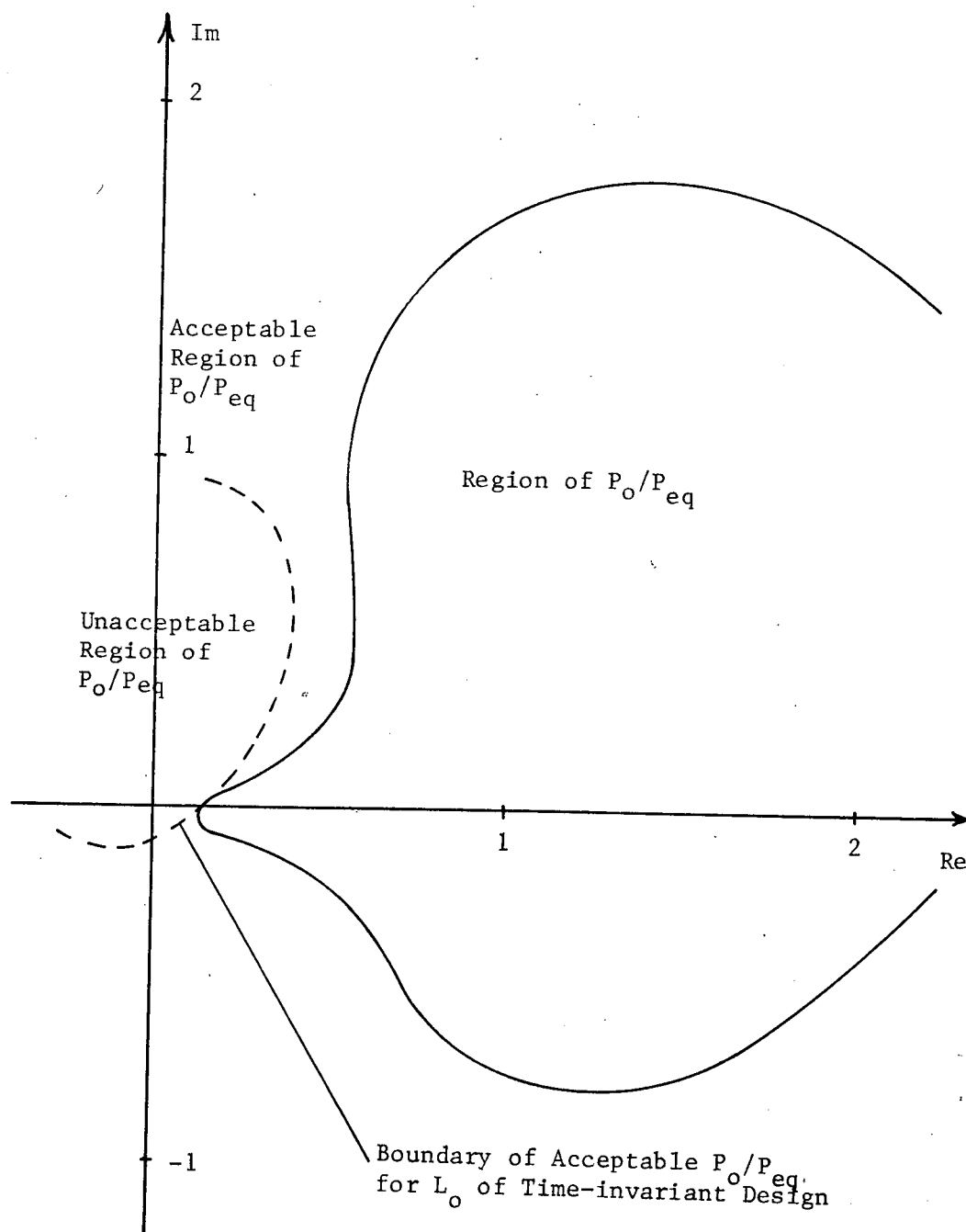


Figure 4.41  
Region of  $P_o/P_{eq}$  for  $\omega = 4.39$

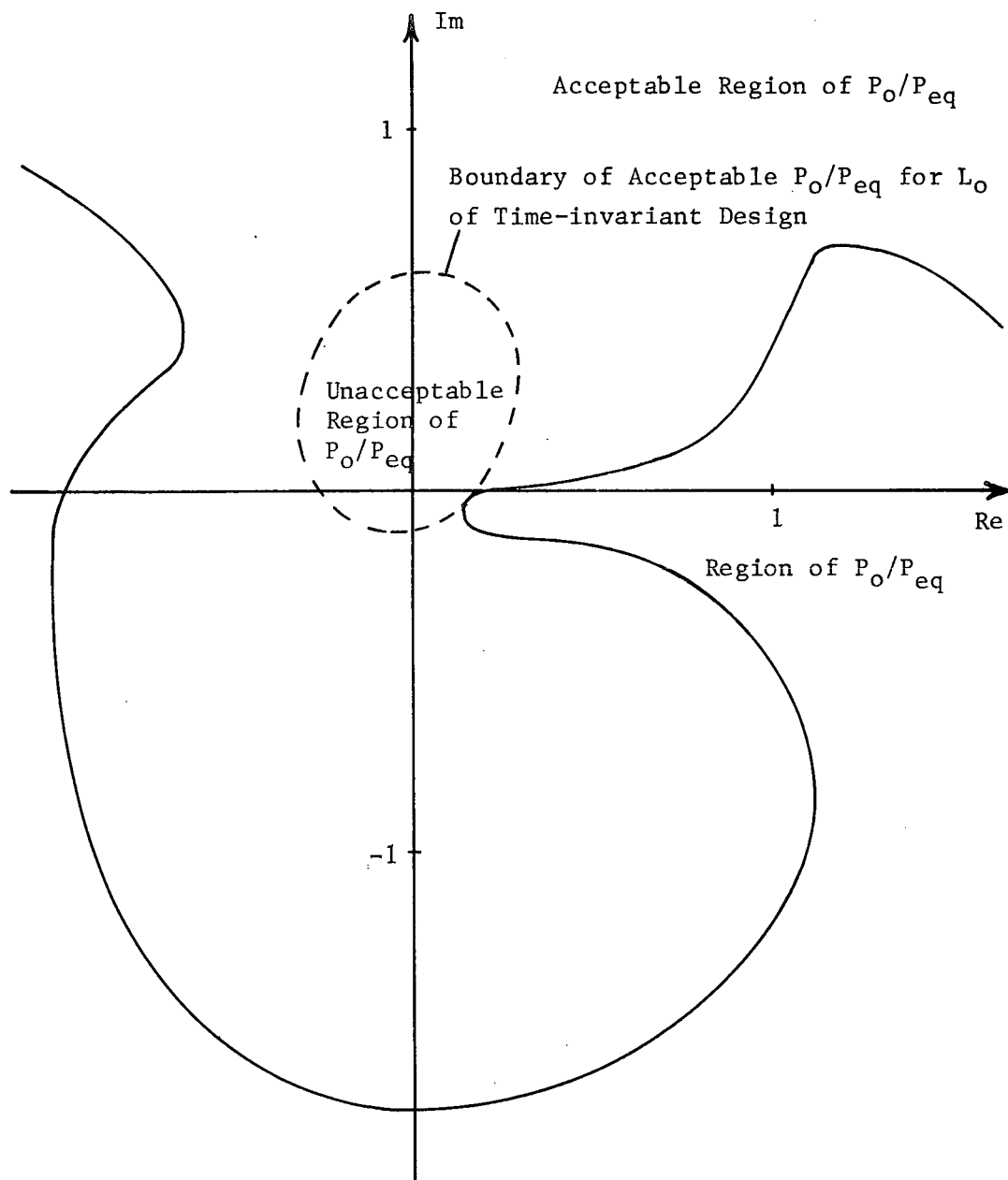


Figure 4.42  
Region of  $P_O/P_{eq}$  for  $\omega = 6.28$

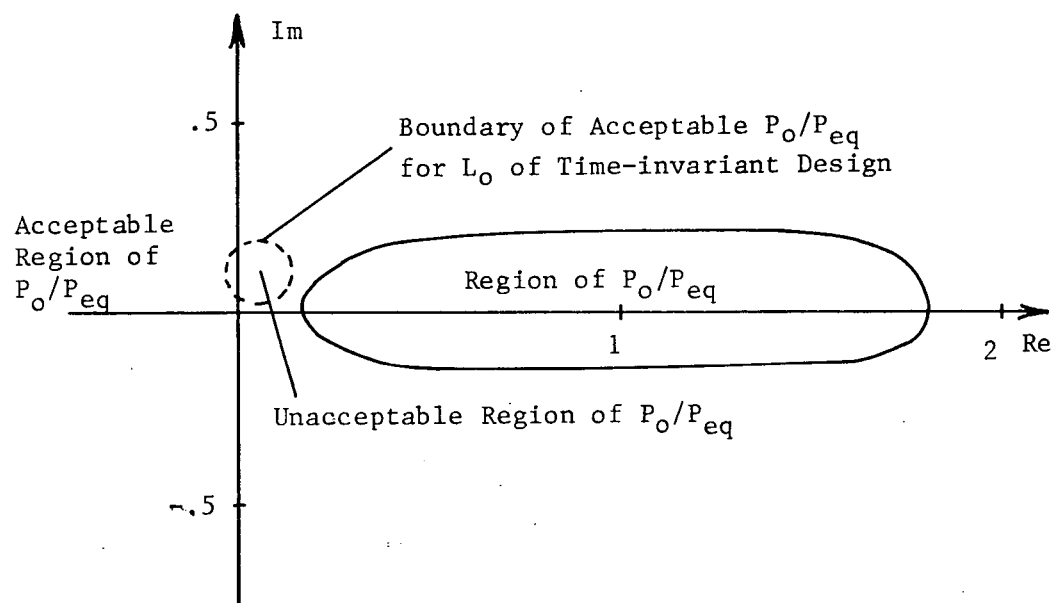


Figure 4.43  
Region of  $P_o/P_{eq}$  for  $\omega = 9.42$

determination.

The regions of  $P_O/P_{eq}$  for frequencies 0.628, 1.25, 1.88, and 9.43 are well concentrated about the region of  $P_O/P_{eq}$  corresponding to the time-invariant case. This concentration is similar to the observations made in the previous chapter and is no surprise; however, the regions of  $P_O/P_{eq}$  for frequencies 4.39 and 6.28 do not show this concentration which was an unexpected result.

The region of  $P_O/P_{eq}$  for 6.28 is especially interesting since it extends into the left half of the complex plane and a good distance into the lower half plane. In fact, points were found as low as  $-j6$ . However, such large magnitudes of  $P_O/P_{eq}$  are not unacceptable as is seen in Figure 4.42. Note what large values of  $P_O/P_{eq}$  imply about the system output  $C(j\omega)$ . Since  $P_O$  is a constant,  $P_O/P_{eq}$  becomes large only if  $P_{eq}$  becomes small. Since  $P_{eq}$  is defined as the plant output divided by the plant input,  $P_{eq}$  becomes small only if the time-varying plant does not effectively transfer the signal at the frequency of interest. In other words,  $P_O/P_{eq}$  will be large if the frequency content of the output is small while that of the input is not so small. In the example the frequency content of the output at 6.28 cannot only be small or even zero, but can actually be at some finite magnitude  $180^\circ$  out of phase with the desired plant output, thus allowing portions of  $P_O/P_{eq}$  to lie in the left half plane.

Figures 4.38 through 4.43 clearly illustrate why the design is satisfactory for the time-varying gain at frequencies of 1.25 and above. The time-variations do have a significant effect on

the system as shown by the increased size of the region of  $P_o/P_{eq}$ . However, when the specification region of acceptable  $P_o/P_{eq}$  is made large enough to enclose the region of  $P_o/P_{eq}$  for the time-invariant system, it also encloses a great deal of additional area which is large enough to allow for the increased size of the region of  $P_o/P_{eq}$  in the time-varying system. That is, the design is not only acceptable for the range of  $P_o/P_{eq}$  in the time invariant system, but it is also large enough to accept the much larger region of  $P_o/P_{eq}$  in the time-varying system. It is speculated that if the region of  $P_o/P_{eq}$  for the time-invariant system came closer to filling the specification region of  $P_o/P_{eq}$  such as would occur if a plant pole could take on a range of values, the region of  $P_o/P_{eq}$  for the time-varying system would not be able to lie entirely within the acceptable region of  $P_o/P_{eq}$ .

It is also of interest to observe some of the step responses and error functions of the system for time-variations other than those resulting in the maximum value of  $|E|$ . Seven typical step responses with their corresponding time-variations and error functions are shown in Figures 4.44 through 4.50. The time duration of the randomly selected error functions was placed at seven seconds since, as has been previously observed, faster time variations and variations after seven seconds have little effect on the error. The step responses are well behaved despite the time-varying gain. The maximum overshoot appears to be not over 30% and the settling time of the function is not over seven or eight seconds in the worst case. Although fast rise time is



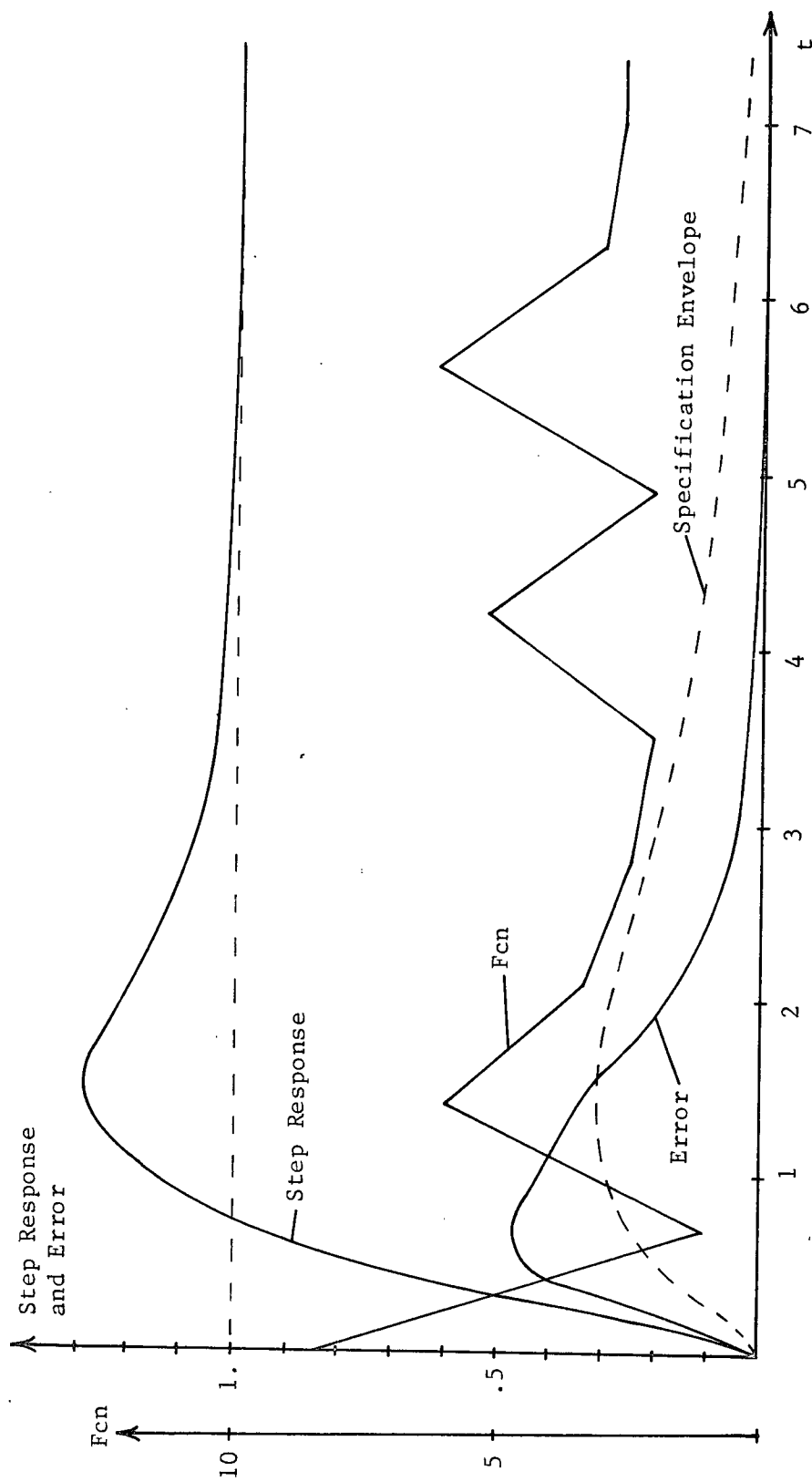


Figure 4.44  
Step Response of Time-Varying System  
Time-Invariant Design

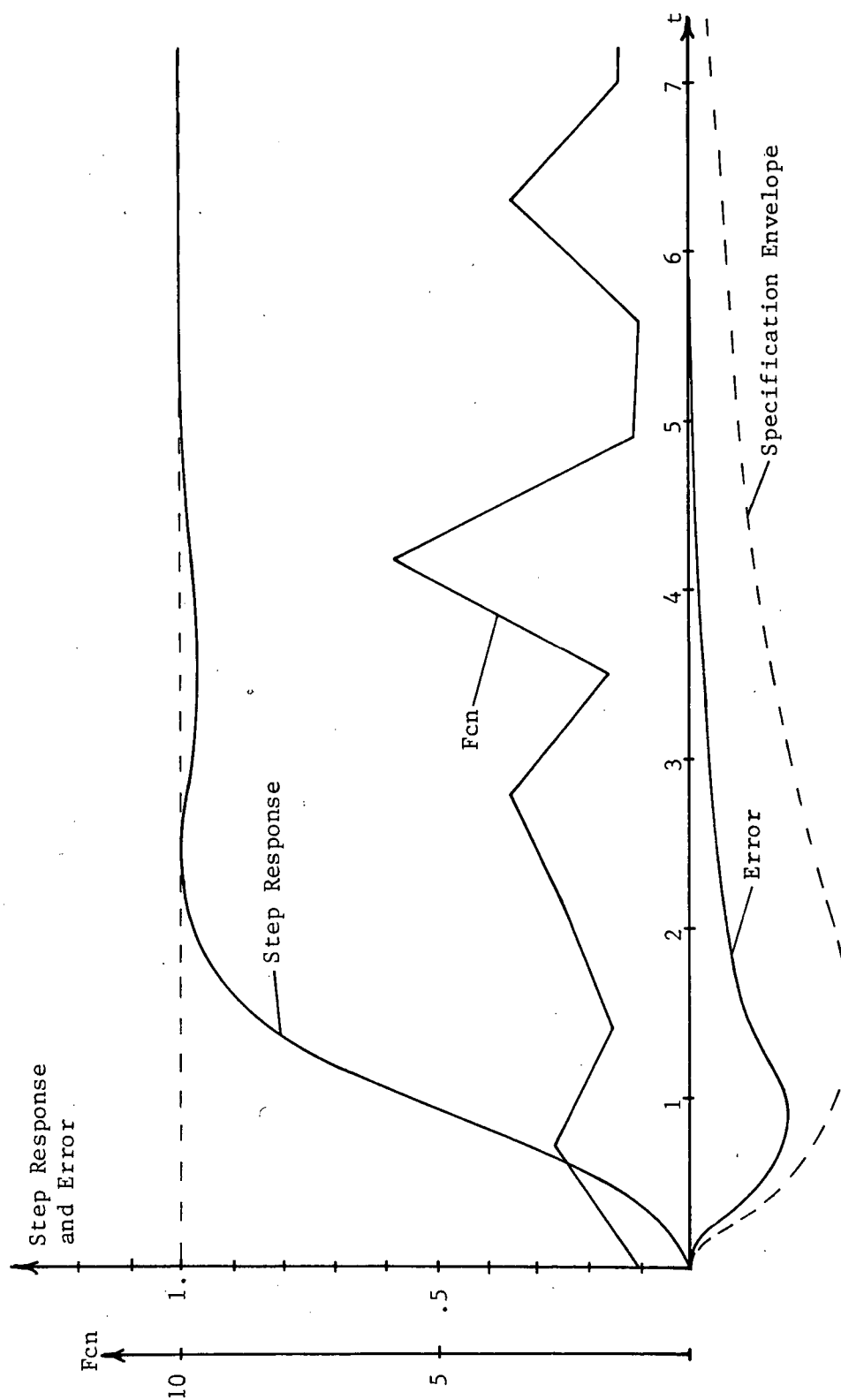


Figure 4.45  
Step Response of Time-Varying System  
Time-Invariant Design

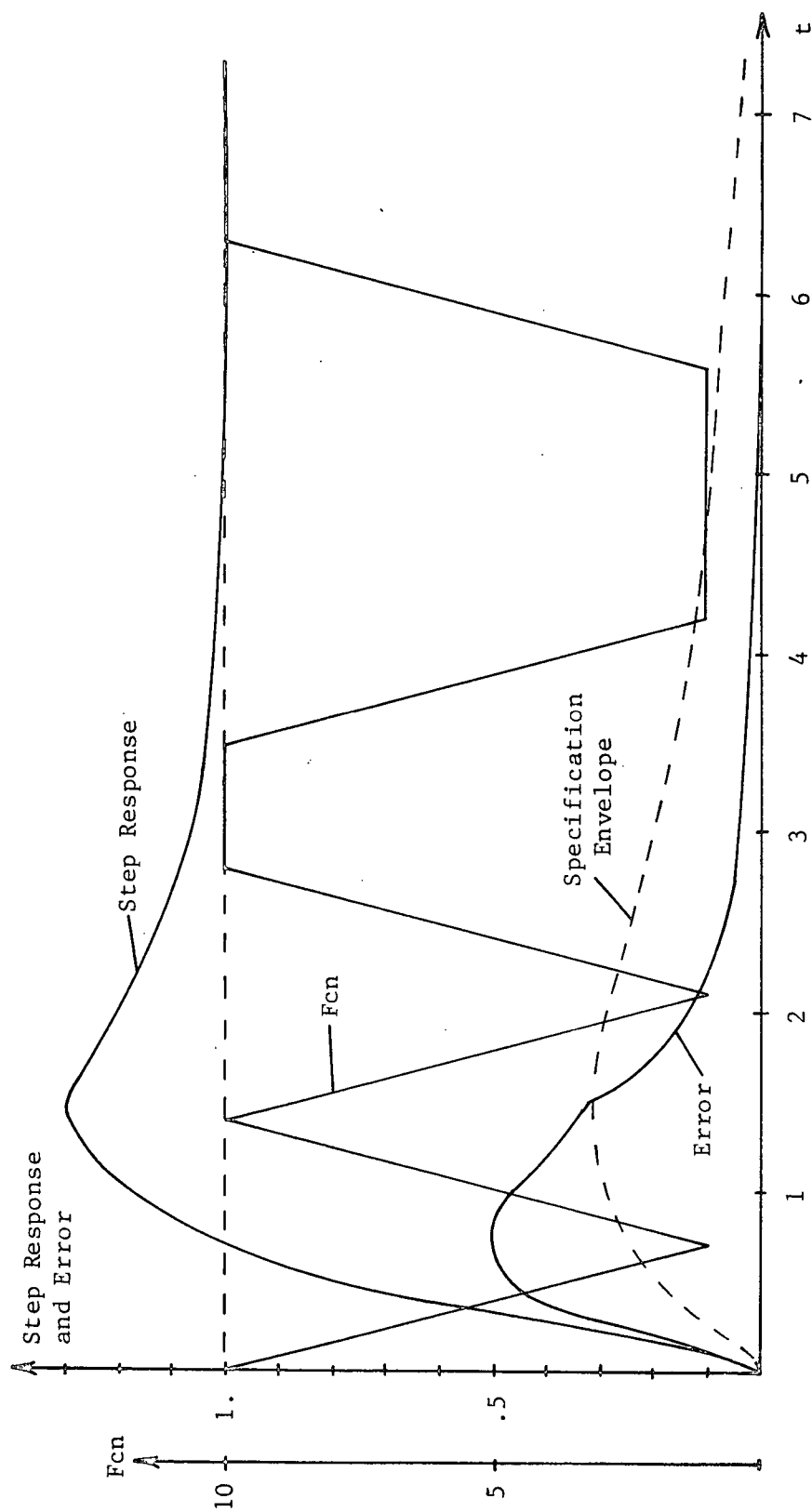


Figure 4.46  
Step Response of Time-Varying System  
Time-Invariant Design

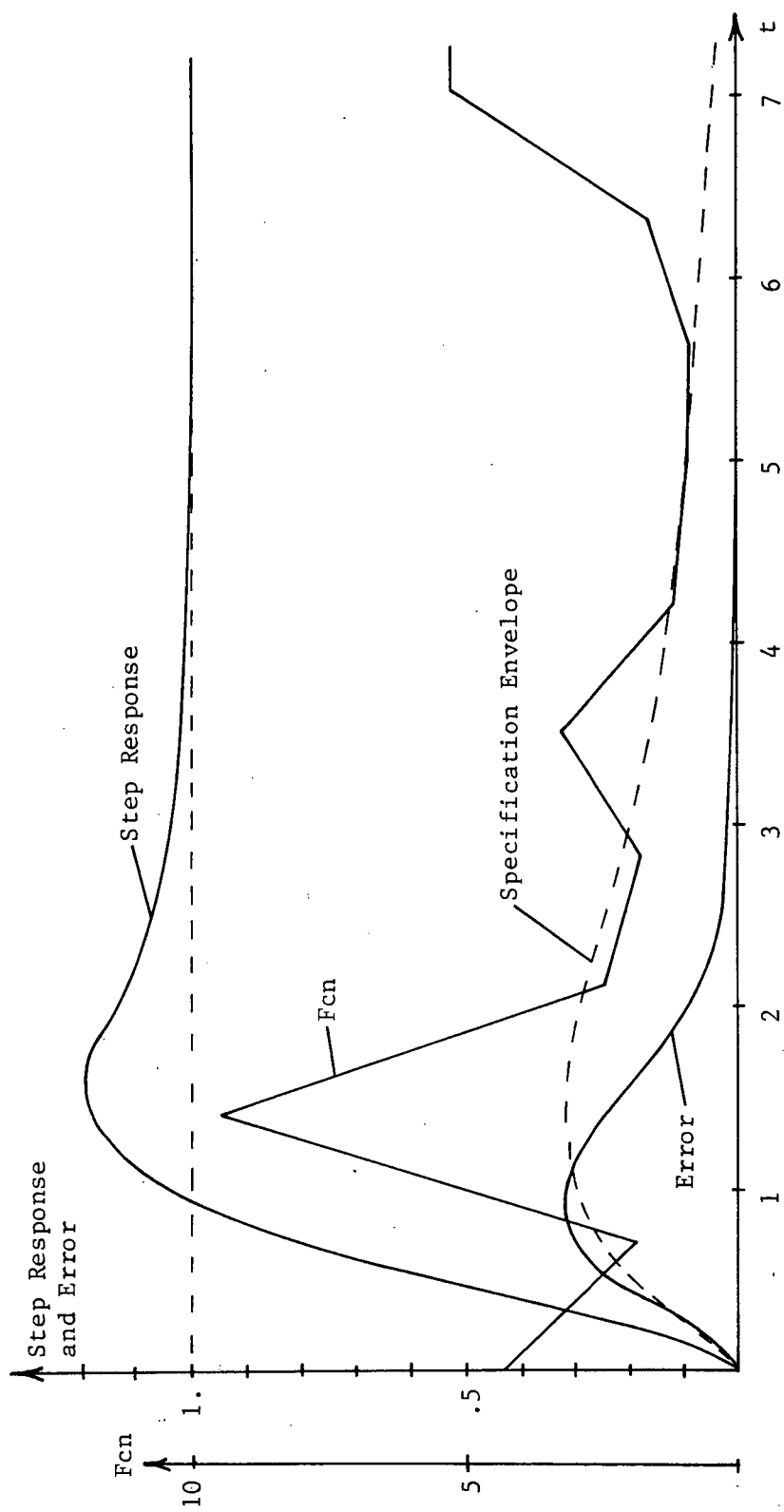


Figure 4.47  
Step Response of Time-Varying System  
Time-Invariant Design

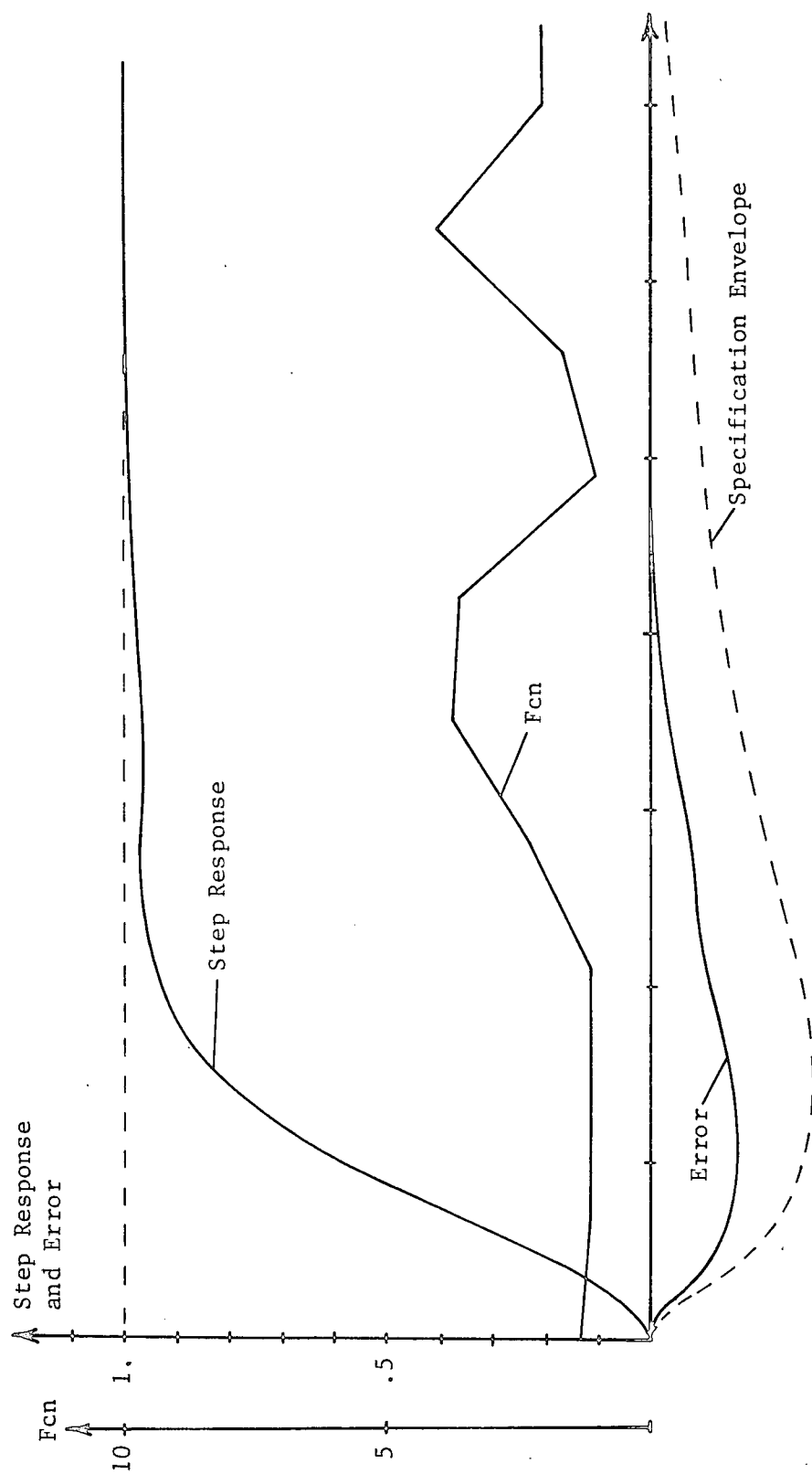


Figure 4.48  
Step Response of Time-varying System  
Time-invariant Design

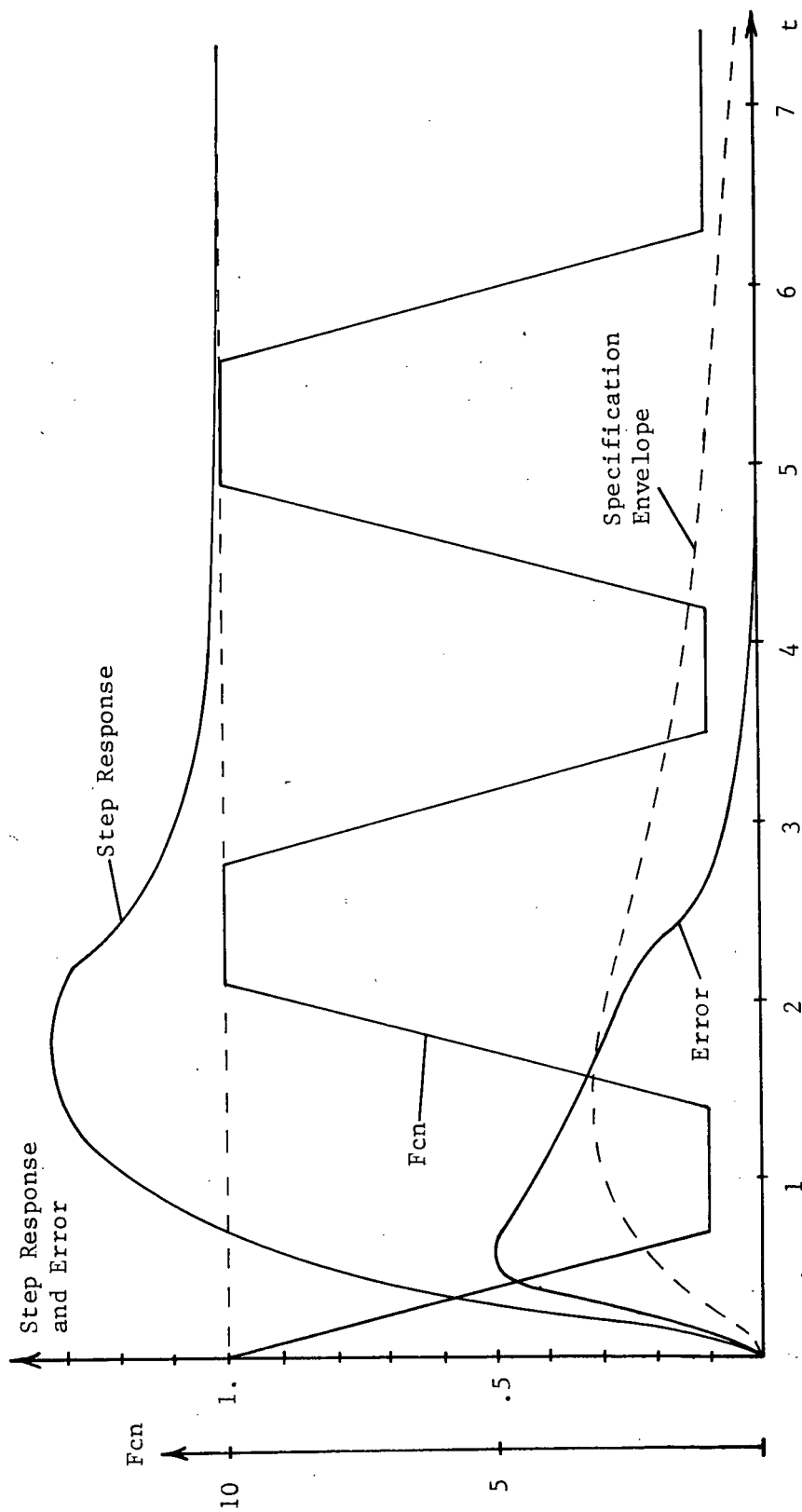


Figure 4.49  
Step Response of Time-varying System  
Time-Invariant Design

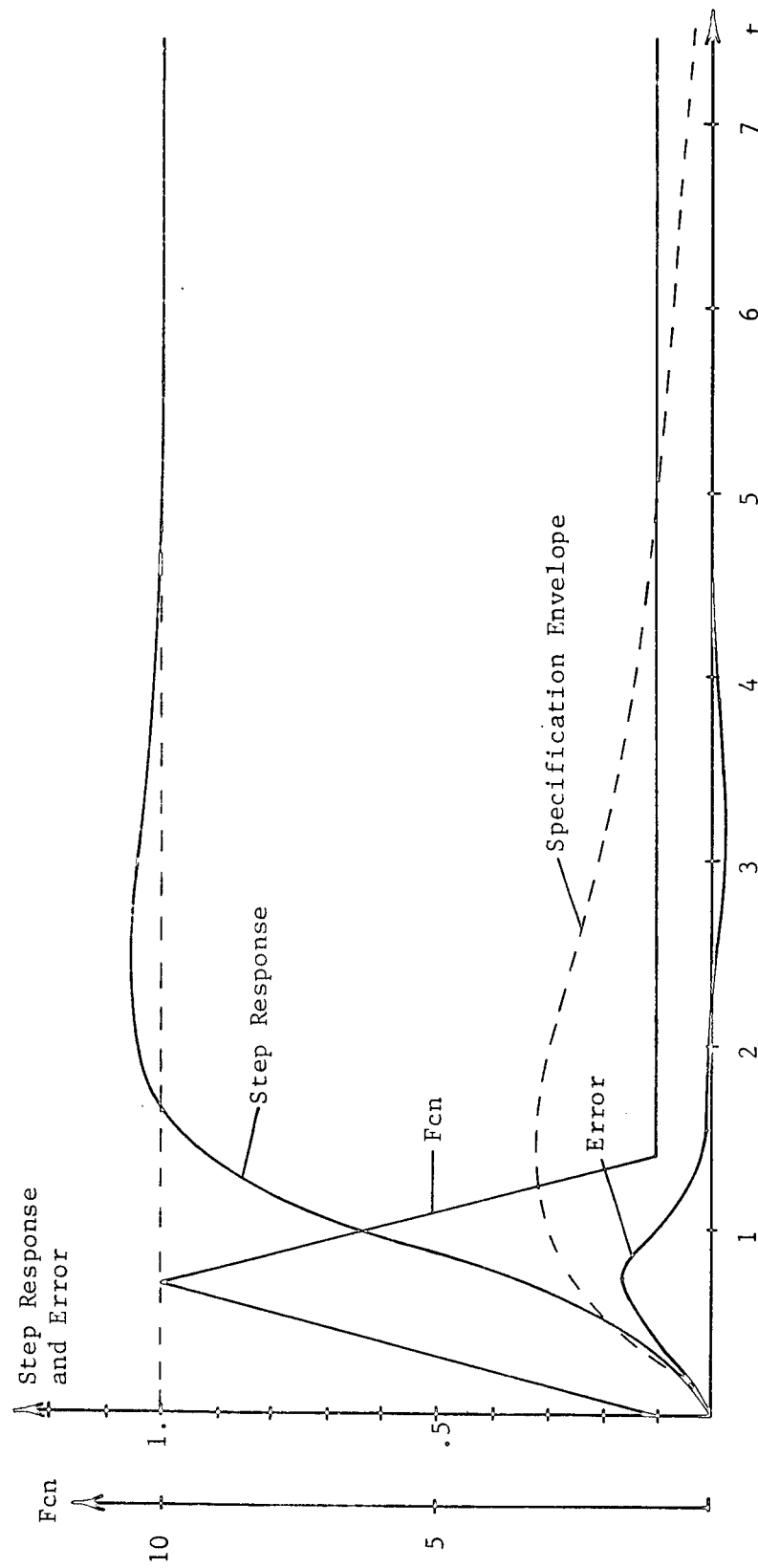


Figure 4.50  
Step Response of Time-varying System  
Time-invariant Design

usually not considered an undesirable property, it is fast rise time that is responsible for the large values of the error functions shown in Figures 4.44, 4.46, and 4.49. The time-varying gain in the responses having large values of error start at or near ten, while functions starting at or near one such as shown in Figures 4.45, 4.48, and 4.50 result in step responses having little or no overshoot with a relatively slow rise time and thus smaller values of error. It is evident from these figures that the form of the step response and thus the error function is highly dependent upon the starting value of the time-varying gain and is less sensitive to subsequent variations. This basically is the same observation made earlier in the determination of the maximum value of  $|E|$ .

Since the time-invariant system design is unsatisfactory for the system under time-varying conditions, a second design must be made. The second design will first be made using design procedure one.

#### 4.5 Second Design: Procedure One

Equations (3-28) are the design equations for the subsequent designs required in procedure one. The design equations can be written as

$$\frac{E_{om}}{M} \left| 1 + L_o \right| \leq \left| 1 + L_o \right| \quad \text{for } E_{om} \geq M \quad (4-9a)$$

$$\left| 1 + L_o \right| \leq \left| 1 + L_o \right| \quad \text{for } E_{om} < M \quad (4-9b)$$

where  $M$  is the frequency domain specification,  $E_{om}$  is the maximum



error of the previous design,  $L_o$  is the compensation of the previous design and  $L'_o$  is the compensation to be designed.

The minimum values of  $|1 + L'_o|$  are now found from Inequalities (4-9). At zero frequency the magnitude of  $L'_o$  is infinite so that Inequalities (4-9) cannot be applied. However, dividing Inequality (4-9a) by  $P_o$  and setting  $\omega$  equal to zero one obtains

$$\frac{E_{om}}{M} |H(o)| \leq |H'(o)|$$

which sets a minimum value on  $|H'(o)|$ . Table 4-2 gives a summary of the specification  $M$ , the values of  $|1 + L_o|$  and the corresponding  $E_{om}$  of the previous design, and the minimum values of  $|1 + L'_o|$  for the frequencies of interest.

$\omega$	$M$	$E_{om}$	$ 1 + L_o $	$\text{Min} 1 + L'_o $
0	1.13	1.32	$ H(o)  = 1.22$	$ H'(o)  \geq 1.43$
0.628	0.65	0.808	2.34	2.91
1.25	0.51	0.543	1.613	1.72
1.88	0.42	0.42	1.34	1.34
4.39	0.11	0.11	1.01	1.01
6.28	0.05	0.05	0.95	0.95
9.41	0.05	0.23	0.93	0.93

Table 4-2  
Summary of Specifications

The minimum values of  $|1 + L'_0|$  correspond to regions in the complex plane of acceptable  $-L'_0$ . These regions are found to lie outside circles about the point one with radius equal to the minimum value of  $|1 + L'_0|$ .

The regions of acceptable  $-L'_0$  corresponding to the values given in Table 4-2 are shown in Figure 4.51 together with the regions of acceptable  $-L_0$  for the time-invariant system. A shortcoming of design procedure one is now evident. Since the region of unacceptable  $-L'_0$  is assumed to be a circle centered about the point one, it is possible to exclude  $-L'_0$  from large areas in the complex plane which would actually be acceptable, thus resulting in an overdesigned system. This will be especially true at high frequency where a small increase in the radius of the circle results in a much larger required increase in  $|L'_0|$ . Unfortunately, it is at these higher frequencies that  $|L'_0|$  must be decreased to as small a value as possible in order to limit the noise transmission to the plant input. For example, consider the regions corresponding to  $\omega$  equal 6.28. If the boundary of acceptable  $-L_0$  for the time-invariant system were not known, the boundary of acceptable  $-L'_0$  allows  $|L'_0|$  to become as small as can be designed. Such a design could not satisfy even the time-invariant system, much less the time-varying system, so that the radius of the region would have to be increased which would demand a much larger increase in  $|L'_0|$  than would really be required.

It was decided to design  $-L'_0$  so that it would lie within the

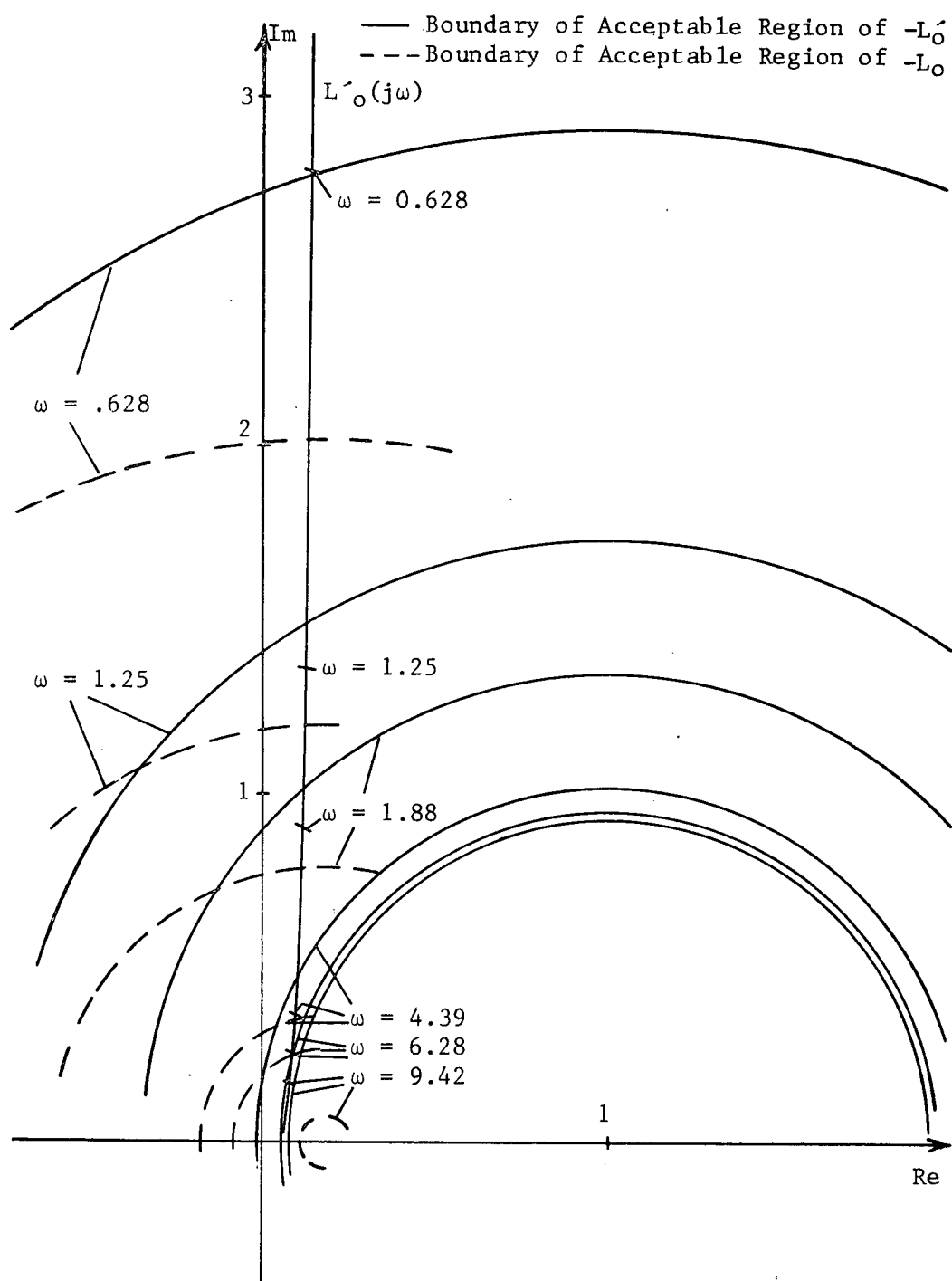


Figure 4.51  
 Polar Plot of  $-L'_0(j\omega)$  with Boundaries  
 of Acceptable Regions of  $-L_0$  and  $-L'_0$

acceptable region of  $-L'_O$  at  $\omega$  equal 0.628 but would lie approximately half way between the boundaries for  $-L_O$  and  $-L'_O$  at  $\omega$  equal to 1.25 and 1.88. At  $\omega$  equal to 4.39, 6.28, and 9.42 only the acceptable regions of  $-L_O$  would be considered. The reason for this is that the specifications were basically satisfied with  $L_O$  except at  $\omega = 0.628$  while a design based solely on the acceptable region of  $-L'_O$  would result in an underdesign at the higher frequencies. The design which was chosen has an  $L'_O(s)$  given by

$$L'_O(s) = 26.88 \frac{(s + 2.2)(s + 5.8)}{s(s + 2)(s + 7)(s + 14)}$$

The polar plot of  $-L'_O$  is shown in Figure 4.51. The corresponding  $H(s)$  is given by

$$H(s) = 14.78 \frac{s^3 + 10s^2 + 28.76s + 25.52}{s^3 + 23s^2 + 140s + 196}$$

and  $G(s)$  is found to be

$$G(s) = 2.2 \frac{s^5 + 25s^4 + 212.88s^3 + 744.8s^2 + 1165.07s + 685.98}{s^5 + 25.8s^4 + 208.4s^3 + 680s^2 + 1108.8s + 784}$$

The higher frequency poles in  $L'_O(s)$  and  $H(s)$  will be added in the final design. The above  $H(s)$  satisfies the specification on  $H'(o)$  given in Table 4-2. More lag is required in  $L'_O$  than in  $L_O$  because of the higher rate of decrease required between the frequencies 0.628 and 1.25.

A comment should be made concerning stability. Since the example has only a time-varying gain, sufficient conditions for

stability are known. A convenient criterion is the circle criterion which is given in Reference (38). The system of this example will be stable if the polar plot of  $-L'_0$  does not lie within or enclose a circle of radius 0.8181 and centered at point one. The above design satisfies this criterion so that the system is assured to be stable.

The new design was tested by simulating the system and determining the maximum magnitude of error. The duration of the time-varying gain as illustrated in Figure 4.30 was set at seven seconds. Since  $L'_0$  is similar to  $L_0$ , faster variations should have little effect on the magnitude of the error as well as variations after seven seconds. As with the first design, it was found that the larger errors occurred for variations that start at ten and decrease quickly to one and that variations starting at values other than near ten produced errors no larger than those observed with the gain held constant at ten. It was also verified that variations occurring after five or six seconds have little effect on the error.

A plot of the maximum error corresponding to this design is shown in Figure 4.52 along with the specification envelope and the maximum error corresponding to the first design. An important observation is that the increase in  $|1 + L'_0|$  at a particular frequency appears to have substantially affected the maximum error only in the vicinity of that frequency. For example, an increase of  $|L'_0|$  at 0.628 did not cause an increase in  $|E|$  at 1.88 as could have occurred in a time-varying system since the

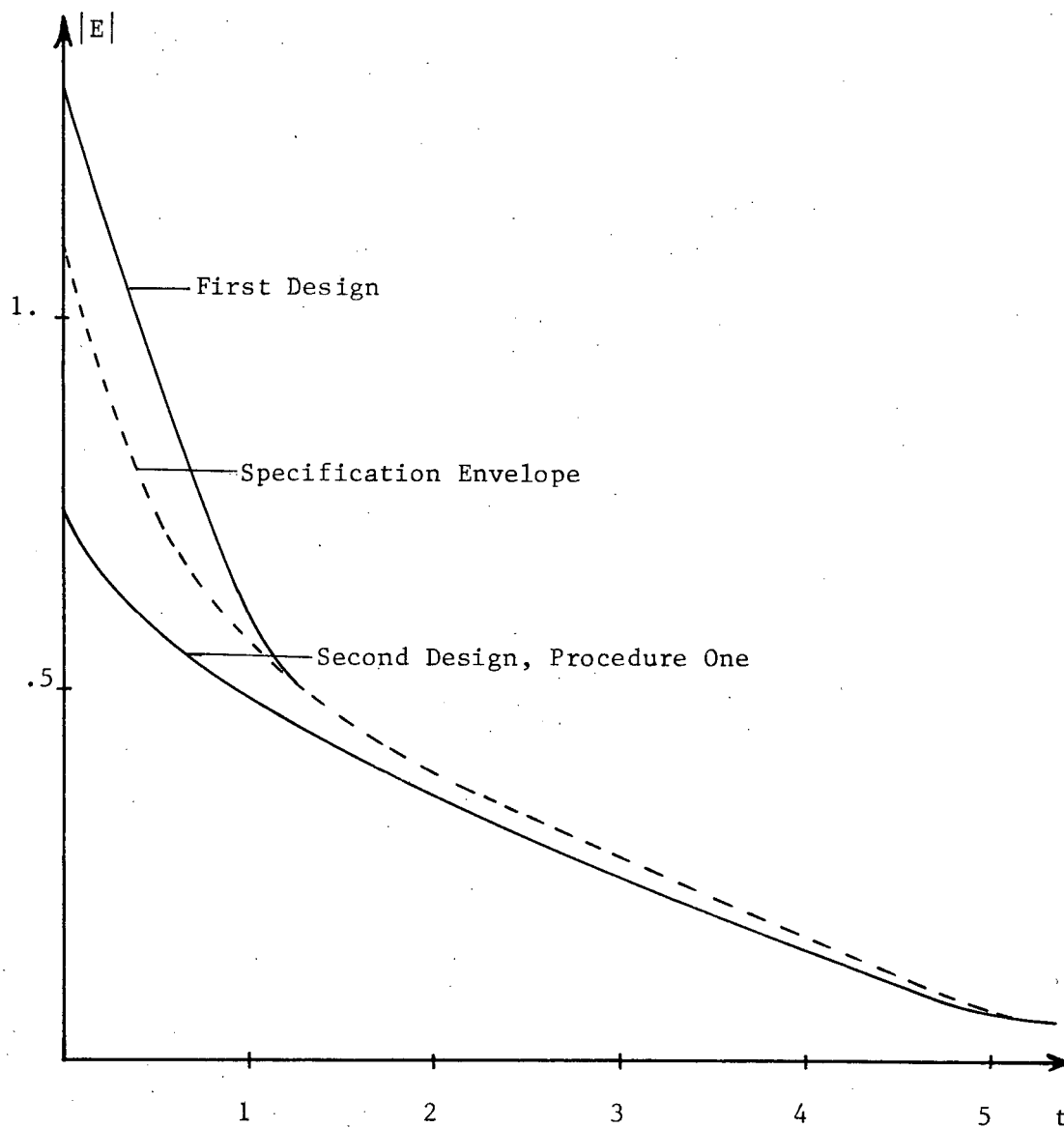


Figure 4.52  
Plot of Maximum  $|E|$   
For Second Design Using Procedure One

frequencies are not independent. As was suspected, the system is overdesigned; that is,  $|E|$  is considerably smaller than the specifications in the low frequency region.

The time variations resulting in the maximum error at  $\omega = 0$  and  $\omega = 0.628$  are shown in Figures 4.53 and 4.54, respectively, with the corresponding step response and error function. Note that these variations are almost identical to the time variations found for the first design shown in Figures 4.31 and 4.34. The step responses and error functions in the second design are also similar to those in the first design. In the second design, however, the peak overshoot is reduced to 19% from 32% in the first design. The settling time in the second design has also been significantly reduced.

Although the design satisfies the frequency domain specification, the error function does not fall within the time domain specification envelope. Nevertheless, the step response is well behaved and would undoubtedly be considered acceptable. In reality, the time domain specification envelope should probably have been chosen to allow larger errors in the range 0 to 1 second since fast rise time is generally not considered an undesirable property in a system. To give an indication of the step response for other variations, variations are shown in Figures 4.55 and 4.56 with their corresponding step responses and error functions.

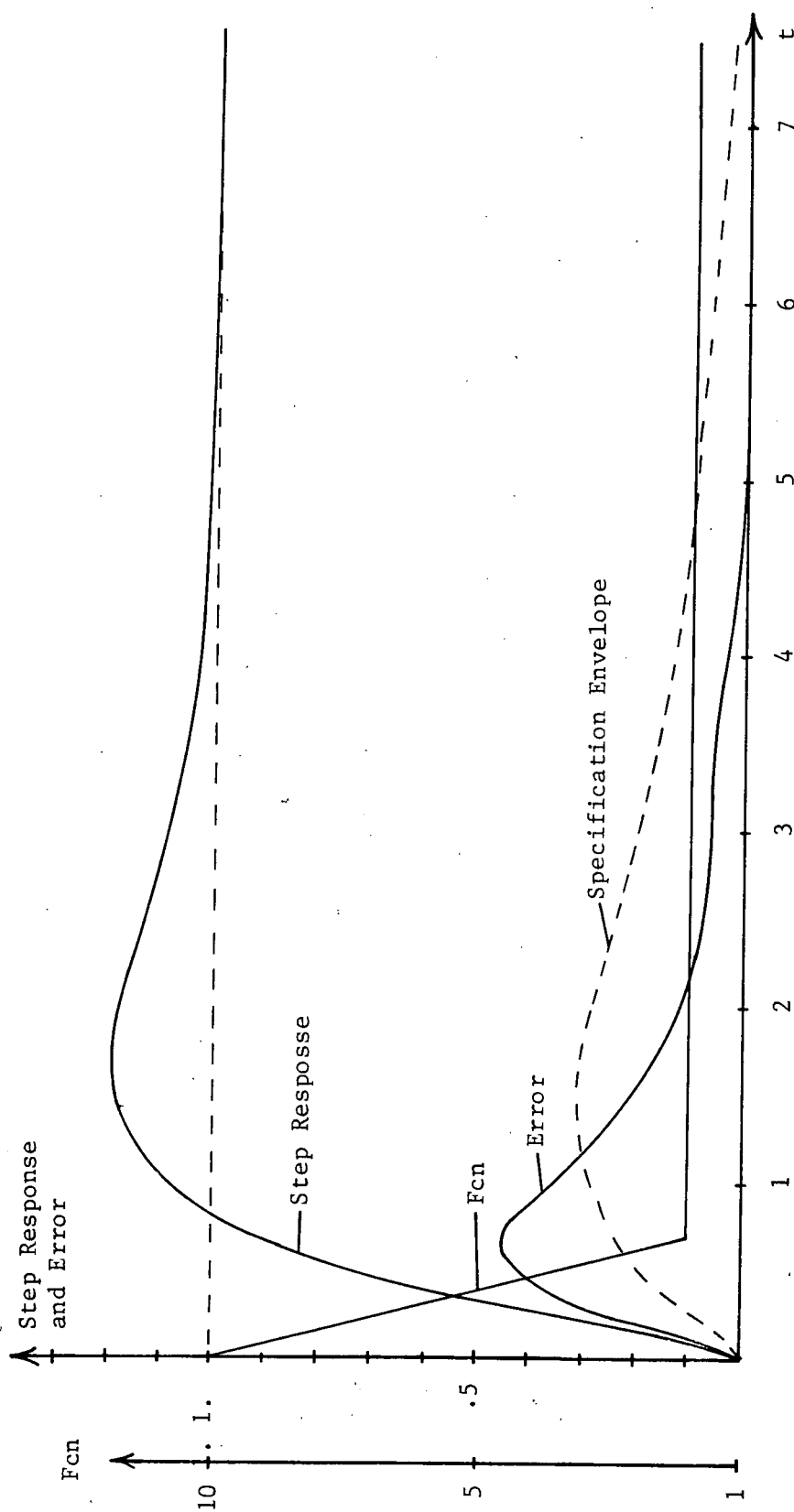


Figure 4.53  
Time Variations Resulting in Maximum  $|E|$   
at  $\omega = 0$  With Corresponding Step Response and Error Function



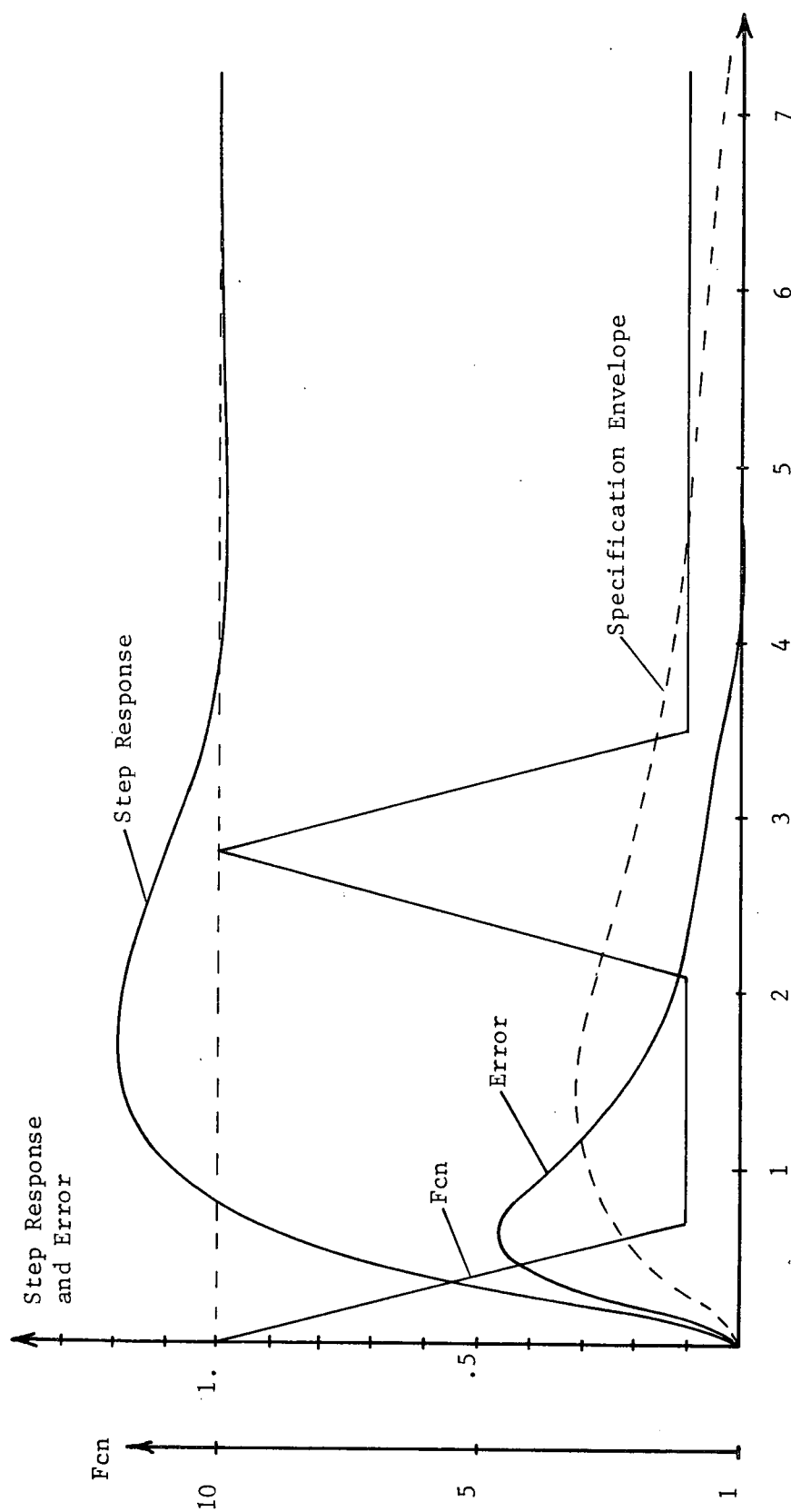


Figure 4.54  
Time Variations Resulting in Maximum  $|E|$   
at  $\omega = 0.628$  with Corresponding Step Response and Error Function

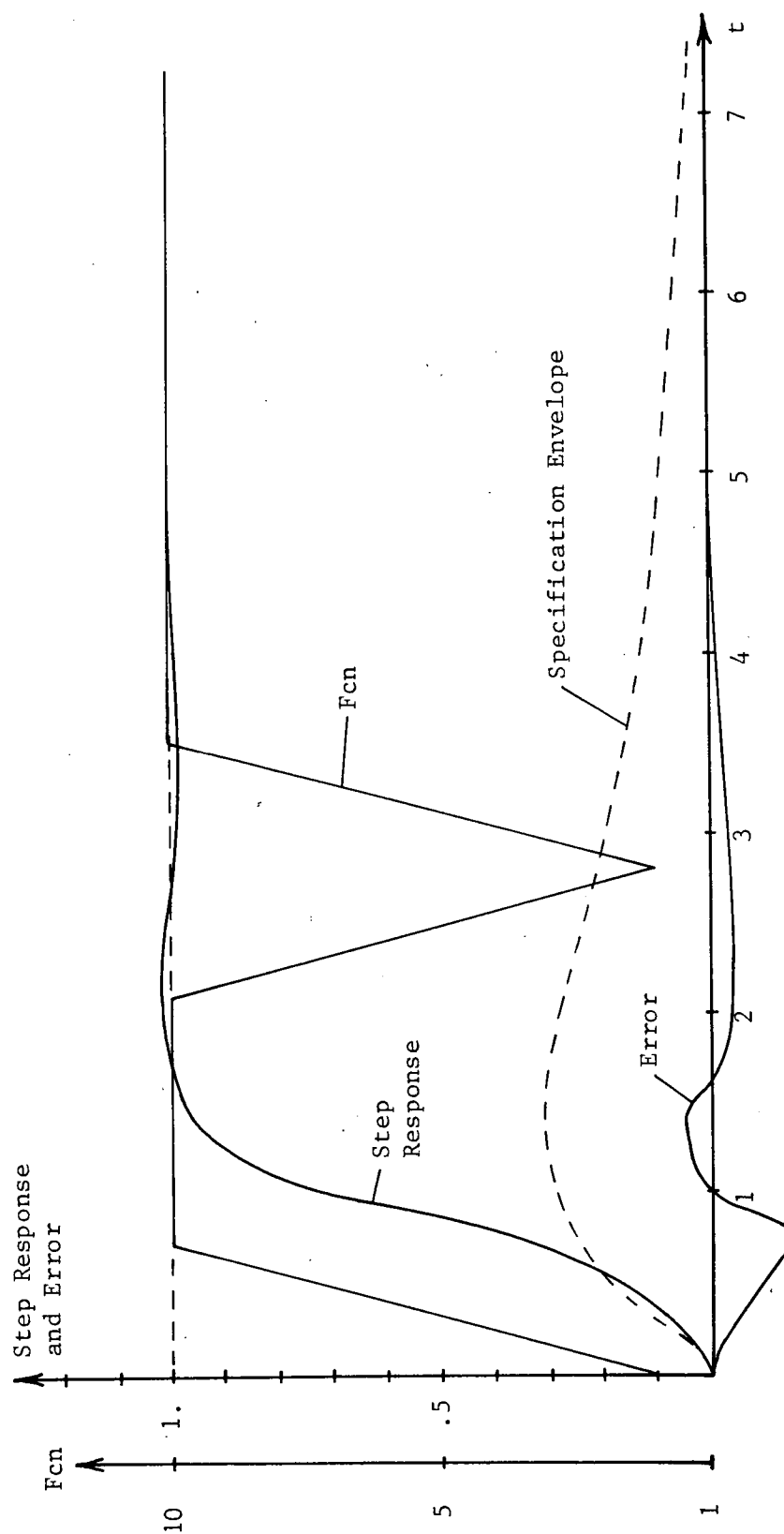


Figure 4.55  
Sample Time Variation with  
Corresponding Step Response and Error Function

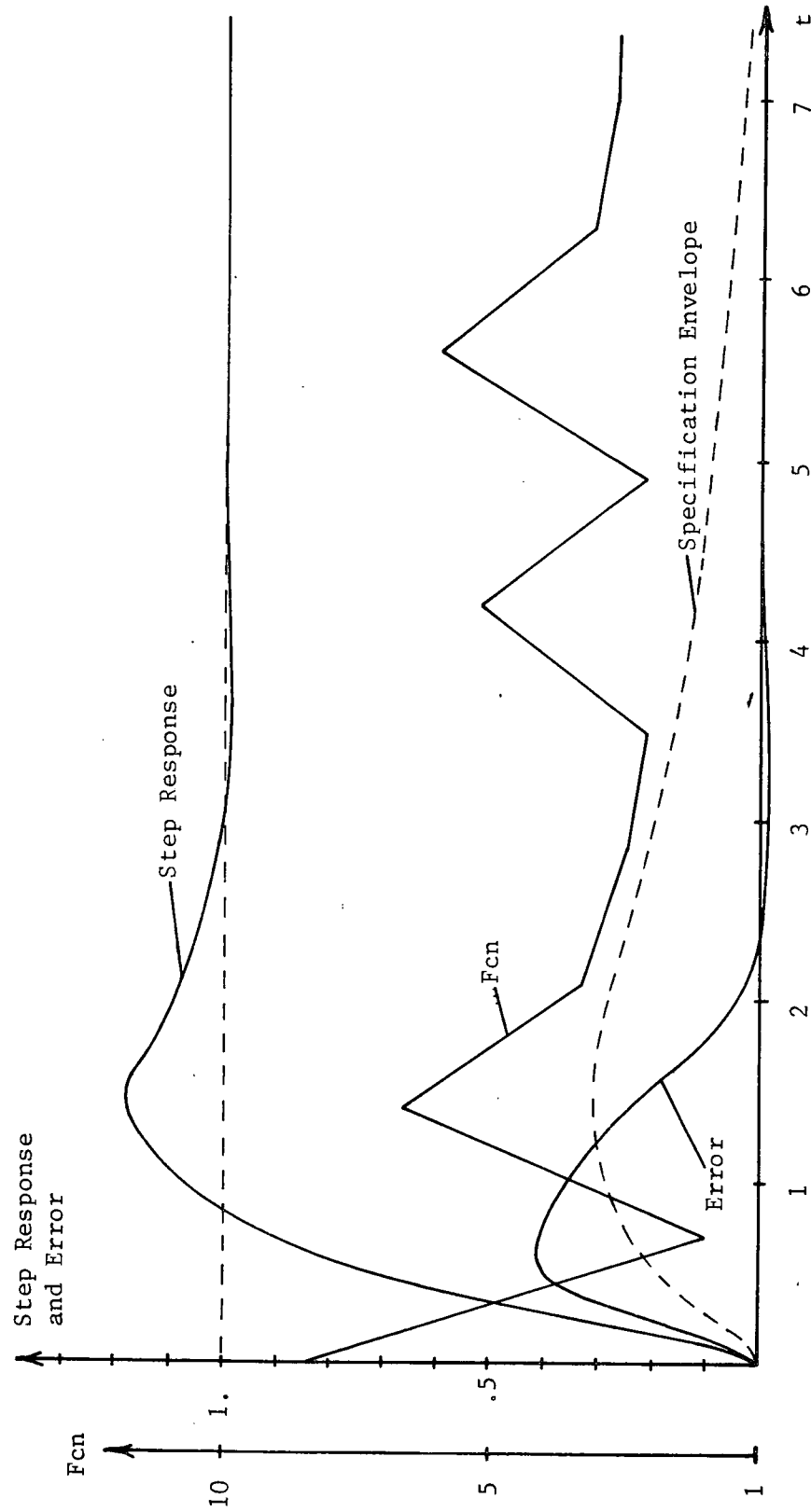


Figure 4.56  
Sample Time Variation with  
Corresponding Step Response and Error Function

#### 4.6 Second Design: Procedure Two

In design procedure two the approach is simply to use the regions of  $P_O/P_{eq}$  from the first design to determine regions of acceptable  $-L'_O$  for the second design. The regions of  $P_O/P_{eq}$  for the first design are shown in Figures 4.38 through 4.43, and the specification regions are given in Figures 4.27a through 4.27f. Using techniques previously described in the first design, the acceptable regions of  $-L'_O$  are determined as shown in Figure 4.57. Except at the frequency 0.628, the acceptable regions of  $-L'_O$  do not require the magnitude of  $-L'_O$  to be substantially greater than was required in the first design. This is expected since the first design satisfied the specifications at frequencies 1.25 and higher.

A design satisfying the specification regions was made by trial and error and the resulting  $L'_O(s)$  is given by

$$L'_O(s) = 25.55 \frac{s + 5}{s(s + 7)(s + 12)}$$

The polar plot of  $L'_O$  is shown in Figure 4.57. The design satisfies the circle criterion for stability which is given in Reference (38) so that system stability is assured. The corresponding expression for  $H(s)$  is

$$H(s) = 15.15 \frac{s^2 + 7s + 10}{s^2 + 19s + 84}$$

and the expression for  $G(s)$  is

$$G(s) = 2.2 \frac{s^4 + 21s^3 + 149.55s^2 + 360.86s + 275.52}{s^4 + 21.8s^3 + 141.2s^2 + 311.2s + 336}$$

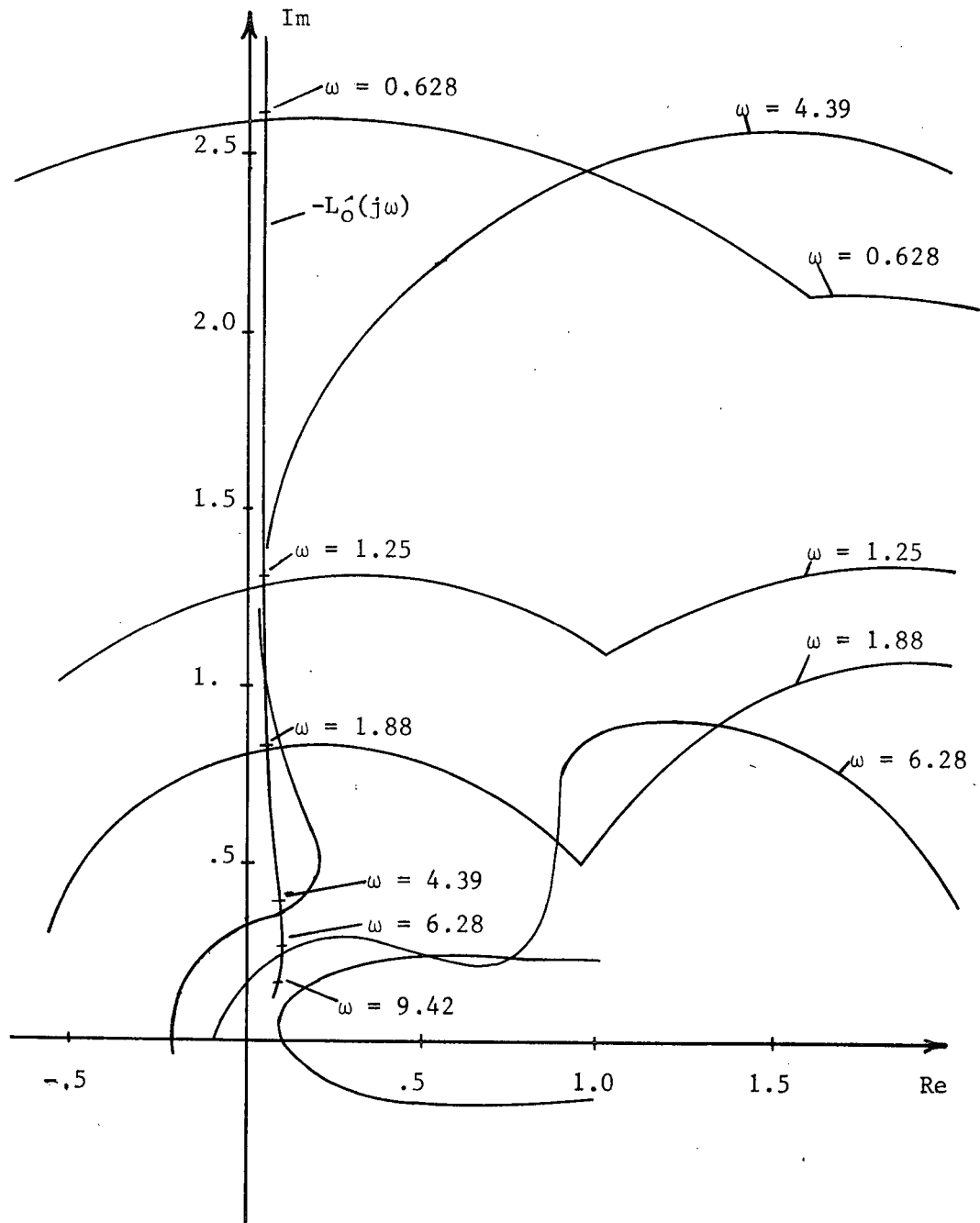


Figure 4.57  
Boundaries of Acceptable Regions of  $-L'_0$  with  
Polar Plot of  $-L'_0(j\omega)$

The high frequency poles will be added in the final design. This design requires more lag than the first design because of the higher rate of decrease between the frequencies 0.628 and 1.25. It should be pointed out that the magnitude of  $E$  is somewhat smaller in this design than in the second design using procedure one. The design was tested by simulating the system and determining the regions of  $P_o/P_{eq}$ . The duration of the time-varying gain illustrated in Figure 4.30 was again set at seven seconds. Simulations were run for over two hundred variations with the variations being both specifically selected and chosen at random. The resulting regions of  $P_o/P_{eq}$  are shown in Figure 4.58 through 4.63, along with the acceptable regions of  $P_o/P_{eq}$  corresponding to  $L'_o$ . The regions of  $P_o/P_{eq}$  fall within the acceptable regions of  $P_o/P_{eq}$  which means that the design satisfies the specifications. However, since the regions of  $P_o/P_{eq}$  do not touch the boundaries of acceptable  $P_o/P_{eq}$  at all frequencies, the system is overdesigned although the overdesign is not appreciable.

Observe that the regions of  $P_o/P_{eq}$  for this second design are almost identical to the regions of  $P_o/P_{eq}$  found for the first design. This result is extremely promising for design procedure two since, for this example at least, the regions of  $P_o/P_{eq}$  do not change appreciably for changes in  $L_o$ . Thus, designing an  $L_o$  based upon regions of  $P_o/P_{eq}$  corresponding to a previous design does not appear to be an unreasonable approach.

To give an indication of the type of step responses which this time-varying system exhibits, a number of step responses with

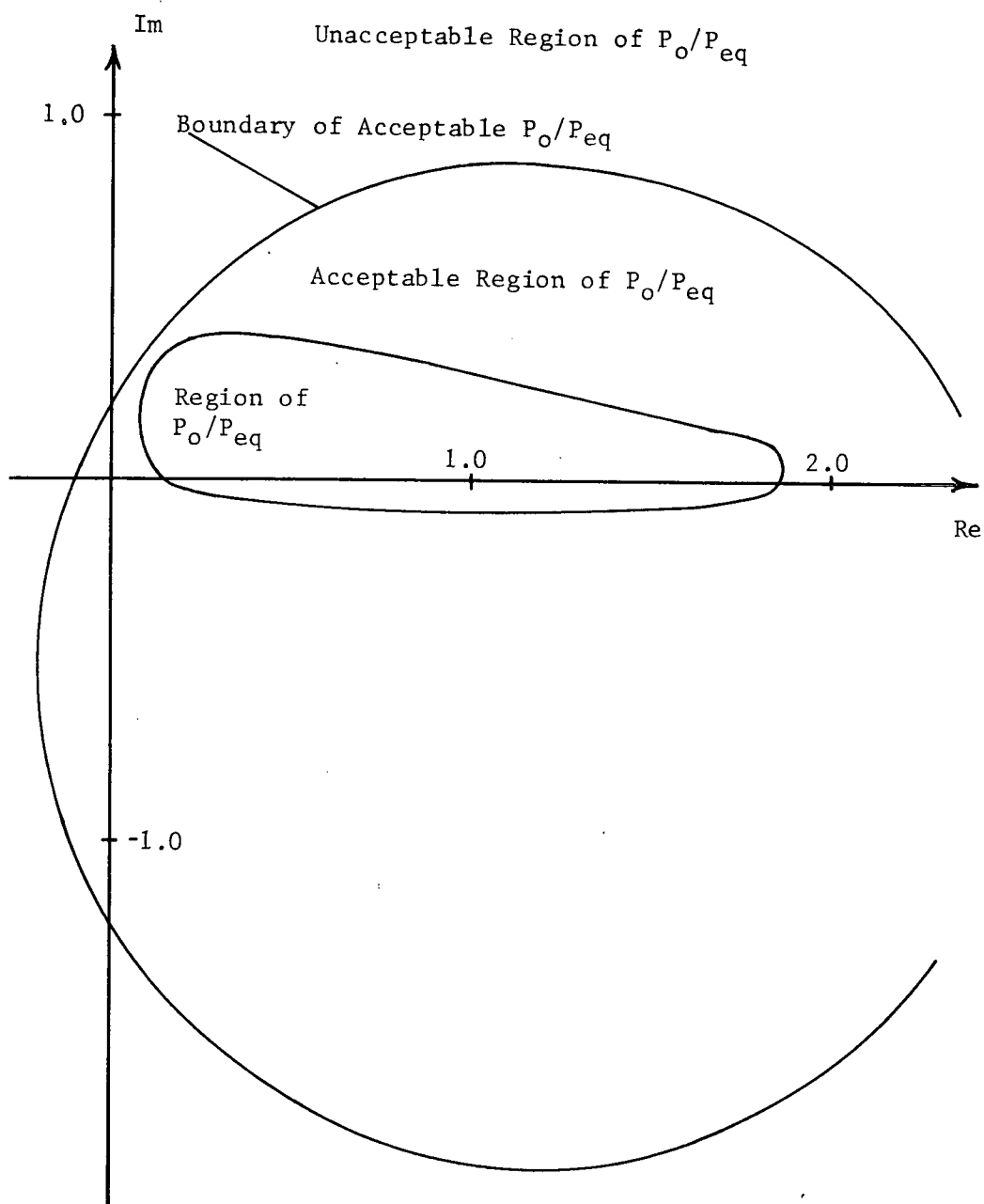


Figure 4.58  
Region of  $P_O/P_{eq}$  for  $\omega = 0.628$

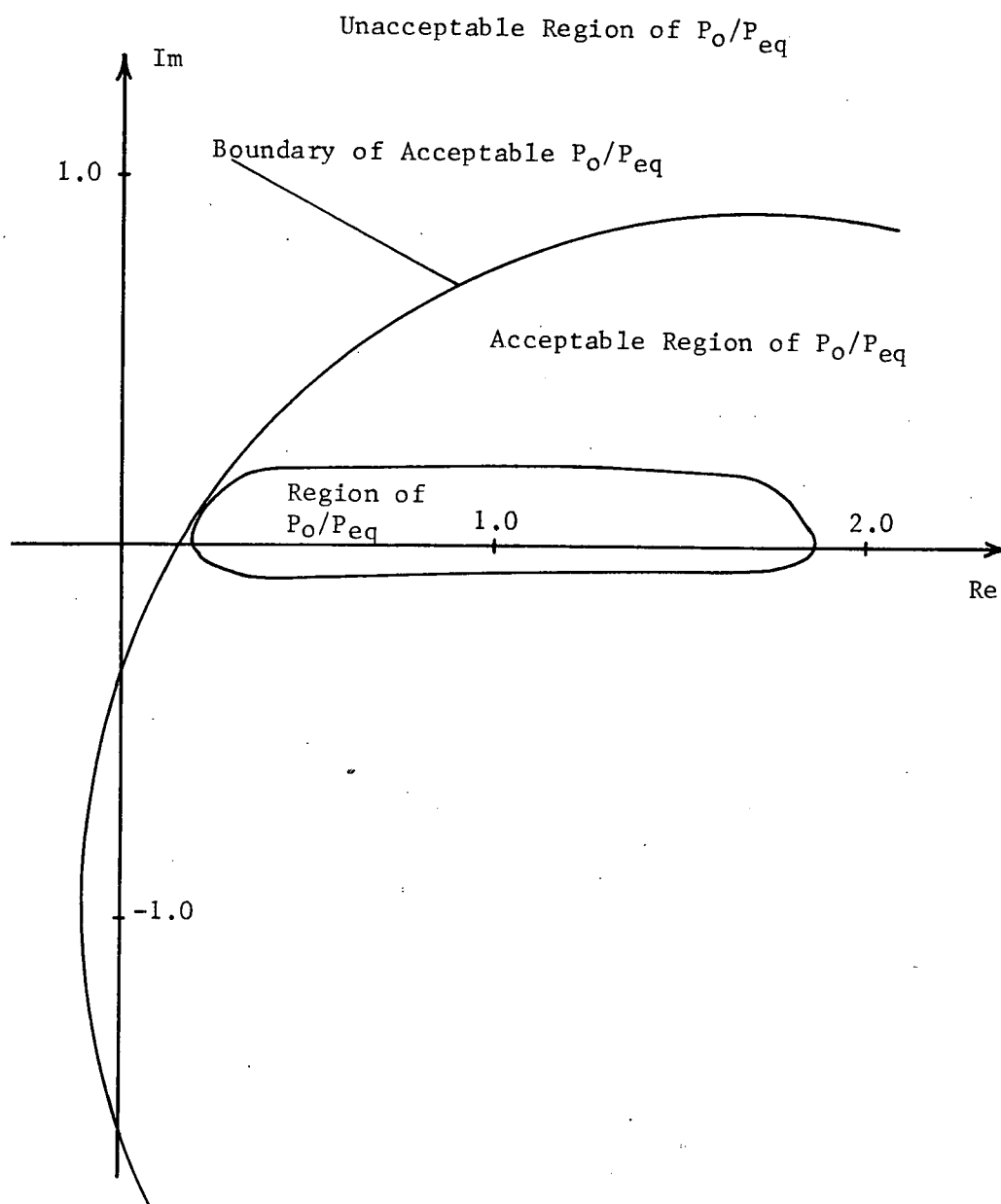


Figure 4.59  
Region of  $P_o/P_{eq}$  for  $\omega = 1.25$



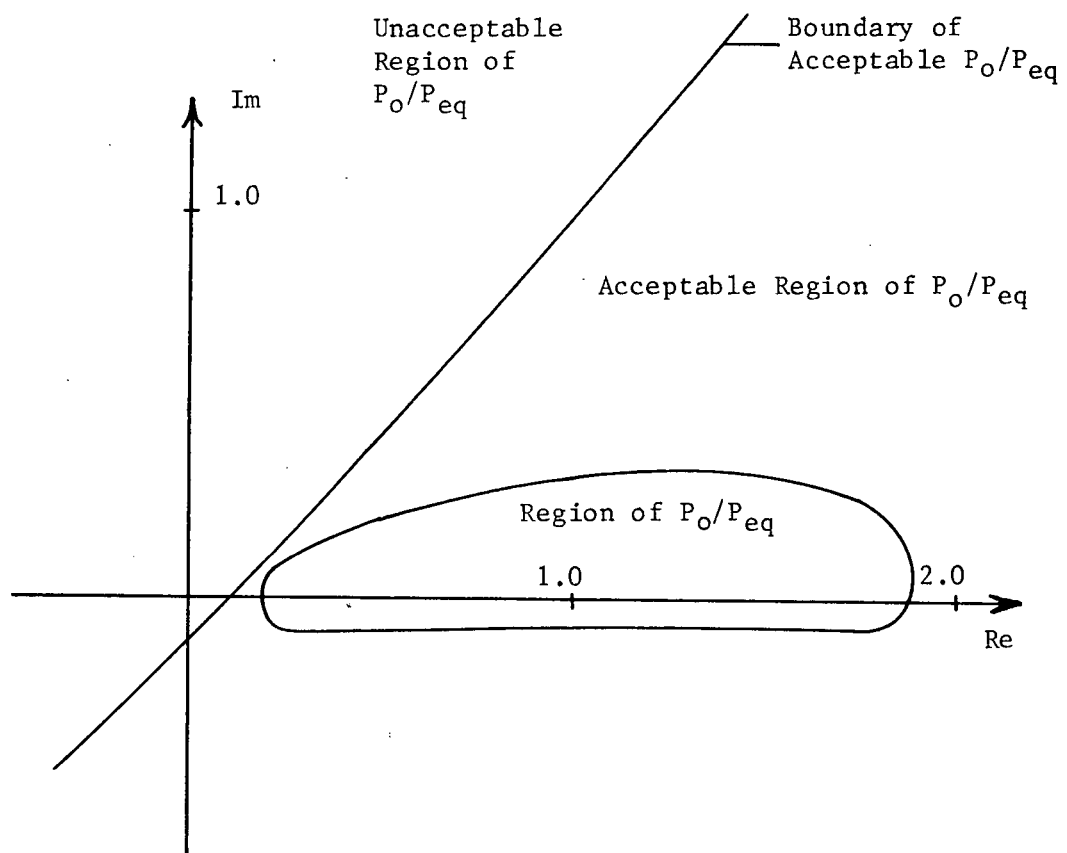


Figure 4.60  
Region of  $P_O/P_{eq}$  for  $\omega = 1.88$

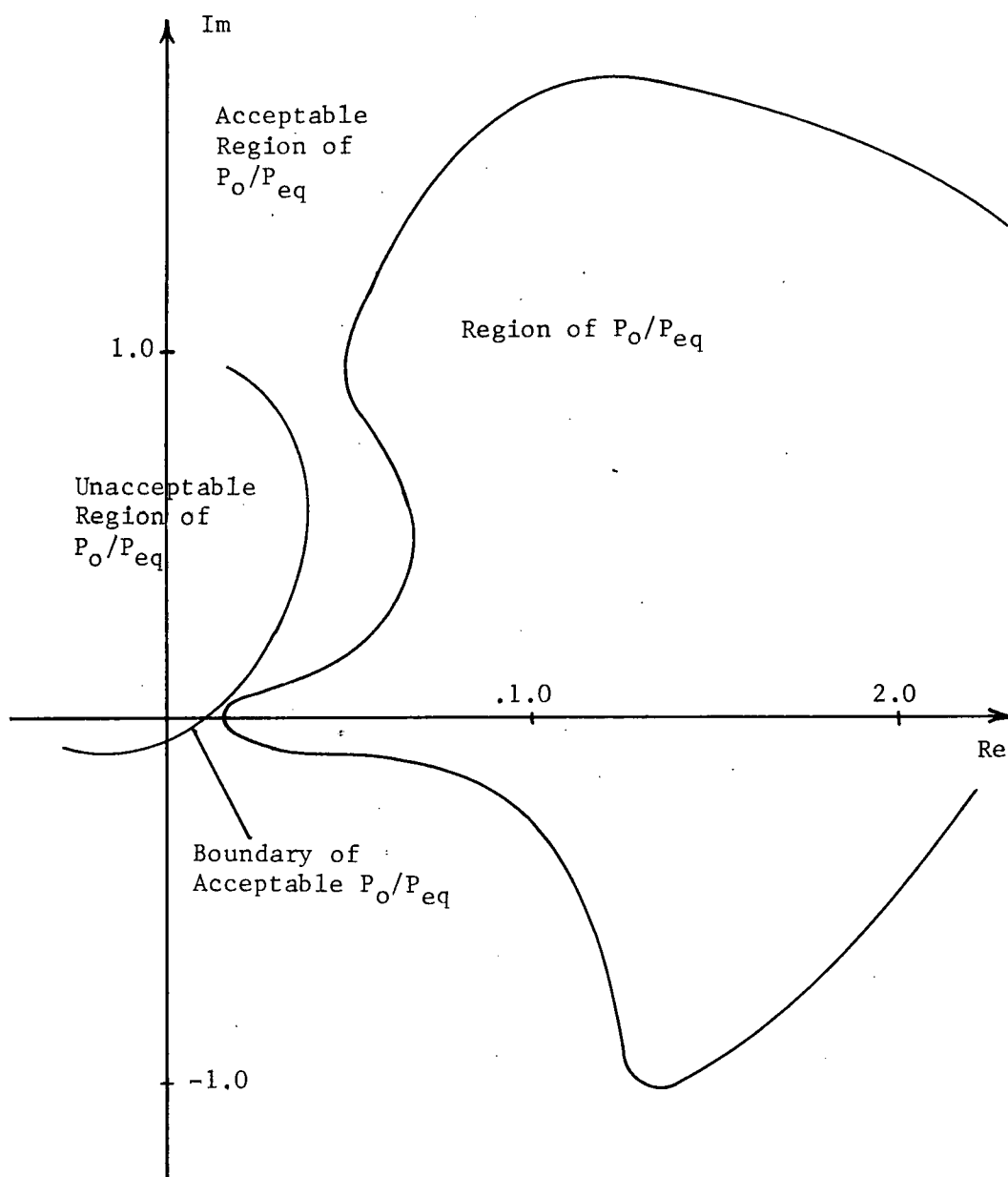


Figure 4.61  
Region of  $P_O/P_{eq}$  for  $\omega = 4.39$

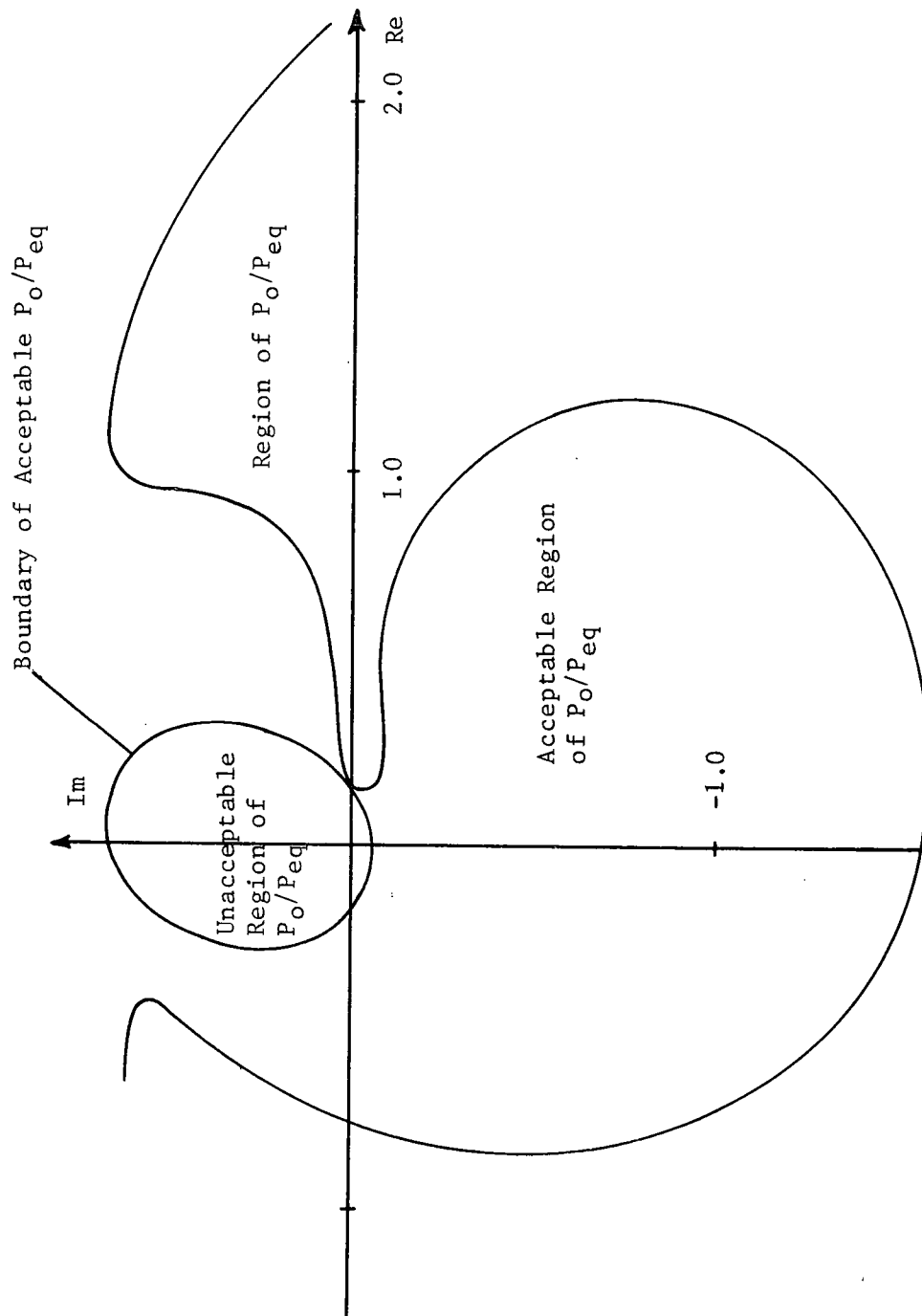


Figure 4.62  
Region of  $P_O/P_{eq}$  for  $\omega = 6.28$

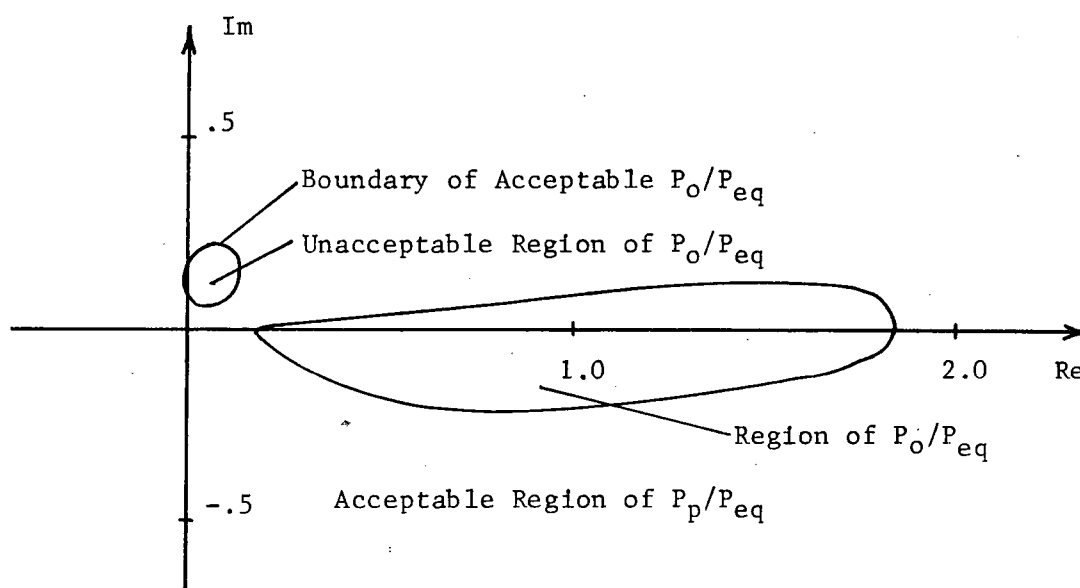


Figure 4.63  
Region of  $P_o/P_{eq}$  for  $\omega = 9.42$

the corresponding error functions and time-variations are shown in Figures 4.64 through 4.71. For comparison, the first two responses correspond to time-invariant conditions with the gain set at ten and one, respectively. As with the earlier designs, the time-variations cause an increase in overshoot and settling time. The maximum overshoot in the time-varying case is approximately 24%, which is an increase over the 19% observed for the second design using procedure one and a decrease over the 32% observed for the first design. Such a result is expected since the magnitude of  $L'_O$  for this design is smaller than the magnitude of  $L'_O$  in the second design using procedure one and is larger than the magnitude of  $L'_O$  in the first design.

#### 4.7 Third Design

In making the second design it was found that a design based on procedure one, which is the technique using the maximum  $|E|$ , will generally result in an overdesigned system because the acceptable regions of  $-L_O$  are assumed to be circular. Use of the second procedure, which is based on the regions of  $P_O/P_{eq}$ , results in the more accurate shape of the acceptable region of  $-L_O$ ; however, the size of the acceptable region cannot be as precisely determined as can be done by the method in procedure one. The third design will be based on a combination of procedures one and two. The shape of the acceptable regions of  $-L_O$  will be assumed to be as was found in the second design using procedure two, while the size will be determined from the maximum error.

The maximum error magnitude was found for the second design

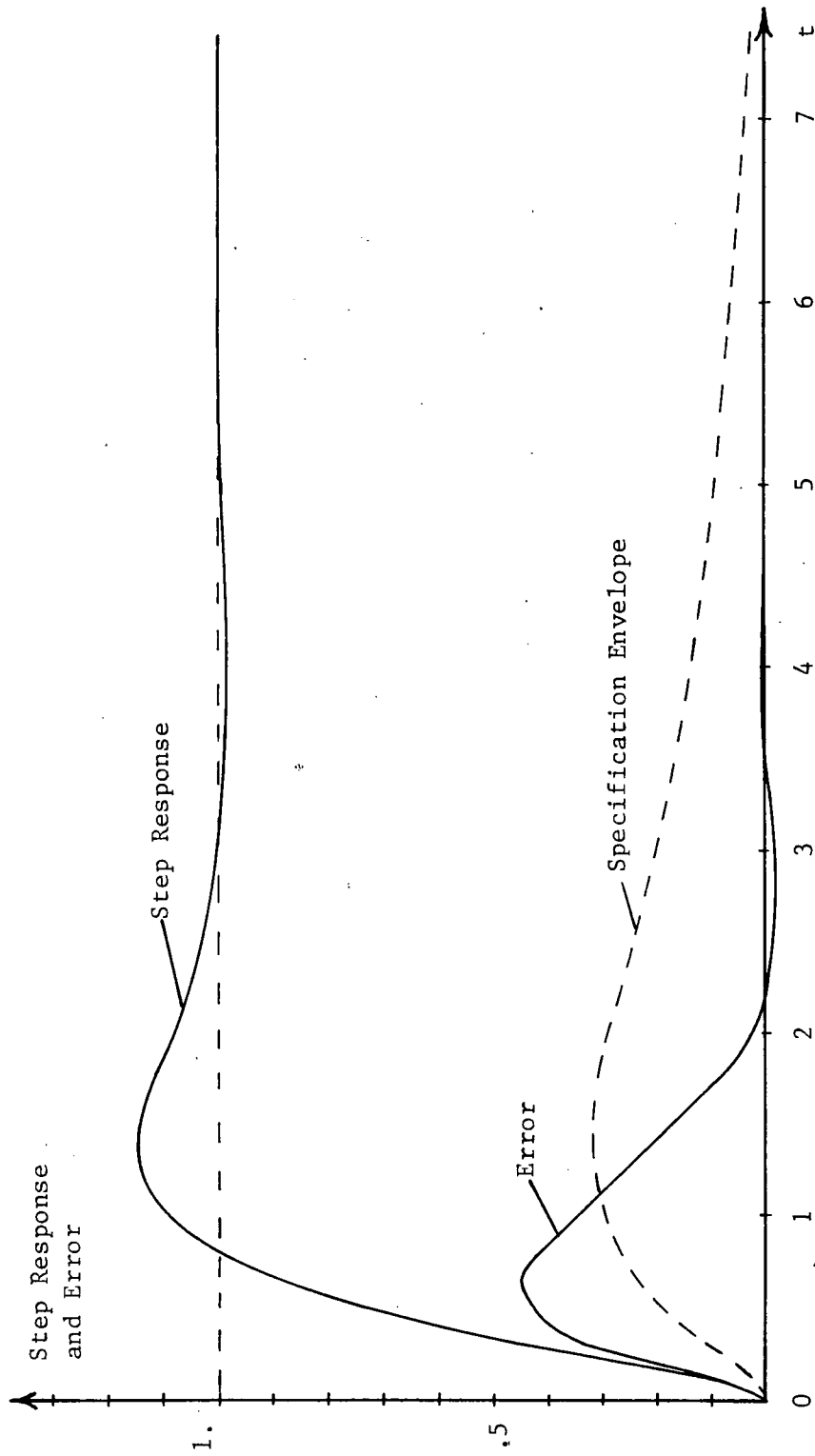


Figure 4.64  
 Step Response of System with Gain  
 Constant at 10, Second Design, Procedure Two

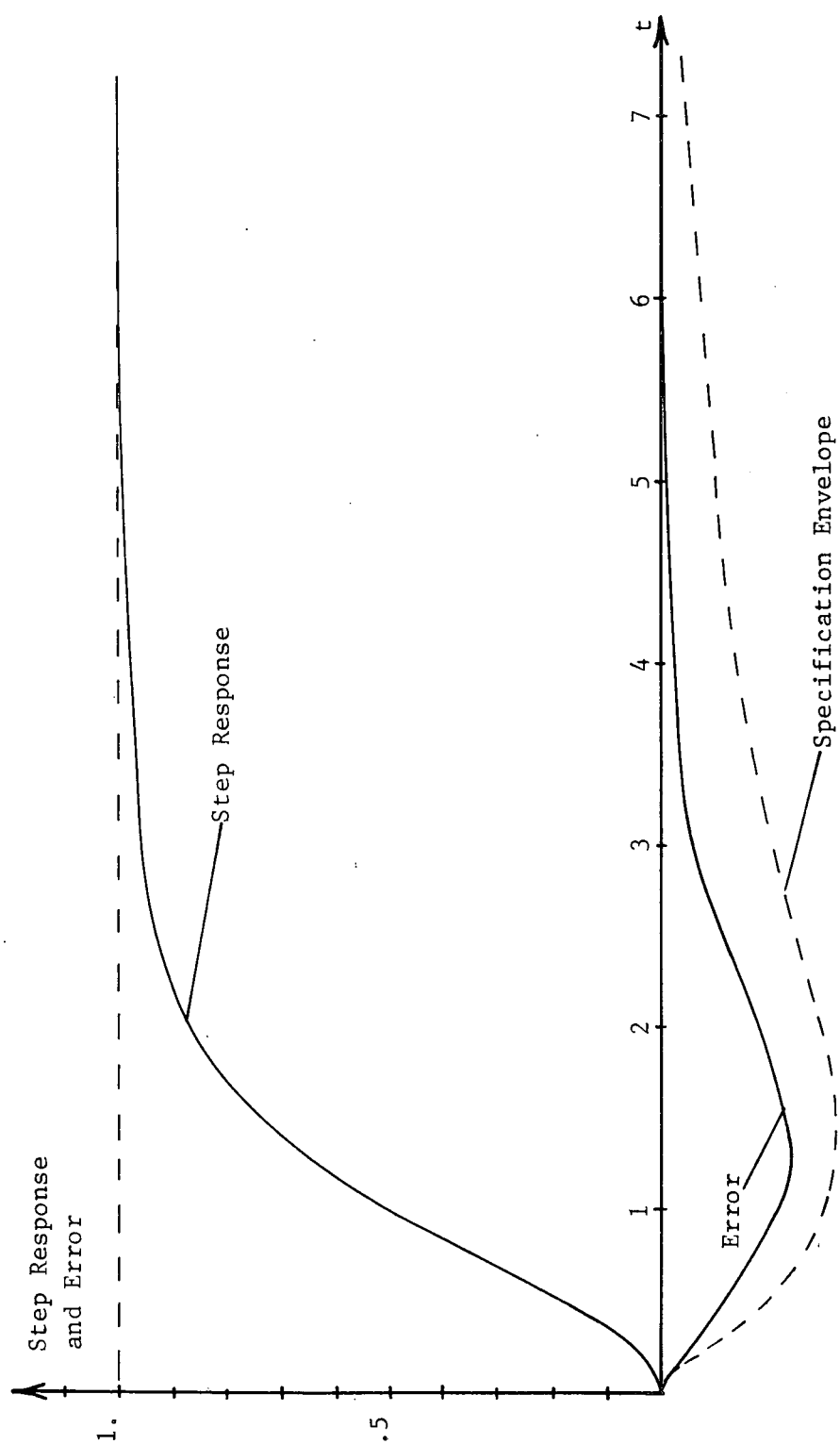


Figure 4.65  
 Step Response of System with Gain  
 Constant at 1, Second Design, Procedure Two

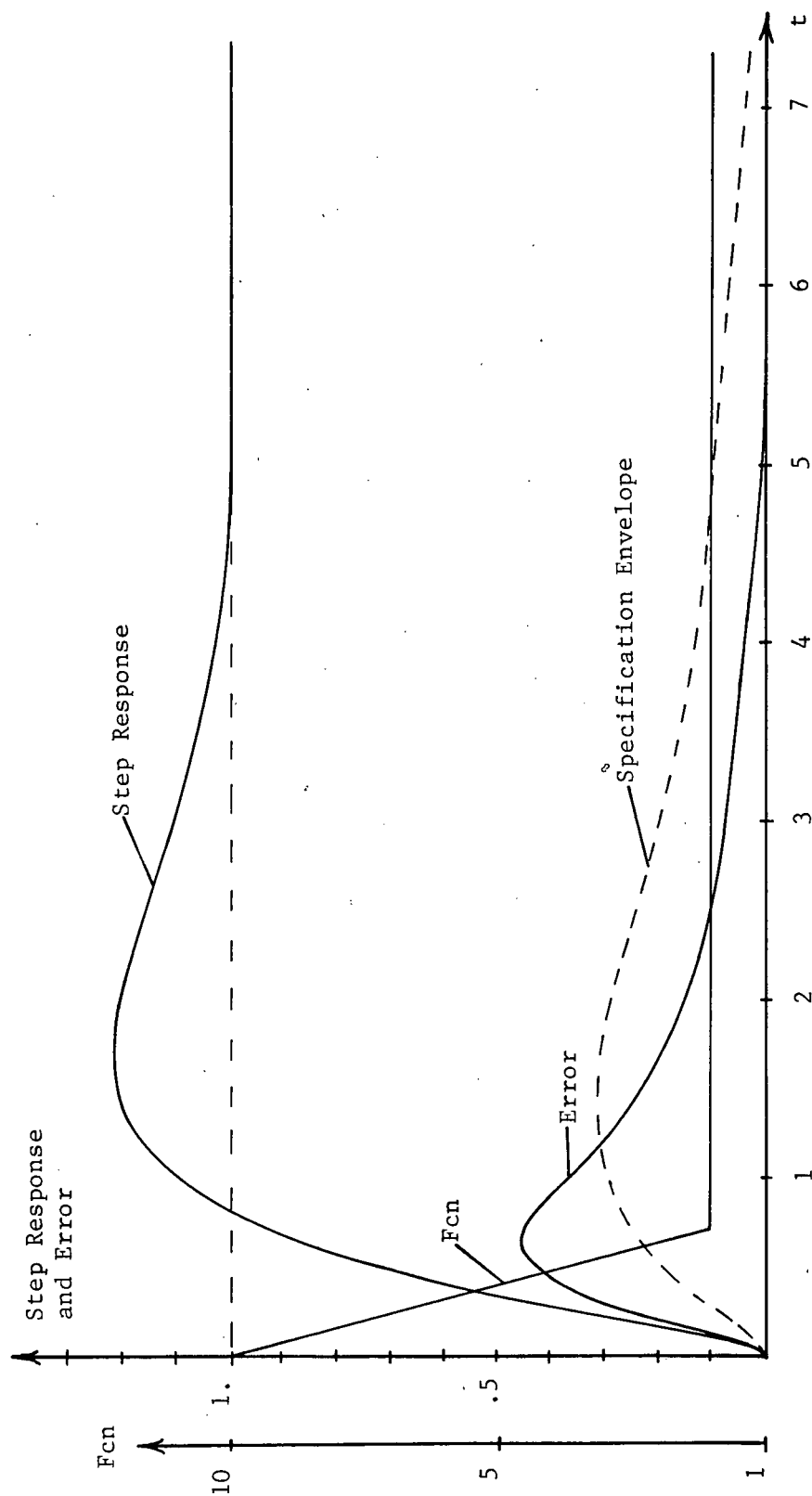


Figure 4.66  
 Sample Step Response of Time-varying System  
 Second Design, Procedure Two



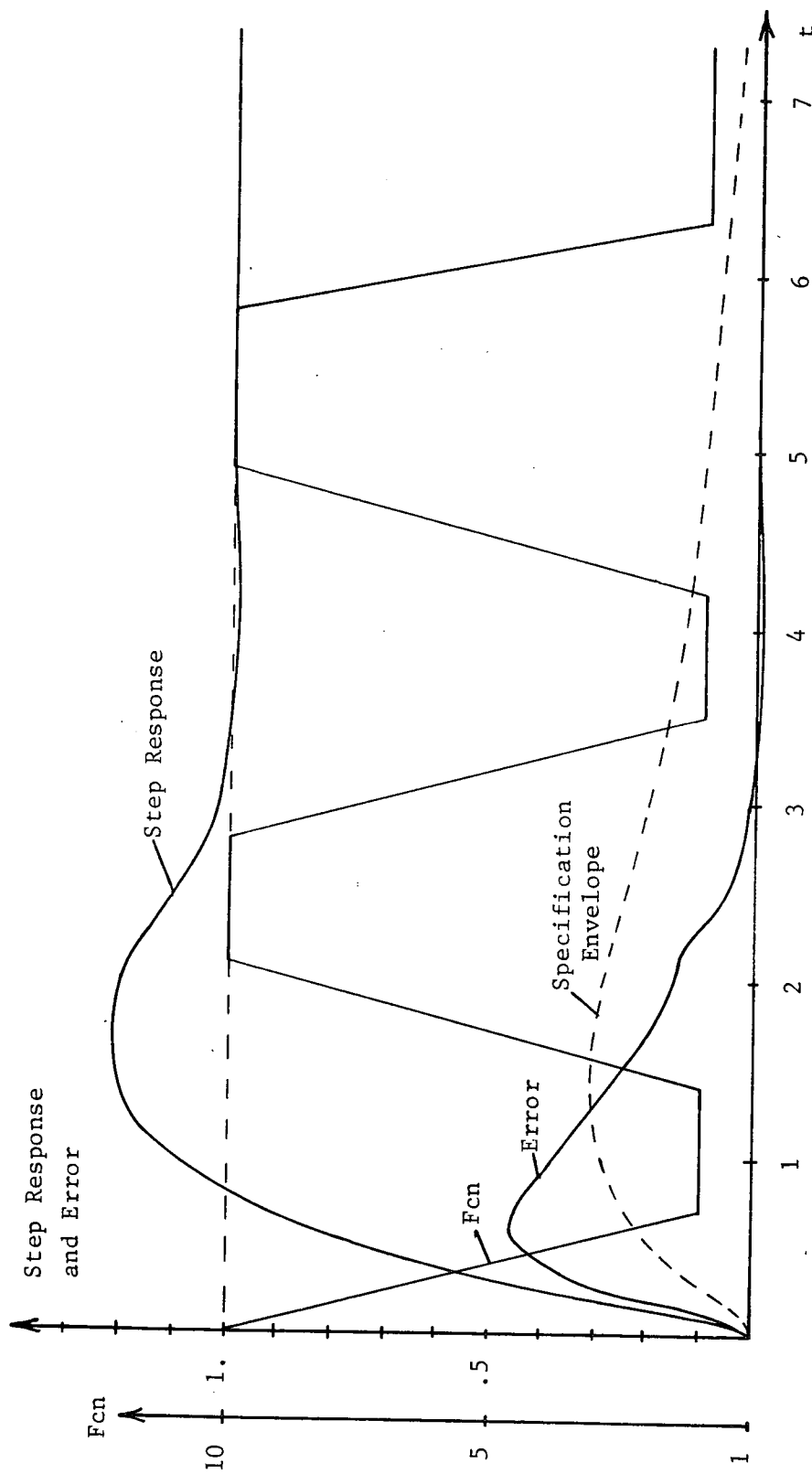


Figure 4.67  
Sample Step Response of Time-varying System  
Second Design, Procedure Two

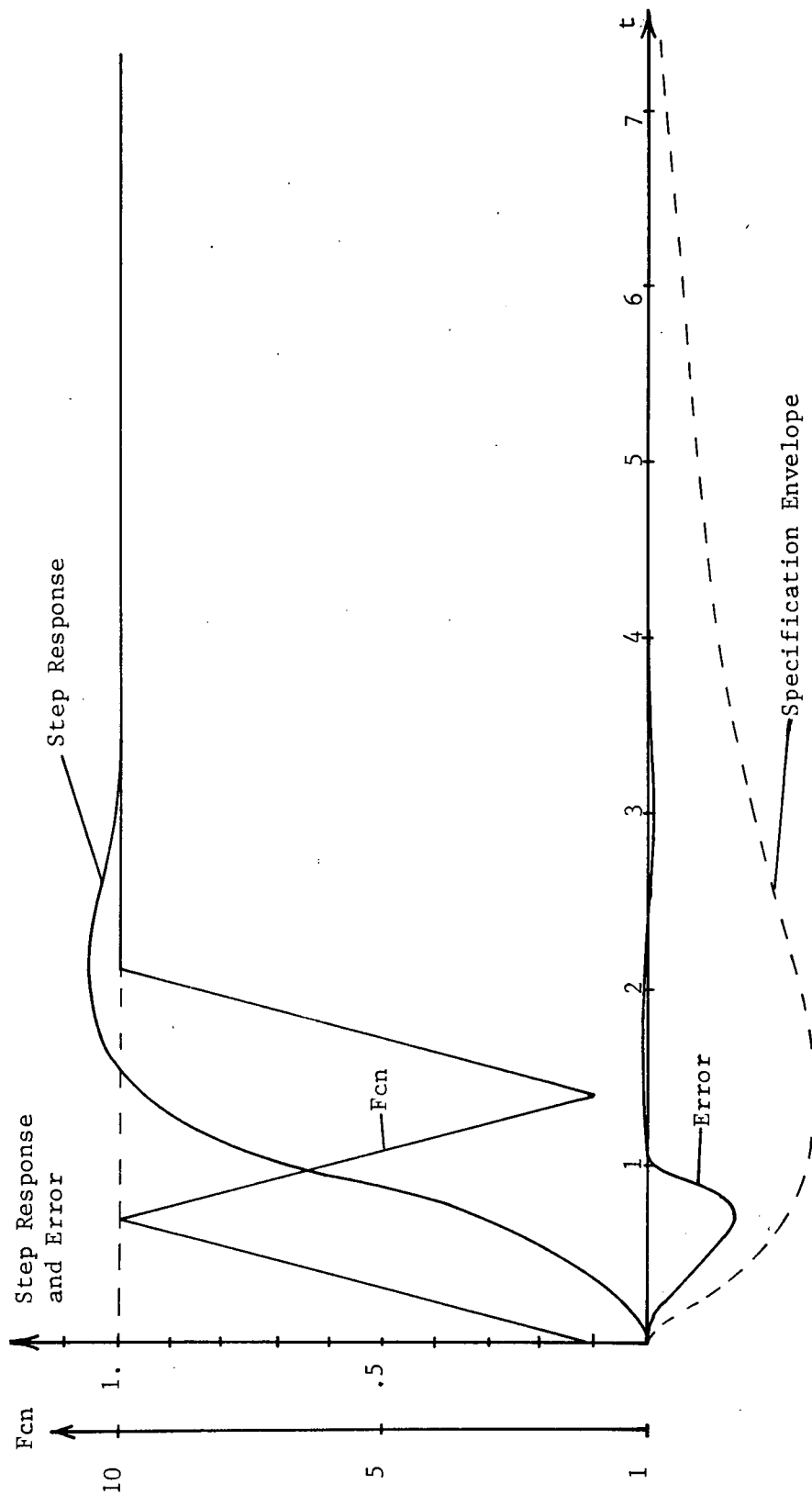


Figure 4.68  
Sample Step Response of Time-varying System  
Second Design, Procedure Two

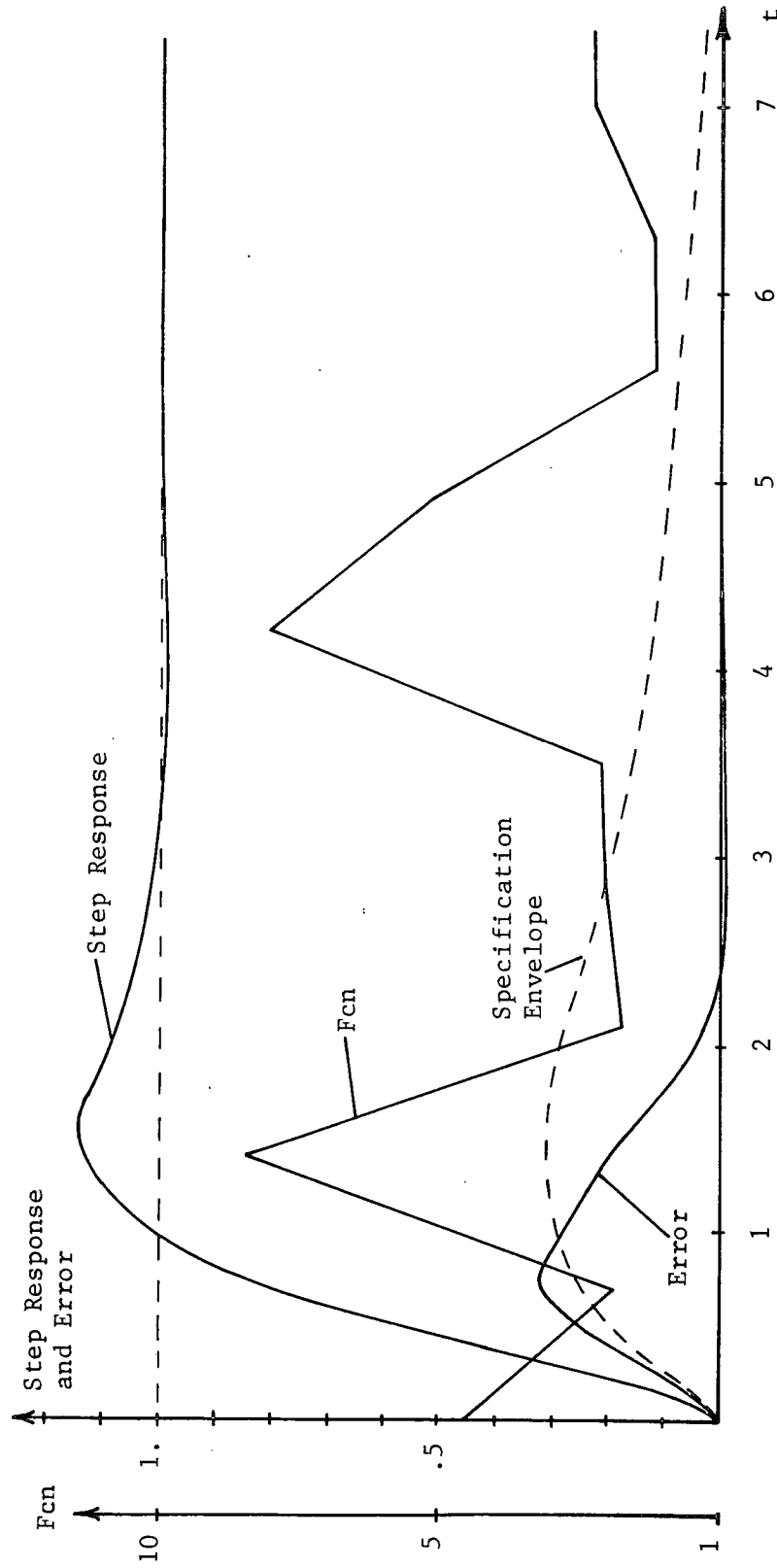


Figure 4.69  
Sample Step Response of Time-varying System  
Second Design, Procedure Two

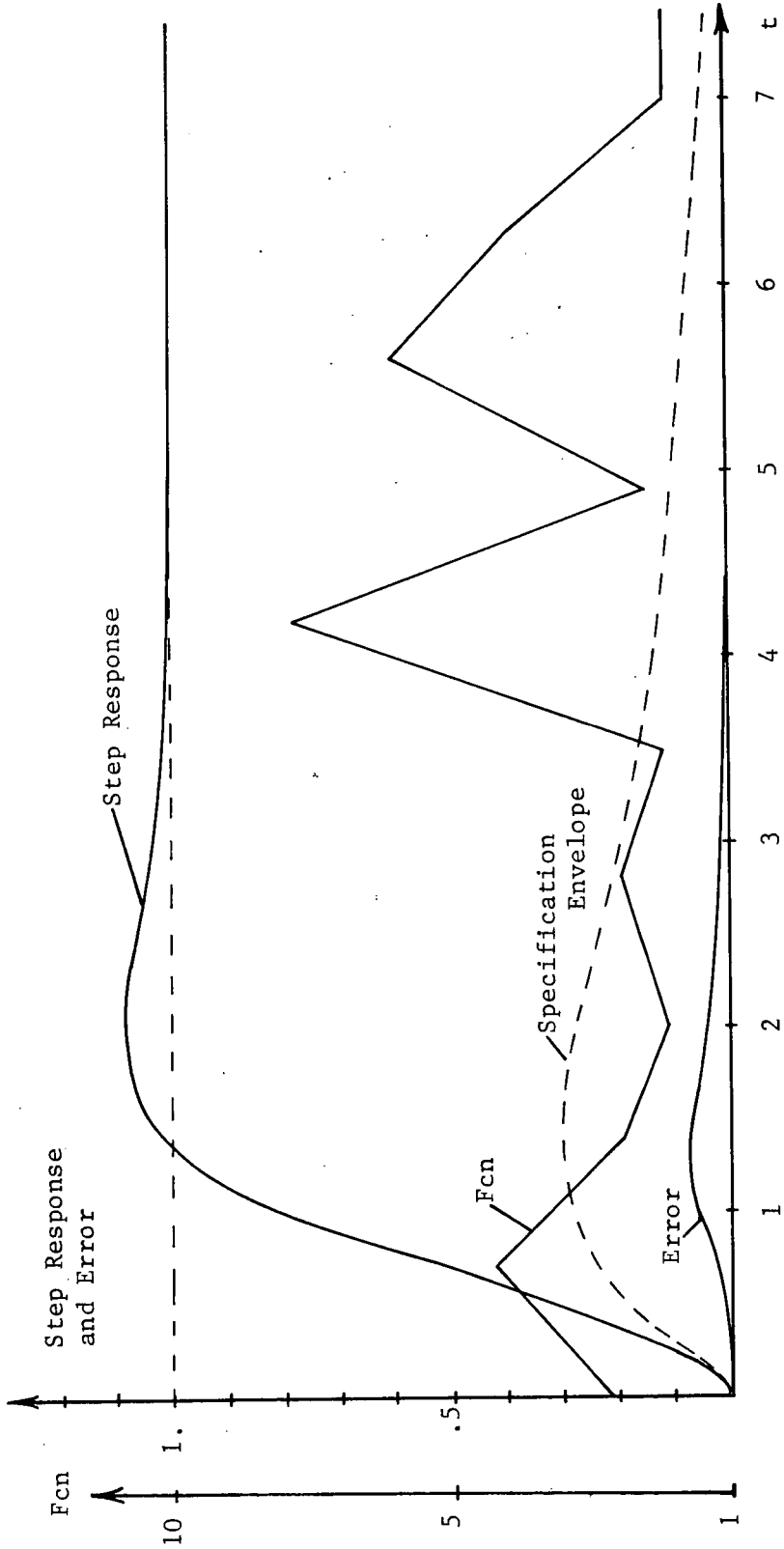


Figure 4.70  
Sample Step Response of Time-varying System  
Second Design, Procedure Two

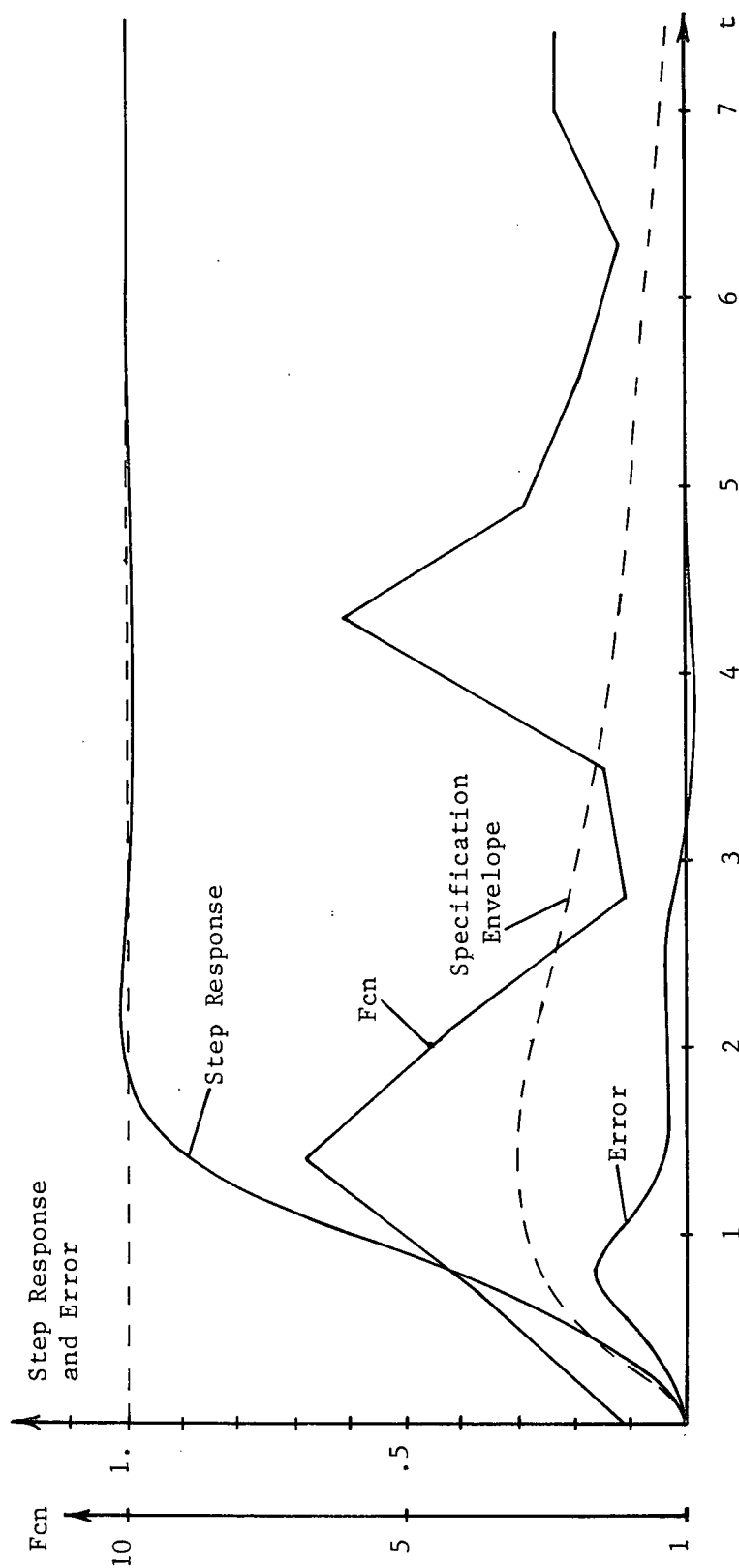


Figure 4.71  
Sample Step Response of Time-varying System  
Second Design, Procedure Two

based on procedure two and is shown in Figure 4.72. Also shown in Figure 4.72 are the maximum error magnitudes for the second design based on procedure one and the maximum error magnitudes for the first design. The first design is not satisfactory, while both of the second designs result in an overdamped system. However, in the second design based on procedure two the magnitude of  $L_0$  needs to be decreased only a small amount at the frequencies 0.628, 1.23 and 1.88 for the error to just lie on the specification curve. To determine the amount of decrease needed at  $\omega = 0.628$ , it will be assumed that the magnitude of the error varies linearly with the magnitude of  $L_0$  between the first design and the second design based on procedure two. The difference in the magnitude of the error of the second design can be increased by .025 which is a 16% change based on the 0.156 difference. The acceptable region of  $-L_0$  at  $\omega = 0.628$  for the third design is then determined as follows.

Figure 4.73 shows a plot of the acceptable region of  $-L_0$  at 0.628 for the first design and for the second design based on procedure two in the area of interest. The magnitude of  $L_0$  for the first design at 0.628 is 2.02 and for the second design is 2.61. The difference in the two magnitudes is 0.59. The boundary of  $-L_0$  at  $\omega$  equal 0.628 for the third design will be placed at 16% of the difference between these two magnitudes as shown in Figure 4.73.

At  $\omega$  equal 1.25 the magnitude of acceptable  $-L_0$  needs to be changed only a little; thus,  $-L_0$  for the third design will be

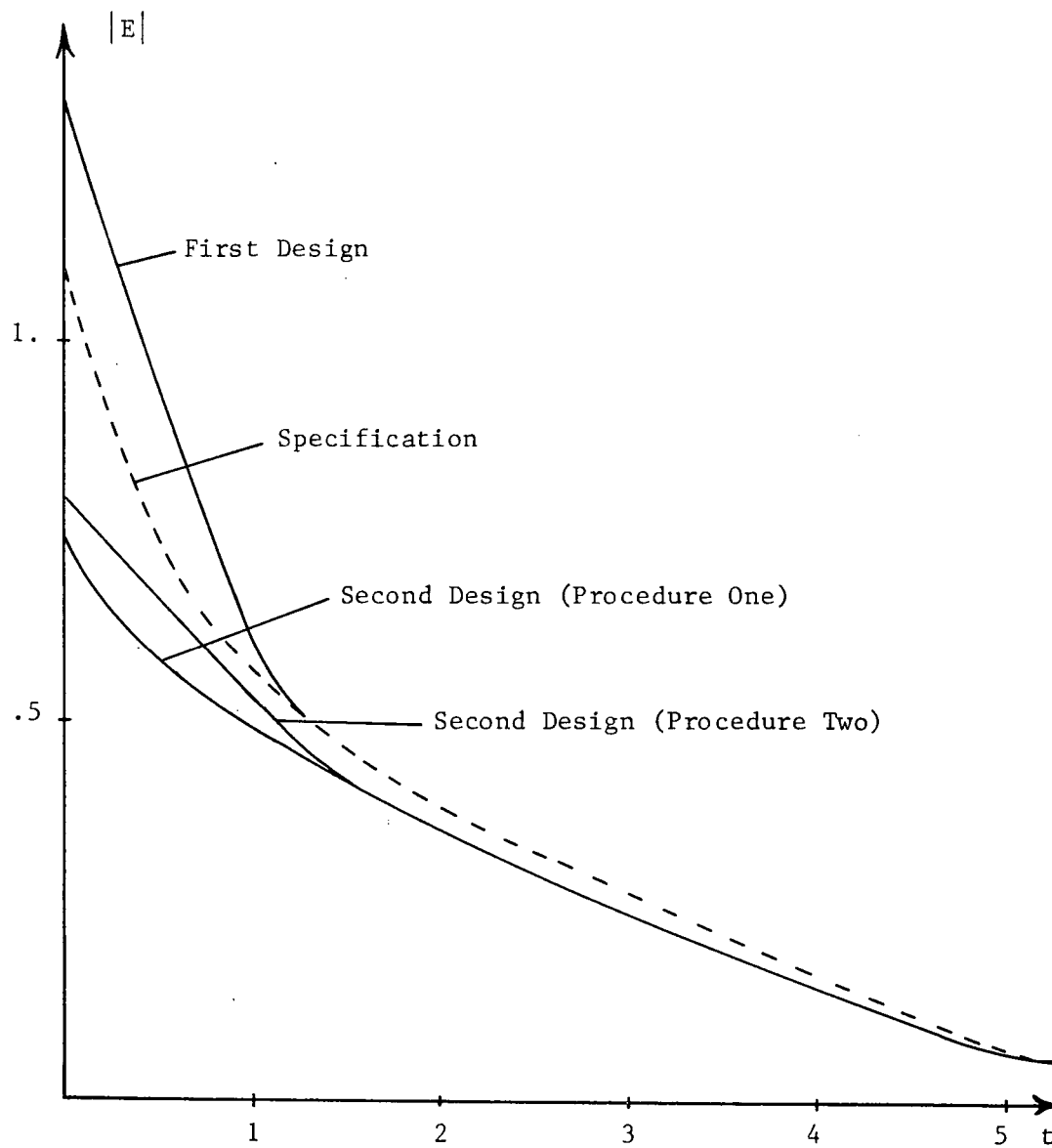


Figure 4.72  
Comparison of Maximum  $|E|$  for  
First and Second Designs

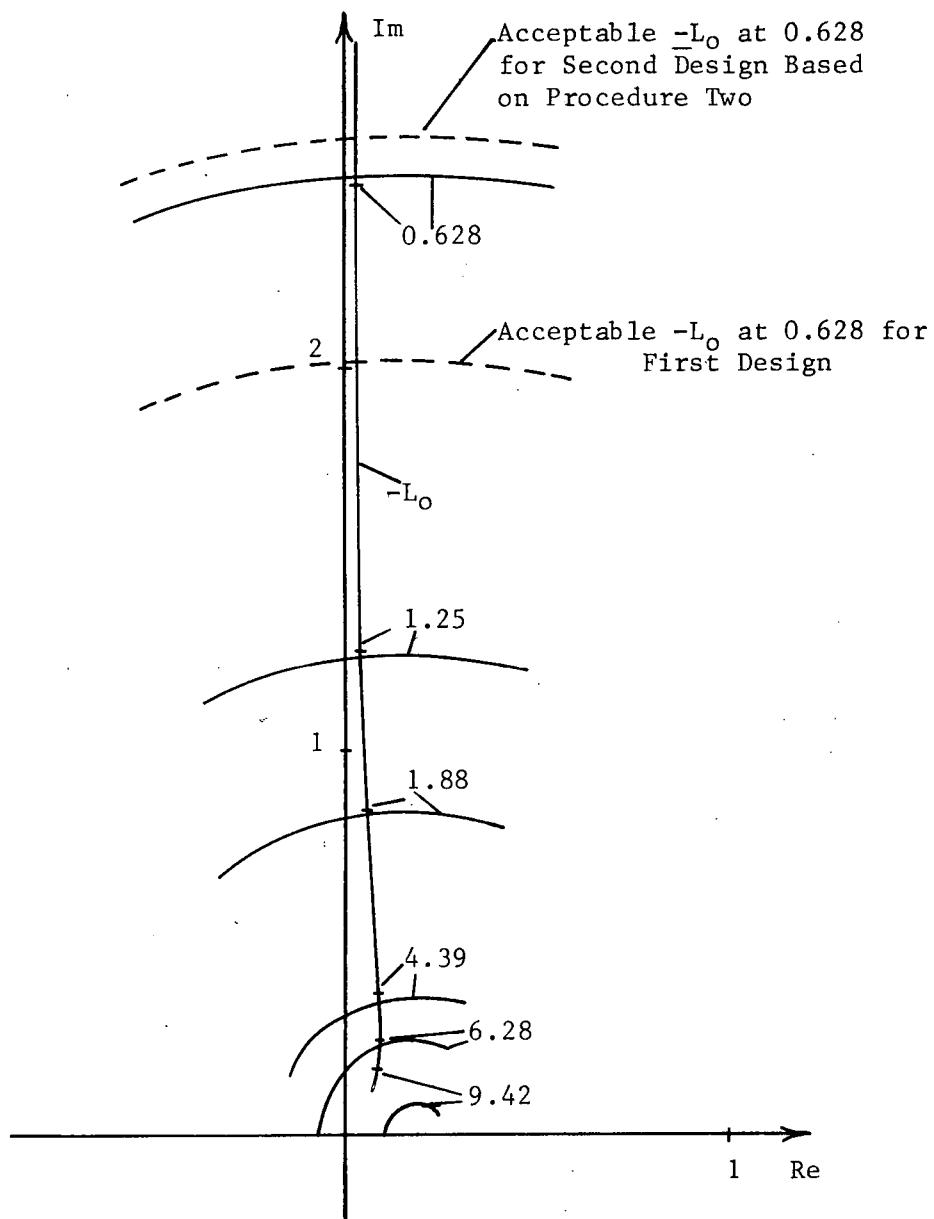


Figure 4.73  
Boundaries of Acceptable  $-L_0$  with Polar  
Plot of  $-L_0$  for the Third Design



chosen to fall approximately half way between the magnitudes of  $-L_0$  for the first design and  $-L_0$  for the second design based on procedure two. At the frequencies 1.88 and higher the magnitude of  $-L_0$  will be chosen the same as the magnitude of  $-L_0$  of the first design since in the first design the specifications are just met at these frequencies. The resulting acceptable regions of  $-L_0$  for the third design are shown in Figure 4.73.

The polar plot of the third design is shown in Figure 4.73 together with the acceptable regions of  $-L_0$ . The expression for  $L_0(s)$  of the third design is

$$L_0(s) = 24.61 \frac{s + 5}{s(s + 8)(s + 10)}$$

This design satisfies the circle stability criterion so that system stability is assured. The corresponding expression for  $H(s)$  is

$$H(s) = 13.54 \frac{s^2 + 7s + 10}{s^2 + 18s + 80}$$

and for  $G(s)$  is

$$G(s) = 2.2 \frac{s^4 + 20s^3 + 140.6s^2 + 332.3s + 246.1}{s^4 + 20.8s^3 + 134.4s^2 + 296s + 320}$$

The high frequency poles will be added in the final design. Note that this design is very similar to the second design based on procedure two. The major difference is the small reduction in the magnitude of  $L_0$  over all frequencies.

The design was tested by simulating the system and determining the regions of  $P_0/P_{eq}$  as well as the magnitude of the error. As

with the second design, the duration of the time-varying gain which is illustrated in Figure 4.30 was set at seven seconds. Almost 300 variations were run with variations being both specifically selected and randomly selected. It is again felt that reasonably accurate results were obtained.

The maximum error magnitude is shown in Figure 4.74 and the regions of  $P_o/P_{eq}$  are shown in Figure 4.75 through 4.80. As was observed in the first design, the maximum errors occurred for time-variations starting at ten and quickly decreasing to one. The only significant increase in error due to the time-variations occurred at the frequencies zero and 0.628. The time variations causing the maximum error magnitude at  $\omega$  equal to zero and 0.628 are shown in Figures 4.81 and 4.82, respectively, along with the corresponding step response and error function. Note in Figure 4.74 that the magnitude of the error is slightly larger than the specifications in the region of 0.628. Otherwise, the system just satisfies the specifications. Figure 4.75 also shows that the specifications are not exactly met at 0.628 since the region of  $\omega$  does not fully lie within the acceptable region of  $P_o/P_{eq}$ .

Since this system is very close to meeting the specifications exactly, it is very likely that this design would be considered acceptable. A series of time-variations with the corresponding step responses and errors are shown in Figures 4.83 through 4.88.

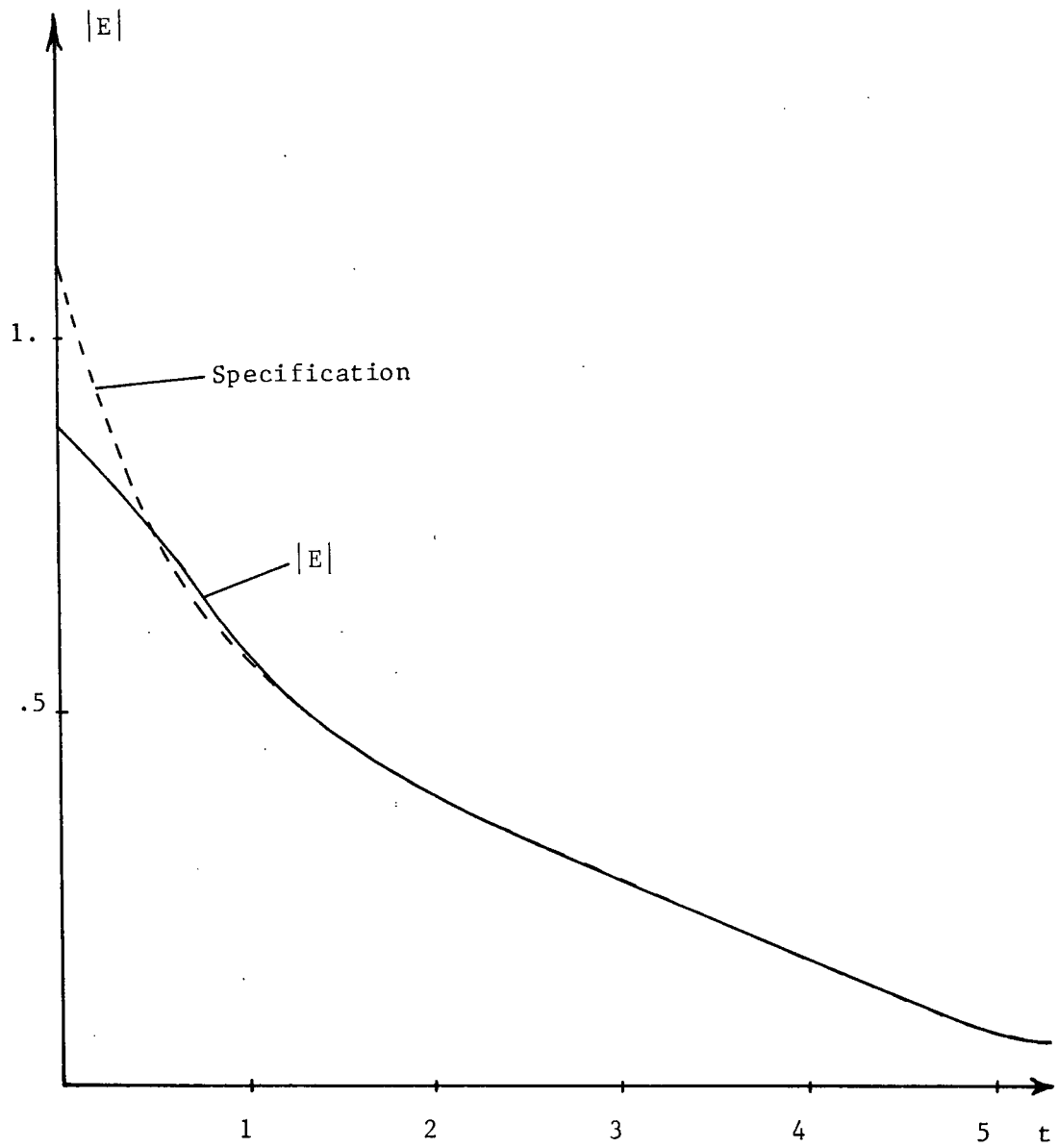


Figure 4.74  
Maximum  $|E|$  for Third Design

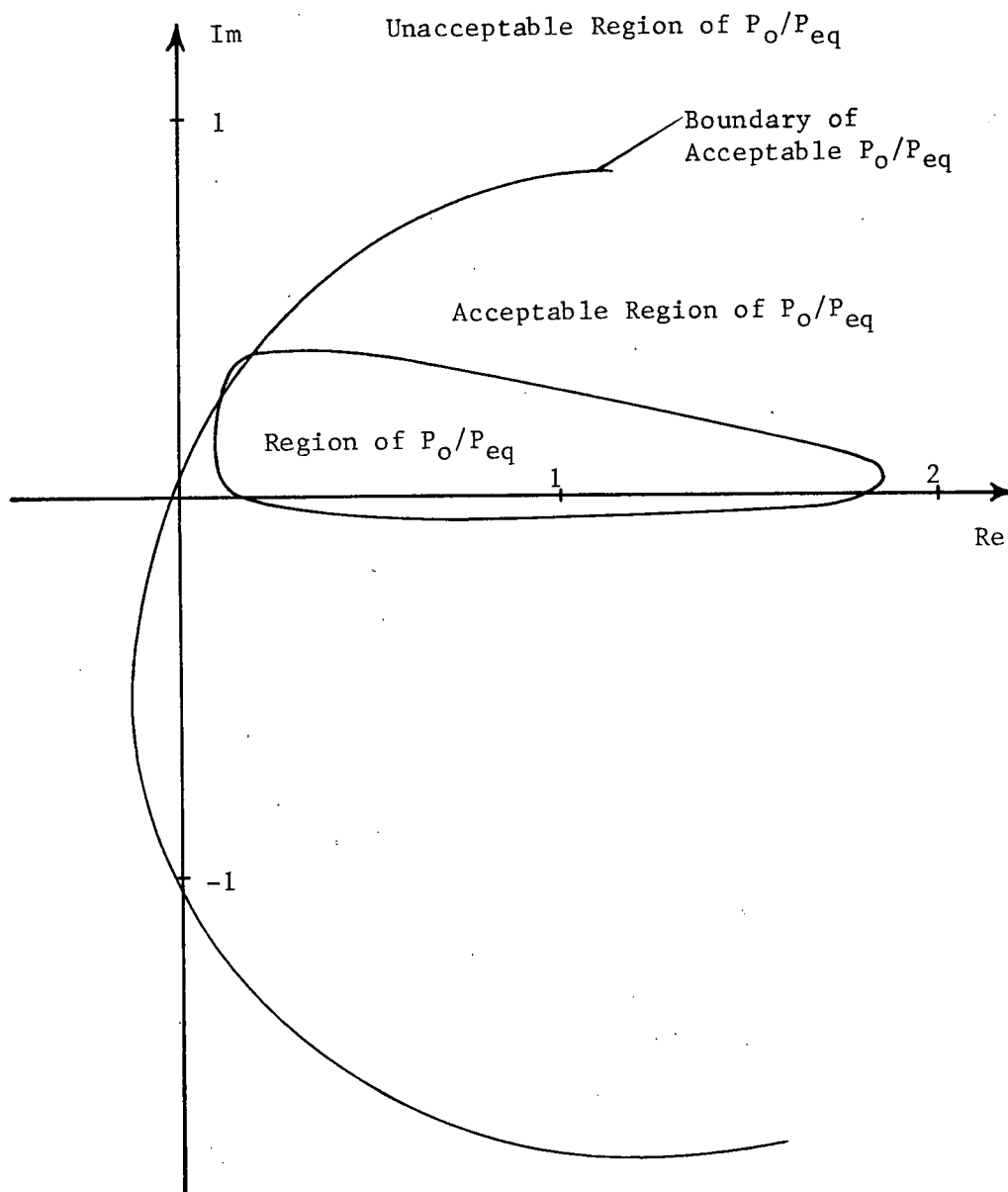


Figure 4.75  
Region of  $P_O/P_{eq}$  for  $\omega = 0.628$ , Third Design

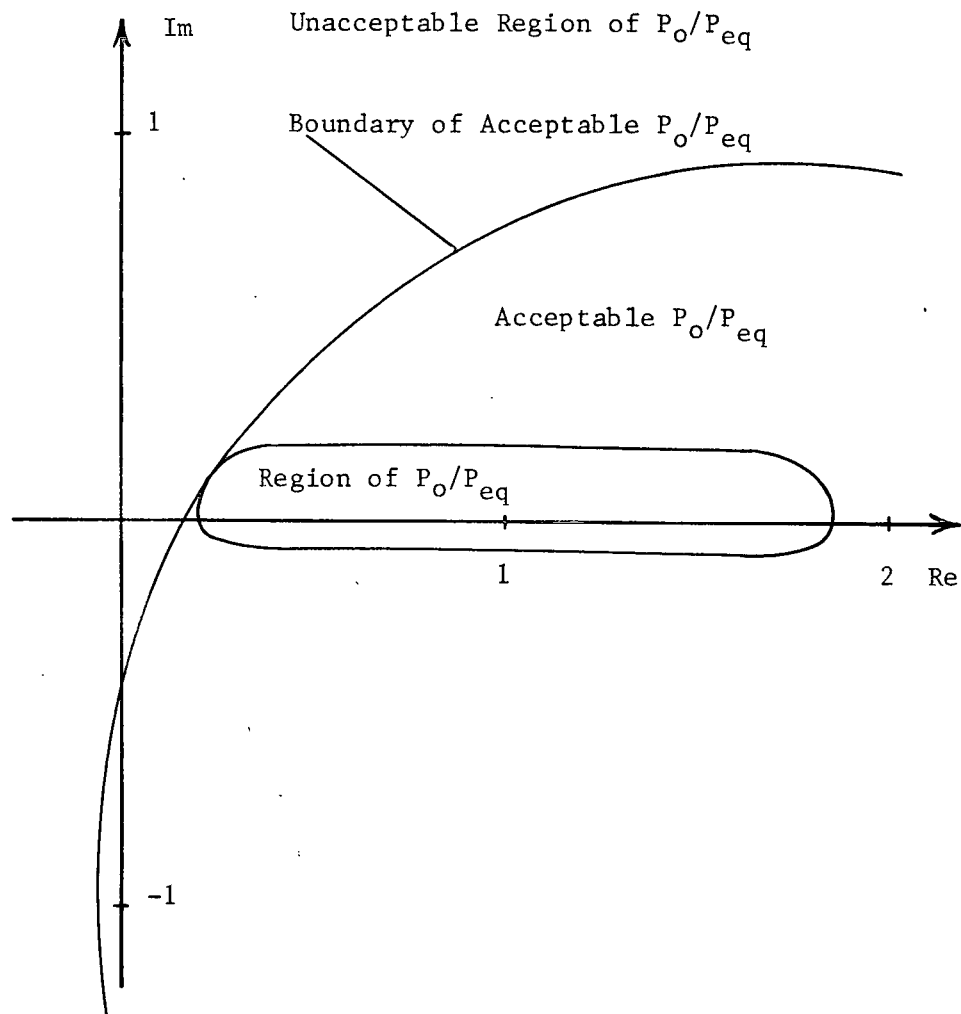


Figure 4.76  
 Region of  $P_o/P_{eq}$  for  $\omega = 1.25$ , Third Design

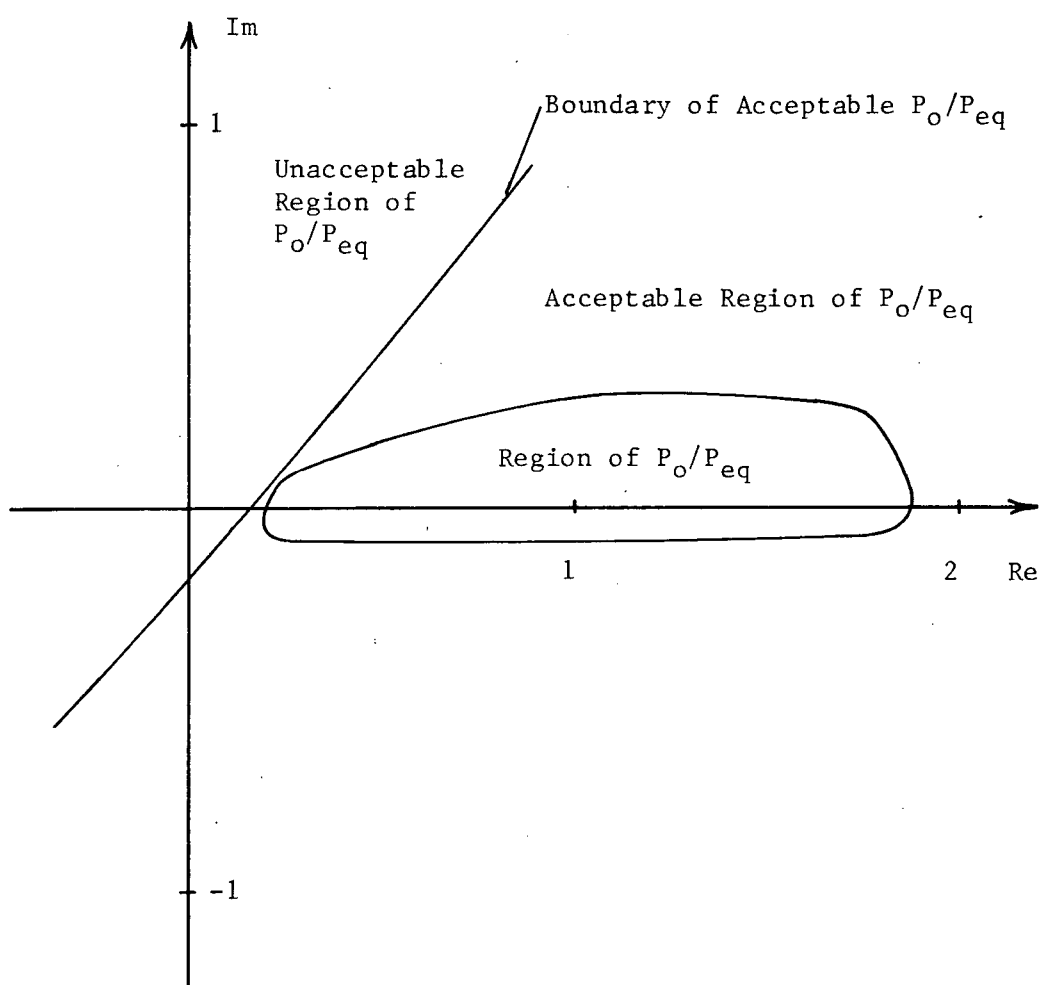


Figure 4.77  
 Region of  $P_o/P_{eq}$  for  $\omega = 1.88$ , Third Design

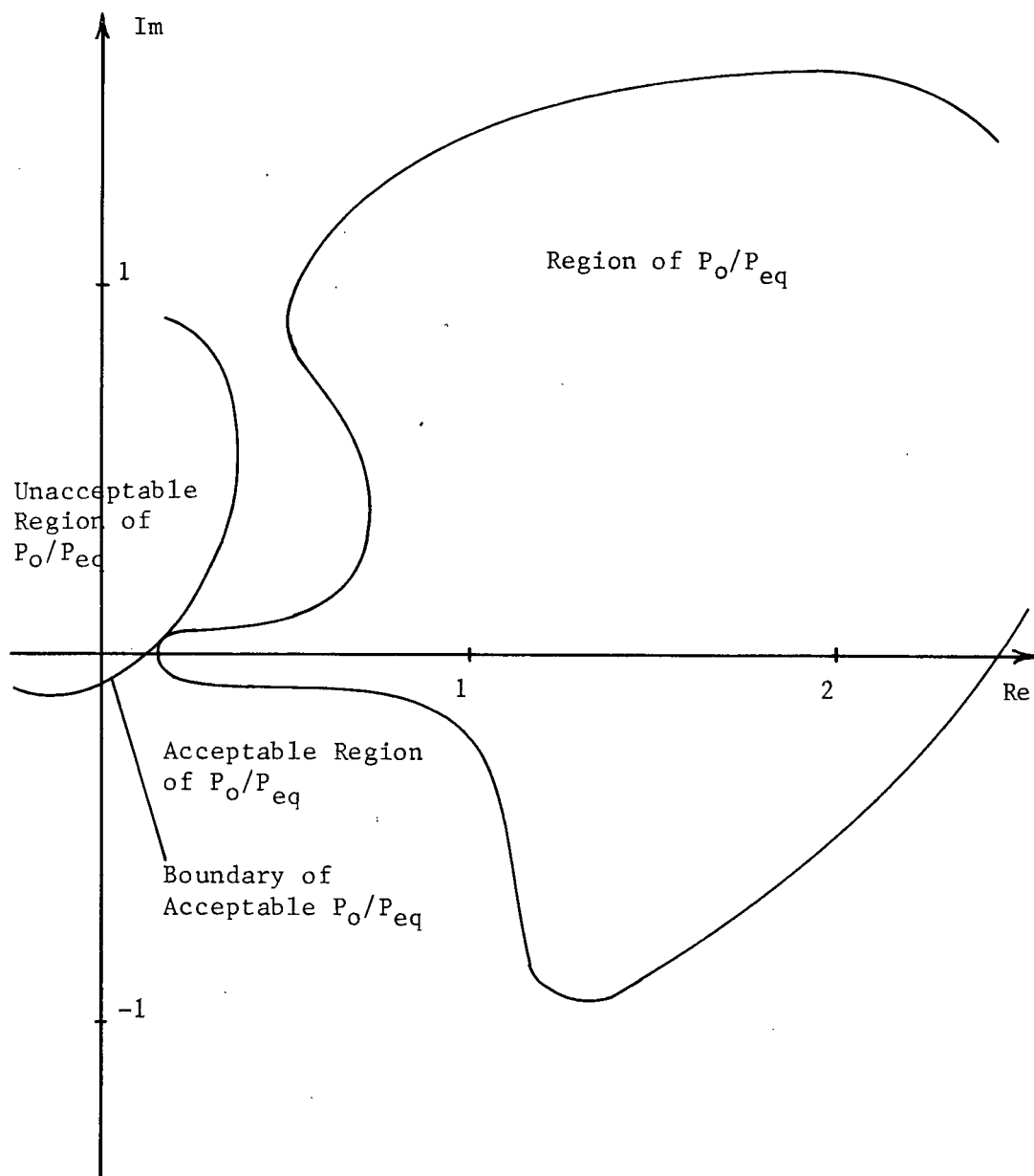


Figure 4.78  
 Region of  $P_o/P_{eq}$  for  $\omega = 4.39$ , Third Design

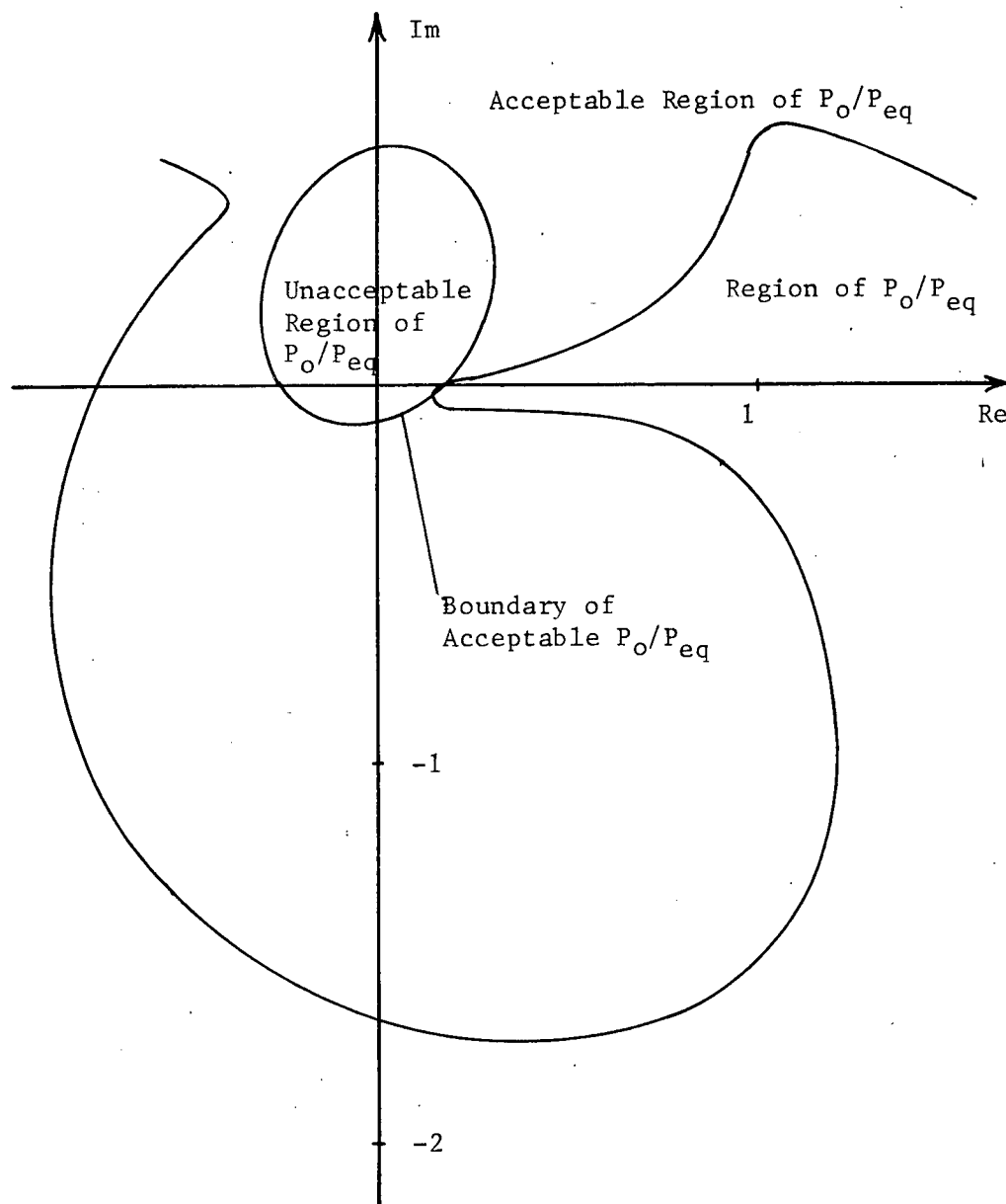


Figure 4.79  
Region of  $P_o/P_{eq}$  for  $\omega = 6.28$ , Third Design



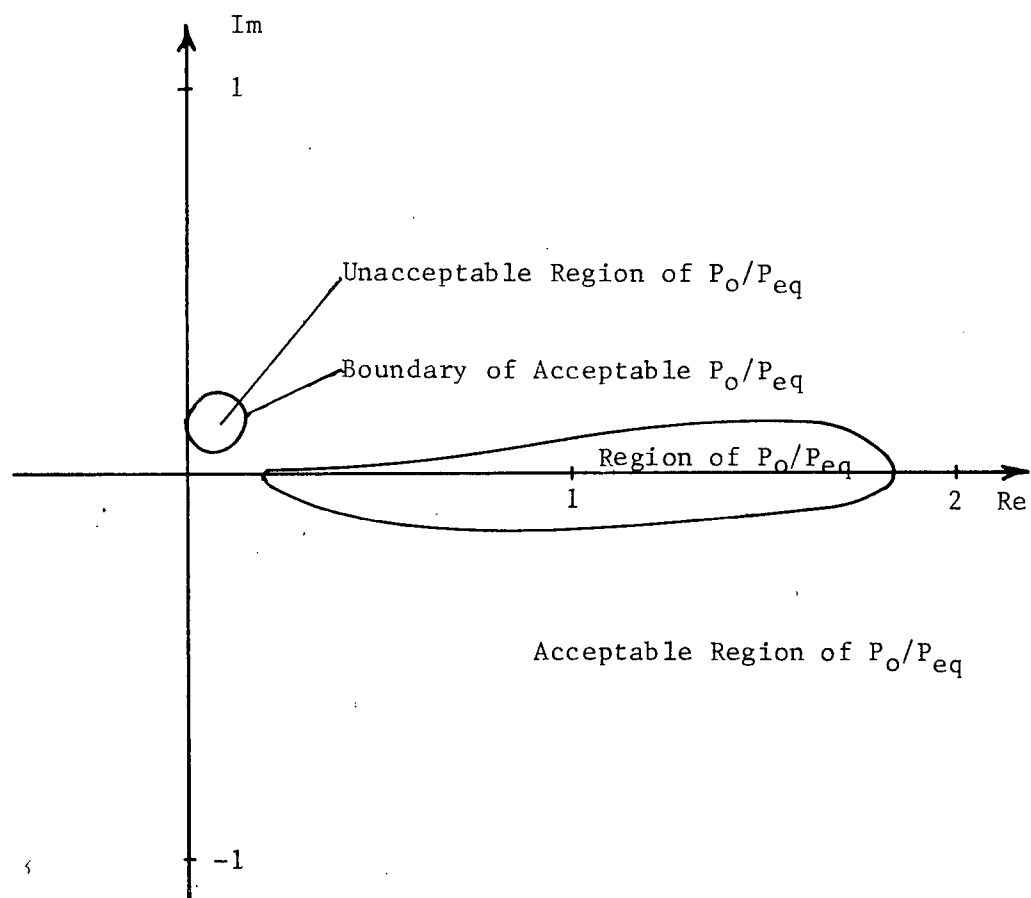


Figure 4.80  
 Region of  $P_O/P_{eq}$  for  $\omega = 9.42$ , Third Design

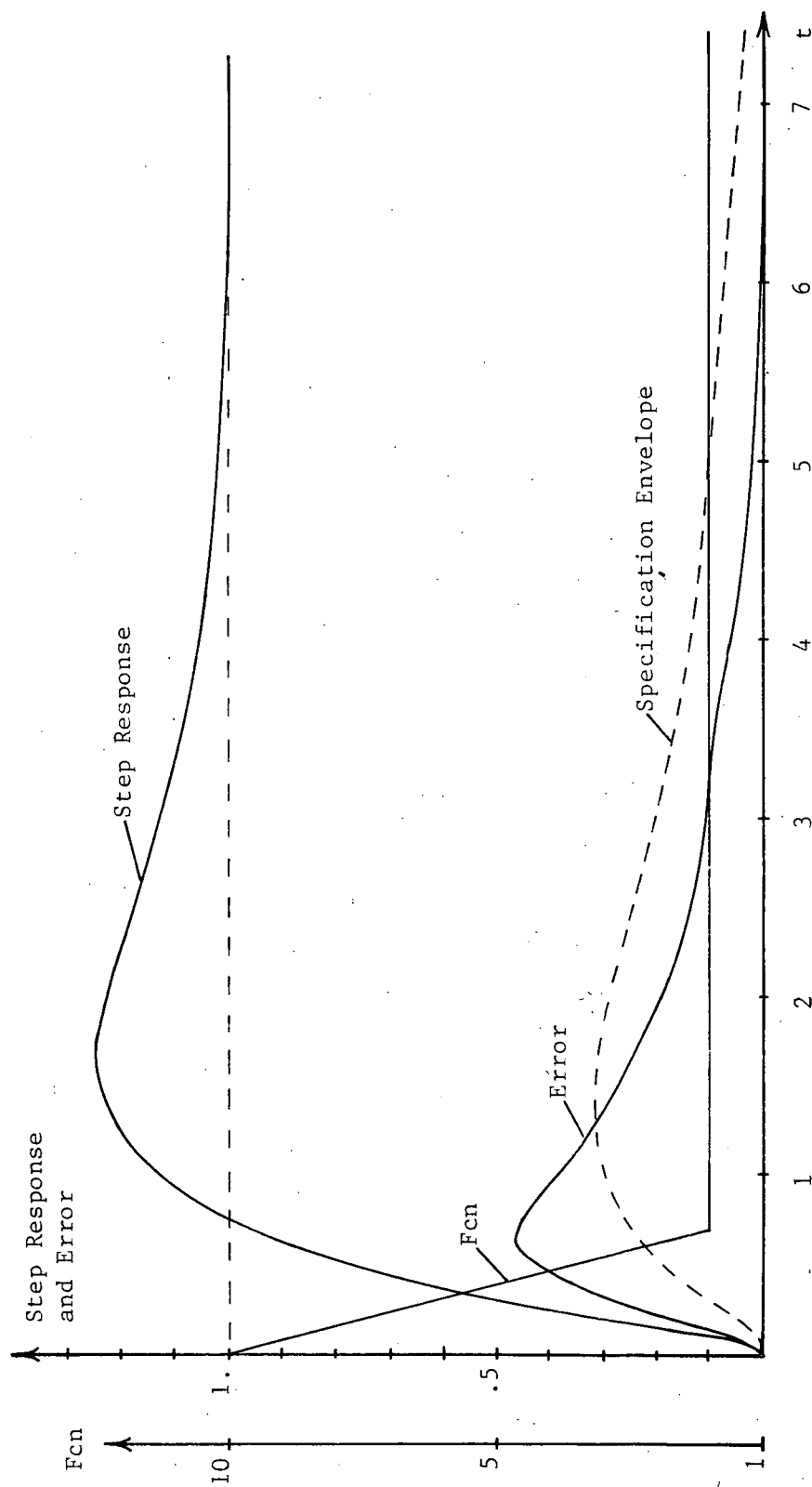


Figure 4.81  
Time-variation Causing Maximum  $|E|$  at  $\omega = 0$ .

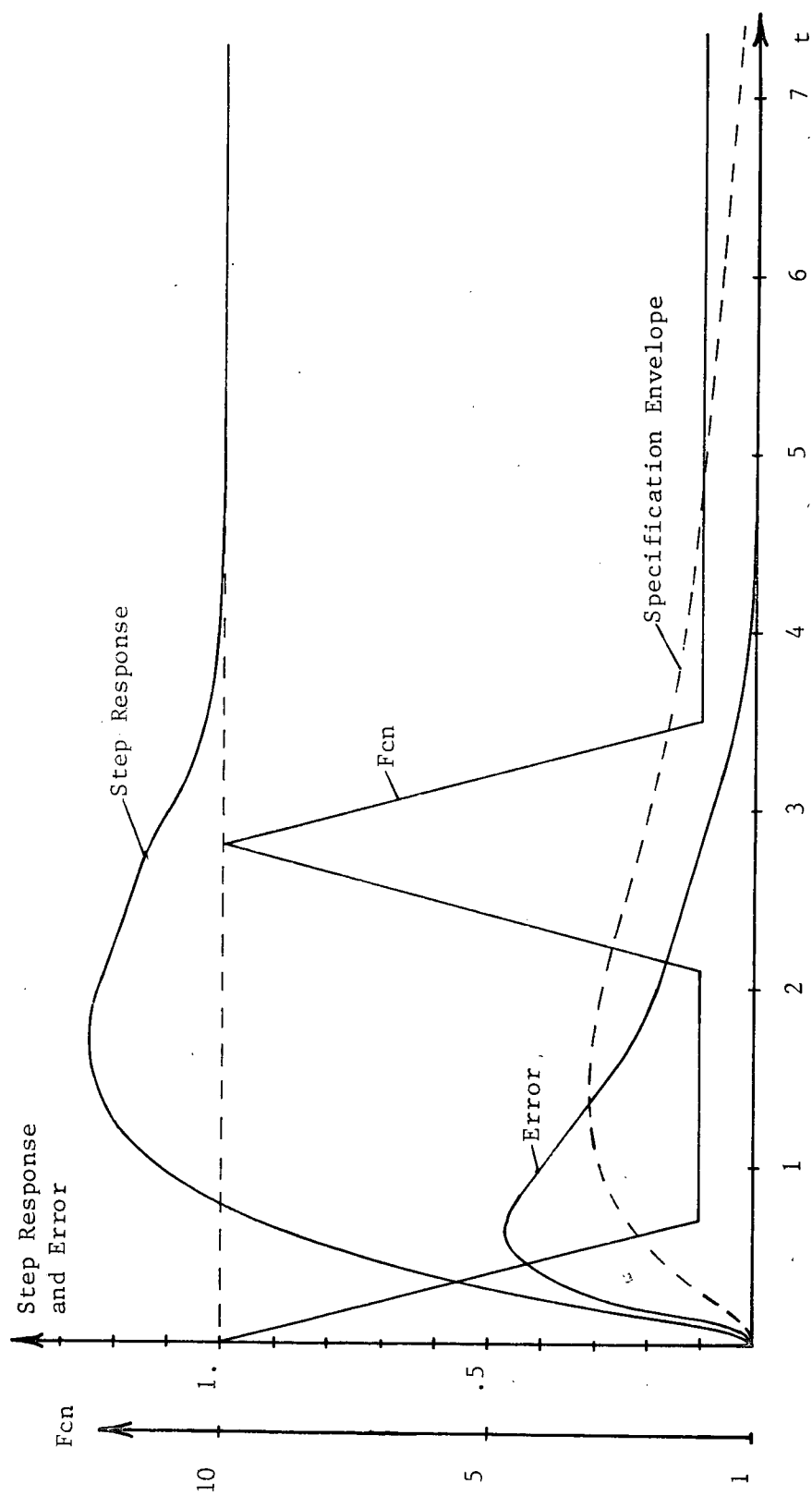


Figure 4.82  
Time-variation Causing Maximum  $|E|$  at  $\omega = 0.628$

C.S.

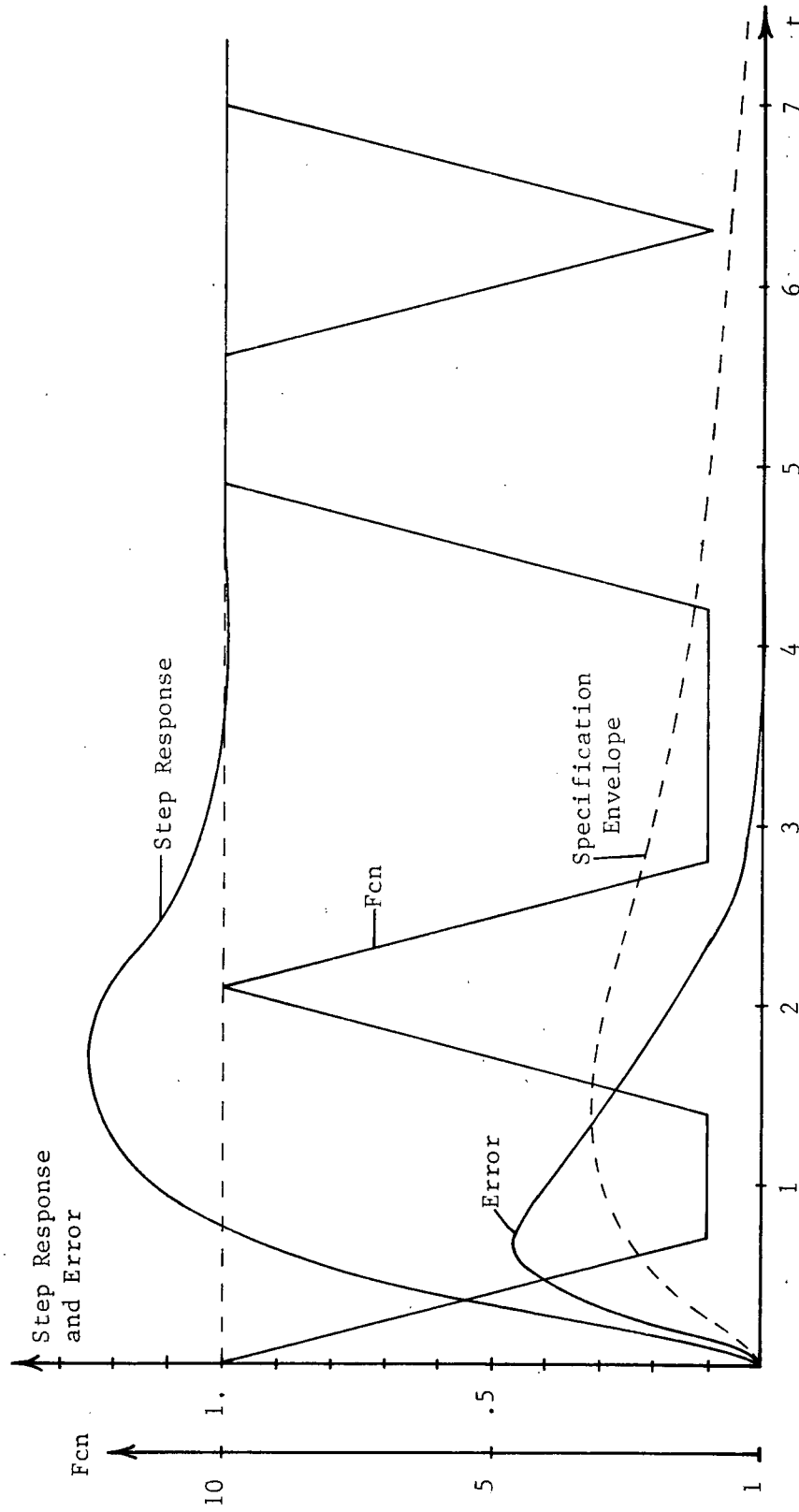


Figure 4.83  
Sample Step Response of Time-varying System  
Third Design

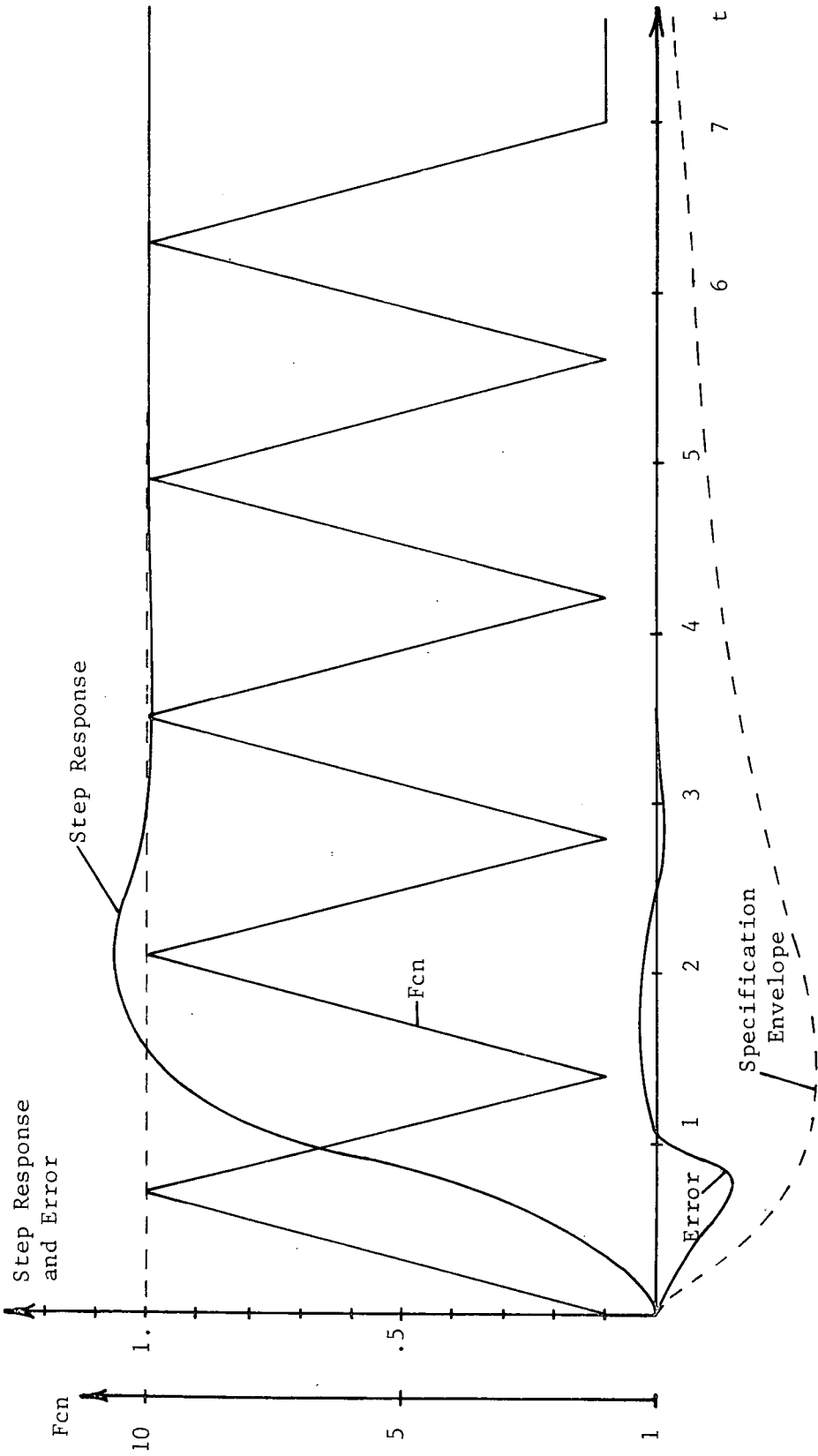


Figure 4.84  
Sample Step Response of Time-varying System  
Third Design

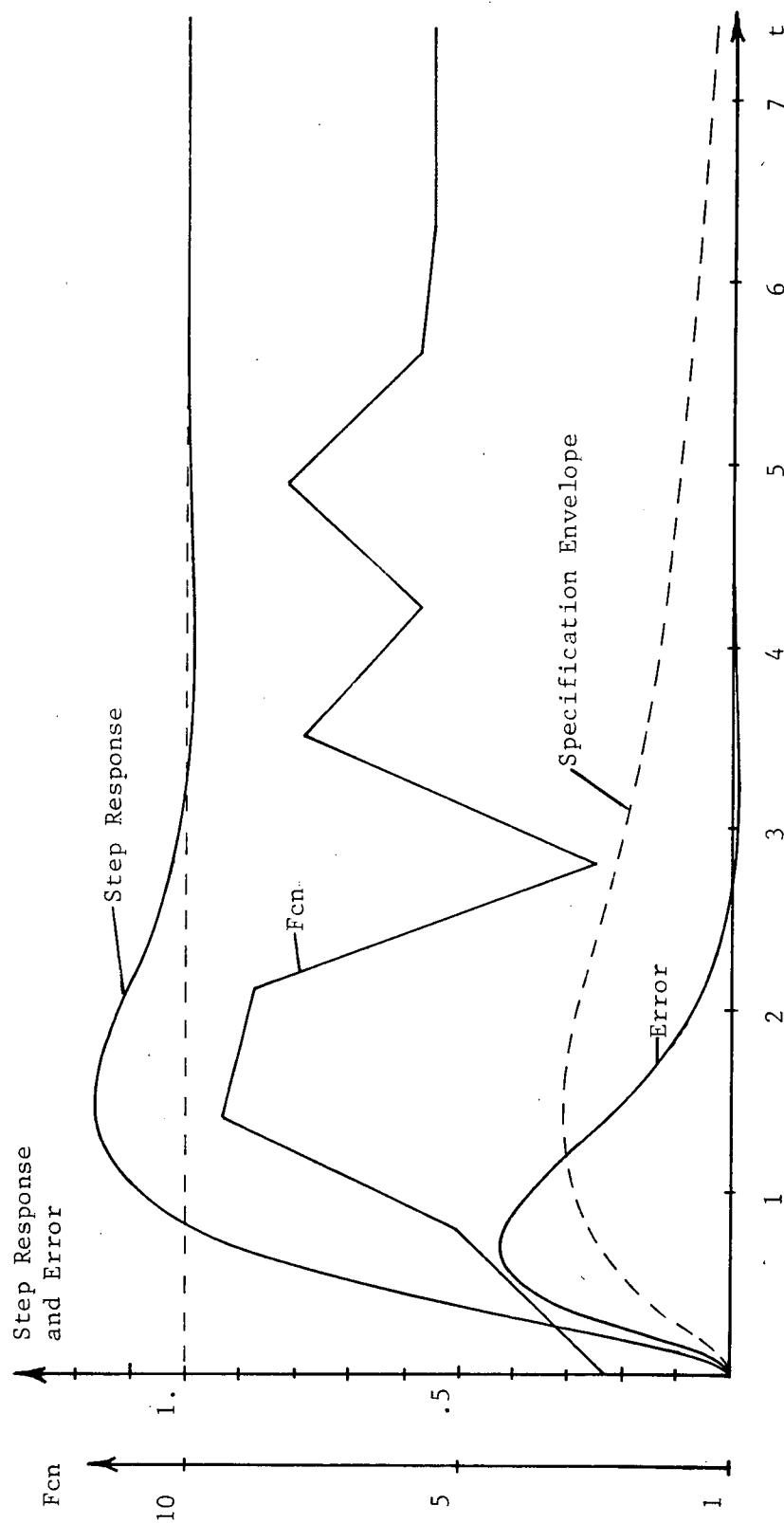


Figure 4.85  
Sample Step Response of Time-varying System  
Third Design

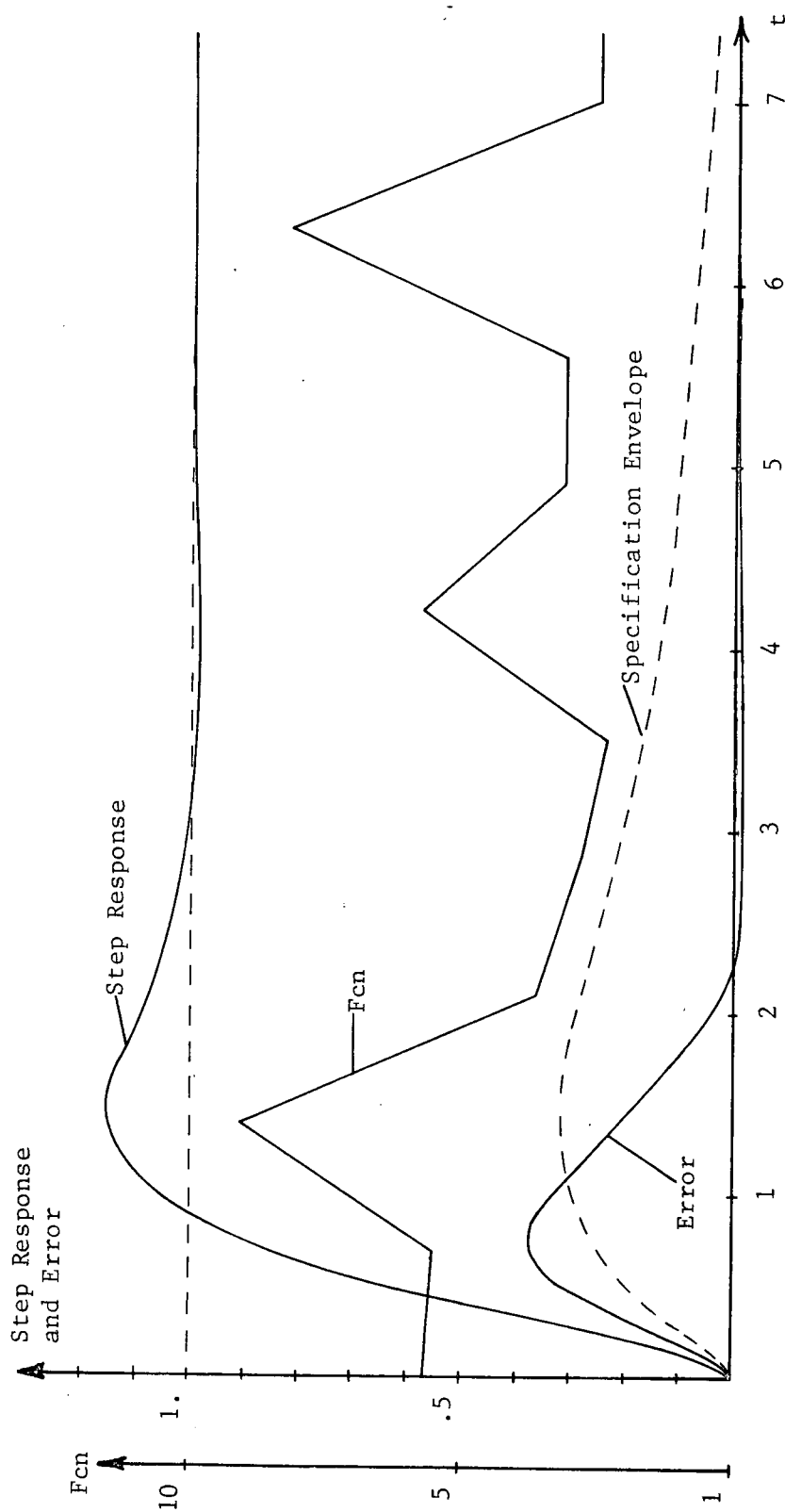


Figure 4.86  
Sample Step Response of Time-varying System  
Third Design

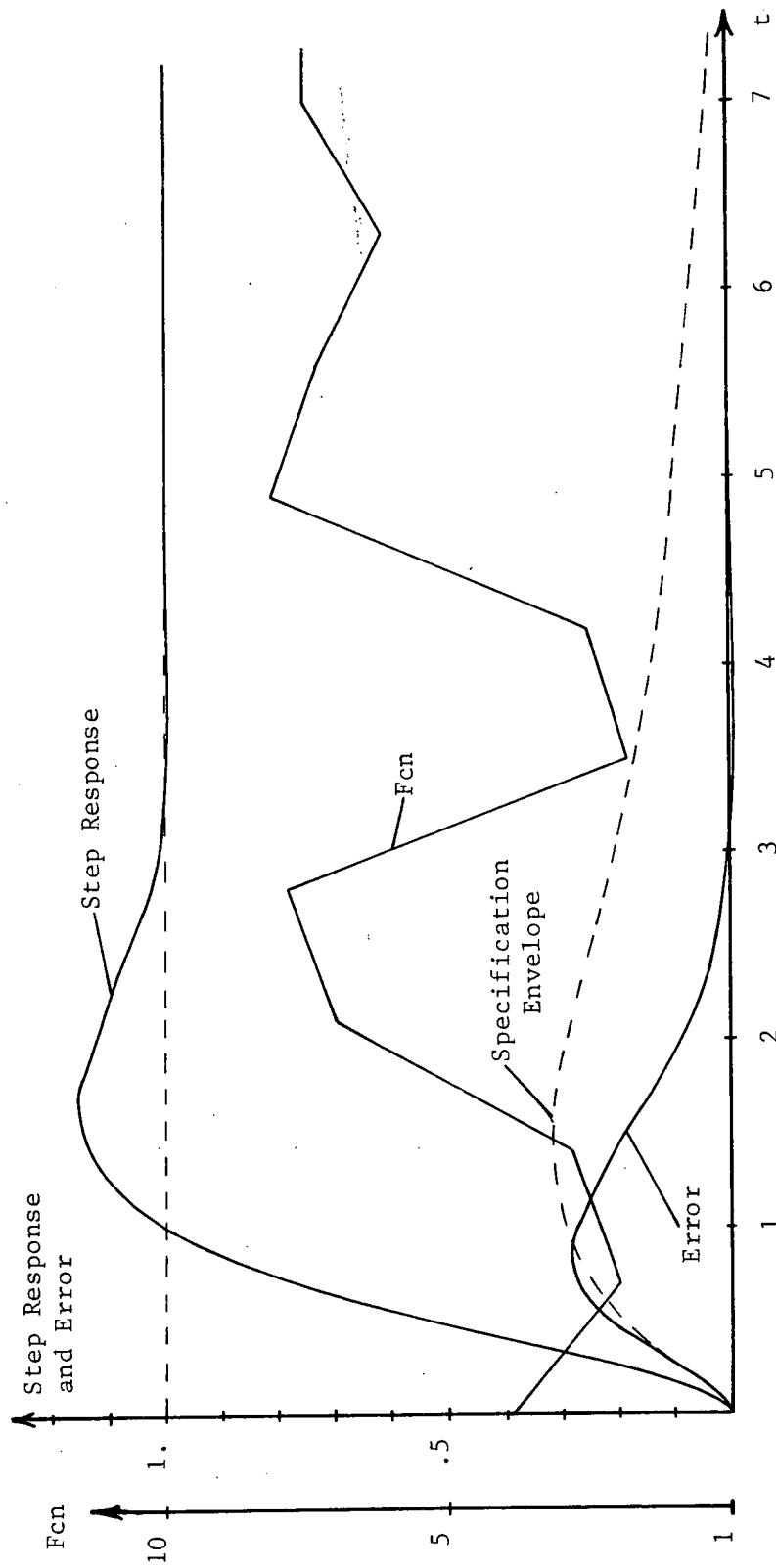


Figure 4.87  
Sample Step Response of Time-varying System  
Third Design



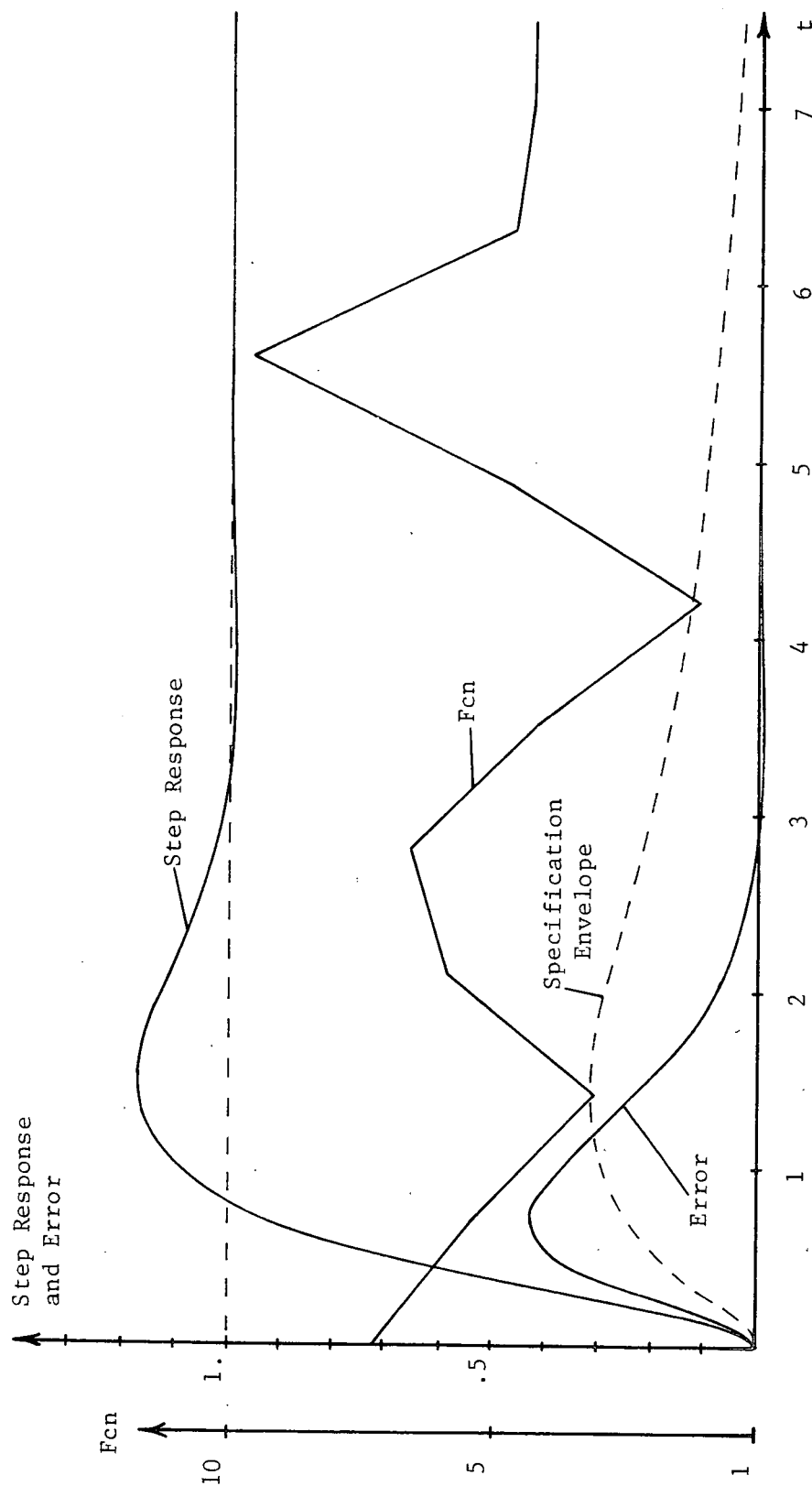


Figure 4.88  
Sample Step Response of Time-varying System  
Third Design

Note that the maximum overshoot is approximately 25% and the maximum settling time is six seconds. The third design is basically satisfactory; however, the system design must be completed by adding the high frequency poles in  $L_0$ . A fourth design will now be made to include the high frequency poles.

#### 4.8 Addition of High Frequency Poles

With only minor modification to  $L_0$  in the region of one radian the third design would be satisfactory from the point of view of system response and noise transmission in the low frequency region; however, it is far from optimal when noise transmission in the high frequency region is considered. The high frequency poles necessary to reduce the noise transmission at high frequencies will now be added.

An analysis of the noise transmission problem can be carried out in basically the same manner as presented by Horowitz<sup>45</sup> for linear time-invariant systems. Due to the linearity of the system, the system input can be assumed to be zero without affecting the results. Referring to Figure 4.1, with the system input zero the plant input  $Z$  is given by

$$Z(j\omega) = -H(j\omega) \left[ N(j\omega) + C(j\omega) \right]$$

which can be written

$$Z(j\omega) \left[ 1 + H(j\omega) \frac{C(j\omega)}{Z(j\omega)} \right] = -H(j\omega) N(j\omega).$$

Rearranging the expression, one can obtain

$$Z(j\omega) = \frac{-\frac{L_O(j\omega)}{P_{eq}(j\omega)}}{\frac{P_O(j\omega)}{P_{eq}(j\omega)} + L_O(j\omega)} N(j\omega) \quad (4-10)$$

where

$$P_{eq}(j\omega) = \frac{C(j\omega)}{Z(j\omega)}$$

and

$$L_O(j\omega) = P_O(j\omega)H(j\omega) .$$

In the low frequency region the characteristics of  $L_O$  are dictated by the system response. That is, at low frequencies  $L_O$  must lie within acceptable regions in the complex plane up to some frequency beyond which  $|L_O|$  may be decreased as quickly as possible. In the high frequency region the characteristics of  $L_O$  are dictated by Equation (4-10) which describes the noise transmission from the noise source to the plant input. To show that it is desirable to decrease  $|L_O|$ , suppose  $|L_O|$  were made large in the low frequency region. The noise transmitted to the plant input would approximately be given by

$$Z(j\omega) \approx \frac{-1}{P_{eq}(j\omega)} N(j\omega) .$$

At high frequencies the transmission of the time-varying plant is greatly reduced so that  $|P_{eq}(j\omega)|$  becomes small which results in large values of noise transmission to the plant input. Thus,  $|L_O|$

should be made as small as possible within the high frequency region.

The reduction of  $|L_O|$  in the high frequency region is accomplished by including high frequency poles in the design of  $L_O$ . A large number of poles cannot be added too low in the frequency range for otherwise instability will result. The procedure is then to add poles at increasing frequencies as quickly as possible while maintaining both a stable system and the proper system response. The problem is now to determine at what frequency one may stop adding poles.

Again consider Equation (4-10). At high frequencies  $|L_O|$  is smaller than  $|P_O/P_{eq}|$  so that the noise component of the plant input  $Z$  can be approximated by the expression

$$Z(j\omega) \approx \frac{\frac{L_O(j\omega)}{P_{eq}(j\omega)}}{\frac{P_O(j\omega)}{P_{eq}(j\omega)}} N(j\omega)$$

or

$$Z(j\omega) \approx \frac{L_O(j\omega)}{P_O(j\omega)} N(j\omega) = H(j\omega) N(j\omega) \quad (4-11)$$

From this expression, which is intuitively evident, it is seen that poles should be added to  $L_O$  until the desired amplification factor between the noise source and plant input is achieved. The desired amplification will depend upon the system and the noise source. In some cases it may be satisfactory to stop adding

poles while  $|H(j\omega)|$  is larger than unity, while in other cases it may be desired to add poles until  $|H(j\omega)|$  is much less than unity. In this example it will be assumed that poles will be added until  $|H(j\omega)|$  becomes less than unity — that is, until  $|L_O(j\omega)|$  becomes smaller than  $|P_O(j\omega)|$  as the frequency is increased.

The approach in making the fourth design is to assume the acceptable regions of  $-L_O$  corresponding to the third design are also acceptable when high frequency poles are added. Note that this does not mean that high frequency poles will merely be added to the third design, because the addition of such poles will cause an unacceptable decrease in  $|L_O|$  in the region of five to ten radians unless they are placed at extremely high frequencies. The high frequency poles must be incorporated as an integral part of a new design based upon the assumed acceptable region of  $-L_O$ .

The polar plot of  $L_O$  for the fourth design is shown in Figure 4.89 together with the acceptable regions and the stability region corresponding to the circle criterion. The expression for  $L_O(s)$  is given by

$$L_O(s) = 56.16 \frac{s + 5}{s(s + 10)(s + 18) \left[ \frac{s}{27} + 1 \right] \left[ \frac{s}{40} + 1 \right] \left[ \frac{s}{60} + 1 \right] \left[ \frac{s}{70} + 1 \right]} \quad (4-12)$$

The expressions for  $H(s)$  and  $G(s)$  were not found as a ratio of polynomials as was done in the previous designs. Instead, the system was simulated by simulating the various components of  $H$  and  $G$ . The expression for  $H(s)$  is

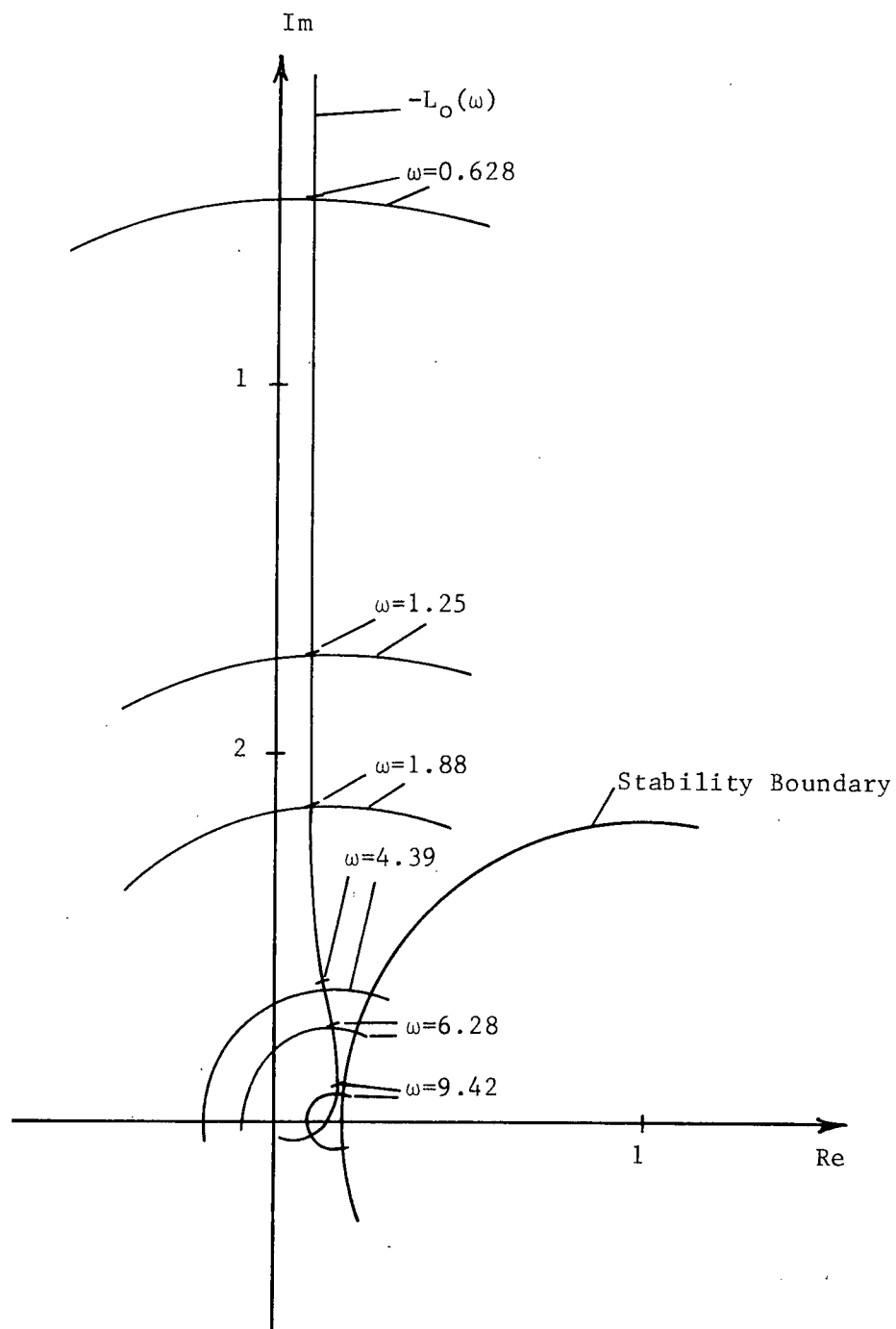


Figure 4.89  
Polar Plot of  $-L_O$  for Fourth Design with  
Boundaries of Acceptable Regions of  $-L_O$

$$H(s) + 30.88 \frac{s^2 + 7s + 10}{s^2 + 28s + 180} \frac{1}{\frac{s}{27} + 1} \frac{1}{\frac{s}{40} + 1} \frac{1}{\frac{s}{60} + 1} \frac{1}{\frac{s}{70} + 1}$$

and the expression for  $G(s)$  is

$$G(s) = \left[ 1 + L_o(s) \right] \frac{2.2s(s + 2)}{s^2 + 2.8s + 4}$$

where  $L_o(s)$  is given above.

In adding the high frequency poles the critical region was found to be between five and ten radians per second. As poles are added at 20 or 30 radians, lag is introduced between five and ten radians which causes  $-L_o$  to enter the circular stability region. Although entering the stability region does not imply an unstable system, system stability is not assured. The magnitude portion of the Bode plot of  $|L_o|$  for the fourth design is shown in Figure 4.90 with the plot of  $|L_o|$  corresponding to the third design and the plot of  $|P_o|$ . Note that the third design and the fourth design are identical below four radians per second. From four to 25 radians the magnitude of  $L_o$  for the fourth design is larger than the magnitude of  $L_o$  for the third design. This increase allows a more rapid decrease of  $|L_o|$  in the region greater than 25 radians. The point where  $|L_o|$  for the fourth design crosses  $|P_o|$  is at 94 radians so that poles are not added above 94 radians.

The fourth design was simulated and the maximum value of  $|E|$  was determined which is shown in Figure 4.91. It is seen that  $|E|$  significantly exceeds the specifications in the region of 0.25 to 1.6 radians. The step response corresponding to a function for

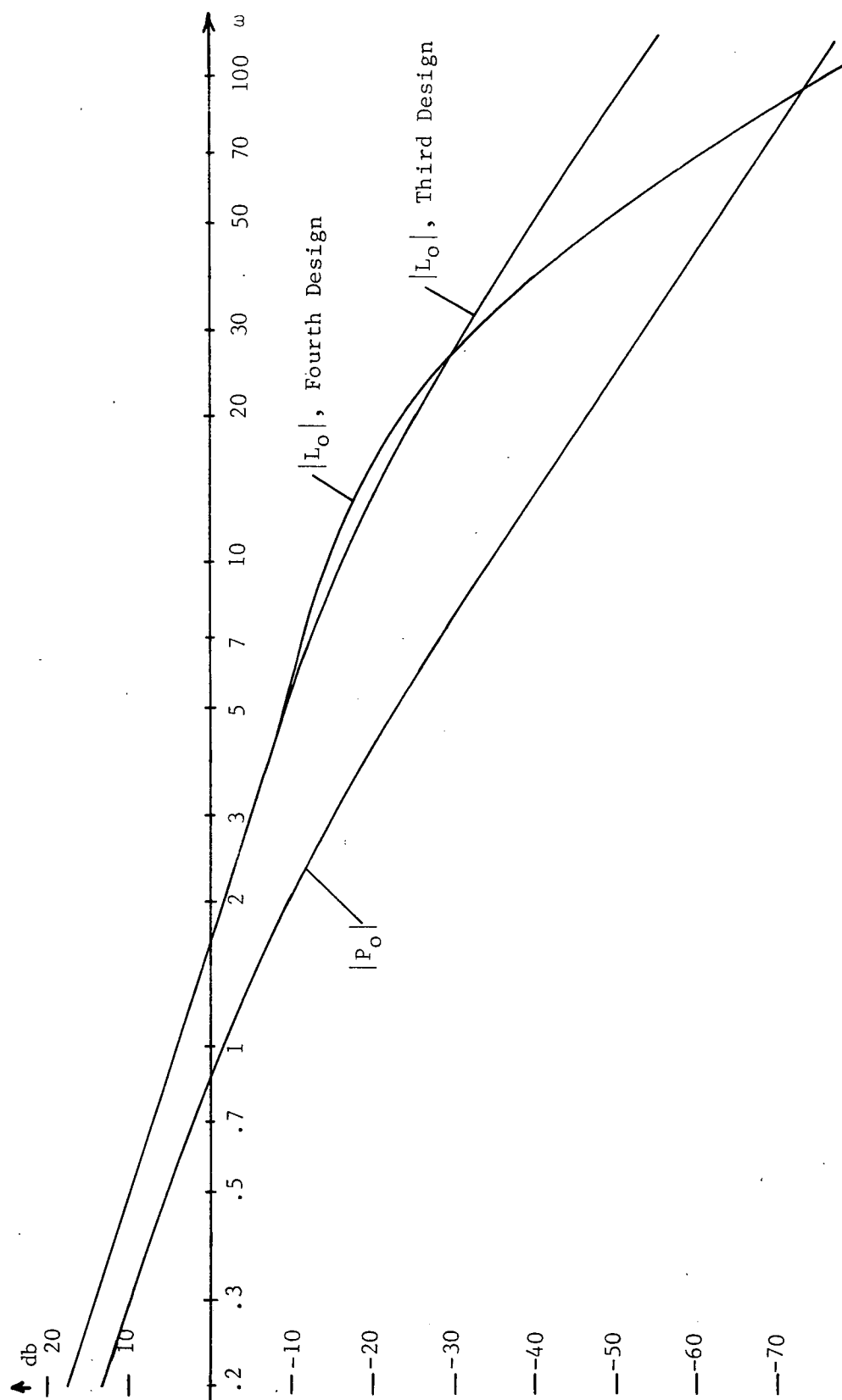


Figure 4.90  
Bode Plot of  $|L_O|$  for Fourth Design,  $|L_O|$  for Third Design and  $|P_O|$



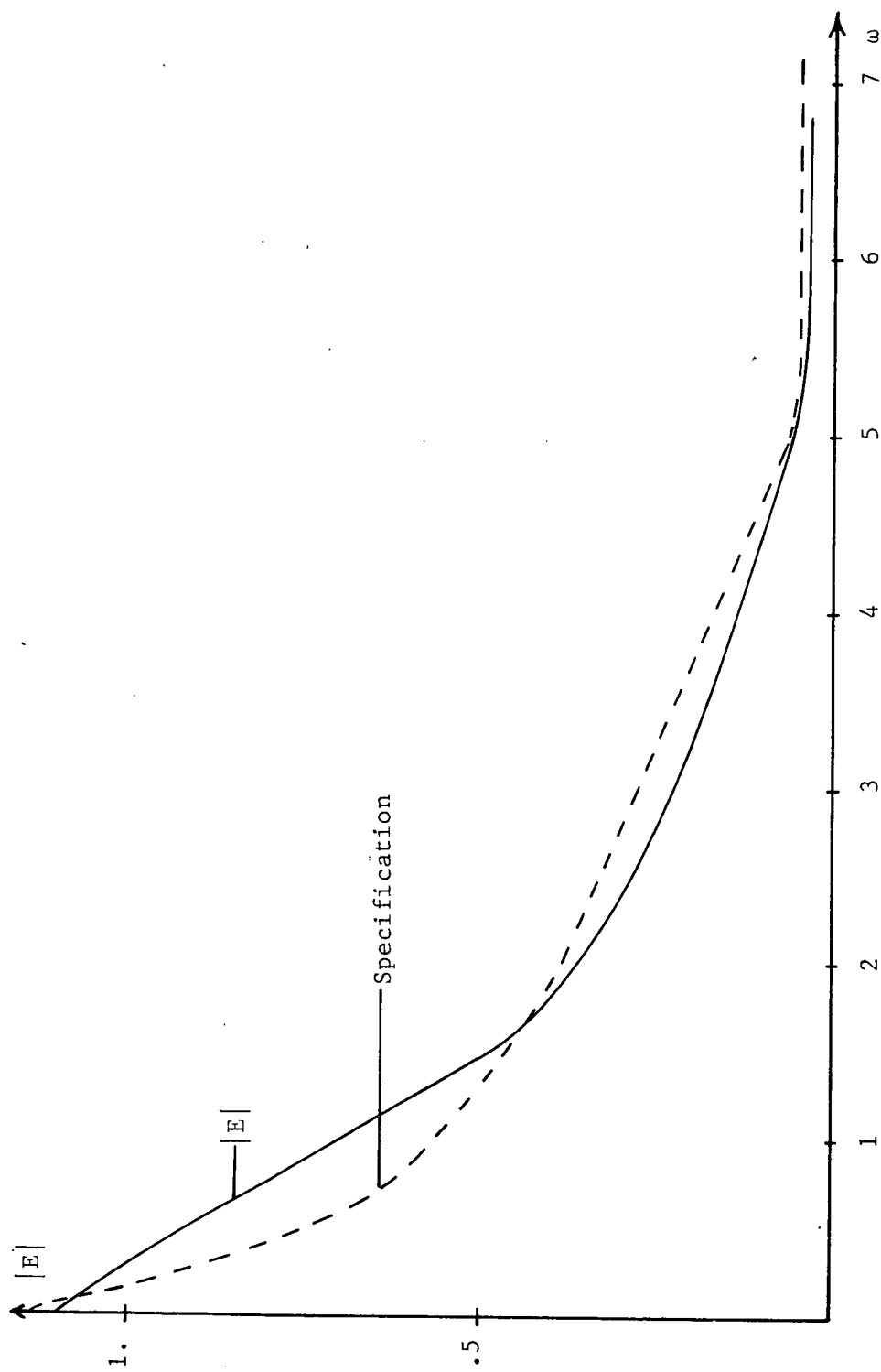


Figure 4.91  
Maximum  $|E|$  for Fourth Design

which the specification is exceeded is shown in Figure 4.92.

Note the "dip" in the error as a function of time in the region of 0.6 seconds. Contrary to what might be expected the "dip" did not result in a violation of the specification. The main frequency component in the "dip" is around 12 radians and the specifications were not violated in this high frequency region, although an increase in  $|L_O|$  was observed in this region over that seen in the third design. The violation of specifications in the region of 0.25 to 1.6 radians is due to the addition of the high frequency poles and is not an unexpected occurrence in a time-varying system.

There are now two possible modifications of  $|L_O|$  which will reduce the value of  $|E|$ . Either the magnitude of  $|L_O|$  may be increased in the appropriate low frequency range or the high frequency poles may be moved to higher frequencies which results in raising  $|L_O|$  in the high frequency range. The design procedures give a formal and systematic approach to increasing  $|L_O|$  in the frequency range where the specifications are violated; however, placement of the high frequency poles must be done on a trial and error basis.

The amplification of the noise from the noise source  $N$  to the plant input is a more severe problem in the higher frequency ranges than in the lower frequency ranges. One reason is that the noise usually has larger components in the higher frequencies than in the lower frequencies. But more important, it is the higher frequencies where  $|P_O/P_{eq}|$  is small and  $|H|$  is large which

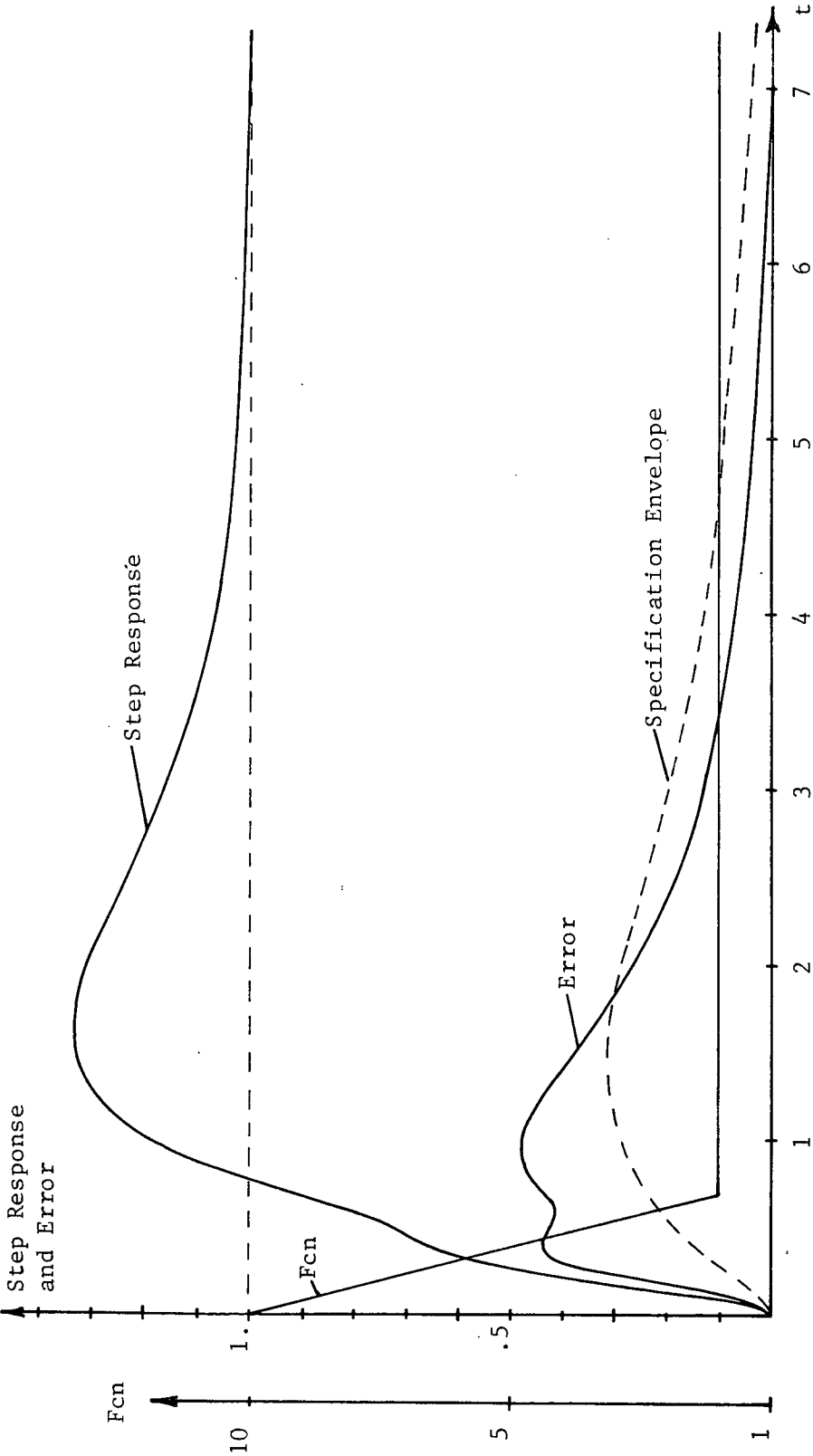


Figure 4.92  
Step Response Sample of Fourth Design

leads to large amplification of the high frequency noise components as is seen from Equation (4-11). Thus, increasing  $|L_O|$  in the lower frequency range is preferred to relocating the high frequency poles to still higher frequencies and thus increasing  $|L_O|$  in the high frequency range.

The fourth design was modified in order to observe the effect of both increasing  $|L_O|$  at low frequencies and relocating the high frequency poles. The effect of relocating the high frequency poles will first be discussed. The last three poles of  $|L_O|$ , Equation (4-12), were moved to 100 radians. This new system will be referred to as the first modification of the fourth design or simply Mod One. The expression for  $L_O(s)$  corresponding to Mod One is

$$L_O(s) = 56.16 \frac{s + 5}{s(s + 10)(s + 18) \left[ \frac{s}{27} + 1 \right] \left[ \frac{s}{100} + 1 \right]^3}$$

The expressions for  $H(s)$  and  $G(s)$  is evident from the corresponding expressions of the fourth design and will not be given. The difference between  $|L_O|$  for the fourth design and for Mod One is most easily observed from Bode plots of the magnitude portion of  $L_O$  for the two systems which are shown in Figure 4.93. Although the difference in the two designs may not appear to be significantly different from inspection of the Bode plot, the difference is actually quite large due to the fact that noise power is calculated from a linear integration over frequency. The maximum value of  $|E|$  for Mod One is shown in Figure 4.94. The specifications are violated in the region of .5 to 1.5 radians, but the

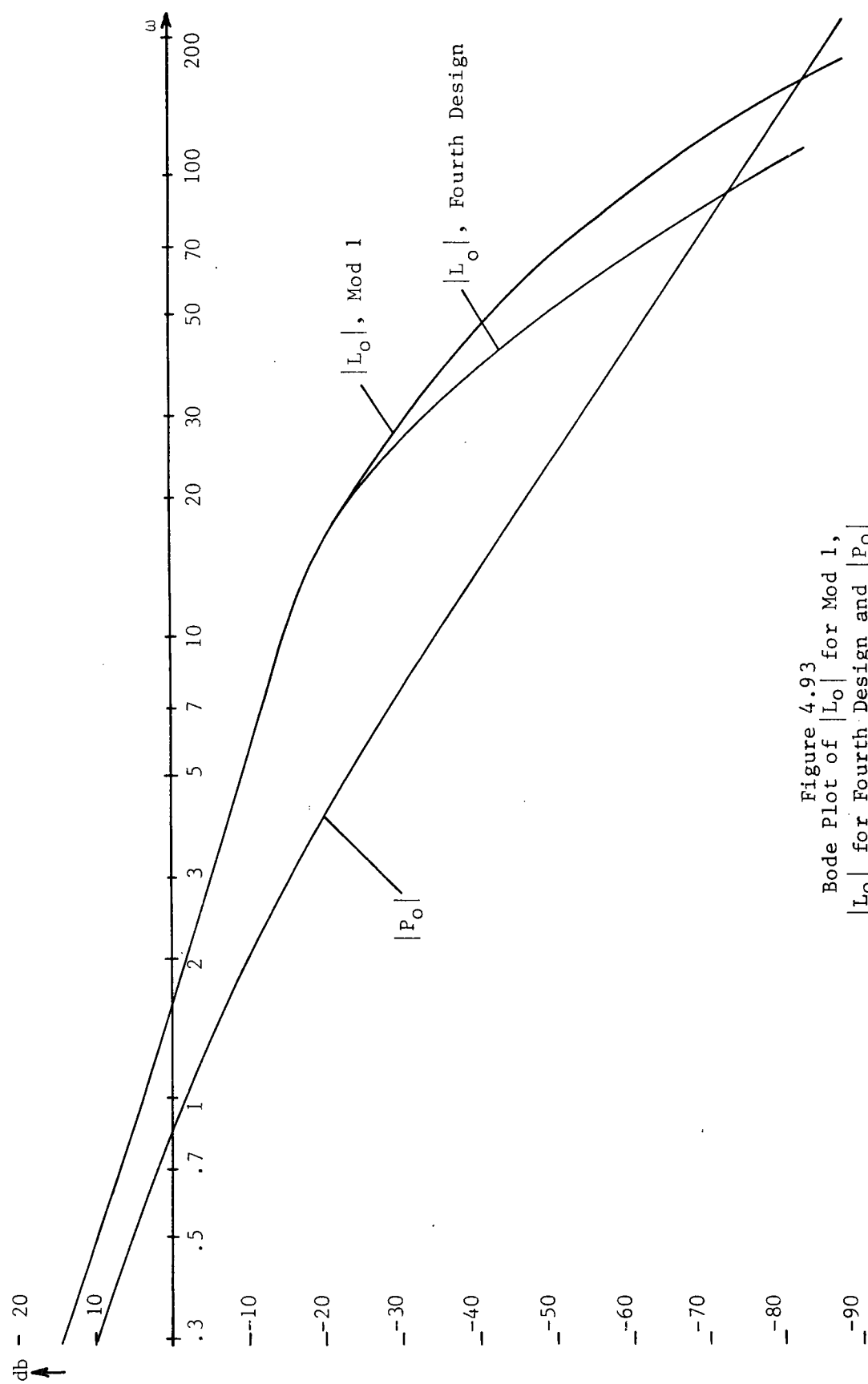


Figure 4.93  
Bode Plot of  $|L_o|$  for Mod 1,  
 $|L_o|$  for Fourth Design and  $|P_o|$

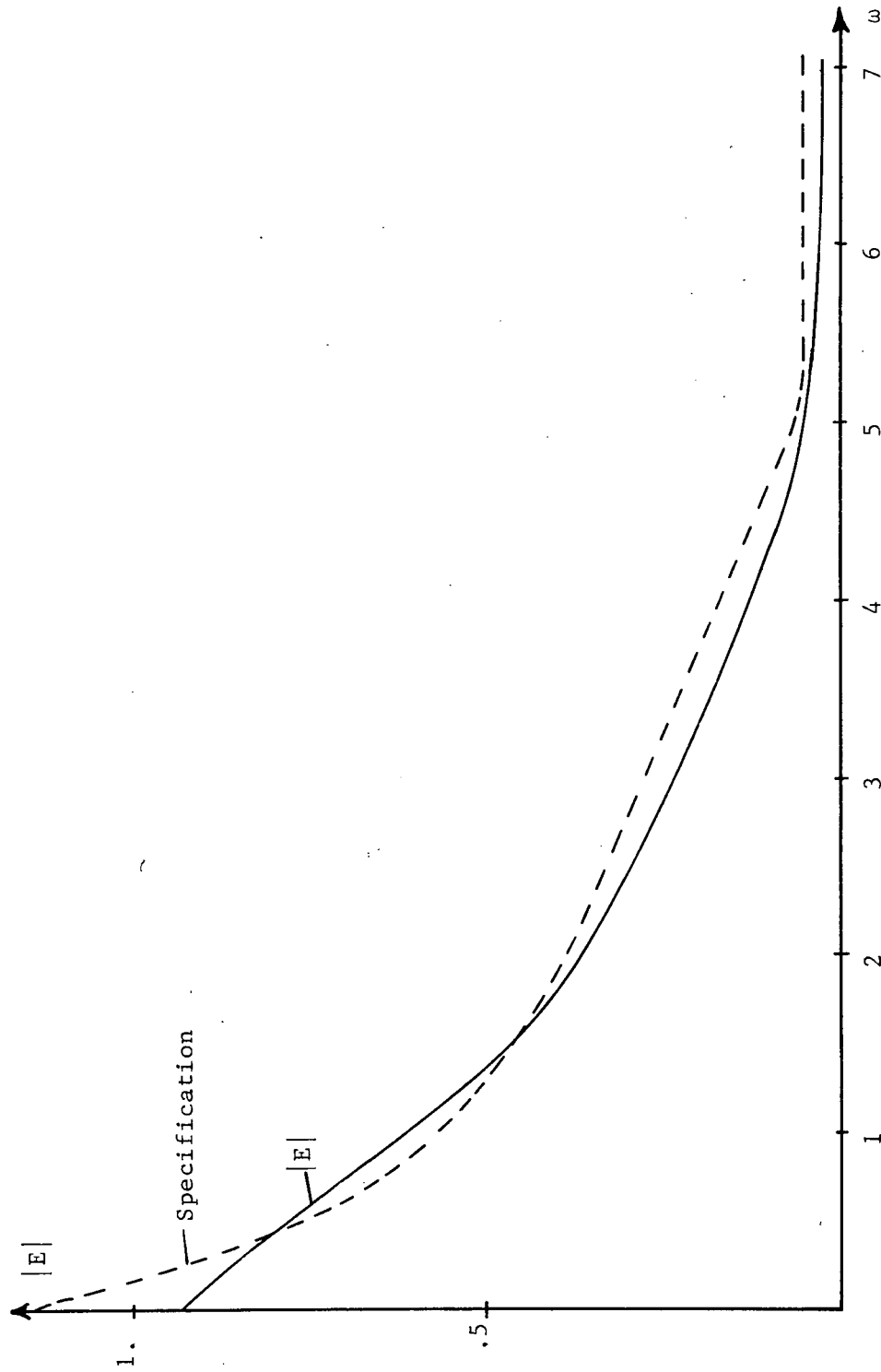


Figure 4.94  
Maximum  $|E|$  for Fourth Design, Mod 1

value of  $|E|$  is shown in Figure 4.95. Note that the "dip" which was observed in the error of the fourth design (see Figure 4.92) is not present in Mod One. This design is unacceptable not only because it violates the specifications but also because it does not represent the fastest decrease in  $|L_O|$  that is possible in the high frequency region.

A second modification was made to the fourth design to observe the effect of increasing  $|L_O|$  in the low frequency region. The modification consisted of increasing the magnitude of  $|L_O|$  in the low frequency range with the high frequency poles unchanged. This new system will be referred to as the second modification of the fourth design or simply Mod Two. As in the third design, a combination of design procedures one and two was used to determine the acceptable regions of  $-L_O$ . The shape of the acceptable region of  $-L_O$  was assumed to be as shown in Figure 4.89 and the design equation, Equation (4-9), was used to determine the proper size of the acceptable regions. The acceptable regions of  $-L_O$  for the second modification are shown in Figure 4.96 together with a polar plot of  $-L_O$  for Mod Two. The magnitude portion of the Bode plots of  $L_O$  for Mod Two together with the fourth design are shown in Figure 4.97. Note that in Mod Two the values of  $|L_O|$  do not come as close to lying on the boundaries of the acceptable regions as does  $|L_O|$  for the fourth design shown in Figure 4.89. This is because it proved to be difficult to have the large magnitude of  $|L_O|$  required at 0.628 radians and at the same time decrease  $|L_O|$  to the minimum magnitude at 1.25 and 1.88 without violating the

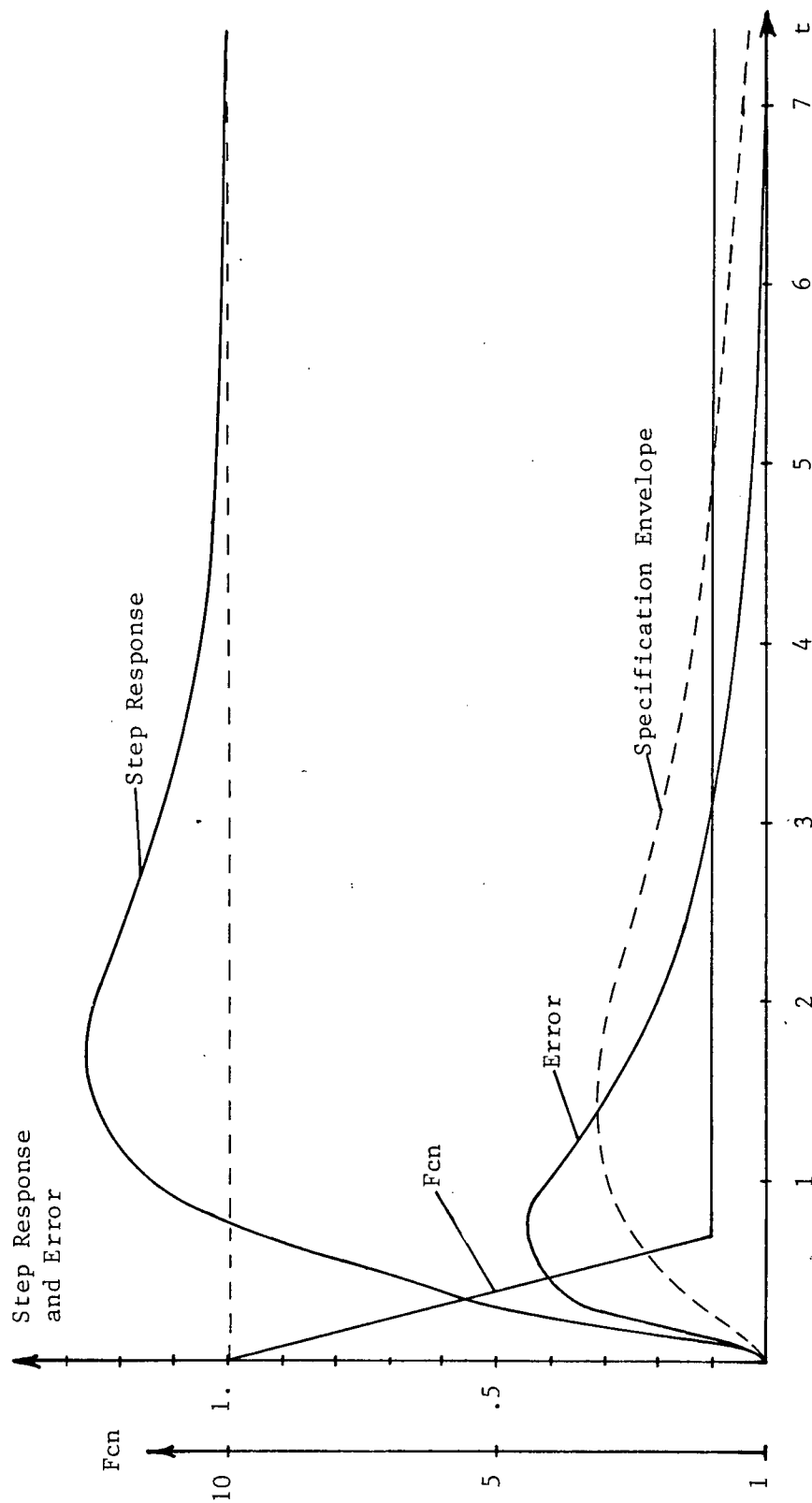


Figure 4.95  
Step Response Sample of Fourth Design, Mod 1



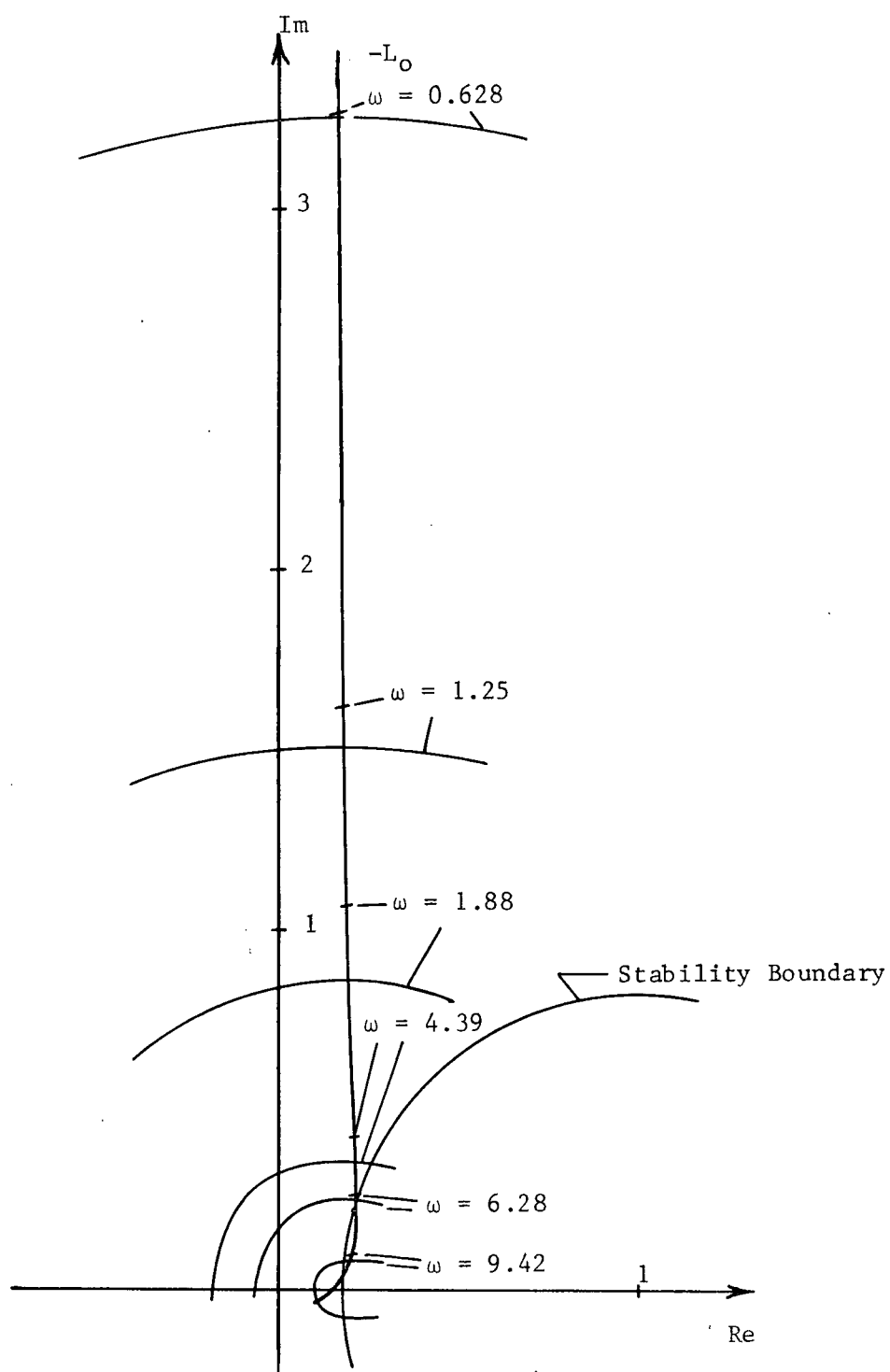


Figure 4.96  
 Boundaries of Acceptable Regions of  $-L_O$   
 With Polar Plot of  $-L_O$  for Fourth Design, Mod 2

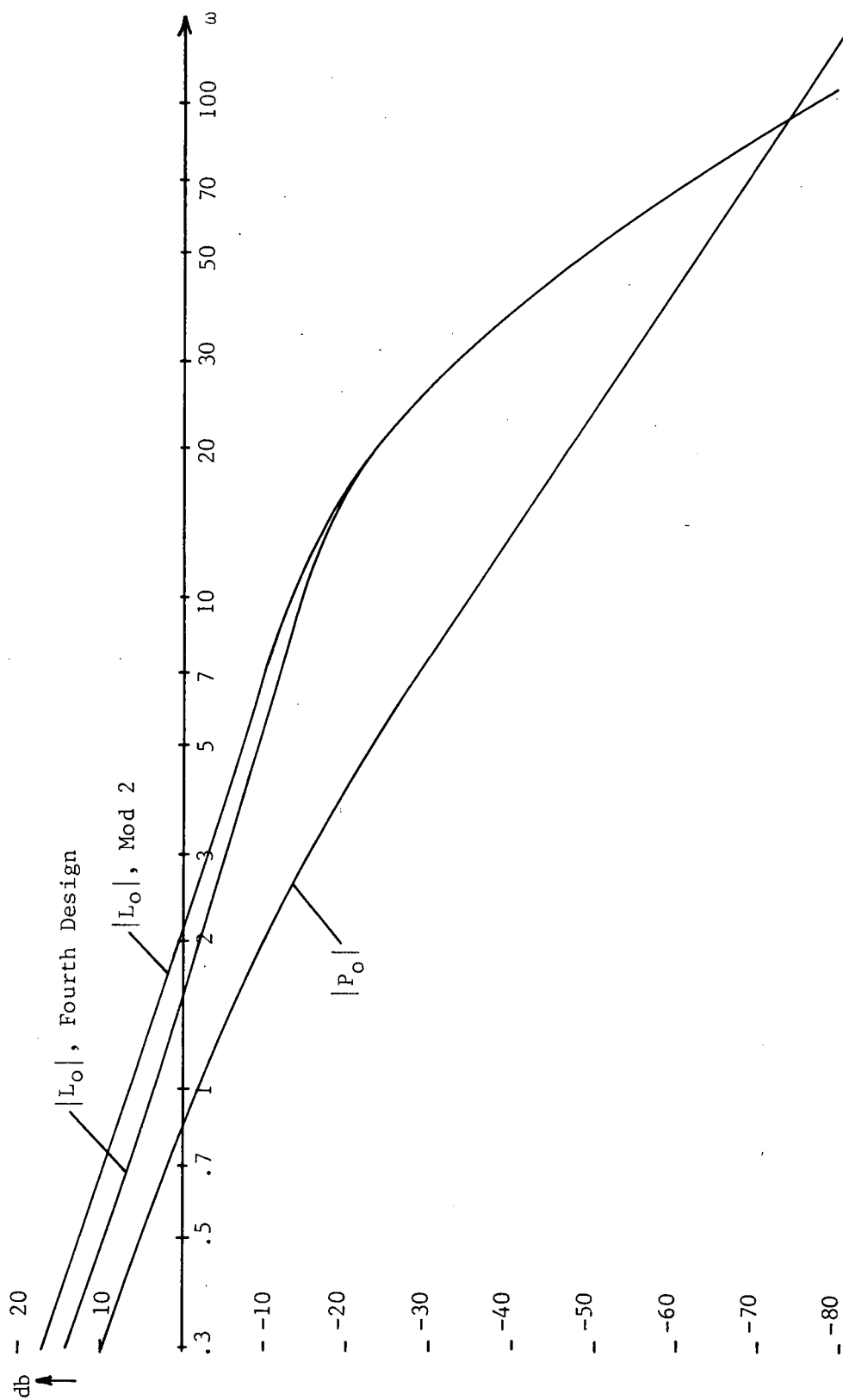


Figure 4.97  
Bode Plot of  $|L_O|$  for Fourth Design,  
 $|L_O|$  for Mod 2, Fourth Design and  $|P_O|$

specifications at 9.42 or even maintaining system stability. Note that if the point 0.1818 on the real axis is enclosed by  $-L_0$ , the system is unstable when the gain is constant at ten from a time-invariant analysis. The plot of  $-L_0$  for Mod Two slightly enters the stability circle so that the system stability cannot be assured. The system proved, however, to be stable for all time-variations tested.

A slight improvement can be made in fitting  $-L_0$  to the acceptable regions of  $-L_0$  by moving the pole which is located at ten radians to eight radians, moving the zero which is located at 6.4 radians to four radians, placing an additional zero at 2.3 radians and placing an additional pole at 1.7 radians. However, this small improvement was not felt to be worth the additional complexity in the system and will not be discussed in detail.

The maximum value of the error magnitude for Mod Two is shown in Figure 4.98. Figure 4.99 shows a step response for one function which corresponds to an extreme value of  $|E|$ . Note that the "dip" in the error at approximately .5 seconds is larger than was observed in the fourth design and is in fact large enough to result in a small violation of the specification in the region of six to ten radians where  $|E|$  reaches a value of 0.6. The specifications are also not met in the region of 0.5 to 1.5 radians. This design would not be considered acceptable for not only does it violate the specifications but also stability is not assured.

A fifth design will now be made. It is expected that  $|L_0|$  for the fifth design should lie somewhere between Mod One and

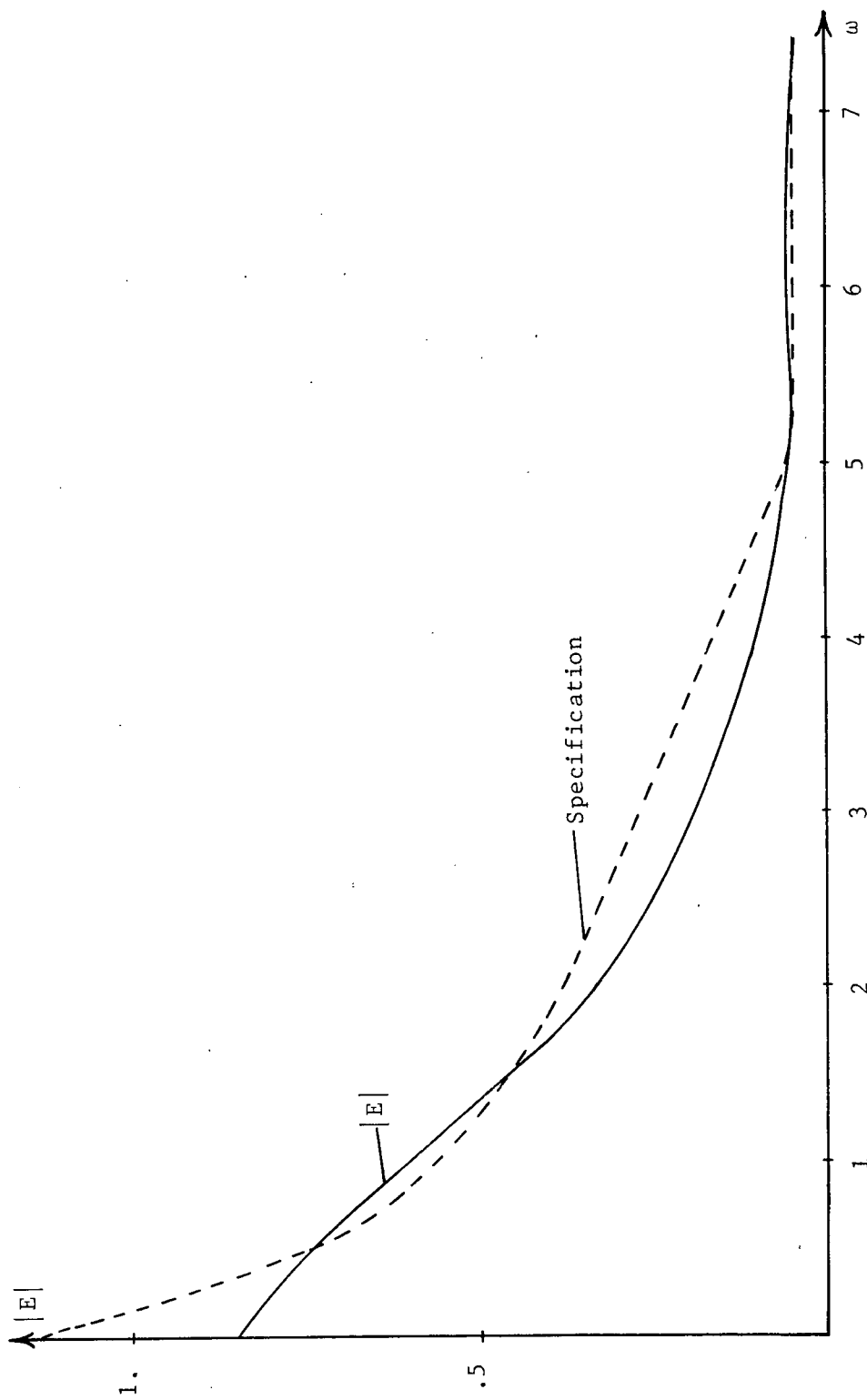


Figure 4.98  
Maximum  $|E|$  for Fourth Design, Mod 2

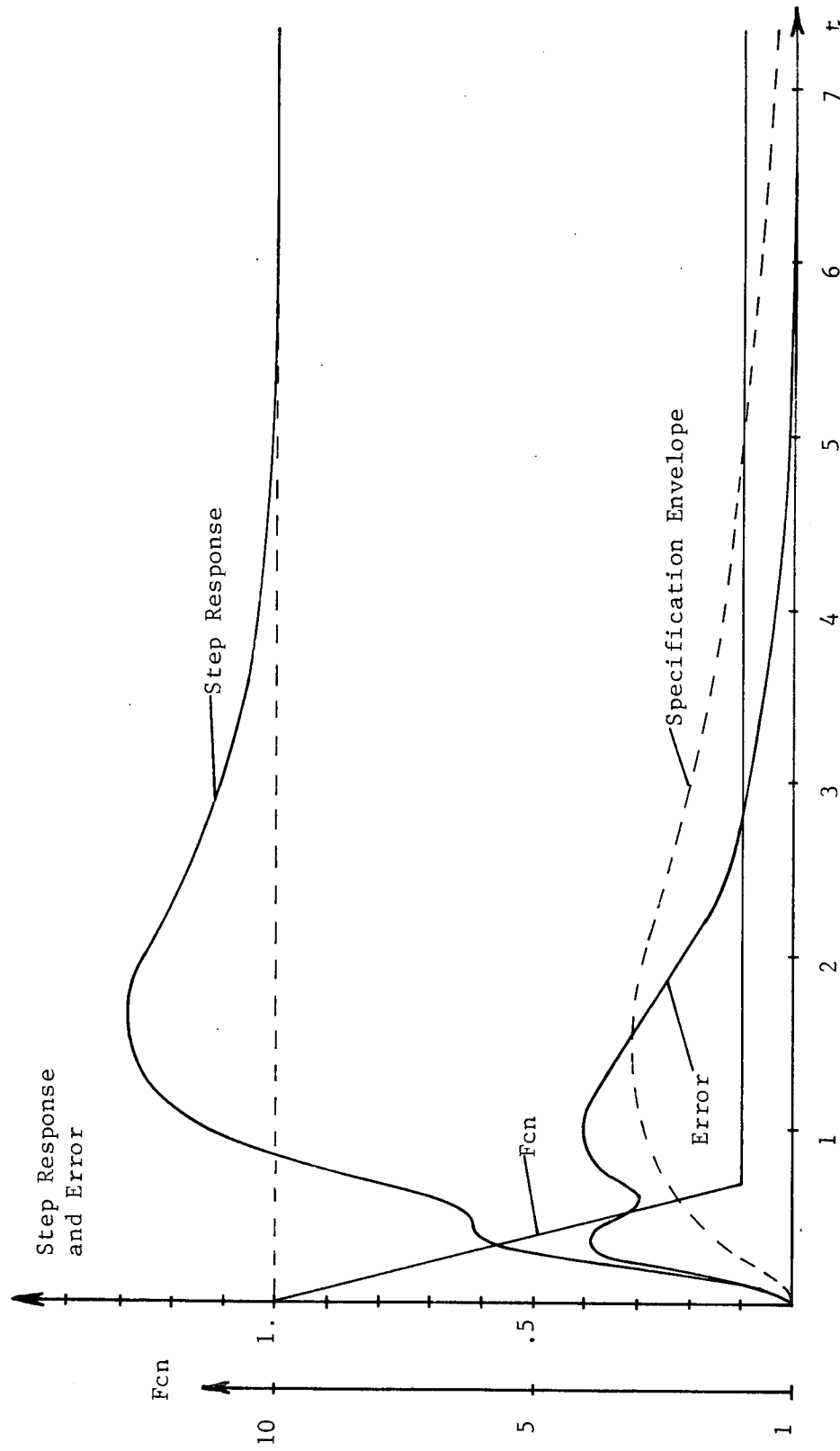


Figure 4.99  
Step Response of Fourth Design, Mod 2

Mod Two, since in Mod One  $|L_O|$  was too large in the high frequency regions and not quite large enough in the low frequency region, while in Mod Two  $|L_O|$  was not large enough in the high frequency region and appeared to be a little too large in the low frequency region. The magnitude of  $|L_O|$  for the fifth design at low frequencies will be chosen to lie approximately half way between the magnitude corresponding to Mod One and Mod Two. The high frequency poles will then be placed so that a polar plot of  $-L_O$  lies just outside the stability circle in order to assure system stability. Note that this approach departs from the design procedure but instead draws upon the insight which has been gained in the previous designs.

The expression for  $L_O(s)$  for the fifth design is given by

$$L_O(s) = 75 \frac{s + 6}{s(s + 12.5)(s + 20) \left[ \frac{s}{30} + 1 \right] \left[ \frac{s}{45} + 1 \right] \left[ \frac{s}{70} + 1 \right] \left[ \frac{s}{85} + 1 \right]}$$

The polar plot of  $-L_O$  is shown in Figure 4.100. For comparison the acceptable regions used in the fourth design are also shown in Figure 4.100. The relatively large magnitude of  $L_O$  in the region of nine radians is necessary in order to be able to reduce  $|L_O|$  more rapidly in the higher frequency regions. This can be more clearly seen from a Bode plot of  $|L_O|$  which is shown in Figure 4.101. Also shown in Figure 4.101 are plots of  $|L_O|$  corresponding to Mod One and Mod Two. Note that the magnitude of  $|L_O|$  for the fifth design lies approximately half way between the magnitudes of  $|L_O|$  of Mod One and Mod Two at both high frequencies and low

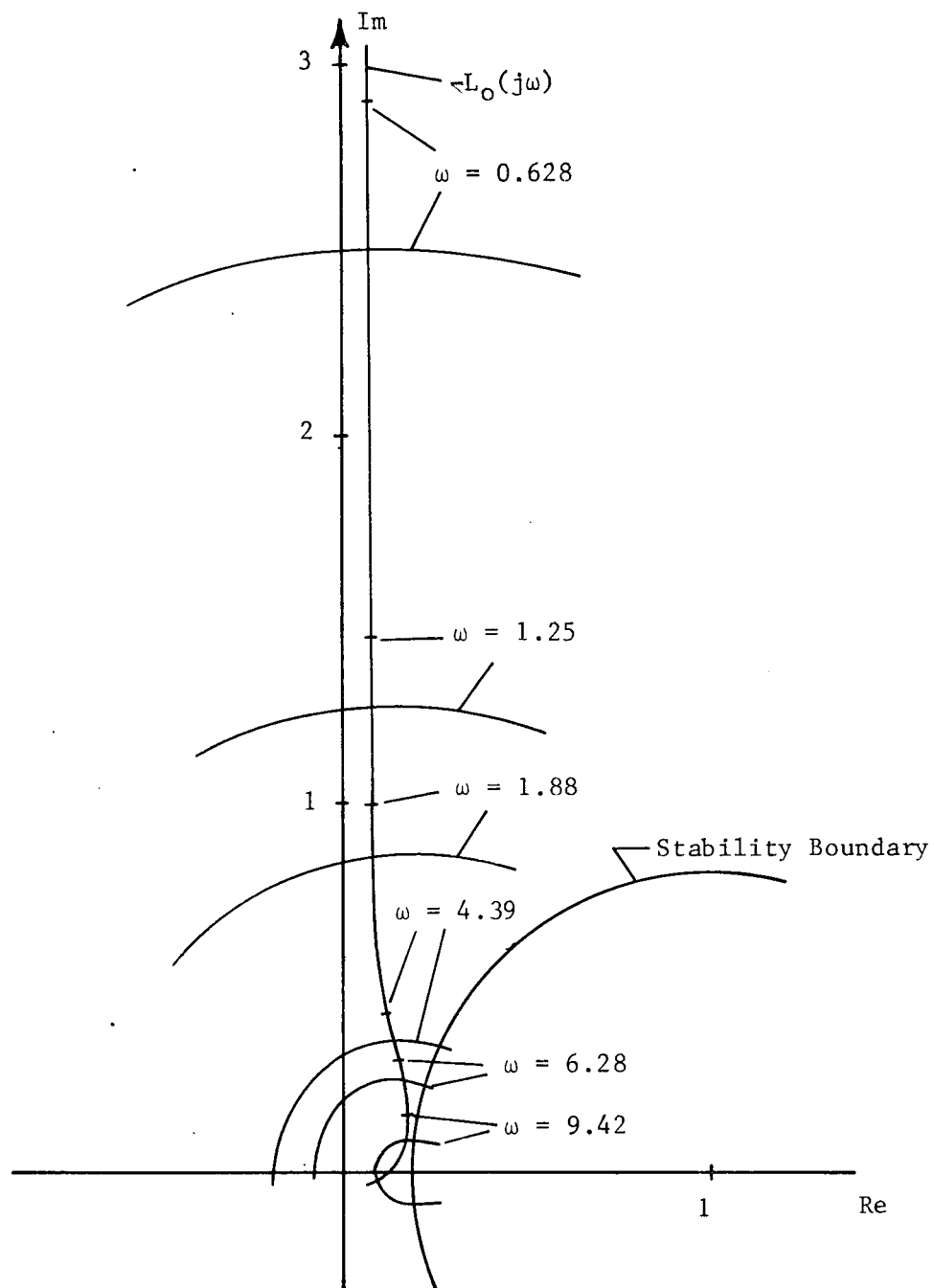


Figure 4.100  
 Polar Plot of  $-L_O$  for Fifth Design  
 With Boundaries of Acceptable Regions of  $-L_O$  for Fourth Design

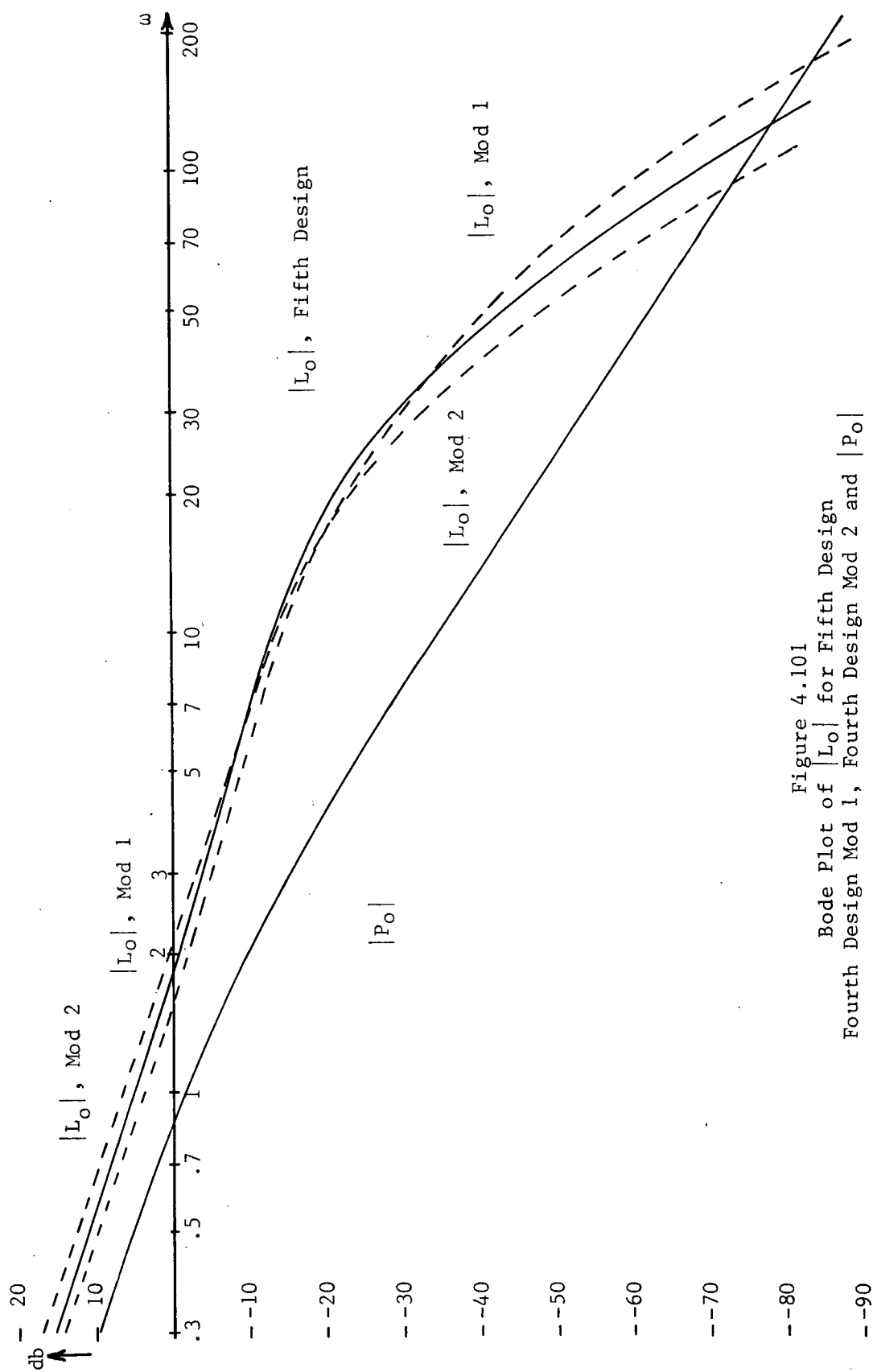


Figure 4.101  
Bode Plot of  $|L_O|$  for Fifth Design  
Fourth Design Mod 1, Fourth Design Mod 2 and  $|P_O|$



frequencies. The plot of the maximum error magnitudes for the fifth design is shown in Figure 4.102. It is seen from Figure 4.102 that the specifications are satisfied. The choice of  $L_0$  was fortunate because the value of  $|E|$  just meets the specifications in the regions of one and 5.5 radians which are the critical frequency regions. In the region between two to four radians  $|E|$  is much smaller than is required by the specification which is due to the difficulty in making  $|L_0|$  as large as required in the region of one and six radians, while at the same time small enough to just meet the specifications in the region between two and five radians.

The fifth design is very close to the best design possible. That is, the design satisfies the specification, but any significant decrease in the magnitude of  $|L_0|$  in any frequency range will either result in a violation of the specifications or an increase of the high frequency noise transmission. As has been mentioned, the critical frequency ranges are around one and 5.5 radians. If the high frequency poles are moved to lower frequencies in order to reduce the noise transmission, the specifications will be violated at both one and 5.5 radians. Decreasing  $|L_0|$  in the low frequency range will result in a specification violation in the region of one radian unless the high frequency poles are moved farther out in the frequency range, thus increasing the noise transmission. The fifth design is thus selected as the final design.

The expression for  $H(s)$  is given by

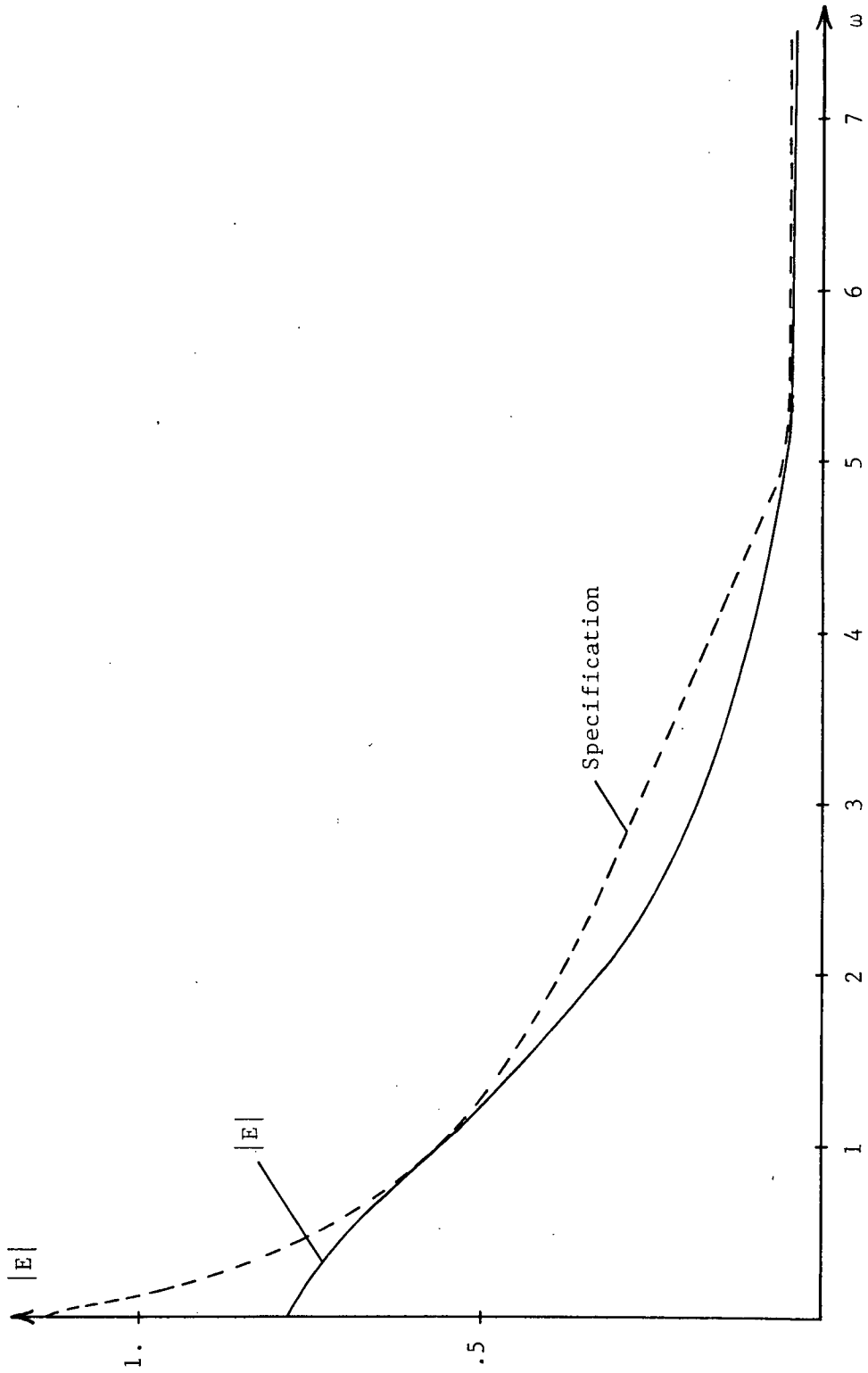


Figure 4.102  
Maximum  $|E|$  for Fifth Design

$$H(s) = 41.25 \frac{(s + 2)(s + 6)}{(s + 12.5)(s + 20) \left[ \frac{s}{30} + 1 \right] \left[ \frac{s}{48} + 1 \right] \left[ \frac{s}{70} + 1 \right] \left[ \frac{s}{80} + 1 \right]}$$

and the expression for  $G(s)$  is found from the relation

$$G(s) = \left[ 1 + L_O(s) \right] \frac{T_O(s)}{P_O(s)}$$

where

$$\frac{T_O(s)}{P_O(s)} = 2.2 \frac{s(s + 2)}{s^2 + 2.8s + 4} .$$

A sampling of step responses for the fifth design is shown in Figure 4.103 through Figure 4.108. The maximum overshoot was found to be 24% and the maximum rise time is six seconds. Observe in Figure 4.103 that the "dip" in the error around 0.5 seconds is still present but its magnitude has been reduced to the point that the specifications are not violated. Note also the high frequency variations present in the error shown in Figure 4.104 and Figure 4.105. These variations are not present in the third design, so are thus a result of the decrease in  $|L_O|$  in the high frequency region.

The regions of  $P_O/P_{eq}$  for the fifth design are shown in Figures 4.109 through Figure 4.114. The regions closely resemble those found for the third design which are shown in Figures 4.75 through Figure 4.80. However, the regions for the fifth design are somewhat larger than those for the third design, especially

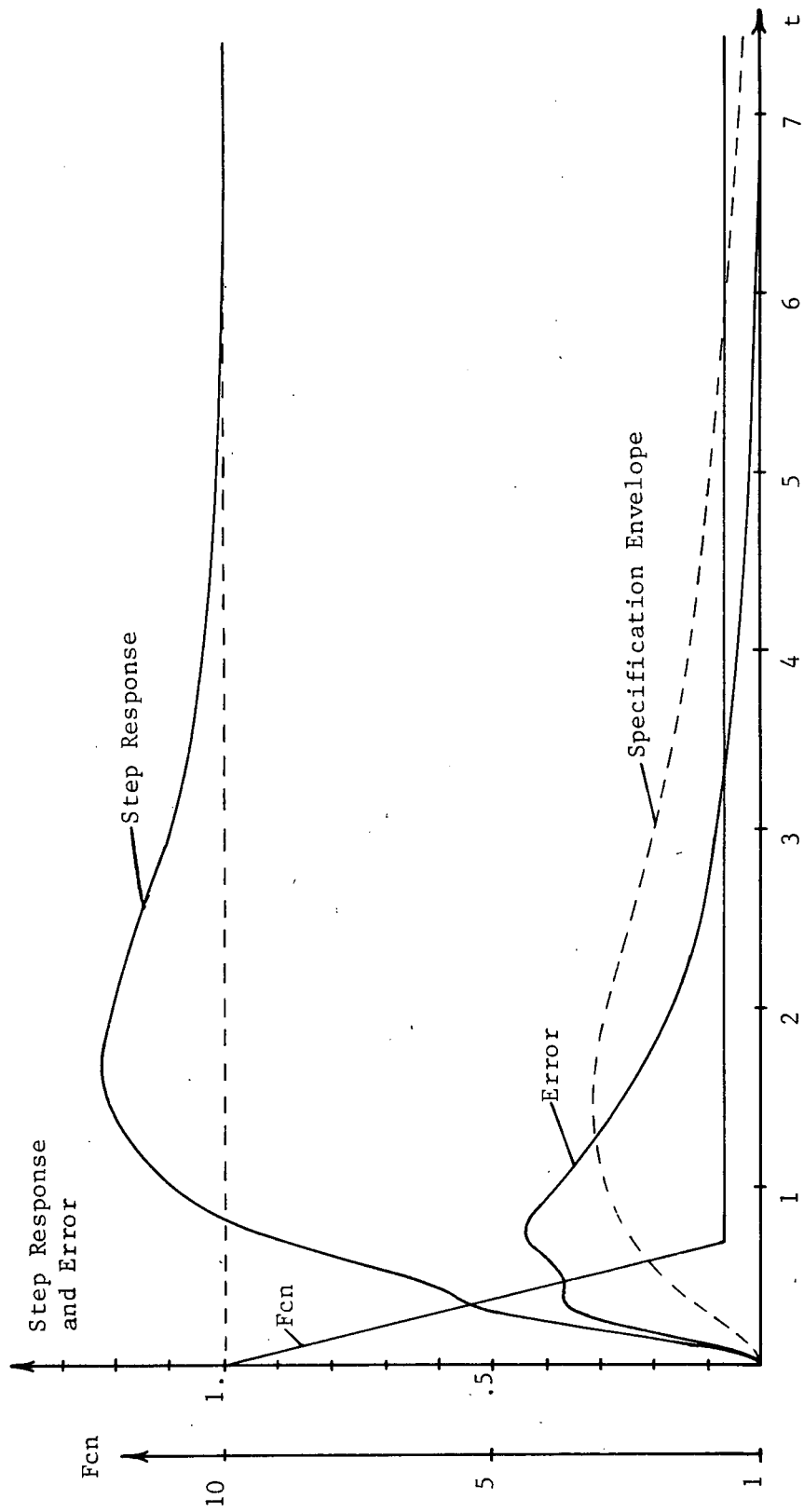


Figure 4.103  
Sample Step Response of Fifth Design

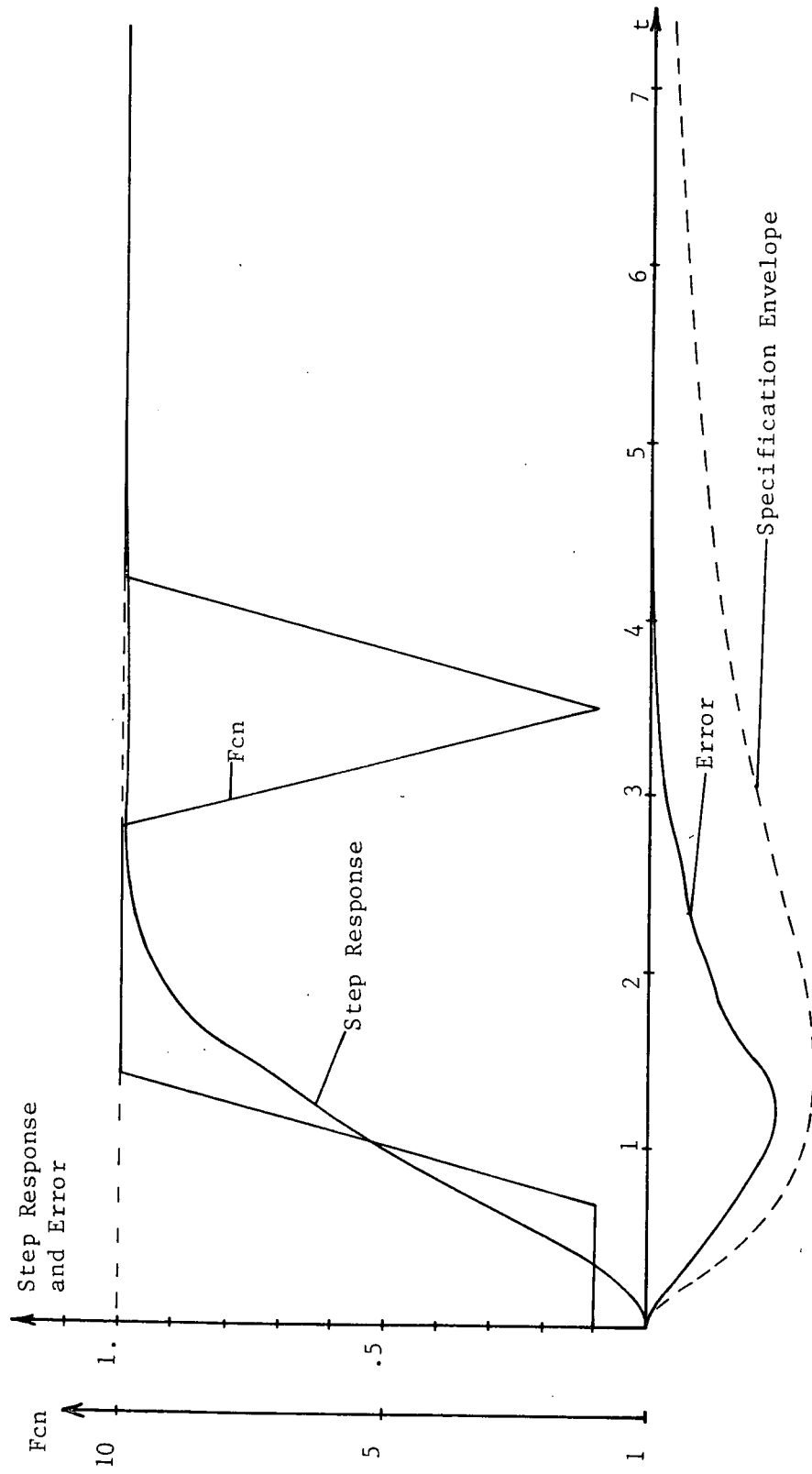


Figure 4.104  
Sample Step Response of Fifth Design

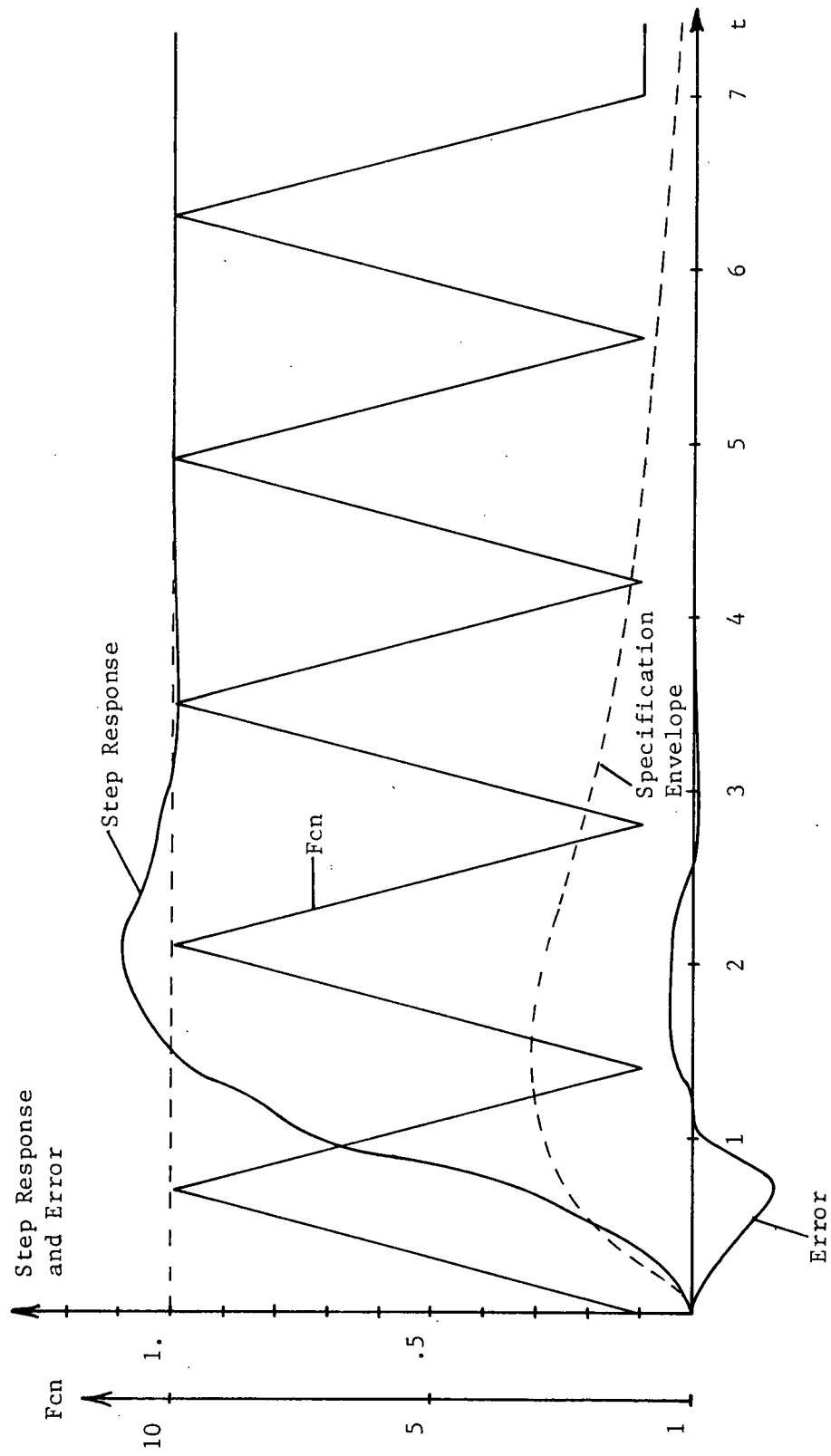


Figure 4.105  
Sample Step Response of Fifth Design

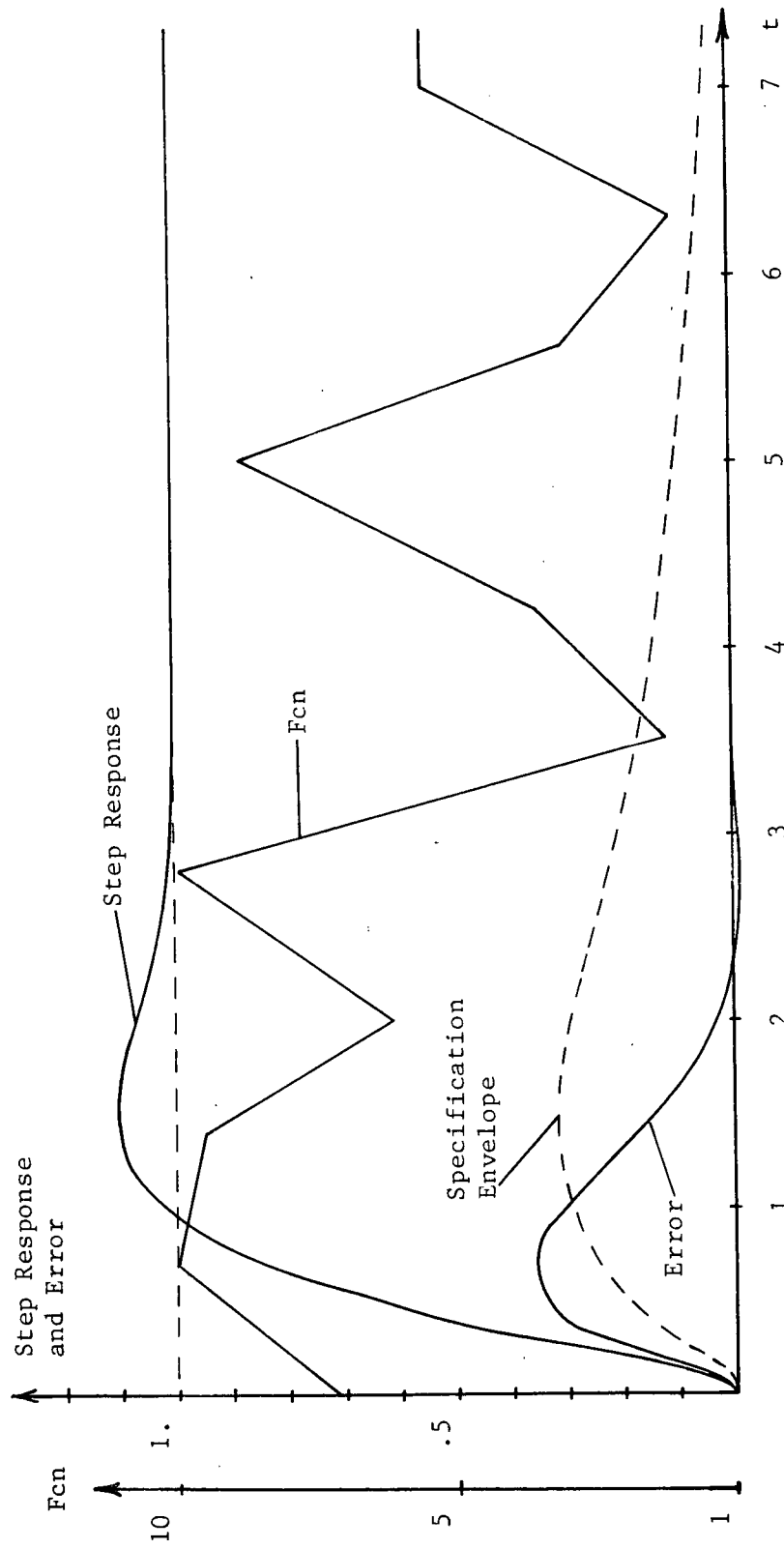


Figure 4.106  
Sample Step Response of Fifth Design

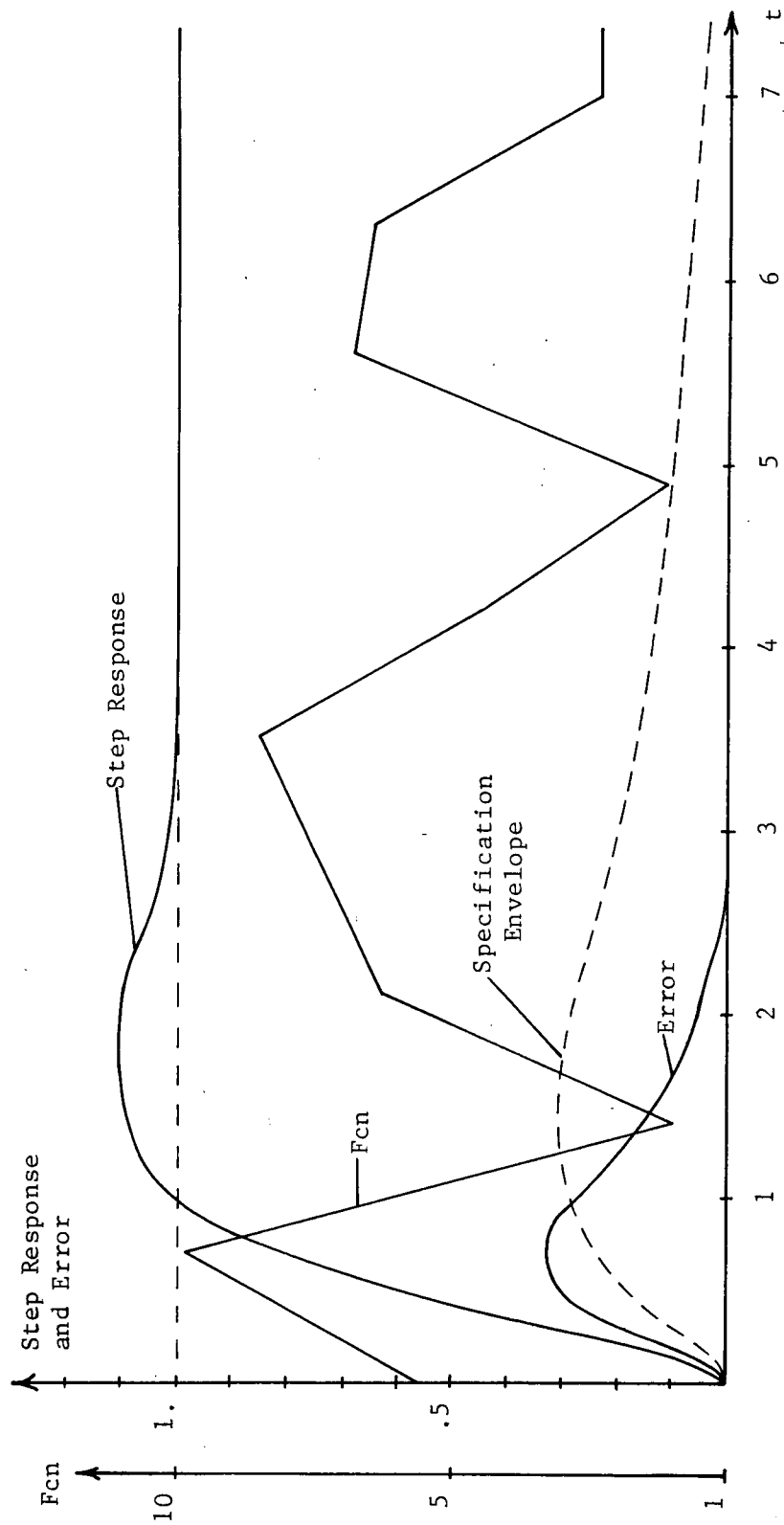


Figure 4.107  
Sample Step Response of Fifth Design



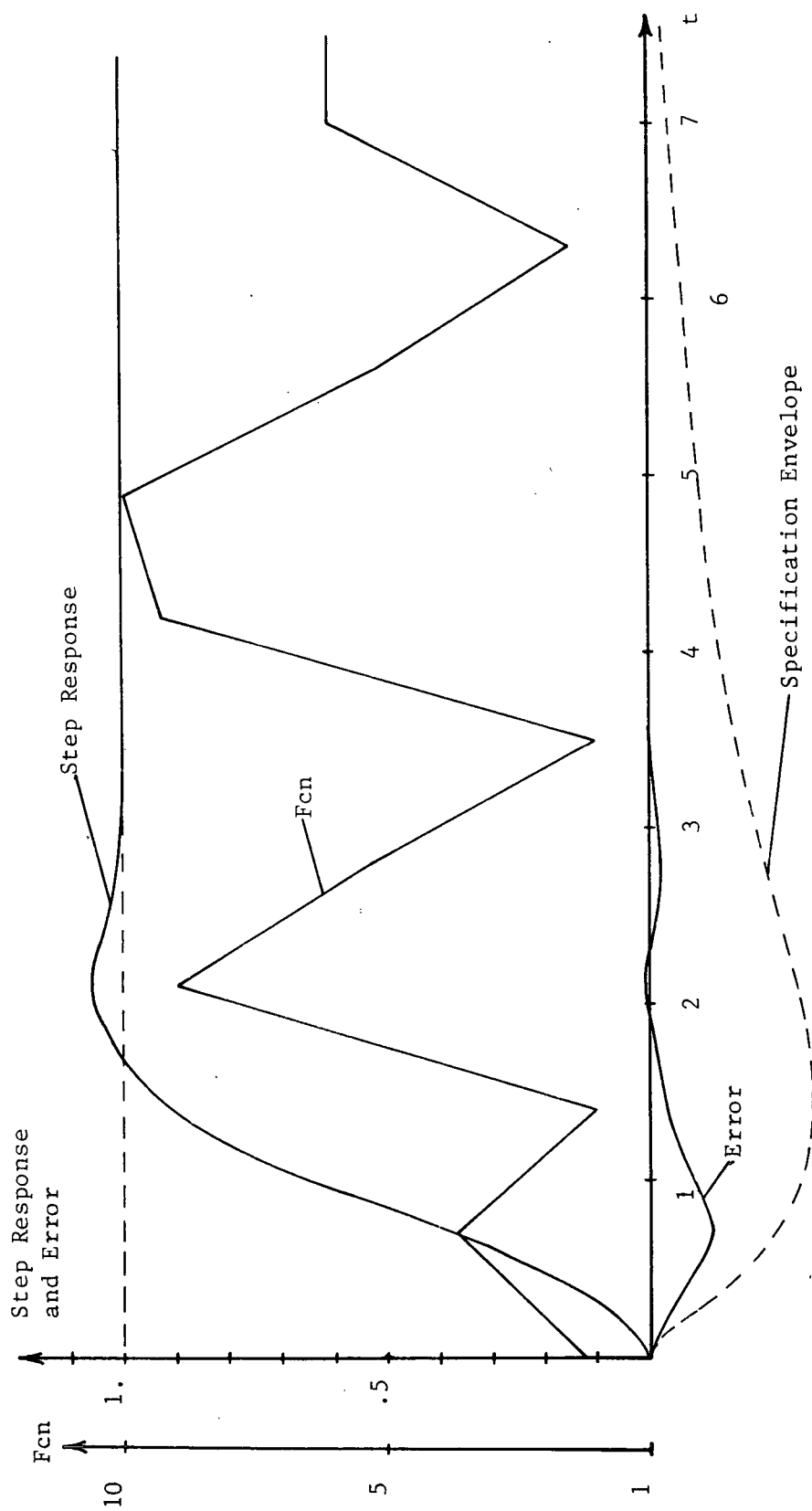


Figure 4.108  
Sample Step Response of Fifth Design

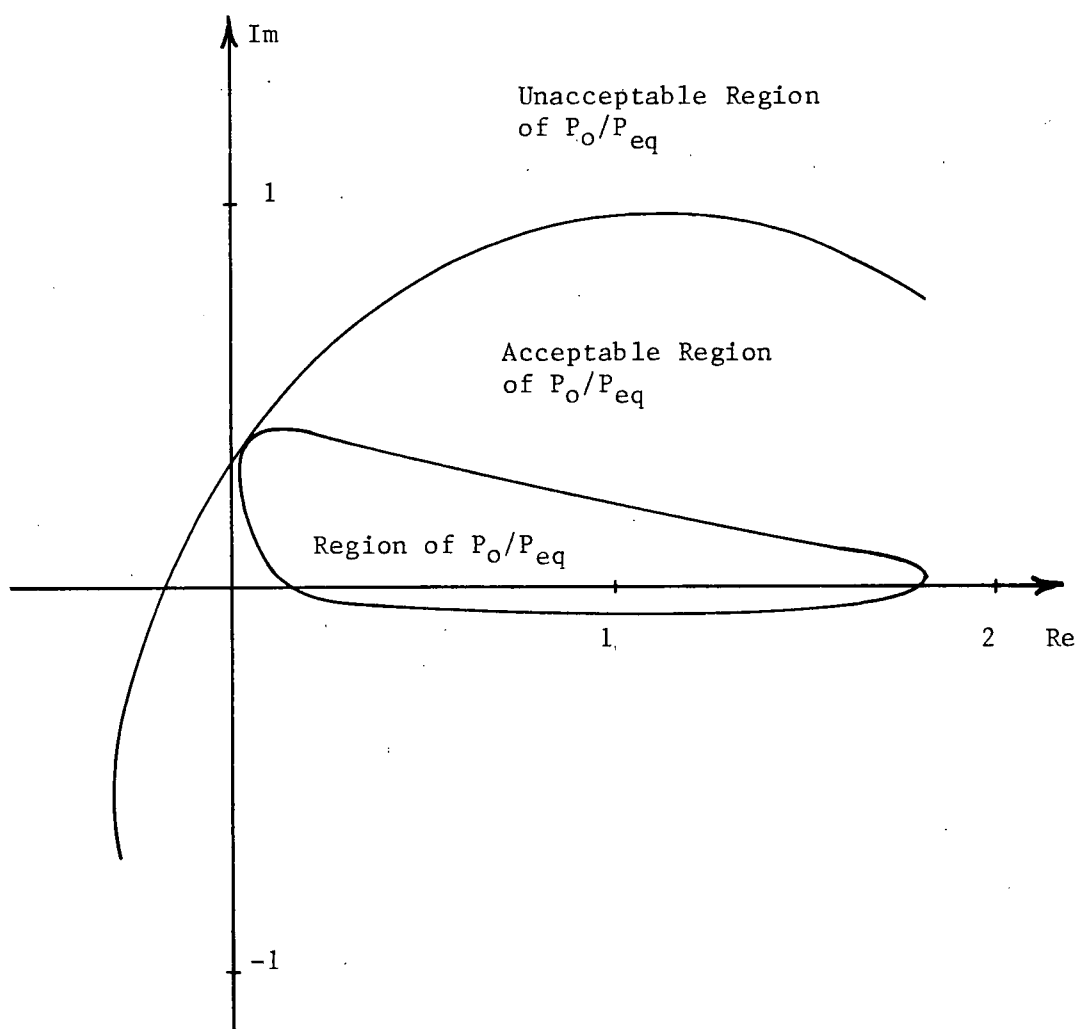


Figure 4.109  
Region of  $P_o/P_{eq}$ , Fifth Design,  $\omega = 0.628$

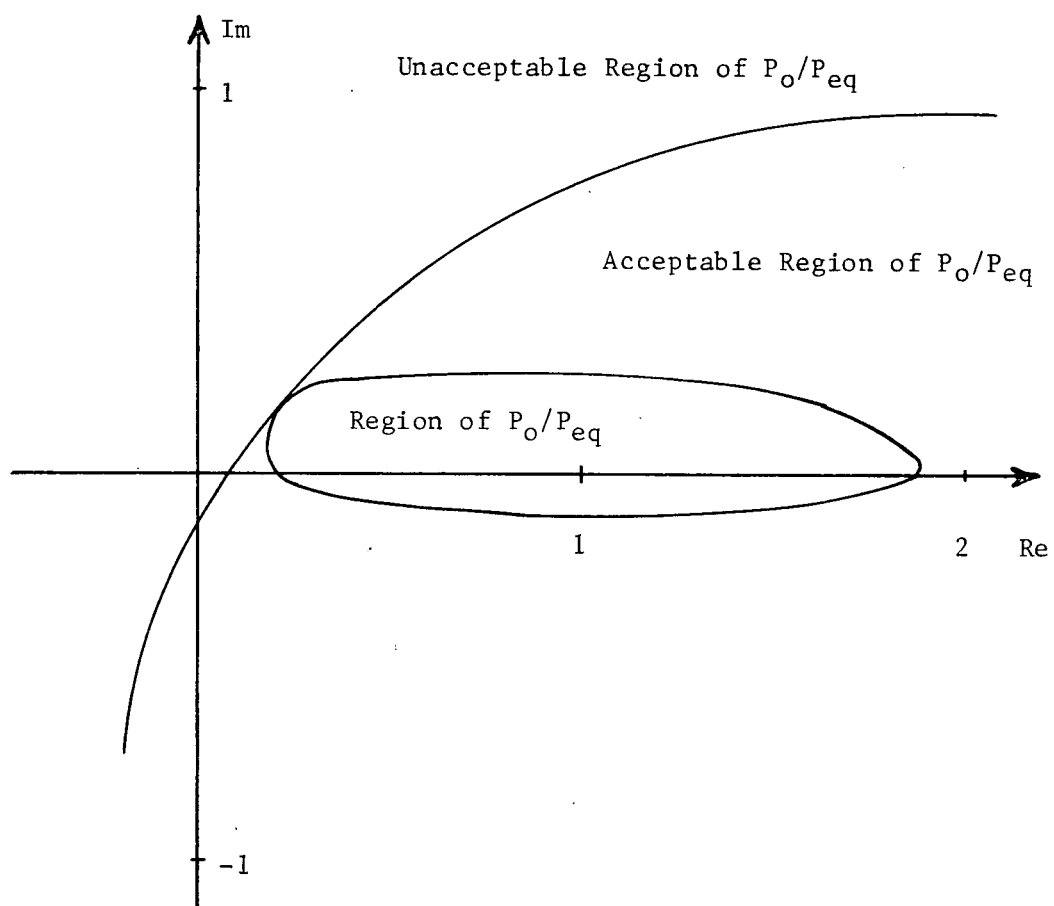


Figure 4.110  
 Region of  $P_O/P_{eq}$ , Fifth Design,  $\omega = 1.25$

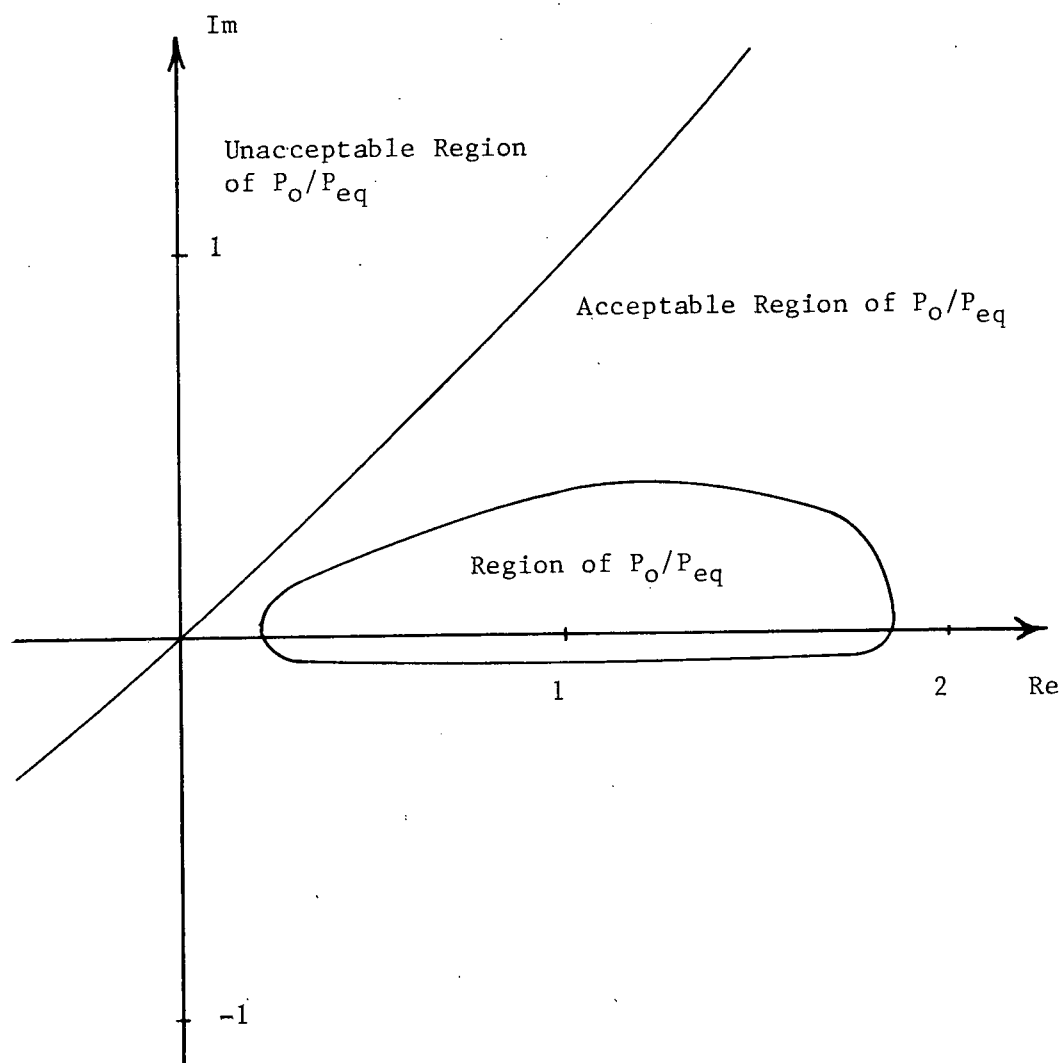


Figure 4.111  
 Region of  $P_O/P_{eq}$ , Fifth Design,  $\omega = 1.88$

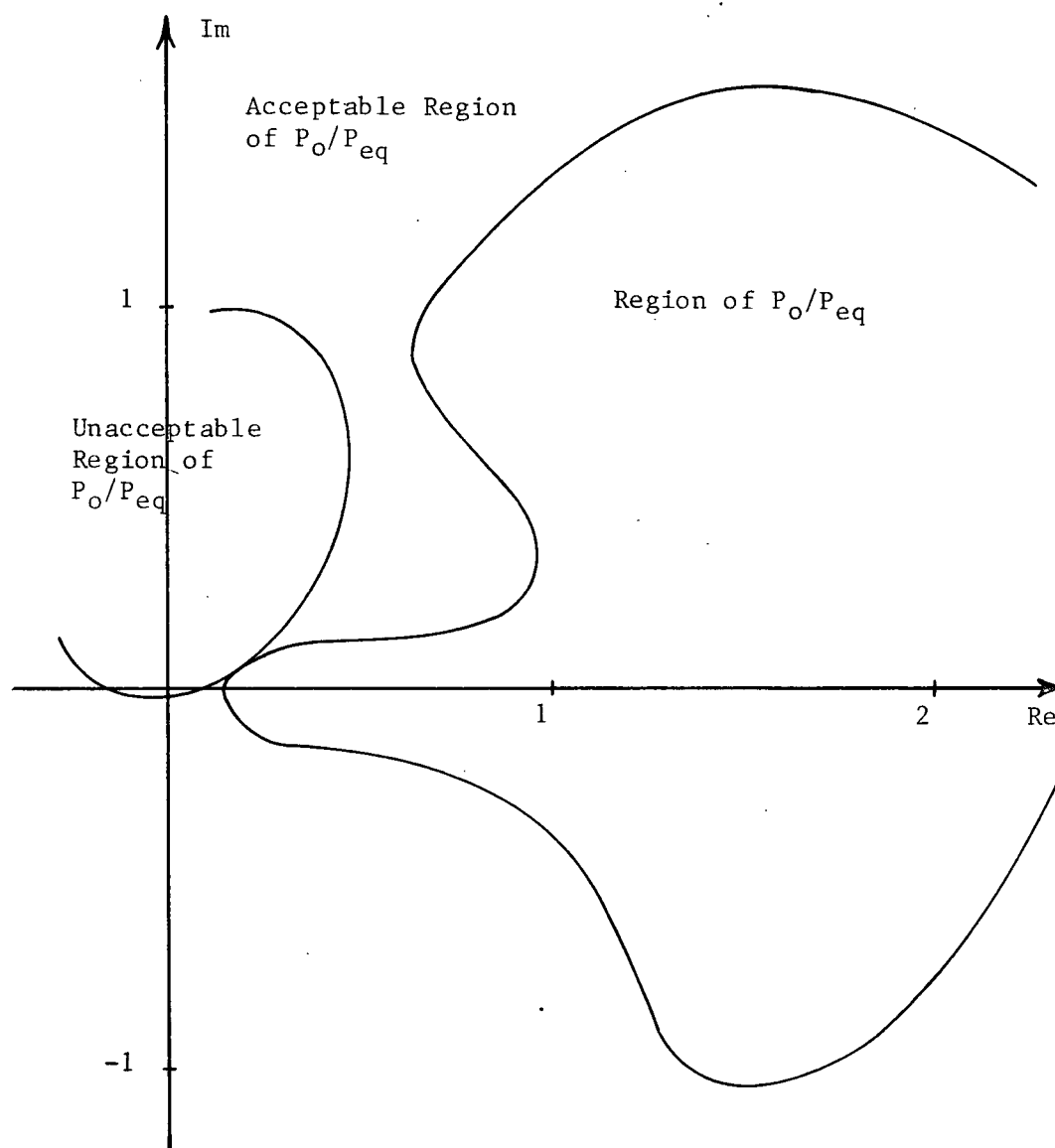


Figure 4.112  
Region of  $P_O/P_{eq}$ , Fifth Design,  $\omega = 4.39$

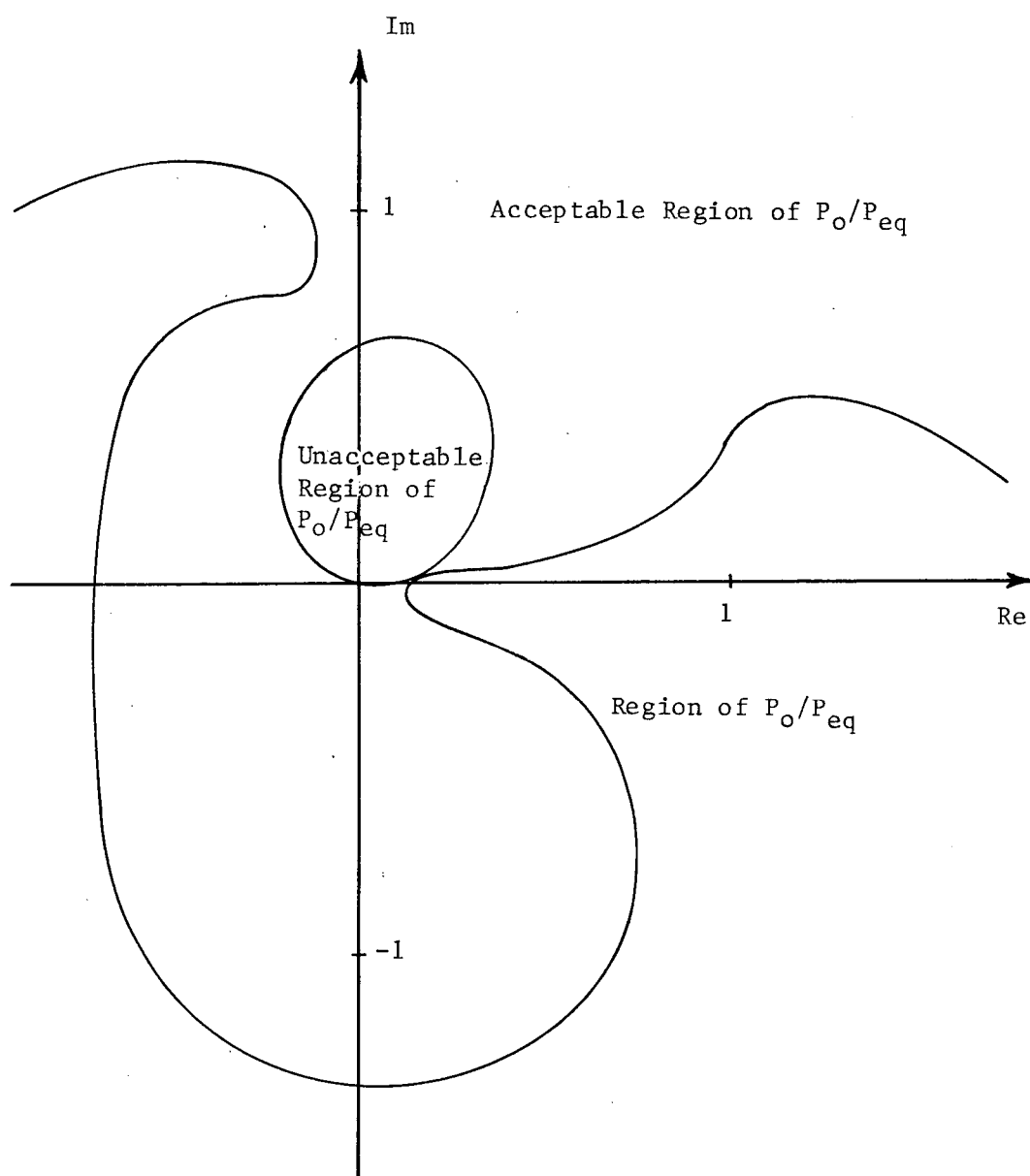


Figure 4.113  
Region of  $P_o/P_{eq}$ , Fifth Design,  $\omega = 6.28$

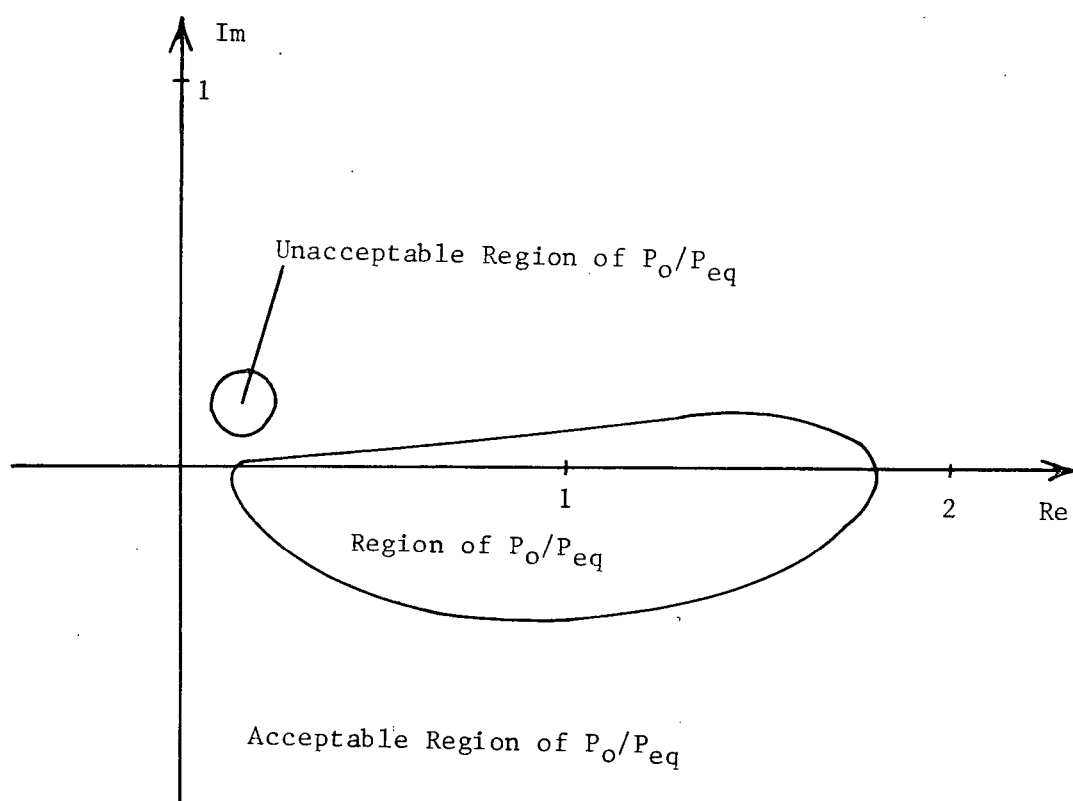


Figure 4.114  
Region of  $P_O/P_{eq}$ , Fifth Design,  $\omega = 9.42$

in the critical area around the origin. The addition of the high frequency poles in  $L_0$  has thus increased the size of the regions of  $P_0/P_{eq}$  but the basic shape is unchanged.

#### 4.9 Summary

A system having a time-varying gain which can range between values of one and ten has been designed to meet a set of frequency domain specifications. The design is close to optimal in the sense that noise transmission to the plant input is minimized. In the process of carrying out the design a good deal of insight about the design procedure and the system was obtained.

The first comment concerns the specifications. The frequency domain specifications which were chosen appear to have been reasonable since the resulting system has a well-behaved step response that would undoubtedly be considered satisfactory. However, the system error as a function of time does not fall within the specification envelope shown in Figure 4.7 which was used to arrive at the frequency domain specifications. This is, of course, due to the fact which was discussed earlier that error functions can satisfy the frequency domain specification and still fall outside the time domain error envelope. The time domain envelope is exceeded only because of a fast system rise time. Since a fast rise time is generally not considered an undesirable system property, it appears that the time domain envelope was not properly selected in the first place. It appears that the time domain envelope should have allowed the system error to deviate much more near the origin than was actually allowed. If it were



desired to have the slower rise time, it would be necessary to modify the frequency domain specifications. More study of the relationship between the time domain specifications and the frequency domain specifications would be necessary, however, to determine the specific changes required.

The approach of using the time-invariant design as a starting point appears quite satisfactory. In the example the time-invariant design indicated the shape of the regions of  $-L_0$  which changed very little during the design. The assumption that small changes in  $L_0$  cause only small changes in the regions of  $P_0/P_{eq}$  proved to be valid for the example. In fact, changes in  $L_0$  that were not so small caused only relatively small changes in the region of  $P_0/P_{eq}$  as was found in the fourth and fifth design when the high frequency poles were added. Although the assumption will have to be verified for other types of systems in order to obtain any generality, its verification in this example is very promising for the use of the regions of  $P_0/P_{eq}$ .

As was mentioned earlier, an additional advantage to using the time-invariant design as a starting point in the procedure is that it allows one to readily observe the additional magnitude of  $L_0$  needed to compensate for the time-variations. Figure 4.115 shows the Bode plot of  $|L_0|$  for the final design together with the plot of  $|L_0|$  for a time-invariant design which includes the high frequency poles. Also shown in Figure 4.115 is the plot of  $|P_0|$ . The magnitude of  $|L_0|$  for the time invariant design is substantially less in both the high frequency and low frequency regions than is

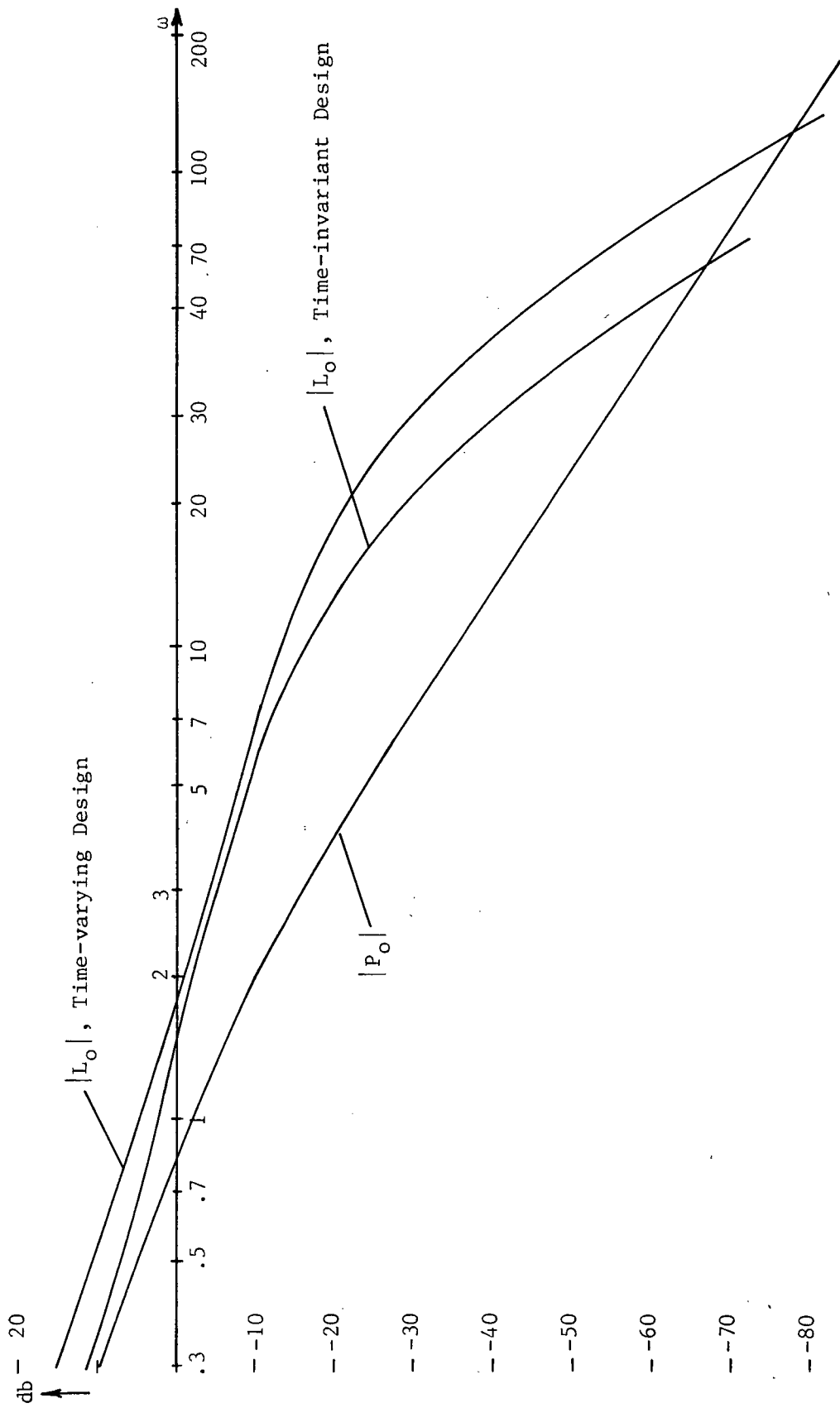


Figure 4-115  
Bode Plot of  $|L_O|$  for Time-varying and Time-invariant Designs

$|L_O|$  for the time-varying design. However, in the region between two and six radians the difference in  $|L_O|$  between the two designs is not large and in fact  $|L_O|$  for the time-varying design could probably be reduced somewhat. Thus the time-variations appear to have little effect on the system response in the range of two to six radians.

The example also pointed up a serious flaw in design procedure one. The flaw, which was found in the second design, is the fact that the acceptable regions of  $-L_O$  are assumed to be circles centered at point one. Such an assumption would undoubtedly lead to an overdesigned system with little indication as to just what to do to eliminate the overdesign. This is especially true in the high frequency region where an overdesign is the most undesirable. A problem is also present with procedure two in that it is difficult to determine precisely the size of the regions of  $P_O/P_{eq}$  which means that the precise size of the regions of acceptable  $-L_O$  is also difficult to determine. It was found that a combination of the strong points of the two procedures resulted in an improvement in the design procedures. The regions of  $P_O/P_{eq}$  of procedure two was used to determine the shape of the acceptable regions of  $-L_O$  while  $|E|$  of procedure one was used to determine how much the regions should be increased or decreased for the next design. This combination appears to result in a more powerful procedure than either design procedure one or two alone.

It was also found in the example that the addition of the high frequency poles in  $L_O$  had a large effect on the low frequency

error. Thus, it would probably be desirable to include the high frequency poles in  $L_0$  from the beginning of the design rather than designing  $L_0$  at low frequencies before adding the high frequency poles as was done in the example. There is, however, an advantage in designing at low frequencies first and then adding the high frequency poles. The advantage is that it is possible to examine the effect of changing only portions of  $L_0$ . If the poles are added early in the design, care must be taken in modifying  $L_0$  since a change in the high frequency part of  $L_0$  affects the low frequency error and vice versa. However, in the example, the low frequency portion of  $L_0$  did not affect the high frequency error as much as the high frequency portion affected the low frequency error.

It is also of interest to note the type of time-varying gain system for which a design is possible. If the time-invariant portion of the plant is minimum phase, that is, all poles and zeroes are in the left half plane, then it is possible to increase the magnitude of  $L_0$  indefinitely without violating the stability criterion (see Figure 4.100) so that the specifications will eventually be met. On the other hand, if the time-invariant portion of the plant is nonminimum phase, then it is not possible to increase the magnitude of  $L_0$  indefinitely without violating the stability criterion. Thus, for such systems it may not be possible to increase the magnitude of  $L_0$  sufficiently to satisfy the specifications. Therefore, if the time-invariant portion of the plant is minimum phase, a design is always possible; otherwise,

the possibility of a design depends upon the particular system and the specifications.

Even though a strict application of the design procedure itself may not lead directly to an optimal design, the procedure does provide a systematic approach to arriving at an acceptable design provided stability can be maintained. In the example the insight gained in applying the design procedures allowed the design to be carried to a point very close to the optimal. It is anticipated that this will generally be the case in applying these design procedures.

The example has demonstrated that suitable frequency domain specifications can be obtained and the design procedures can be successfully applied to systems with a time-varying gain.

## CHAPTER V

### CONCLUSIONS

A study of the time-varying system design problem which was outlined in Section 1.1 has been undertaken. After a review of the previous research in the field of time-varying systems it was decided to employ time-invariant compensation and to design for a desired transfer function for which procedures are well developed rather than attempt to design for an impulse response which would require a study in itself. An effort was first made to obtain an analytical solution of the system equations from which a design procedure could be developed. Unfortunately, the attempt was unsuccessful so that efforts were turned to the utilization of numerical solutions of the system equations which could be obtained from computer simulations.

It was possible to develop two design procedures which are based on the numerical solution of the system equation. The basic difference in the two procedures is that procedure one assumes the acceptable regions of the nominal loop gain  $L_0$  to be circular, while in procedure two the shape of the acceptable region is determined in the process of the design. Examples were presented which illustrated that it was possible to carry out the steps of the procedures using computer simulations.

The procedures as presented do not constitute a complete solution of the time-varying system design problem. One

difficulty which must be resolved is the determination of satisfactory frequency domain specifications. Although it is possible to arrive at specifications which intuitively appear reasonable, the exact relationship between time-domain and frequency domain specifications are unknown. A second difficulty is the determination of a general stability criterion for time-varying systems. Since necessary conditions for stability are known for systems having a time-varying gain, it is usually possible to design such systems so that stability is guaranteed. (It may not be possible to maintain stability if the time-invariant portion of the plant is non-minimum phase; otherwise, there will be no difficulty.) Nonetheless, in the design of a general system the procedures themselves do not assure stability; however, any future stability criterion which is specified in the frequency domain can readily be incorporated into the procedures.

A design example of a system having a time-varying gain was carried out in depth. Practical frequency domain specifications were developed and a design was obtained which is close to the optimal design. At each step the system step responses were examined and were compared to the desired step response. It was seen that the step responses behaved as one might expect and that the step responses of the final design were entirely satisfactory, thus showing that the frequency domain specifications were also satisfactory. This example demonstrated that it was possible to arrive at satisfactory frequency domain specifications and by

employing the insight gained in carrying out the procedures, a design could be obtained which was close to the optimal design. It was seen that in the example the assumption of circular acceptable regions of  $L_0$  which is made in design procedure one was highly inaccurate. In fact, it was found that a combination of procedures one and two gave better results than either of the two procedures individually. The combined method consists of determining the shape of the acceptable regions of  $L_0$  from procedure two, while the size of the acceptable regions are determined from procedure one. On the whole the example indicated that the design procedures could be satisfactorily carried out and would yield acceptable results.

In carrying out the design examples presented in this paper, simulations were successfully carried out on analog, digital, and hybrid computers. The advantage of the analog computer is its ability to solve the system equations quickly; however, it requires constant attention by the operator in order to perform the many runs required in searching for the maximum  $E$  and the region of  $P_0/P_{eq}$ . Operator action also increases the total run time considerably. The advantage of the digital computer is that it can perform the required runs automatically; however, it requires a good deal of time to complete the calculations. The hybrid computer is able to utilize the good features of both the analog and digital computers. The analog portion of the hybrid computer is utilized to obtain a quick solution to the system equations,



while the digital portion is used to control the analog and read out the results. The hybrid operations are much faster than either the digital or analog alone and would be the preferred method of performing the calculations if such a computer were available.

An additional area of research is the determination of worst case time variations. That is, the determination of those variations which result in the maximum value of  $E$  and which fall on the boundary of the region of  $P_O/P_{eq}$ . At present the method of determining the maximum value of  $E$  and the region of  $P_O/P_{eq}$  is to run a large number of possible variations as was done in the examples. This approach is successful when there is no more than one or two time-varying parameters. However, if the system has several time-varying parameters, the number of possible combinations of these variations soon become prohibitively large to try to determine the worst case variations simply by testing representative variations of all possible combinations. If the worst case variations were known, there would be no need for a search and the time required to carry out the design would be greatly reduced.

It can not be stated the design procedures are ready for general application to the design of time-varying systems because of the problem of system stability and the problem of determining the worst case variations for systems having a number of time-varying parameters. However, the procedures can be successfully employed on systems having a time-varying gain. In addition, the

concepts apply to any time-varying system; so, depending upon the case, it may be possible to apply the procedures to more general systems. Thus, even though the procedures are limited, they are a useful tool in the practical design of time-varying systems.

## BIBLIOGRAPHY

1. W. R. Bennett, "A General Review of Linear Varying Parameter and Non-Linear Circuit Analysis." Proc. IRE, vol. 38, pp. 259-263; March 1950.
2. D. Grahan, E. Brunelle, W. Johnson, H. Passmore, Engineering Analysis Methods for Linear Time-Varying Systems, Technical Documentary Report ASD-TDR-62-362, Wright-Patterson Airforce Base, pp. 41-55, 1963.
3. W. Kaplan, Operational Methods for Linear Systems, Addison-Wesley, Reading, Mass., pp. 89-93, 1962.
4. B. Friedland, "A Technique for the Analysis of Time-Varying Sampled Data System," Transaction AIEE, vol. 75, Pt. II, pp. 407-414, 1956.
5. J. B. Cruz, Jr., "Sensitivity Considerations for Time-Varying Sampled Data Feedback Systems", IRE Transactions on Automatic Control, vol. AC-6, no. 2, pp. 228-236, 1961.
6. J. B. Cruz, Jr., "A Generalization of the Impulse Train in the Time Domain", IRE Transactions on Circuit Theory, vol. CT-6, no. 4, pp. 393-394, 1959.
7. J. B. Cruz, Jr. and M. F. Van Valkenburg, "The Synthesis of Models for Time-Varying Linear Systems", Proceedings of the Symposium on Active Networks and Feedback Systems, Polytechnic Press, N.Y., pp. 527-544, 1960.
8. S. Darlington, "Nonstationary Smoothing and Prediction Using Network Theory Concepts". IRE Transactions on Circuit Theory, May (Supp.), pp. 1-11, 1959.
9. A. V. Solodov, Linear Automatic Control Systems with Varying Parameters, American Elsevier Publishing Co., Inc., N.Y., pp. 44-95, 1966.
10. A. R. Stubberud, Analysis and Synthesis of Linear Time-Variable Systems, University of California Press, Berkeley and Los Angeles, California, pp. 11-20, 1964.
11. F. R. Gerardi, "Application of Mellin and Hankel Transforms to Networks with Time-Varying Parameters", Trans IRE, CT-6, no. 2, pp. 197-208, 1959.
12. A. Erdelyi, (Ed.), Tables of Integral Transforms, Vols I and II, Bateman Manuscript Project, California Institute of Technology, McGraw-Hill Book Co., pp. 56-65, 1954.

13. J. A. Aseltine, "A Transform Method for Linear Time-Varying Systems", Journal of Applied Physics, vol. 25, pp. 761-764, 1954.
14. A. W. Naylor, "Generalized Frequency Response Concepts for Time-Varying, Discrete-Time Linear Systems", IEEE Transactions on Circuit Theory, vol. CT-10, pp. 428-440, Sept. 1963.
15. A. W. Naylor and F. M. Waltz, "On the Design of Time-Varying, Linear Closed Loop Systems with the Aid of a New Transform Technique", IEEE Transactions on Automatic Control, vol. AC-11, no. 4, pp. 716-723, Oct. 1966.
16. L. A. Zadeh, "A General Theory of Linear Signal Transmission Systems", Journal of the Franklin Institute, vol. 253, no. 4, pp. 293-312, April 1952.
17. L. A. Zadeh, "Frequency Analysis of Variable Networks", Proceedings of the IRE, vol. 38, pp. 291-299, 1950.
18. L. A. Zadeh, "Circuit Analysis of Linear Varying-Parameter Networks", Journal of Applied Physics, vol. 21, pp. 1171-1177, Nov 1950.
19. L. A. Zadeh, "General Input-Output Relations for Linear Networks", Proceedings of the IRE, vol. 40, pg. 103, 1952.
20. J. B. Cruz, Jr., "On the Synthesis of Time-Varying Linear Systems", Technical Note No 9, Contract No. AF49(638)-63, Project No. 47501, File No 2-1-23, Air Force Office of Scientific Research, pp. 14-23, 1959.
21. W. Kaplan, Operational Methods for Linear Systems, Addison-Wesley, Reading, Mass., pp. 515-526, 1962.
22. Gerlach, "A Time-Variable Transform and its Application to Spectral Analysis", Trans. IRE, CT-2, no 1, pp. 22-25, 1955.
23. M. C. Herrero, "Resonance Phenomena in Time-Varying Circuits", Trans. IRE, CT-2, no. 1, pp. 35-41, 1955.
24. K. S. Narendra, "Integral Transforms for a Class of Time-Varying Linear Systems", IRE Transactions on Automatic Control, vol. AC-6, no. 3, pp. 311-318, 1961.
25. L. Weiss, "On System Functions with the Separability Property", International Journal of Control, vol. 1, no. 5, pp. 487-496, 1965.
26. I. M. Horowitz, Synthesis of Feedback Systems, Academic Press, New York, pp. 1-2, 1963.

27. W. C. Schultz and V. C. Rideout, "Control System Performance Measures: Past, Present, and Future", IRE Transactions on Automatic Control, vol. AC-6, no. 1, pp. 22-35, 1961.
28. I. M. Horowitz, Synthesis of Feedback Systems, Academic Press, New York, pp. 188-194, 1963.
29. F. H. Raven, Automatic Control Engineering, McGraw-Hill, Inc., N.Y., pp. 62-629, 1968.
30. C. E. Bradford, M. W. DeMerit, "Relation Between Transient and Frequency Response", Handbook of Automation, Computation, and Control, John Wiley & Sons, Inc., N.Y., vol 1, pp 22-01 to 22-61, 1958.
31. H. D'Angelo, Linear Time-Varying Systems: Analysis and Synthesis, Allyn and Bacon, Inc., Boston, Mass., pp. 269-271, 1970.
32. R. C. Dorf, Time-Domain Analysis and Design of Control Systems, Addison-Wesley, Reading, Mass., pp. 134-157, 1965.
33. L. Zadeh and C. Desoer, Linear System Theory, McGraw-Hill, New York, pp. 1-56, 1963.
34. I. Sandberg, "A Frequency-Domain Condition for the Stability of Feedback Systems Containing a Single Time-Varying Non-Linear Element," Bell System Technical Journal, vol. 43, pp. 1601-1608, 1964.
35. Z. Rekasius and J. Rowland, "A Stability Criterion for Feedback Systems Containing a Single Time-Varying Element," IEEE Transactions on Automatic Control Theory, vol. AC-10, no. 3, pp. 352-354, 1965.
36. A Gersho, "Properties of Time-Varying Linear Systems", Research Report EE552, Cornell University, Ithaca, New York, pp. 1-14, 1962.
37. T. Kailath, "Sampling Models for Linear Time-Variant Filters", Technical Report 352, MIT Research Laboratory of Electronics, Cambridge, Mass., pp. 5-12, 1959.
38. H. D'Angelo, Linear Time-Varying Systems: Analysis and Synthesis, Allyn and Bacon, Inc., Boston, Mass., pp. 70-71, 1970.
39. V. Borskii, "On the Properties of the Impulsive Response Function of Systems with Variable Parameters", Automation and Remote Control, vol. 20, no. 7, pp. 822-830, 1959.

40. J. B. Cruz, Jr., "On the Realizability of Linear Differential Systems", IRE Transactions on Circuit Theory, pp. 347, 348, 1960.
41. J. J. D'Azzo and C. H. Houpis, Feedback Control System Analysis and Synthesis, McGraw-Hill Book Co., Inc., N.Y., pg. 113, 1960.
42. F. G. Tricomi, Integral Equations, Interscience Pub, Inc., New York, pp. 161-217, 1957.
43. D. Graham, E. Brunelle, W. Johnson, H. Passmore, Engineering Analysis Methods for Linear Time-Varying Systems, Technical Documentary Report ASD-TDR-62-362, Wright-Patterson Airforce Base, pg. 133, 1963.
44. D. E. Dick and H. J. Wertz, "Analog and Digital Computations of Fourier Series and Integrals", IEEE Transactions on Electronic Computers, vol. EC-16, no. 1, pp. 8-13, 1967.
45. I. M. Horowitz, Synthesis of Feedback Systems, Academic Press, New York, New York, pp. 267-270, 1963.
46. A. J. Rault, "Stability of Time-Varying Feedback Systems", Ph.D. Dissertation, University of California, Berkeley, pp. 99-118, 1966.
47. D. D. Siljak, Non-Linear Systems, John Wiley & Sons, Inc., New York, pp. 326-330, 1969.
48. R. W. Hamming, Numerical Methods for Scientists and Engineers, McGraw-Hill Book Co., Inc., New York, pp. 67-78, 1962.
49. A. Papoulis, The Fourier Transform and Its Applications, McGraw-Hill Book Co., Inc., New York, pp 7-52, 1962.
50. K. Knopp, Theory of Functions, Dover Publications, Inc., New York, pg. 61, 1945.
51. I. M. Horowitz, Synthesis of Feedback Systems, Academic Press, New York, pp. 441-452, 1963.
52. W. Kaplan, Operational Methods for Linear Systems, Addison-Wesley, Reading, Mass. pp. 436-442, 1962.

## APPENDIX A

In this appendix it will be shown that if the system remains stable, the magnitude of the error can be reduced to as small a value as desired by increasing the magnitude of the feedback compensation  $H(j\omega)$ .

Employing the abbreviated notation of Section 3.2, the design equation, Equation (3-9), is given by

$$P_o^{-1}E + HE = -\Delta P^{-1}(C_o + E) \quad (A-1)$$

The expressions for  $E$  and  $\Delta P^{-1}$  are

$$E = C - C_o$$

$$\Delta P^{-1} = P^{-1} - P_o^{-1}.$$

Substituting these expressions into Equation (A-1) it is possible to obtain

$$HC + P^{-1}C = HC_o + P_o^{-1}C_o \quad (A-2)$$

It is important to understand the meaning of Equation (A-2). A block diagram of the system is shown in Figure A.1.

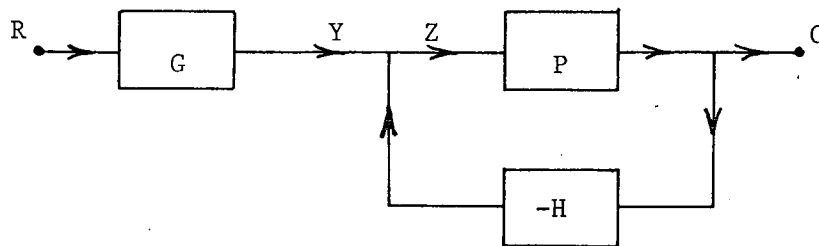


Figure A.1  
Block Diagram of System Under Study

The system equation is

$$GR = P^{-1}C + HC \quad (A-3)$$

Comparing the system equation with Equation (A-2) it is seen that one can write

$$HC + P^{-1}C = GR = HC_0 + P_0^{-1}C_0$$

That is, both the right hand side and the left hand side of Equation (A-2) are equal to the output of the prefilter. This, of course, is due to the fact that in Equation (A-2) the plant input is considered a constant and the difference in  $C$  and  $C_0$  is due only to the difference in the plant  $P$  and the nominal plant  $P_0$ . Thus, the output of the prefilter is always the same irregardless of the plant. The system output in turn is such that the relation  $P^{-1}C + HC$  is always equal to the prefilter output.

Another point that should be recalled is that in Equation (A-3) the plant output is not unique for a given plant input. This is due to the fact that the system output is made up of the system input and the complementary solution which is uniquely determined by the system's initial conditions.<sup>52</sup> In determining the step response of a stable system the initial conditions are set to zero so that the complementary solution is also zero and the output consists only of the forced solution which is uniquely determined by the system input. If the system is unstable, however, the complementary solution will grow without bound once



an initial condition is displaced slightly from zero by noise. Thus, if the system is unstable, the complementary solution will not be zero so that the system output will not be uniquely determined by the system input. Thus, in Equation (A-2), if the system is stable,  $C$  is uniquely determined by  $C_0$  and vice versa since the initial conditions are set equal to zero in the determination of the system step response. If the system is unstable, however, this uniqueness does not hold.

In describing the system it is convenient to borrow notation from classical linear time-invariant system analysis. Let the system type number of a time-varying system be the same as the type number if the plant parameters were time-invariant.<sup>41</sup> That is, if the plant parameters were time-invariant, then the plant of a type 0 system has no poles at the origin, while the plant of a type 1 system has a pole of order one at the origin, the plant of a type 2 system has a pole of order two at the origin, and so forth.

Consider next the relationship between the nominal plant and the desired step response. The desired step response  $C_0$  must be chosen such that it can be delivered by the nominal plant  $P_0$  as a result of a reasonable plant input. That is, it must not be necessary that the plant input contain impulse functions or derivatives of impulse functions in order for the nominal plant to deliver the desired step response when the plant is the nominal plant. This will only be true if the input to the plant is

physically possible. Thus, if the system is stable, the input to the nominal plant  $P_o$  must be bounded. In addition, if the system is type 0,  $e(t)$  will settle to a constant and if the system is type 1 or higher,  $e(t)$  will settle to zero. Therefore, for type 0 systems the Fourier transform of the plant input will only have a pole at frequency zero and no other poles, (i.e., all the poles of the Laplace transform of  $z(t)$  will be in the left half plane except for one pole at the origin). For type 1 systems or higher the Fourier transform of the plant input will have no poles (i.e., all poles of the Laplace transform of  $z(t)$  will lie in the left half plane). The Fourier transform of the input to the nominal plant is given by

$$Z = P_o^{-1}C_o$$

which is independent of the feedback  $H$ ; thus, the magnitude of  $P_o^{-1}C$  is independent of  $H$  and is bounded for all  $\omega$  except in type 0 systems where  $P_o^{-1}C_o$  has a pole at  $\omega = 0$ .

The desired objective is to show that the magnitude of the error goes to zero as the magnitude of  $H$  goes to infinity provided the system remains stable. Since the system is assumed stable and for step responses the system initial conditions are zero, Equation (A-2) uniquely describes  $C$  in terms of  $C_o$  and vice versa. Equation (A-2) can be written in the form

$$C - C_o = \frac{1}{H} \left[ P_o^{-1}C_o - P^{-1}C \right].$$

Returning to the full notation, one obtains

$$E(j\omega) = C(j\omega) - C_o(j\omega) =$$

$$\frac{C_o(j\omega)P_o^{-1}(j\omega)}{H(j\omega)} - \int_{-\infty}^{\infty} P^{-1}(j\omega, j\gamma) \frac{C(j\gamma)}{H(j\omega)} d\gamma. \quad (A-4)$$

Note that the nominal plant is time-invariant and can thus be represented by its transfer function which is denoted  $P_o^{-1}(j\omega)$ . From the previous discussion it is seen that the first term on the right hand side of Equation (A-4) goes to zero as  $|H|$  goes to infinity except for type 0 systems at  $\omega = 0$ . This is because  $P_o^{-1}C_o$  is independent of  $H$  and is bounded except for the one case.

It is not so obvious, however, that the integral term goes to zero as  $|H|$  goes to infinity since the system output  $C$  is dependent upon  $H$ . It will be shown by contradiction that the integral term does in fact go to zero as the magnitude of  $H$  increases without bound. Suppose that the magnitude of the integral term does not go to zero as  $|H|$  goes to infinity. That is

$$\lim_{|H| \rightarrow \infty} \int_{-\infty}^{\infty} P^{-1}(j\omega, j\gamma) \frac{C(j\omega)}{H(j\omega)} d\gamma > K. \quad (A-5)$$

Observe that  $H(j\omega)$  is not a function of the variable of integration and thus just represents a complex number that grows in magnitude with the limiting process. Interchanging the order of the limiting process and the integration procedure and noting that  $P^{-1}(j\omega, j\gamma)$  is independent of the limiting process since it is independent of  $H$ , one can write

$$\left| \int_{-\infty}^{\infty} P^{-1}(j\omega, j\gamma) \lim_{|H| \rightarrow \infty} \frac{C(j\gamma)}{H(j\omega)} d\gamma \right| > K. \quad (A-6)$$

In this form it is evident that the magnitude of  $C$  must increase at least as fast as the magnitude of  $H$ , for otherwise, the magnitude of  $C/H$  would tend to zero and the magnitude of the integral would also tend to zero. Thus,  $C$  must have the property

$$\lim_{|H| \rightarrow \infty} |C| \rightarrow A|H|^b, \quad b \geq 1, \quad A > 0.$$

Observe, therefore, that

$$\lim_{|H| \rightarrow \infty} |C - C_0| \rightarrow A|H|^b.$$

Thus, from Equation (A-4), one now obtains

$$\lim_{|H| \rightarrow \infty} |C - C_0| |H| = \left| \int_{-\infty}^{\infty} P^{-1}(j\omega, j\gamma) \lim_{|H| \rightarrow \infty} C(j\gamma) d\gamma \right|$$

or

$$\lim_{|H| \rightarrow \infty} A|H|^b |H| \leq \int_{-\infty}^{\infty} |P^{-1}(j\omega, j\gamma)| \lim_{|H| \rightarrow \infty} A|H|^b d\gamma.$$

Dividing by  $|H|^{b+1}$ , the expression becomes

$$A \leq \int_{-\infty}^{\infty} |P^{-1}(j\omega, j\gamma)| \lim_{|H| \rightarrow \infty} \frac{A}{|H|} d\gamma.$$

Since the term  $A/|H|$  goes to zero as the magnitude of  $H$  goes to infinity, the integral is zero or

$$A \leq 0$$

which is a contradiction. The original supposition that the integral term of Equation (A-4) does not go to zero is thus false, and it can only be concluded that the integral term does indeed go to zero as the magnitude of  $H$  goes to infinity.

Since both terms on the right hand side of Equation (A-4) go to zero as the magnitude of  $H$  increases, the magnitude of the error must also go to zero.

In summary, it has been shown that as the magnitude of the feedback compensation  $H$  is increased without bound, the magnitude of the error tends to zero provided system stability can be maintained.

APPENDIX B  
DERIVATION OF  $I_o(j\gamma)$

In this appendix the expression for  $I_o(j\gamma)$  of design example two is derived. The expression for  $I_o(j\gamma)$  is given by

$$I_o(j\gamma) = \int_{-\infty}^{\infty} P^{-1}(j\gamma, j\omega) C_o(j\omega) d\omega - \int_{-\infty}^{\infty} P_o^{-1}(j\gamma, j\omega) d\omega$$

which is equivalent to the Fourier transform of the plant input when the plant output is equal to  $c_o(t)$  minus the Fourier transform of the nominal plant input when the output is equal to  $c_o(t)$ . Referring to design example two it is seen that if the plant output is  $c_o(t)$  then the plant input is given by

$$y(t) = g(t)\ddot{c}_o(t) + f(t)\dot{c}_o(t),$$

and if the input to the nominal plant is  $c_o(t)$  its output is

$$y(t) = 0.505\ddot{c}_o(t) + 0.175\dot{c}_o(t).$$

Thus the expression for  $I_o(j\gamma)$  can be written

$$I_o(j\gamma) = \int_{-\infty}^{\infty} \left\{ (g(t) - 0.505)\ddot{c}_o(t) + (f(t) - 0.175)\dot{c}_o(t) \right\} e^{-j\gamma t} dt. \quad (B-1)$$

Substituting the expressions for  $g(t)$ ,  $f(t)$  and  $c_o(t)$  from design example two into this equation one obtains

$$\begin{aligned} I_o(j\gamma) = \int_{-\infty}^{\infty} \left\{ \left[ G_1 - 0.505 + G_2(1 - e^{-b(t-\tau_2)})u(t-\tau_2) \right] \right. \\ \left[ 4e^{-1.4t}\cos(1.414t) - 3.96e^{-1.4t}\sin(1.414t) \right] u(t) + \\ \left[ F_1 - 0.175 + F_2(1 - e^{-a(t-\tau_1)})u(t-\tau_1) \right] \\ \left. \left[ 2.83e^{-1.4t}\sin(1.4.4t)u(t) \right] \right\} e^{-j\gamma t} dt. \end{aligned}$$

Note that the evaluation of this integral depends upon the values of  $\tau_1$  and  $\tau_2$ . Let

$$G_3 = G_1 - 0.505$$

and

$$F_3 = F_1 - 0.175 .$$

In order to simplify the expression the following functions are defined:

$$A_1(j\gamma) = \int_0^{\infty} G_3 \left[ 4e^{-1.4t} \cos(1.414t) - 3.96e^{-1.4t} \sin(1.414t) \right] e^{-j\gamma t} dt$$

$$A_2(j\gamma) = \int_0^{\infty} G_2 (1 - e^{-b(t-\tau_2)}) \left[ 4e^{-1.4t} \cos(1.414t) - 3.96e^{-1.4t} \sin(1.414t) \right] e^{-j\gamma t} dt$$

$$A_3(j\gamma) = \int_{\tau_2}^{\infty} G_2 (1 - e^{-b(t-\tau_2)}) \left[ 4e^{-1.4t} \cos(1.414t) - 3.96e^{-1.4t} \sin(1.414t) \right] e^{-j\gamma t} dt$$

$$B_1(j\gamma) = \int_0^{\infty} F_3 2.83e^{-1.4t} \sin(1.414t) e^{-j\gamma t} dt$$

$$B_2(j\gamma) = \int_0^{\infty} F_2 (1 - e^{-a(t-\tau_1)}) 2.83e^{-1.4t} \sin(1.414t) e^{-j\gamma t} dt$$

$$B_3(j\gamma) = \int_{\tau_1}^{\infty} F_2 (1 - e^{-a(t-\tau_1)}) 2.83e^{-1.4t} \sin(1.414t) e^{-j\gamma t} dt$$

Evaluating these integrals one obtains:

$$A_1(j\gamma) = G_3 \frac{4j\gamma}{(j\gamma + 1.4)^2 + 2}$$

$$A_2(j\gamma) = G_2 \left\{ \frac{4j\gamma}{(j\gamma + 1.4)^2 + 2} - \frac{4 e^{b\tau_2} (j\gamma + b)}{(j\gamma + 1.4 + b)^2 + 2} \right\}$$

$$A_3(j\gamma) = G_2 e^{-(j\gamma+1.4)\tau_2} \left\{ \frac{4j\gamma \cos(1.414\tau_2) - 3.96(j\gamma+2.8)\sin(1.414\tau_2)}{(j\gamma + 1.4)^2 + 2} - \frac{4(j\gamma+b)\cos(1.414\tau_2) - 3.96(j\gamma+2.8+b)\sin(1.414\tau_2)}{(j\gamma + 1.4 + b)^2 + 2} \right\}$$

$$B_1(j\gamma) = F_3 \frac{4}{(j\gamma + 1.4)^2 + 2}$$

$$B_2(j\gamma) = F_2 \left\{ \frac{4}{(j\gamma + 1.4)^2 + 2} - \frac{4 e^{a\tau_1}}{(j\gamma + 1.4 + a)^2 + 2} \right\}$$

$$B_3(j\gamma) = F_2 e^{-(j\gamma+1.4)\tau_1} \left\{ \frac{4\cos(1.414\tau_1)+2.8(j\gamma+1.4)\sin(1.4\tau_1)}{(j\gamma+1.4)^2+2} - \frac{4\cos(1.414\tau_1)+2.8(j\gamma+1.4+a)\sin(1.414\tau_1)}{(j\gamma+1.4+a)^2+2} \right\}$$

$I_o(j\gamma)$  is thus given by the following expressions.

For  $\tau_1 \leq 0$  ,  $\tau_2 \leq 0$

$$I_o(j\gamma) = A_1(j\gamma) + A_2(j\gamma) + B_1(j\gamma) + B_2(j\gamma)$$

For  $\tau_1 \leq 0$  ,  $\tau_2 \geq 0$

$$I_o(j\gamma) = A_1(j\gamma) + A_2(j\gamma) + B_1(j\gamma) + B_3(j\gamma)$$

For  $\tau_1 \geq 0$  ,  $\tau_2 \leq 0$

$$I_o(j\gamma) = A_1(j\gamma) + A_3(j\gamma) + B_1(j\gamma) + B_2(j\gamma)$$

For  $\tau_1 \geq 0$  ,  $\tau_2 \geq 0$

$$I_o(j\gamma) = A_1(j\gamma) + A_3(j\gamma) + B_1(j\gamma) + B_3(j\gamma)$$



APPENDIX C  
DERIVATION OF  $P_o(j\omega)/P_{eq}(j\omega)$

In this appendix the expression for  $P_o(j\omega)/P_{eq}(j\omega)$  of design example three is determined. Referring to Equation (3-55)

$P_o(j\omega)/P_{eq}(j\omega)$  is seen to be given by

$$\frac{P_o(j\omega)}{P_{eq}(j\omega)} = \frac{P_o(j\omega)}{C_o(j\omega)} \int_{-\infty}^{\infty} P^{-1}(j\omega, j\gamma) C_o(j\gamma) d\gamma .$$

The transfer function of the nominal plant is given by

$$P_o(j\omega) = \frac{1}{0.505(j\omega)^2 + 0.175j\omega}$$

and  $C_o(j\omega)$  is given by

$$C_o(j\omega) = \frac{4}{j\omega [(j\omega)^2 + 2.8j\omega + 4]} .$$

Let

$$Y(j\omega) = \int_{-\infty}^{\infty} P^{-1}(j\omega, j\gamma) C_o(j\gamma) d\gamma .$$

This integral is the Fourier transform of the plant input when the plant output is  $c_o(t)$ . Thus the integral can be expressed as

$$Y(j\omega) = \int_{-\infty}^{\infty} \left\{ g(t) \dot{c}_o(t) + f(t) \dot{c}_o(t) \right\} e^{-j\omega t} dt . \quad (C-1)$$

Comparing Equation C-1 with Equation B-1 of Appendix B it is seen that the two are the same with the exception of two constant terms in Equation B-1. Thus the development given in Appendix B applies directly to obtaining  $Y(j\omega)$  with the exception that  $G_3$  is set equal to  $G_1$  and  $F_3$  is set equal to  $F_1$ . That is

$$Y_o(j\omega) = I_o(j\omega)$$

where

$$G_3 = G_1$$

and

$$F_3 = F_1 .$$

The expressions for  $P_o(j\omega)/P_{eq}(j\omega)$  are

For  $\tau_1 \leq 0$  ,  $\tau_2 \leq 0$

$$\frac{P_o(j\omega)}{P_{eq}(j\omega)} = \frac{P_o(j\omega)}{C_o(j\omega)} \left[ A_1(j\omega) + A_2(j\omega) + B_1(j\omega) + B_2(j\omega) \right]$$

For  $\tau_1 \leq 0$  ,  $\tau_2 \geq 0$

$$\frac{P_o(j\omega)}{P_{eq}(j\omega)} = \frac{P_o(j\omega)}{C_o(j\omega)} \left[ A_1(j\omega) + A_2(j\omega) + B_1(j\omega) + B_3(j\omega) \right]$$

For  $\tau_1 \geq 0$  ,  $\tau_2 \leq 0$

$$\frac{P_o(j\omega)}{P_{eq}(j\omega)} = \frac{P_o(j\omega)}{C_o(j\omega)} \left[ A_1(j\omega) + A_3(j\omega) + B_1(j\omega) + B_2(j\omega) \right]$$

For  $\tau_1 \geq 0$  ,  $\tau_2 \geq 0$

$$\frac{P_o(j\omega)}{P_{eq}(j\omega)} = \frac{P_o(j\omega)}{C_o(j\omega)} \left[ A_1(j\omega) + A_3(j\omega) + B_1(j\omega) + B_3(j\omega) \right]$$

where the functions  $A_1(j\omega)$ ,  $A_2(j\omega)$ ,  $A_3(j\omega)$ ,  $B_1(j\omega)$ ,  $B_2(j\omega)$ , and  $B_3(j\omega)$  are given in Appendix B with  $G_1$  equal to  $G_3$  and  $F_1$  equal to  $F_3$ .

## APPENDIX D

This appendix discusses the computer simulation of the design example presented in Chapter 4.

The simulation was carried out on an IBM 1130 digital computer using the Continuous System Modeling Program or CSMP for the 1130. The computer had a core storage of 16K and a memory access time of four microseconds. The CSMP program simulates an analog computer with the input in the form of functional blocks such as an integrator, summer, multiplier, etc. The system to be simulated must thus be represented by a block diagram in much the same manner as is done in setting up an analog computer simulation. The program is limited to a maximum of 25 integrators and a total of 85 functional blocks. This size proved to be adequate for the systems simulated in the example. The method of performing the integration in the program is by a second order Range-Kutta which is carried out at one half the integration interval specified by the user.

Modifications to the CSMP program were necessary in order to save and store the plant input and output signals as well as to calculate the necessary Fourier transforms. The algorithm given in Reference (48) was used in the subroutine for the Fourier transform computation. Modifications were also made in the program for selecting a different time-varying function at each run. The function parameters could either be selected at random from a random function generator or, if desired, could be chosen by the

operator and read in from cards. Provisions were made for calculating and printing the error  $E(j\omega)$  and the ratio  $P_o(j\omega)/P_{eq}(j\omega)$  at selected values of  $\omega$ . In addition, the actual signals themselves could be printed out if desired. As an aid in determining the regions of  $P_o/P_{eq}$ , a plotting scheme was devised whereby the points of  $P_o/P_{eq}$  were stored for each calculation and after all time-variations had been run, the points were "plotted" by the printer for each value of  $\omega$ . This technique eliminates the necessity of manually plotting each value.

The calculation of the Fourier transform of the various signals requires special consideration. In the definition of the Fourier transform, the limits of integration are from plus to minus infinity. Obviously, the numerical integration cannot be performed over such a range; however, if the function to be integrated is zero outside a finite range, the integration need only be performed over this finite range and the numerical integration can be performed satisfactorily. Consider the error function

$$e(t) = c(t) - c_o(t).$$

At  $t$  less than or equal to zero,  $c$  and  $c_o$  are both zero so that  $e$  is also zero. If there is an integrator in the plant, the final value of  $c$  will equal the final value of  $c_o$ , so that the final value of  $e$  is also zero. Practically, one finds that  $e$  is essentially zero after some finite time  $T$ . Thus, the numerical calculation of  $E(j\omega)$  is accomplished by integrating over the

interval zero to  $T$ . Difficulty is encountered in the numerical evaluation of the Fourier transform of the step response  $c(t)$ . Note that  $c$  is zero for  $t$  less than or equal to zero but goes to some finite value  $C_\infty$  as  $t$  goes to infinity. Thus, the numerical evaluation of  $C(j\omega)$  cannot be made from  $c(t)$  directly. This difficulty can be circumvented by defining a new function  $\tilde{c}(t)$  as

$$\tilde{c}(t) = C_\infty u(t) - c(t)$$

where  $u(t)$  is the unit step function. After some time  $T$ ,  $c(t)$  is essentially equal to  $C_\infty$  so that  $\tilde{c}(t)$  is zero for  $t$  greater than  $T$ . Also,  $\tilde{c}(t)$  is zero for  $t$  less than zero so that the numerical Fourier transform of  $\tilde{c}(t)$  can easily be calculated by integrating over the interval zero to  $T$ . The Fourier transform of  $u(t)$  for  $\omega$  greater than zero is known to be

$$u(t) = \frac{1}{j\omega}$$

so that the Fourier transform of  $C$  can be obtained from the relation

$$\begin{aligned} C(j\omega) &= C_\infty \mathcal{F}[u(t)] - \mathcal{F}[\tilde{c}(t)] \\ &= \frac{C_\infty}{j\omega} - \tilde{C}(j\omega) \end{aligned}$$

The function  $\tilde{c}(t)$  can easily be obtained in the simulation from which  $\tilde{C}(j\omega)$  and  $C(j\omega)$  are then calculated. The calculation of the Fourier transform of the plant input presents no particular problem since in the example the plant input signal goes to zero as time goes to infinity.

The integration step size in the program must be selected by the operator and is unchanged throughout the run. A number of step sizes were examined in order to determine the proper values which would yield as rapid a solution as possible and still maintain accuracy. The size selected was 0.01 seconds. Tests were run on time-invariant systems to check the accuracy of the Fourier transform calculation and it was found that the computer computations error was well within 5% up to 30 radians. As an additional test, each time-varying design was run with the gain held constant at values of 1, 1.818, and 10, and the results compared against analytical calculations. This procedure not only verified the accuracy of the calculation but also insured against an error in the simulation.

Despite efforts to reduce computation time, the calculations were fairly lengthy. It required from seven to ten minutes of computer time to calculate ten seconds of simulated system time and an additional two minutes were required to compute  $|E|$  and  $P_o/P_{eq}$  for the frequencies of interest. A complete design evaluation consisting of from 250 to 300 runs required from 35 to 40 hours of computer time.